A

THESIS

entitled

DEVELOPMENT OF GEOCHEMICAL EXPLORATION TECHNIQUES FOR MASSIVE SULPHIDE ORE DEPOSITS, EASTERN BLACK SEA REGION, TURKEY

Submitted for the degree of

DOCTOR OF PHILOSOPHY

in the

Faculty of Science of the University of London

by

MEMET NAMIK ÇAĞATAY

Royal School of Mines
Imperial College of
Science and Technology

June 1977

ABSTRACT

Three types of volcanogenic sulphide mineralizations were studied in the Eastern Black Sea Ore Province of Turkey: (1) massive sulphide type (Madenköy, Kutlular, and Tunca deposits), (2) pyritic stockwork type (Kotarak Dere and Murgul stockwork deposits and the slightly mineralized Sirtköy occurrence), and (3) pyritic impregnation type (Sarisu barren pyrite impregnation occurrence).

In all cases the sulphide bodies and occurrences are associated with the Dacitic Series of Upper Cretaceous age; the hanging-wall rocks consist of the Upper Basic Series comprising basic lavas interclated with tuffaceous sediments and limestone members. Tectonic events are marked by broad regional folding and block faulting; the latter feature has played a major role in exposing the Dacitic Series.

Geochemical exploration in the Eastern Black Sea Ore Province is dependent upon a sound knowledge of the genetic and structural features of the various deposit types, the chemistry and alteration characteristics of the host rocks, and the parameters controlling secondary dispersion of pathfinder and indicator elements.

A well developed drainage pattern associated with block faulting makes stream sediment surveys an ideal method for outlining initial target areas of potential mineralization. Drainage surveys indicate that As is the best elemental pathfinder for outlining the sulphide deposits, the strongest anomalies being observed for concealed ore bodies with exposed mineralized stockworks. Zinc, Pb, Ag, and Cd exhibit anomalies which are dependent on the type of mineralization present, the strongest anomalies being associated with massive sulphide deposits, whereas weaker and more specific anomalies (mainly Cu and Mo) are related to barren stockwork and impregnation occurrences.

Studies were made of the primary dispersion of twenty-seven elements in the footwall and hanging-wall formations of the various mineralized zones. The most effective results were obtained from the analysis of the dacitic footwall rocks. Fluorine, As, Cu, Zn, Pb, and Ba exhibit halos of high anomaly contrast in the dacites which are the host rocks for the ores. Fluorine and As increase significantly in the direction of massive sulphide mineralization (e.g. Madenköy) and can, therefore, be used as directional vectors during drilling programs. Primary halos of As, F, Pb, Cu, Zn, Mo, Ba, and Mn in the hanging-wall hematitized pumice tuffs, and anomalous contents of F, Pb, and Ag in the basalts in the cover rock sequence of the Madenköy massive ore body, were detected; the lateral extent of these halos is about 300 m. The dispersion of Hg is restricted, and this element is not a good indicator of mineralization despite its concentration of up to 7 ppm in the Madenköy massive ore. The dacitic-tuff breccia overlying the concealed Kutlular massive ore body is also enriched in As, Mo, Cu, Zn, and Pb. For the barren mineralized zones, the overlying basalts or spilites contain either increased

concentrations of As and Cu only (e.g. Sirtköy) or exhibit no recognizable primary halos (e.g. Sarisu). When present (as at Madenköy and Tunca), the hematitized rock units directly overlying the Dacitic Series were found to be the best sampling media for detecting primary halos as far as cover rocks are concerned.

On a regional basis the potential of exposed stockwork and pyritic impregnation zones can be assessed by their elemental content. Barren pyritic impregnation deposits generally register only anomalous Fe and to a lesser extent Cu contents. Pyritic stockwork deposits with no associated massive sulphides are enriched in Fe, As, and Cu, whereas those accompanying massive sulphides are marked by enrichments of some or all of Fe, As, Cu, Pb, Zn, Ag, Cd, and Mo. The barren, mineralized dacites are also characterized by higher contents of V, Ti, Co, and Sc but not Ni or Mg.

Hydrothermal alteration characteristics were evaluated by a simple, semi-quantitative X-ray diffraction technique. The ratio, clay (illite-sericite + kaolinite + montmorillonite)/feldspar, was found to be effective in detecting hydrothermally altered zones related to mineralization.

Limited data on the trace element chemistry of pyrite from the stockwork and impregnation zones of the various deposits suggest that higher Co and Ni, and lower As contents occur in pyrite from barren pyritic deposits compared with massive sulphide deposits.

Soils in the Eastern Black Sea Region can be effectively used as an alternative or adjunct sampling medi to rocks in areas of poor bedrock exposure. Lead, Zn, As, and Cu were found to be excellent indicators of massive sulphides. Selective extraction studies involving EDTA, hydroxylamine hydrochloride, and ammonium oxalate solutions indicated that the first two extractants were the most effective in increasing anomaly contrast. The hydroxylamine hydrochloride and EDTA extractions were also found to be better at enhancing hydromorphic anomalies of Zn and Pb over the concealed Madenköy massive ore body.

Based on the present studies, guidelines for geochemical exploration for volcanogenic sulphide deposits in the Eastern Black Sea Ore Province have been formulated.

ACKNOWLEDGEMENTS

The author would like to thank the following persons and organizations for their help in his research:

Dr. D.R. Boyle - for supervising the research and critically discussing and reading the manuscript.

Dr. W.T. Meyer.- for supervising the initial stages of the research.

Professor J.S. Webb - for making the analytical facilities of the Applied Geochemistry Research Group available to the author.

Dr. M. Thompson and Mr. A.J. Thompson - for their guidance in analytical aspects of the research.

The Analytical Staff of the Applied Geochemistry Research Group - for carrying out the direct reading optical spectrographic analysis.

Mr. R. Curtis - for his help and guidance in X-ray diffraction techniques.

M.T.A. (Mineral Research and Exploration Institute of Turkey) geologists in the Eastern Black Sea Region - for their assistance in the field.

M.T.A. - for financially supporting the project.

Geological Survey of Canada - for permitting the author to use its library facilities during the thesis preparation.

TABLE OF CONTENTS

		Page
ABSTRACT		(i)
ACKNOWLEDGMENTS		(ii)
TABLE OF CONTENTS		(iv)
LIST OF TABLES		
LIST OF FIGURES		
INTRODUCTION		1
CHAPTER 1	REVIEW OF THE GEOLOGY OF VOLCANOGENIC MASSIVE SULPHIDE DEPOSITS	5
1.1	INTRODUCTION	5
1.2	GENERAL FEATURES OF VOLCANOGENIC MASSIVE SULPHIDE DEPOSITS	5
1.3	CLASSIFICATION OF VOLJANOGENIC MASSIVE SULPHIDE DEPOSITS	6
1.4	EXAMPLES OF VOLCANOGENIC MASSIVE SULPHIDE DEPOSITS	11
1.4.1	Copper-Zinc Deposits in the Keewatin Greenstone Belts of Canada	11
1.4.2	Cyprus Massive Sulphide Deposits	14
1.4.3	Massive Sulphide Bodies of Elazig Ophiolite Nappe, Southeastern Turkey	16
1.4.4	Küre Massive Sulphide Deposit, Northern Turkey	19
1.4.5	Bedded Pyritic Copper Deposits of the Shikoku Province of Japan	21
1.4.6	The "Kuroko" Ore Deposits of Japan	22
CHAPTER 2	REVIEW OF GEOCHEMICAL EXPLORATION FOR VOLCANOGENIC MASSIVE SULPHIDE DEPOSITS	30
CHAPTER 3	PHYSIOGRAPHY, REGIONAL GEOLOGY, AND MINERALIZATION OF THE EASTERN BLACK SEA ORE PROVINCE	37
3.1	LOCATION OF STUDY AREA	37
3.2	CLIMATE	40
3.3	TOPOGRAPHY AND DRAINAGE	40
3.4	SOILS	42
3.5	HISTORY OF TECTONIC AND MAGMATIC DEVELOPMENT IN THE EASTERN BLACK SEA REGION	43
3.6	STRATIGRAPHY	47
3.6.1	Crystalline Basement	50
3.6.2	Lower Basic Series	51
3.6.3	Dacitic Series	51
3.6.4	Upper Basic Series	52
3.6.5	Flysch and Interbedded Volcanics	52
3.6.6	Quartz-feldspar Porphyries	53
3.6.7	Tertiary Igneous Intrusions	53
3.6.8	The Young Basic Series	54
3.6.9	Glacial Moraines	54
3.7	STRUCTURAL GEOLOGY OF THE EASTERN PONTIDS	55

3.8	MINERALIZATION	57
3.8.1	Plate Tectonics and Mineralization in the Tethyan Region with Special Reference to Turkey	57
3.8.2	Mineralization in the Eastern Black Sea Ore Province	59
3.8.2.1	Ore Deposits associated with the Upper Cretaceous-Eocene Calc-alkaline Volcanic Suite	59
3.8.2.2	Deposits Genetically Associated with Eocene-Oligocene Granitic and Granodioritic Intrusions	68
CHAPTER 4	LOCAL GEOLOGY AND MINERALIZATION	70
4.1	INTRODUCTION	70
4.2	MADENKÖY (1) AREA	73
4.2.1	Previous Work	73
4.2.2.1	Dacitic Series	75
4.2.2.2	Upper Basic Series	79
4.2.2.2.1	Pumice Tuffs	79
4.2.2.2.2	Basalt flows	82
4.2.2.2.3	Andesitic Tuff-Breccias	84
4.2.2.2.4	Limestone-Marl-Sandstone Series	84
4.2.2.3	Basic Dykes	84
4.2.3	Mineralization	85
4.2.3.1	Occurrence	85
4.2.3.2	Ore Mineralogy	86
4.3	SIRTKÖY STOCKWORK MINERALIZATION	93
4.4	SARISU BARREN PYRITIC IMPREGNATION OCCURRENCE	95
4.5	KUTLULAR MASSIVE SULPHIDE DEPOSIT	95
4.6	KOTARAK DERE STOCKWORK DEPOSIT	99
4.7	TUNCA MASSIVE SULPHIDE DEPOSIT	100
4.8	MURGUL STOCKWORK DEPOSIT	103
CHAPTER 5	ANALYTICAL METHODS	106
5.1	INTRODUCTION	106
5.2	ATOMIC ABSORPTION SPECTROMETRY	107
5.3	DIRECT READING OPTICAL SPECTROMETRY ANALYSIS	109
5.4	COMPARISON OF RESULTS OBTAINED BY ATOMIC ABSORPTION ANALYSIS AND DIRECT READING SPECTROGRAPHIC ANALYSIS	111
5.5	COLORIMETRIC ANALYSIS	115
5.5.1	Arsenic Analysis	115
5.5.2	Molybdenum Analysis	117
5.6	FLUORINE ANALYSIS BY ION SELECTIVE ELECTRODE	121
5.7	MERCURY ANALYSIS BY FLAMELESS ATOMIC ABSORPTION METHOD	121
5.8	SELECTIVE EXTRACTION METHODS	124
5.8.1	EDTA Extraction	124
5.8.2	Acidified Hydroxylamine Hydrochloride Extraction	125
5.8.3	Ammonium Oxalate Extraction	127
5.9	pH DETERMINATIONS	127

5.9.1	Determination of Soil pH	127
5.9.2	Determination of the pH of Stream Waters	127
5.10	X-RAY DIFFRACTION ANALYSIS	128
5.11	SELENIUM ANALYSIS	131
5.11.1	Purpose of Selenium Analysis	131
5.11.2	Review of Present Methods of Selenium Analysis	132
5.11.3	Colorimetric Method of Selenium Analysis	133
5.11.3.1	Discussion	134
5.11.4	Microwave Induced Argon Plasma Analysis	136
5.11.4.1	Introduction	136
5.11.4.2	Research and Development on an Inductively Coupled Microwave Plasma System for Selenium Analysis	139
5.11.4.2.1	Introduction	139
5.11.4.2.2	Instrumentation	139
5.11.4.2.3	Preparation of Standards	142
5.11.4.2.4	Investigations	143
5.11.4.2.5	Discussion	148
5.11.4.2.6	Conclusions and Recommendations	150
CHAPTER 6	CHEMISTRY OF THE SULPHIDES	153
6.1	INTRODUCTION	153
6.2	CHEMISTRY OF THE ORES	153
6.3	MINOR ELEMENT CHEMISTRY OF THE PYRITE	164
6.3.1	Previous Work and Objectives of the Study	164
6.3.2	Results	167
CHAPTER 7	HYDROGEOCHEMICAL EXPLORATION	173
7.1	INTRODUCTION	173
7.2	DATA PROCESSING AND INTERPRETATION	174
7.3	pH OF SPRING AND STREAM WATERS	175
7.4	ANALYSIS OF SIZE FRACTIONS	182
7.5	SELECTIVE EXTRACTION ANALYSIS	184
7.6	HYDROGEOCHEMICAL DISPERSION OF METALS	188
7.6.1	Introduction	188
7.6.2	Dispersion of Metals	189
7.7	SUMMARY AND CONCLUSIONS	212
CHAPTER 8	LITHOGEOCHEMICAL EXPLORATION	214
8.1	INTRODUCTION	214
8.2	HYDROTHERMAL ALTERATION	214
8.2.1	Introduction	214
8.2.2	Hydrothermal Alteration in the Madenköy Deposit	217
8.2.3	Hydrothermal Alteration in the Sirtköy Pyritic Stockwork Occurrence	224
8.2.4	Hydrothermal Alteration in the Sarisu Pyritic Impregnation Occurrence	226
8.2.5	Hydrothermal Alteration in the Kutlular Massive Sulphide Deposit	226
8.2.6	Hydrothermal Alteration in the Kotarak Dere Stockwork Deposit	228

8.2.7	Hydrothermal Alteration in the Tunca Massive Sulphide Deposit	229
8.2.8	Discussion	231
8.2.9	Hydrothermal Alteration as a Guide to Ore	236
8.2.9.1	Introduction	236
8.2.9.2	Use of Feldspar Alteration as a Guide to Ore	236
8.3	BEDROCK GEOCHEMISTRY	244
8.3.1	Introduction	244
8.3.2	Data Processing and Presentation	246
8.3.3	Reconnaissance Bedrock Survey in the Cayeli Area	249
8.3.4	Detailed Bedrock Surveys	261
8.3.4.1	Primary Halos in Dacitic Host Rocks	261
8.3.4.2	Primary Halos in Hanging-wall Rocks	268
8.3.5	Regional Assessment of Mineralized Stockwork and Impregnation Zones	272
CHAPTER 9	PEDOGEOCHEMICAL EXPLORATION	280
9.1	INTRODUCTION	280
9.2	DATA PROCESSING AND PRESENTATION	281
9.3	THE pH OF SOILS	283
9.4	DISPERSION OF METALS IN SOILS	283
9.4.1	Introduction	283
9.4.2	Dispersion of Metals	287
9.5	SELECTIVE EXTRACTION TECHNIQUES	302
9.5.1	Introduction	302
9.5.2	Results	306
9.6	DISCUSSION AND CONCLUSIONS	316
CHAPTER 10	GUIDELINES FOR EXPLORATION AND RECOMMENDATIONS FOR FURTHER RESEARCH	318
10.1	GUIDELINES FOR EXPLORATION	318
10.2	RECOMMENDATIONS FOR FURTHER RESEARCH	322
REFERENCES		324
APPENDIX A	SAMPLE COLLECTION AND SAMPLE PREPARATION	338
A.1	SAMPLE COLLECTION	338
A.1.1	Rock and Ore Sampling	338
A.1.2	Soil Sampling	338
A.1.3	Stream Sediment Sampling	339
A.2	SAMPLE PREPARATION	339
A.2.1	Introduction	339
A.2.2	Preparation of Rock Samples	339
A.2.3	Preparation of Soil Samples	339
A.2.4	Preparation of Stream Sediment Samples	340
A.2.5	Clay Separation technique for Rock Samples	340
A.2.6	Pyrite separation technique for Mineralized Samples	340
APPENDIX B	ANALYTICAL METHODS	342

B.1	SAMPLE DIGESTION PROCEDURES FOR ATOMIC ABSORPTION SPECTROMETRY	342
B.1.1	Nitric Acid Digestion	342
B.1.2	Nitric/Perchloric Acid Digestion	342
B.1.3	Bromine/Nitric Acid Digestion for Sulphide Analysis	343
B.2	DIRECT READING OPTICAL SPECTROGRAPHIC ANALYSIS SAMPLE PREPARATION AND OPERATING CONDITIONS	344
B.3	COLORIMETRIC ANALYSIS	345
B.3.1	Arsenic Analysis	345
B.3.2	Molybdenum Analysis	346
B.4	FLUORINE ANALYSIS	347
B.5	MERCURY ANALYSIS-FLAMELESS ATOMIC ABSORPTION METHOD	350
B.5.1	Total Mercury Analysis	350
B.5.2	Mercury Thermal Evolution Profile Analysis	352
B.6	SELECTIVE EXTRACTION METHODS	352
B.6.1	EDTA Extraction	352
B.6.2	Acidified Hydroxylamine Hydrochloride Extraction	353
B.6.3	Ammonium Oxalate Extraction	354
B.7	COLORIMETRIC METHOD OF SELENIUM ANALYSIS	355
APPENDIX C	DATA PROCESSING	359
APPENDIX D	BEDROCK DATA FOR KUTLULAR, KOTARAK DERE, AND TUNCA AREAS	363

LIST OF TABLES

Table No.		Page
CHAPTER 1		
1.1	Characteristics of different types of volcanogenic massive sulphide deposits	8
1.2	Base metal, Co and Ni concentrations of the Ergani, Madenköy, and Küre (Turkey) and Skauritissa, Mathiati, Agrokipia and Kokkinoyia (Cyprus) massive sulphide deposits	17
1.3	Cu, Zn, Pb, Co, and Ni contents of the Kuroko-type ores of Japan	27
1.4	Cu, Zn, Pb, Co, and Ni contents of some volcanogenic massive sulphides in the Eastern Black Sea Ore Province	28
CHAPTER 3		
3.1	Stratigraphy of Eastern Black Sea Region, Turkey	48
3.2	General stratigraphy of the Eastern Black Sea Region, Turkey	49
3.3	Ore and gangue minerals in volcanogenic sulphide deposits in the Eastern Black Sea Ore Province, Turkey	63
CHAPTER 4		
4.1	Volcanogenic sulphide mineralization, Eastern Black Sea Province, Turkey	72
4.2	Vertical distribution of three ore-forming phases in ore samples from drill-hole 110	92
CHAPTER 5		
5.1	Analytical characteristics of the elements analysed by atomic absorption spectrophotometry	108
5.2	Extractability of metals with nitric acid and nitric acid/perchloric acid digestions	110
5.3	Analytical characteristics of the elements determined by the direct reading spectrographic system	112
5.4	Comparison of atomic absorption (nitric acid digestion) and direct reading spectrographic methods of analysis	113
5.5	Comparison of atomic absorption and direct spectrographic methods for ore samples	114
5.6	Effect of the $KHSO_4$ and NaOH fusion techniques on the analysis of arsenic in sulphide samples	116
5.7	Effects of solution acidity on arsenic determinations	118

5.8	Precision at 95% confidence level of the Gutzeit method as determined by replicate analyses of two rock samples	118
5.9	Modification of the pH of the EDTA solution (pH:4.65) by soil and hematitized tuff samples	126
5.10	Characteristic reflections of minerals at which peak intensities were measured by X-ray diffraction	129
5.11	Identification of clay minerals by X-ray powder diffraction	130
5.12	Comparison of duplicate selenium analyses obtained for two different batch analyses	135
5.13	The effect of microwave generator power on the signal obtained by running a solid standard containing 5 ppm selenium	144
5.14	The effect of argon flow rate on the sensitivity of the signal obtained by running a 5 ppm selenium solid standard	144

CHAPTER 6

6.1	Analysis of samples from different zones of the Madenköy massive sulphide deposit in drill-hole 110	155
6.2	Analysis of samples from different zones of the Madenköy massive sulphide deposit in drill-hole 101	156
6.3	Analysis of ore samples from drill-hole K-10 of the Kutlular massive sulphide deposit	158
6.4	Analysis of ore samples from the Kotarak Dere sulphide deposit	159
6.5	Analysis of surface ore samples from the Tunca ore deposit	160
6.6	Analysis of ore samples from the Sirtköy barren stockwork-impregnation mineralization	162
6.7	Analysis of mineralized surface samples from the Sarisu barren pyrite-impregnation mineralization	163
6.8	Trace element contents of pyrite from the Madenköy massive sulphide deposit	168
6.9	Trace element contents of pyrite from Murgul, Kutlular, Tunca, Kotarak Dere, Sirtköy, and Sarisu	169
6.10	The As/(Co-Ni) ratio of pyrite samples from the stockwork and dissemination zones of various types of mineralization	171

CHAPTER 7

7.1	Statistical summary of total stream sediment data	176
7.2	Statistical summary of stream sediment data from background areas	177

7.3	Analysis of size fractions of stream sediments from Maden stream draining Madenköy deposit	183
7.4	Analysis of size fractions of stream sediments from Latum River near Madenköy deposit	183
7.5	Arsenic contents of size fractions of sediments from Maden stream and Latum River, Madenköy area	185
7.6	Arsenic content of ground and unground stream sediment samples from the Madenköy area	185
7.7	Percentage of extractability of various metals from Madenköy stream sediments using 0.05 M EDTA solution	187
7.8	Percentage of extractability of various metals from Madenköy stream sediments using 1 M acidified hydroxylamine hydrochloride solution	187
7.9	Correlation coefficients for stream sediment data from the Madenköy, Sirtköy, and Sarisu areas	202

CHAPTER 8

8.1	Clay and carbonate mineral distribution in the Madenköy massive sulphide deposit	223
8.2	X-ray reflections of nacrite in pumice tuffs	224
8.3	X-ray diffraction properties of mixed-layer illite-montmorillonite clay	225
8.4	Composition of dacitic rocks associated with volcanogenic sulphide mineralization in the Eastern Black Sea Region	247
8.5	Composition of cover rocks associated with volcanogenic sulphide mineralization in the Cayeli area, Eastern Black Sea Region	248
8.6	Mean extractabilities of metals from 16 pumice tuff drill-core samples for three types of extraction procedures	270
8.7	Variations in some major element contents of dacitic rocks from various mineralized areas compared with unmineralized dacites from the Madenköy area	278

CHAPTER 9

9.1	Statistical summary of total soil data	282
9.2	Mercury phase analysis of selected soil samples	303
9.3	Solubility of sulphides in three types of extraction media	307
9.4	Extractability of elements from soil samples by 0.05 ammonium EDTA	308
9.5	Extractability of elements from soil samples by 1 M hydroxylamine hydrochloride solution in acetic acid	309

9.6 Extractabilities of elements from soil samples by 0.157 M ammonium oxalate solution 310

APPENDIX D

Table D.1 Bedrock data, Kutlular area 363
Table D.2 Bedrock data, Kotarak Dere area 363
Table D.3 Bedrock data, Tunca area 364

LIST OF FIGURES

		Page
CHAPTER 1		
1.1	Simplified model illustrating the tectonic environments of the four types of volcanogenic massive sulphide deposits	9
CHAPTER 3		
3.1	Location of the Eastern Black Sea Ore Province	38
3.2	Location map of study areas	39
3.3	Distribution of atmospheric precipitation for the year 1969	41
3.4	Geology of eastern part of Eastern Black Sea Region, Turkey	44
3.5	Principal mineral deposits of the Eastern Black Sea Ore Province, Turkey	60
CHAPTER 4		
4.1	Geology of Cayeli area	71
4.2	Geology of Madenköy (1) area	75
4.3	Geological cross sections, Madenköy massive sulphide deposit	76
4.4	Geological cross section along strike, Madenköy massive sulphide deposit	77
4.5	Plot of FeO (total Fe expressed as FeO)/ MgO vs. SiO_2 for Madenköy basalts and andesitic dykes on variation diagram of Miyashiro (1974)	83
4.6	Geology of Sirtköy area	94
4.7	Geology of Sarisu area	94
4.8	Geology of Kutlular area	96
4.9	Geology of Kotarak Dere area	96
4.10	Geological cross section of Kutlular massive sulphide deposit	97
4.11	Geology of Tunca area	101
4.12	Geology of Murgul area	101
4.13	Geological cross section of the Tunca massive sulphide deposit	102
4.14	Geological cross sections of Murgul mine area	104
CHAPTER 5		
5.1	Effect of acidity on molybdenum determination	120
5.2	Apparatus for mercury analysis	123
5.3	Schematic diagram of microwave-induced argon plasma emission system	141
5.4	Effect of argon flow rate on calibration	145
5.5	Typical signals obtained with different crucibles	147

5.6	Calibration curves for selenium	149
5.7	Vapor evolution profiles for different forms of selenium	151

CHAPTER 6

6.1	Vertical distribution of As, Mo, and Hg in the Madenköy sulphide ores (drill-hole 110)	157

CHAPTER 7

7.1	Stream sediment sample sites and the pH of stream and spring waters, Cayeli area	178
7.2	Stream sediment sample sites and the pH of stream and spring waters, Madenköy area	179
7.3	Stream sediment sample sites and the pH of stream and spring waters, Kutlular area	180
7.4	Dispersion of arsenic in stream sediments, Cayeli area	190
7.5	Dispersion of copper in stream sediments, Cayeli area	191
7.6	Dispersion of zinc in stream sediments, Cayeli area	192
7.7	Dispersion of lead in stream sediments, Cayeli area	193
7.8	Dispersion of silver in stream sediments, Cayeli area	194
7.9	Dispersion of molybdenum in stream sediments, Cayeli area	195
7.10	Dispersion of barium in stream sediments, Madenköy and Sirtköy areas, Cayeli	196
7.11	Dispersion of arsenic in stream sediments, Kutlular area	197
7.12	Dispersion of copper in stream sediments, Kutlular area	198
7.13	Dispersion of zinc in stream sediments, Kutlular area	199
7.14	Dispersion of lead in stream sediments, Kutlular area	200
7.15	Dispersion of arsenic in stream sediments, Madenköy area	203
7.16	Dispersion of copper in stream sediments, Madenköy area	204
7.17	Dispersion of zinc in stream sediments, Madenköy area	205
7.18	Dispersion of lead in stream sediments, Madenköy area	206
7.19	Dispersion of silver in stream sediments, Madenköy area	207
7.20	Dispersion of iron in stream sediments, Cayeli area	210
7.21	Dispersion of manganese in stream sediments, Cayeli area	211

CHAPTER 8

8.1	The most abundant zones of occurrence of Clay minerals at the Madenköy massive sulphide deposit	219
8.2	The most abundant zones of occurrence of carbonate minerals	220
8.3	Vertical zonation of hydrothermal alteration halo at the Madenköy massive sulphide deposit	221
8.4	Vertical distribution of minerals in the Kutlular massive sulphide deposit	227
8.5	Vertical distribution of minerals in the Kotarak Dere deposit	227
8.6	Vertical zonation of hydrothermal alteration halo at the Tunca massive sulphide deposit	230
8.7	Field of formation of ore and hydrothermal mineral assemblages within massive ore and hydrothermal mineral assemblages within massive ore, stockwork and impregnation zones and pumice tuffs at the Madenköy massive sulphide deposit in the Cu-Fe-S-O system at 250°C and 0.1 molar total sulphur	232
8.8	Idealized cross section showing the spatial association of the Madenköy massive sulphide deposit and the hydrothermal alteration zones.	234
8.9	Clay/feldspar ratio of bedrocks, Cayeli area	239
8.10	Clay/feldspar ratio of bedrocks, Madenköy area	241
8.11	Clay/feldspar ratio of bedrocks, Kutlular area	242
8.12	Clay/feldspar ratio of bedrocks, Kotarak Dere area	242
8.13	Clay/feldspar ratio of bedrocks, Tunca area	243
8.14	Vertical elemental profiles in drillholes 4, 73, and 37, the Madenköy deposit	250
8.15	Vertical elemental profiles in drillholes 110, 101, and 30, the Madenköy deposit	251
8.16	Vertical elemental profiles in drillholes 106, and 108, 105, the Madenköy deposit	252
8.17	Vertical elemental profiles in drillhole K-8, the Kutlular deposit	253
8.18	Vertical elemental profiles in drillhole 1, the Kotarak Dere deposit	253
8.19	Vertical elemental profiles in drillholes T-1 and T-5, the Tunca deposit	254
8.20	As content of bedrocks, Cayeli area	256
8.21	F content of bedrocks, Cayeli area	257
8.22	Pb content of bedrocks, Cayeli area	258
8.23	Zn content of bedrocks, Cayeli area	259

8.24	Cu content of bedrocks, Cayeli area	260
8.25	As content of bedrocks, Madenköy area	263
8.26	F content of bedrocks, Madenköy area	264
8.27	Pb content of bedrocks, Madenköy area	265
8.28	Zn content of bedrocks, Madenköy area	266
8.29	Cu content of bedrocks, Madenköy area	267

CHAPTER 9

9.1	Location of soil traverses, Cayeli area	284
9.2	Soil sample locality map, Madenköy (1) area	285
9.3	Location of soil traverses, Kutlular area	286
9.4	Location of soil traverse, Kotarak Dere area	286
9.5	Elemental profiles along soil traverse 2M-2M', Madenköy (2) area	288
9.6	Elemental profiles along soil traverse R-R', south of the Madenköy area	289
9.7	Elemental profiles along soil traverse 2S-2S', Sirtköy area	290
9.8	Elemental profiles along soil traverse A-A' over the Madenköy massive sulphide deposit	291
9.9	Elemental profiles along soil traverse B-B' over the Madenköy massive sulphide deposit	292
9.10	Hg and Ba contents, and the pH of soils along traverse B-B' over the Madenköy massive sulphide deposit	293
9.11	Elemental profiles along soil traverse C-C' over the Madenköy massive sulphide deposit	294
9.12	Elemental profiles along soil traverse 1K-1K' over the Kutlular massive sulphide deposit	296
9.13	Elemental profiles along soil traverse 2K-2K' over the Kutlular massive sulphide deposit	297
9.14	Elemental profiles along soil traverse D-D' over the Kotarak Dere deposit	298
9.15	Elemental profiles along soil traverse 1S-1S', Sirtköy area	299
9.16	Elemental profiles along soil traverse 1SS-1SS', Sarisu area	301
9.17	EDTA extractable Cu, Zn, and Pb in soils along traverse B-B' over the Madenköy massive sulphide deposit	313
9.18	Hydroxylamine hydrochloride extractable Cu, Zn, and Pb in soils along traverse B-B' over the Madenköy massive sulphide deposit	314
9.19	Ammonium oxalate extractable Cu, Zn, and Pb in soils along traverse B-B' over the Madenköy massive sulphide deposit	315

APPENDIX C

C.1	Statistical parameters for 14 elements in all surface rock samples as computed by program "MRSTAT"	360
C.2	Histogram for log(10) transformed Cu concentrations of 221 soil samples as plotted by program "RAWFREQ"	361
C.3	Probability plot of cumulative frequency distributions for log(10) transformed Cu concentrations in 221 soil samples as plotted by program "RAWFREQ"	362

INTRODUCTION

Many economic volcanogenic sulphide deposits genetically related to a calc-alkaline volcanic series (Dacitic Series) of Upper Cretaceous age occur in the Eastern Black Sea metallogenic province of Turkey. This region presents many similarities to the Kuroko-type massive sulphide bearing Green Tuff regions of Japan. It has been known for its copper production since medieval times, and some of the deposits, such as Murgul (in operation at present), have been worked many times throughout history.

Mineral exploration in the province is hindered by a high topographic relief, a dense vegetation cover, and limited accessibility. The economic sulphide deposits found so far are those that outcrop or sub-outcrop and occur in relatively accessible areas. Large areas remain to be explored for concealed mineral deposits, and many others contain pyritic stockwork and impregnation zones that have not as yet been assessed as possible indicators of hidden ore. The main problems facing the exploration geochemist in this area are: (a) the formulation of cost effective and efficacious reconnaissance surveys in an area where accessibility and mobility are severely restricted; (b) the detection of blind ore deposits manifested by primary halos and alteration zones in the host dacitic and cover rocks; (c) the determination of geochemical vectors in the exposed stockwork and impregnation zones for outlining massive sulphide mineralization under the covered flanks of the felsic volcanics; and (d) the assessment of geochemical methods of fingerprinting

exposed stockwork and impregnation zones to determine their possible association with concealed massive sulphide orebodies.

Solutions to these problems were investigated by means of detailed geochemical studies over massive and stockwork sulphide orebodies, and over pyritic impregnation and barren sulphide occurrences. These include the Madenköy, Kutlular, and Tunca massive sulphide deposits; the Kotarak dere stockwork sulphide deposit; and the Sirtköy and Sarisu barren pyritic stockwork and impregnation-type occurrences. The following studies were undertaken in the above mentioned areas:

(a) Prior to any exploration work, a study of the geology and mineralization of the Eastern Black Sea Region was made on the basis of field work by M.T.A. and the published literature up to 1976. The author has also reviewed the features of volcanogenic massive sulphides in general, discussing the distribution and occurrence of these deposits in the Eastern Black Sea Province in light of recent advances in this field.

(b) The ore mineralogy, texture, and chemistry of the sulphide orebodies and occurrences was investigated. A knowledge of the chemistry of the ores was considered especially necessary to find the most effective indicator and pathfinder elements for use in geochemical exploration.

(c) Orientation stream sediment surveys were carried out to investigate their efficacy in this region. Detailed drainage sampling was done in mineralized areas in an attempt to develop criteria for distinguishing economic and barren mineralized zones.

(d) In the Eastern Black Sea ore province the volcanogenic sulphide deposits generally have associated hydrothermal

alteration zones. Detailed mineralogical studies of surface and core samples from these alteration zones were carried out to formulate diagnostic parameters as guides to the location of ore.

The lateral and vertical dispersion of several elements in the footwall and hanging-wall formations of the sulphide deposits were studied. All of the volcanogenic sulphide deposits in the region are associated with dacitic rocks which are usually exposed as small windows by block faulting. Special emphasis was, therefore, placed on these rocks, their major and minor element chemistry in the vicinity of different mineralizations being investigated to determine parameters for differentiating between exposed mineralized zones associated with concealed massive ore and those related to barren mineralization.

(e) Pedogeochemical surveys were carried out with a view to using the soils as an alternative sampling medium to rocks, particularly in areas where weathering and limited exposure makes bedrock surveys difficult. Selective extraction studies of the soils were made in an attempt to enhance anomalies over cover rocks and possibly differentiate these from those obtained over stockwork and impregnation zones.

Most of the bedrock studies summarized above were concentrated in and around the Madenköy massive sulphide deposit mainly because this is the type of deposit usually sought, and also because extensive diamond drilling ensured adequate samples of the ore and host rocks. In some of the study areas surface rock sampling was restricted by weathering and poor exposure. In the Sirtköy and Sarisu areas no

drilling programs have been initiated, and drilling at the Kutlular and Kotarak Dere deposits was still in progress at the time field work was carried out. In the Murgul area the prolonged mining and smelting activity, beginning in Medieval times, has resulted in considerable contamination and stripping of the wall rocks. The drill cores, which have been exposed to the atmosphere for about ten years, are all thus also contaminated and weathered. No attempt was made, therefore to sample this deposit.

CHAPTER 1

REVIEW OF THE GEOLOGY OF VOLCANOGENIC MASSIVE SULPHIDE DEPOSITS

1.1 INTRODUCTION

The present state of our knowledge of volcanogenic massive sulphides is reviewed, including their general characteristics, their tectonic environment of formation, their associated volcanic rocks, and their mineralogy and chemistry. A voluminous literature exists concerning these deposits, only a part of which is reviewed in the following.

Effective geochemical exploration techniques for volcanogenic massive sulphide deposits are dependent upon a sound knowledge of their genesis, mineralogy and chemistry. With this in mind, a review of this nature was considered imperative.

1.2 GENERAL FEATURES OF VOLCANOGENIC MASSIVE SULPHIDE DEPOSITS

Volcanogenic massive sulphide deposits are stratiform, massive, pyritic, base metal sulphide bodies, occurring in volcano-sedimentary rocks. They contain variable proportions of pyrite, chalcopyrite, sphalerite, and galena. The ores are commonly overlain by ferrugenous cherts and iron- and manganese-rich sediments of a mudstone and/or tuffaceous nature. The deposits often exhibit a vertical mineralogical zoning. Many bodies are associated with stockwork mineralizations in extensively altered, sulphide impregnated volcanic or pyroclastic rocks constituting the footwall. The associated volcanic rocks range in composition from basic pillow lavas to felsic calc-alkaline volcanics and pyroclastics.

Studies of younger deposits (e.g., those in Cyprus and the Kuroko deposits of Japan) as well as the present day formation of exhalative-sedimentary sulphide deposits in different geologic environments (e.g., Vulcano, Tyrrhenean Sea (Honnorez et al., 1973) and Talasea, New Britain, P.N.G. (Ferguson et al., 1974)), has changed the concensus of opinion about the genesis of these deposits from one of hydrothermal replacement to a process of syngenetic volcanic-sedimentary formation. These deposits are now largely believed to have been formed on the sea-floor by fumarolic activity associated with subaqueous volcanism. There are, however, still many exponents of the hydrothermal-replacement theory for some of the type deposits described below.

1.3 CLASSIFICATION OF VOLCANOGENIC MASSIVE SULPHIDE DEPOSITS

Several classifications of massive sulphide deposits have been proposed. Waltham (1968) classified the early Paleozoic massive sulphide deposits of Norway into five types on the bases of their sulphide mineralogy and texture: 1) magnetite ore, 2) magnetite-pyrite ore, 3) coarse-grained pyrite ore, 4) fine-grained pyrite ore, and 5) pyrrhotite-chalcopyrite ore.

Gilmour (1971) suggested a classification based on observable features, such as mineralogy, texture, and tectonic setting of the deposits. He stressed that multiple features rather than individual ones should be used to characterize a class of deposits, and thought all classes were parts of a continuous series. His series cover a spectrum of deposits in shales and siltstones (e.g. Mount Isa); felsic members of

calc-alkaline rocks (e.g. Buchans, Newfoundland; East Shasta, California; Matagami, Quebec; and Kuroko deposits, Japan); and basic rocks (e.g. Cyprus deposits).

Hutchinson (1973), in his review of volcanogenic massive sulphide deposits, distinguished three types based on the type of igneous activity associated with the deposits, base and precious metal content of the ores, and the evolutionary tectonics. His three classes are: 1) Cu-Zn-type in mafic to felsic volcanic rocks, also producing Au and Ag; 2) Pb-Zn-Cu-pyrite-type in calc-alkaline volcanics, also containing Ag; and 3) Cu-pyrite-type in ophiolites containing Au).

Geochemical studies, especially the rare earth element geochemistry of the volcanic rocks genetically associated with the massive sulphide deposits, are contributing greatly to our understanding of the tectonic environment of these deposits. Pearce and Gale (1976), as a result of this geochemical approach, distinguished five different types of volcanogenic massive sulphide deposits: 1) Cyprus type-back arc type, 2) Lokken type-back arc type, 3) Noranda type-ocean basin type, 4) Joma type-continental margin type, and 5) Kuroko type-acid island arc type.

An approach similar to that of Hutchinson (1973) will be followed here in classifying these deposits. Associated volcanic rocks and sediments, tectonic environment, mineralogy, texture, and Co and Ni contents of the ores are taken as the bases for the classification. Table 1.1 summarizes the above-mentioned characteristics of different volcanogenic sulphide deposits, and Figure 1.1 illustrates the tectonic environments of the four types of deposits.

Table 1.1 Characteristics of different types of volcanogenic massive sulphide deposits

Type of deposit	Associated volcanic rocks and sediments	Tectonic environment	Co and Ni contents of ores	Ore mineralogy	Examples
1. Cu-Zn-type	Differentiated volcanics comprising the full range from basalt to rhyolite. The magma type is island-arc tholeiite. Cherts and iron-rich sediments, greywackes and pyroclastics.	Early development of island-arc systems, possibly ocean-island environment	High Co, intermediate Ni concentrations	Pyrite, chalcopyrite sphalerite, pyrrhotite, magnetite, minor cubanite and valleriite.	Deposits in the Keewatin greenstone belts of Canada: Noranda and Matagami mine areas
2. Cu-Zn-type	Ophiolite complexes, (pillow lavas-ultramafics pelagic sediments). Ocean-floor and island arc tholeiitic magma type. Cherts, Fe- and Mn-rich chemical sediments.	Marginal basin environment	Generally low Co and Ni concentrations	Pyrite, chalcopyrite, sphalerite, marcasite, covellite, digenite and traces of mackinawite and pyrrhotite. Quartz and gypsum occur as gangue minerals.	Cyprus, Oman, and Løkken-type (Norway) deposits
3. Cu-Zn-type	Ophiolite complexes, possibly of ocean-floor tholeiitic origin. Shales, mudstones and argillites with intercalated limestones.	Small ocean basin, near continental	Generally high Co and Ni concentrations	Pyrite, chalcopyrite, sphalerite, pyrrhotite, magnetite. Minor and traces of linnaeite, valleriite. Quartz and barite occur as gangue.	Ergani and Küre deposits in Turkey; Besshi-type deposits in Japan and Joma-type deposits in Norway
4. Cu-Zn-Pb-Ag-type	Felsic rocks of the calc-alkaline volcanic suite. Pyroclastics: Fe- and Mn-rich tuffs and mudstones intercalated with limestones.	Submarine, island-arc environment	Low Co and Ni concentrations	Pyrite, chalcopyrite, sphalerite, galena, sulphosalts. Barite and quartz as gangue minerals. Associated gypsum deposits.	Kuroko-type deposits in Japan; massive sulphide deposits of Eastern Black Sea Ore Province, Turkey

Miyashiro (1973) and Pearce (1975), as a result of geochemical studies, showed that the Troodos ophiolite complex of Cyprus probably formed in an island-arc "sensu stricto", or related marginal basin environment, instead of along ocean ridge. It is now widely excepted that most of the volcanogenic massive sulphide deposits are formed in island-arc or marginal basin environments.

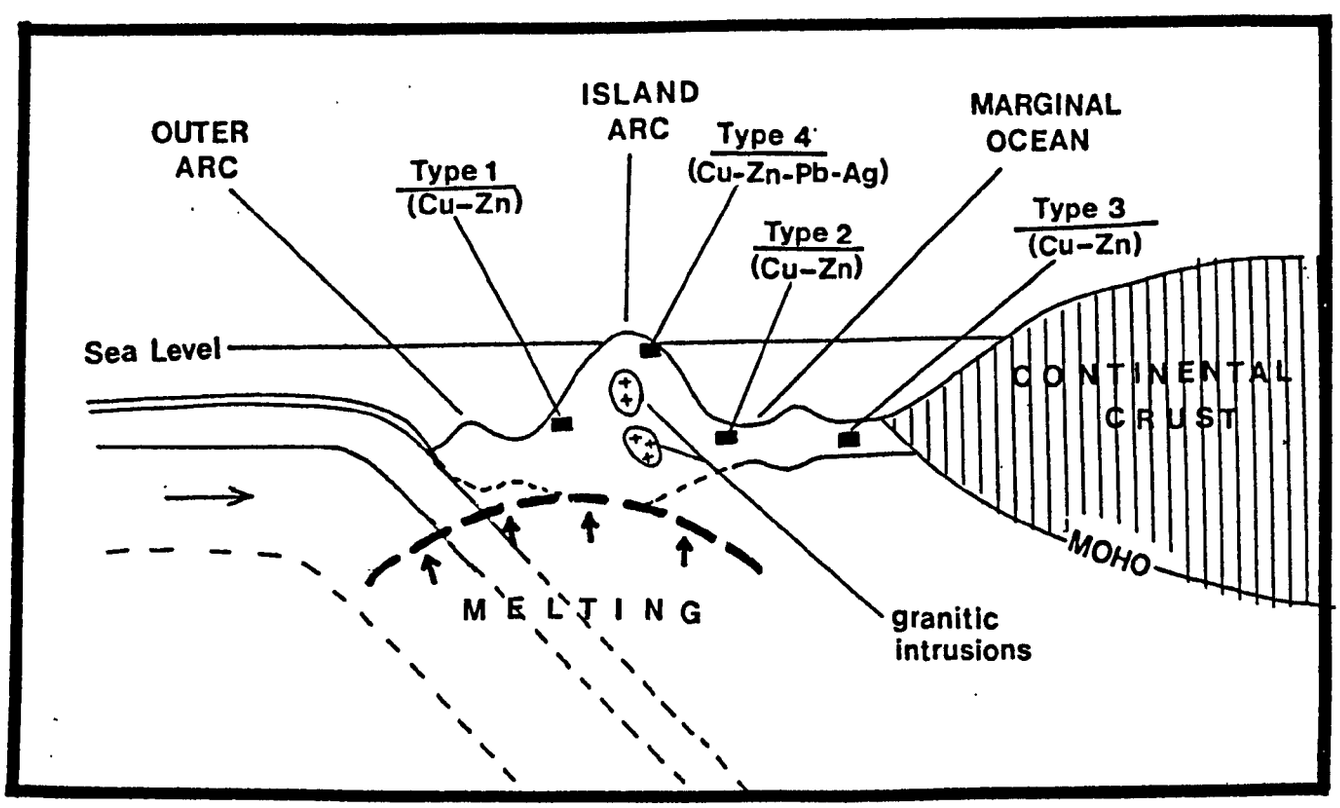


Fig. 1.1 Simplified model illustrating the tectonic environments of the four types of volcanogenic massive sulphide deposits.

The four types of volcanogenic massive sulphides appear to have a sequential formation that is related to the evolutionary tectonics of island-arc orogenies. Thus, in an orogenic belt, type 1 (Cu-Zn) deposits are formed first, followed by the others according to the type of tectonic evolution of that particular island-arc system. Examples of

this sequence are well illustrated by some orogenic belts. For instance in the Pontids of Turkey the Küre deposit (type 3) is of Jurassic age, whereas the Eastern Black Sea massive sulphides (type 4) are of late Cretaceous age. A further example is the Cyprus deposits (type 2), and the Ergani deposit (type 3) of Southeastern Turkey. The two are believed to be on the same Alpine orogenic belt. But the former is of early Cretaceous, and the latter is of upper Cretaceous age. This age difference could, however, be explained by different spreading rates at the two sites (Smith, 1971). Thus, in an orogenic belt it is highly likely for more than one type of volcanogenic massive sulphide deposits to occur. In the old orogenic belts, for example, the Keewatin greenstone belt of Canada, and the Caledonian greenstone belt of Norway, in which the characteristics of island-arcs have disappeared, almost certainly more than one type occurs. Indeed in the latter, two types, Joma-type and Løkken-type, have already been distinguished by Pearce and Gale (1976) by a comparison of their tectonic environments. At present, a great deal of geochemical work has yet to be done on the igneous rocks associated with these deposits in order to define the true nature of their tectonic environments.

The Ni and Co contents of sulphide samples, especially the latter element have often been used in assigning sulphide deposits to sedimentary or hydrothermal origin (Fleischer, 1955). The Co and Ni contents were found to be useful in the classification, but variable amounts were found even between two deposits from the same mining area.

1.4 EXAMPLES OF VOLCANOGENIC MASSIVE SULPHIDE DEPOSITS

1.4.1 Copper-zinc Deposits in the Keewatin Greenstone Belts of Canada

The Precambrian Keewatin belt of the Canadian shield is a typical eugeosynclinal assemblage that includes massive sulphide deposits of the Noranda and Matagami mining areas (Hutchinson, 1965). The volcanic rocks have been considered to be of calc-alkaline affinity by Goodwin and Ridler (1970). However, an earlier geochemical study by Baragar (1968) suggested that they have tholeiitic features. Hutchinson (1973) believes that these rocks are probably similar to the island-arc tholeiites described by Jakes and White (1972). They possibly characterise the early development of an island-arc system. These volcanics represent a well differentiated compositional series, from basalt to rhyolite, and are intercalated with tuffaceous sedimentary rocks, greywacke and cherts. The whole succession has undergone metamorphism and deformation during the Kenoran orogeny.

Sangster (1972) has reviewed the Precambrian volcanogenic massive sulphide deposits of Canada. His account of the important geological features of these deposits can be summarized as follows:

(a) The deposits are clustered in circular areas of acid volcanic rocks, probably representing volcanic centres and occur at stratigraphically favourable horizons at the contacts of felsic rocks. These favourable horizons are marked by "exhalites" which are chemical sediments composed of ferruginous chert and/or iron formation.

(b) The deposits are associated with a single felsic formation in a particular region, in spite of the presence of several felsic formations.

(c) The sulphide deposits are structurally controlled and tend to align themselves along linear faults or rifts which probably determined the distribution of fumaroles and volcanic centres.

The above features are well illustrated in the Noranda and Matagami Lake areas where the metamorphism and deformation have been less intense than in many other parts of the Canadian Shield. The ore bodies in the Keewatin greenstone belts, as in the case with all Precambrian volcanogenic massive sulphide bodies consist of two types of ore: massive ore and stockwork-dissemination ore. The massive ores commonly pass down into a stockwork zone that consists of stringers and disseminations of sulphides within strongly altered felsic lavas and pyroclastics. The alteration is pipe-like in form and in some cases extends about 1000 m below the massive ore. According to Gilmour (1965) the core of the alteration generally consists of massive chlorite, disseminated sulphides, and magnetite grading into zones with sericite-rich margins. The chloritized and sericitized rocks grade into massive and siliceous country rock. The massive ores are conformably overlain by "exhalites" and tuffs. The alteration does not extend into the hanging-wall rocks (Sangster, 1972).

The massive ore contains variable proportions of pyrite, pyrrhotite, chalcopyrite, sphalerite, and magnetite with small amounts of cubanite and valleriite (Hutchinson, 1965). Sphalerite and chalcopyrite are generally concentrated

at the top of a massive ore body, and pyrrhotite is more common towards the stockwork zone.

The ore textures vary from colloform (banded structures usually involving melnikovite pyrite, and sometimes chalcopyrite and sphalerite) to cataclastic, and boundinage structures may be present. Some deposits such as the Horne mine show brecciation of the massive ore (Sinclair, 1971). The ore-wallrock relationships are well illustrated by Sinclair (1971) in the latter mine. The massive sulphide ore bodies of the Horne mine occur in rhyolitic flows, tuffs, and breccias, and the H ore body occurs below the No. 5 ore body. According to Sinclair (1971) the ore formation took place syngenetically as a result of fumarolic activity related to felsic volcanism. Pyrite in the No. 5 zone contains 12 to 60 ppm Co whereas pyrite from the H ore body contains Co contents of approximately 1000 ppm. Sinclair (1971) attributed this to the probable independent formation of the two ore bodies. However, trace element contents of pyrite and pyrrhotite from the Matagami and Noranda area massive sulphides generally show high levels of both Co and Sn and intermediate amounts of Ni. The maximum median contents of these elements in pyrite are 600, 250, and 130 ppm respectively (Roscoe, 1965).

The lead isotope data obtained by Roscoe (1965) gives an age of 2.95 billion years for the Matagami area sulphides and somewhat younger ages for the Noranda deposits. The volcanic rocks that host the Noranda orebodies are also younger than the Matagami rocks. This relationship is suggestive of the hypothesis that the formation of the

massive sulphides and associated volcanic rocks are coeval as Roscoe (1965) has suggested.

Recent geochemical work by Pearce and Gale (1976) suggests that the Noranda-type massive sulphides are formed on the ocean floor in an island-arc type volcanic environment.

1.4.2 Cyprus Massive Sulphide Deposits

Many Cu-Zn massive sulphide deposits occur within the pillow lava and sediment succession of the Troodos ophiolitic complex of Cyprus. This complex consists of an ultrabasic and basic intrusive core surrounded by two pillow lava units which are unconformably overlain by the Cretaceous Parapedhi sediments.. The whole complex represents a typical segment of the oceanic crust, and until recently it has been regarded to have been generated along a mid-ocean ridge. This hypothesis has, however, been questioned by Miyashiro (1973) and Pearce (1975), as stated earlier. Miyashiro (1973) suggested that the Troodos massif, and probably some other ophiolite complexes, were formed as a result of basaltic volcanism in an island-arc setting. He based his argument on the differentiation trends of the Lower Pillow Lava unit and the sheeted complex which follow a calc-alkaline trend. More recently Pearce (1975), studying the geochemical characteristics of the basalts, determined a probable tectonic setting for Cyprus. He suggested the probable development of the Troodos massif first in an inter arc basin with the extrusion of alkali basalts (within-plate) followed by island-arc tholeiite basalts.

The massive sulphides of Cyprus occur as lenticular lenses at the top of the Lower Pillow Lava sequence, and are

covered conformably by the Cretaceous Parapedhi formation consisting of shales, limestones, marls, and chemical sediments. The ore bodies are locally overlain by iron-rich, but manganese-poor ochres, containing sulphides in places. The orchres are believed to have been formed by the submarine oxidation of the sulphides (Constantinou and Govett, 1972). They are in turn commonly overlain by umbres (manganese- and iron-rich sediments). The massive ores are accompanied by a stockwork-impregnation zone in the silicified and brecciated lavas below them. The ore consists of pyrite, which is dominant, and interstitial chalcopyrite, covellite, digenite, sphalerite, and marcasite. Traces of mackinawite and pyrrhotite have also been recorded (Constantinou and Govett, 1973). The amount of chalcopyrite and sphalerite increases towards the top. The top of the massive ore is characterized by a conglomeratic ore with blocks of sulphides in a matrix of sugary pyrite and is underlain by a compact massive ore (Constantinou and Govett, 1973). The collomorphic banding and framboidal textures are characteristic of this top zone. The massive ore passes into the stockwork zone through a zone consisting dominantly of quartz and pyrite. The underlying lavas exhibit extensive alteration comprising a silicified zone surrounded by a chlorite zone.

The zoning and textures of the ores are explained by Constaninou and Govett (1973) in the following way: The primary ore composed of pyrite with traces of chalcopyrite and sphalerite formed in a caldera-like basin. This primary deposit was then subjected to submarine leaching, oxidation, and secondary enrichment, which probably explains the origin

of the ochre. The whole process of ore deposition is presumed to have taken place during a break in the volcanism.

The isotopic evidence from the Troodos complex strongly suggests the involvement of sea water (Sheppard, 1976). He suggested that the sea water circulation in a tectonic environment of high geothermal gradient was responsible for the metamorphism of the pillow lava units and that the sheeted complex belongs to the zeolite and amphibolite facies. He further postulated that the circulating sea water, descending to 2.5 km (to the layered gabbro of the Troodos massif), leached the base metals and deposited them at the points of its discharge on the sea-floor, thus forming the sulphides and the umbre (Spooner and Heaton, 1976).

The Ni and Co contents of the ores are generally low, except for the Skourotissa ores which have a mean Co concentration of 485 ppm and a Co:Ni ratio of 13.8 (Table 1.2).

1.4.3 Massive Sulphide Bodies of the Elâzig̃ Ophiolite Nappe, Southeastern Turkey

The rocks of the Alpine orogeny in south Eastern Turkey consist mainly of spilites, keratophyres, and mafic tuffs of submarine extrusive character intercalated with mudstones, radiolarites, and limestones. Diabase, gabbro, chromitite, and serpentinite also occur in the belt. This sequence of Alpine rocks has been thrust over the younger sediments of the Arabian platform during the Miocene. In the eastern part of this belt, a second thrust zone appears to the north of the former along which the Permian rocks of the Bitlis massif have been thrust over the Alpine ophiolitic complex to the south.

Table 1.2 Base Metal, Co and Ni concentrations of the Ergani, Madenköy, and Küre (Turkey) and Skauritissa, Mathiati, Agrokipia and Kokkinoyia (Cyprus) massive sulphide deposits

Massive Sulphide Deposit	%Cu	%Zn	%Pb	ppm Co	ppm Ni	Co:Ni Ratio	Remarks - References
a) Weiss mine Ergani (Elâzig), Turkey	5.2	3.2	-	820	394	2.1	2 m.t. of pyritic Cu-Zn massive sulphides associated with stockwork-impregnation zone (Çagatay, 1968)
b) Anayatak mine Ergani (Elâzig), Turkey	10.0	3.0	-	2500	700	3.6	6 m.t. of pyritic Cu-Zn massive sulphides associated with stockwork veins (Griffits et al., 1972)
c) Madenköy (Siirt) Turkey	1.0	0.04	0.0015	59	75	0.8	15 m.t. of massive and stockwork-impregnation type sulphides. Average of 90 ore samples from drill-hole M-1 (Çalgin, 1976)
d) Küre (Kastamonu) Turkey	2.75	<0.01	0.02	1525	<15	>100	Bakibaba and Asiköy Mines: together 13 m.t. of massive and impregnation type sulphides (Bailey et al., 1966) Cobalt and Ni analysis by the M.T.A. laboratories (average of 4 ore samples)
e) Skauritissa, Cyprus	2.15	0.08	-	330	24	13.8	6 m.t. of pyritic copper massive sulphides. Average of 10 ore samples (Constantinou and Govett, 1972)
f) Mathiati, Cyprus	1.47	0.29	-	51	33	1.5	3 m.t. of pyritic copper massive sulphides. Average of 56 ore samples (Constantinou and Govett, 1972)
g) Agrokipia, Cyprus	1.0	-	-	41	34	1.2	65,000 t of pyritic massive sulphides. Average of 27 ore samples (Constantinou and Govett, 1973)
h) Kokkinoyia, Cyprus	1.5	0.2	-	63	63	1.0	1 m.t. of pyritic massive ore. Average of 42 ore samples (Constantinou and Govett, 1973)

In the Elâzīg ophiolite belt, a number of massive sulphide deposits occur. The larger and better known of these, listed from west to east, are Elmali in the province of Maraş, Ergani in the province of Elâzīg, and Madenköy in the province of Siirt. The orebodies in the Ergani area are overlain by limestone, basic tuff, and spilitic agglomerate of upper Cretaceous age; and underlain by a silicified pillow lava unit, impregnated and veined with sulphides. The zone of silicification is surrounded by a more extensive chlorite zone. According to Çagatay (1968) the ore minerals consist of pyrite, chalcopyrite, pyrrhotite, sphalerite, and magnetite. Less abundant minerals are cubanite, valleriite, marcasite, anatase, altered chromite, cobalt-pentlandite, linnaeite, and glaucodot . Covellite, cattierite, and digenite occur as secondary minerals. Quartz and barite are the gangue minerals. The mineral paragenesis indicates a relatively high temperature of ore formation. The occurrence of magnetite and chromite, and especially linnaeite, are an important feature of these deposits, and the last mineral has been taken as the diagnostic mineral of these deposits in this belt by Çagatay (in press). The occurrence of cobaltiferous minerals, such as pentlandite, linnaeite, and glaucodot make the deposits being quite rich in cobalt (Table 1.2). The Co contents of pyrite from the Ergani deposit appear to be variable, ranging from 20 to 2000 ppm. (Griffits et al., 1972).

The ores vary in texture from colloform-framboidal to euhedral and subhedral. The replacement of primary magnetite, and the partial replacement of chromite, are

common. These features, together with the wall-rock relationships led Çağatay (1968) and Griffits et al. (1972) to conclude that these deposits are of hydrothermal replacement origin formed as a result of the replacement of mafic rocks by ore solutions. Çağatay (in press) suggests that the sulphide bodies are post-orogenic and closely related to the thrust zones. Griffits et al. (1972), by K/Ar dating on adularia from quartz-epidote veins, determined an age of 31.5 ± 0.8 m.y., corresponding to Middle Oligocene for the Ergani massive sulphides. Although the above evidence supports a hydrothermal replacement origin one can argue that the epigenetic features of these deposits are due to the intense tectonic movements which probably imposed a second phase of hydrothermal activity and thus greatly modified the original, syngenetic deposits. The conformable mudstone hanging walls and colloform, framboidal textures of the massive ores of the sulphide bodies suggests that these deposits are most probably of exhalative-sedimentary origin related to subaqueous mafic volcanic activity. Although the mineral paragenesis of these deposits differs from the "Besshi-type" pyritic copper massive sulphides of Japan (Mitchell and Bell, 1973), they are quite similar in many respects.

1.4.4 Küre Massive Sulphide Deposit, Northern Turkey

Two economic ore bodies, Asiköy and Bakibaba, occur in the Küre mine area of Kastamonu province in northern Turkey. They are massive pyritic copper deposits, closely associated with pillow lavas and generally overlain by argillites. Two pillow lava units, intercalated with two

argillite-greywacke units, occur in the area. The whole sequence is of Jurassic age (Bailey et al., 1966). The ore-bodies occur between the younger pillow lavas and the overlying argillite-greywacke unit. Intrusive rocks are also present in the area. These range from dunite and peridotite to silicic dacite with associated gabbro and diorite. The peridotites are altered to serpentinites. According to Bailey et al. (1966) two types of ore are present in a single ore body, a massive ore consisting of pyrite and chalcopyrite and a lower grade ore in the footwall containing mainly pyrite disseminations in a mafic pillow lava breccia. These ores are characterized by high Co and low Ni concentrations (Table 1.2). The ore bodies occur near a thrust fault, but Bailey et al. (1966) think that the sulphide bodies have no genetic relationship to this structure; on the contrary they postulate that the ores were epigenetically formed by replacement of the pillow lavas and breccias, possibly during the Tertiary. The epigenetic nature of stockwork zones is a general feature common to all volcanogenic deposits, but this feature does not necessarily make the associated massive ore epigenetic. In the Küre mine area the massive ore body may also be syngenetic. Further study is needed in this area before any statement about the origin of these ores can be made. The deposits with their associated rocks and high Co contents are similar to the Ergani deposit, although some of the ore minerals in the latter deposit have not been reported from the Küre ore bodies. The geological environment of these ores is similar to that of the Besshi-type pyritic-copper ores of Japan.

1.4.5 Bedded Pyritic Copper Deposits of the Shikoku Province of Japan

These deposits occur in abundance in the Sanbagawa metamorphic belt of late Mesozoic age. Kanehira and Tatsumi (1970), reviewing the bedded cupriferous iron sulphide deposits in Japan, summarized the following general features of these deposits as follows:

(i) The ores are mainly compact and generally consist of pyrite and some chalcopyrite. Pyrrhotite increases in amount towards the base of the deposits

(ii) The ores occur as bedded and lenticular bodies

(iii) The deposits are associated with metamorphosed submarine basic volcanics, their tuffs and associated black shales of Paleozoic age. They follow definite stratigraphic horizons.

The most characteristic deposit of this type is the Besshi pyritic copper deposit (Mitchell and Bell, 1973). It is a conformable orebody consisting of three types of materials: a compact mass of pyrite, chalcopyrite, and sphalerite with a small amount of gangue consisting of hematite, magnetite, sphene, muscovite, chlorite, and calcite; a banded ore, composed of sulphides and silicates; and an impregnated ore, containing mainly pyrrhotite. Sphalerite, bornite, and tetrahedrite occur in trace amounts. Laterally the orebody gives way to specularite-magnetite seams (Smirnov et al., 1969). The deposit is associated with the Palaeozoic Minawa Formation which consists of metamorphosed basic lavas and black shales. The rock assemblage is typically eugeosynclinal. The occurrence of continentally derived-clastic

sediments in the form of quartzitic schists and shales is suggestive of a marginal oceanic environment.

According to Kanehira and Tatsumi (1970, p. 62) the Co contents of pyrite from several deposits of this type ranged from 15 to 150 ppm with an average of 40 ppm. The Ni/Co ratios were in the range of 1/17-1/20. However, some ore samples of mixed pyrite and chalcopyrite gave Co contents up to 4000 ppm and Ni contents between 10 and 500 ppm. The Ni/Co ratios for these samples were between 1 and 1/30.

1.4.6 The "Kuroko" Ore Deposits of Japan

The Kuroko deposits of Japan are stratiform, base metal sulphide deposits, commonly showing mineralogical zoning. They are related to the Miocene felsic volcanic and pyroclastic rocks of the calc-alkaline suite in the Green Tuff regions of Japan. These deposits have been the subject of intensive study in Japan and in a number of other countries. They have been summarized in two review papers by Matsukuma and Horikoshi (1970), and Lambert and Sato (1974). More detailed descriptions of the Kosaka mining district have been made by Horikoshi (1969), and that of the Hanaoka-Matsumime mine by Ogura (1972). The following summary is largely based on these works.

The Kuroko deposits are important producers of copper, zinc, lead, silver, and gold in Japan. The orebodies are often oval, lens-like in shape. They are overlain by tuffs, clay shales, and mudstones, and underlain by a stockwork and disseminated zone in the footwall. A single

ore body exhibits a common vertical zoning from black ore (kuroko), composed of sphalerite, galena, chalcopyrite, pyrite, and barite on the top, into a pyrite-chalcopyrite-rich yellow ore (oko); this ore grades downward into a pyrite-rich ore (ryukako) and finally into a siliceous stock-work-disseminated ore (keiko) at depth. Enargite, bornite, chalcocite, covellite, and stromeyerite are accompanied by various sulphosalts and electrum (Au-Ag alloy) commonly in the black and to a lesser extent in the yellow ore. The above zoning is not always strictly obeyed, and some of the zones may be missing. The sulphide ore bodies are commonly accompanied by gypsum ore (sekkoko) which is usually inter-bedded with pyroclastic rocks. The stratigraphic position of the gypsum ore in relation to the sulphides is variable. The ore textures also show a variation from the stockwork to the black ore on the top. The stockwork-impregnation zones are usually characterized by anhedral pyrite crystals, and the amount of colloform and framboidal pyrite increases towards the top of the massive ore. The brecciation in the ores is common in the black ore, which probably indicates steam explosions and sedimentation.

Distribution of the Kuroko deposits indicates that they are concentrated in a narrow belt, extending for 1200 km, close to the boundary between the tholeiitic and the high alumina basaltic belts (Lambert and Sato, 1974). The latter belt is known as the Green Tuff region of Japan where intense submarine calc-alkali volcanism of Miocene age took place. The Kuroko deposits were formed towards the more felsic, waning stages of volcanism. The stratigraphic successions

in the mining regions indicates that the Kuroko mineralization in all Green Tuff regions is restricted to the upper half of the Nishikurosawa stage (Middle Miocene) (Matsukuma and Horikoshi, 1970). The Kuroko deposits are generally associated with submarine volcanic and pyroclastic rocks of dacitic and rhyolitic composition (Horikoshi, 1969). The latter rocks generally occur as lava domes in the vicinity of the kuroko ores. The rocks of the Green Tuff regions, with their low Rb and radiogenic Pb, were most probably derived from the partial melting of young crustal rocks within a thick crust. The compositional changes from basalt through andesite to rhyolite were obtained by fractionation of basic and intermediate magmas within the crust (Lambert and Sato, 1974).

The Kuroko deposits are marked by extensive alteration zones, especially in the footwall, and to a lesser extent in the hanging wall rocks.

The alteration commonly appears as argillization and silicification. According to Shirozu (1974), and Iijima (1974) four argillic alteration zones concentrically envelope the deposits and are in turn surrounded by zeolite zones that may extend several kilometres from the orebodies. As one approaches a deposit these argillic zones are:

(a) a montmorillonite zone (30-100 m in thickness)

(b) a sericite - mixed-layer illite - montmorillonite - Fe, Mg chlorite zone (variable, up to 200 m in thickness in deep-seated deposits)

(c) a sericite - mixed-layer sericite - montmorillonite - kaolinite - Mg chlorite zone (approximately 100 m in thickness)

(d) a quartz + sericite zone (approximately 20 m in thickness).

The clay alteration zones, according to Lambert and Sato (1974), developed not only during the Kuroko ore formation, but also for a few million years afterwards, thus extending the alteration zones into the hanging-wall tuffs and sediments.

The concensus of opinion is that the Kuroko volcanogenic massive sulphides are of volcanic-exhalative origin and formed on the sea-floor. The δS^{34} values for sulphides increase from the top to the bottom in an orebody. Kajiwara (1971) explained this in terms of pysico-chemical conditions of ore deposition. He suggested mixing of low pH, low Eh, and high T^{o} ($250^{o}C$) hydrothermal ore solutions with high Eh, high pH, and low T^{o} Miocene sea water for the deposition of the sulphide ores. Gypsum and anhydrite were precipitated as a result of a temperature rise and/or dilution of brines according to the same author. Sato (1973) developed a chloride-complex model from his thermodynamic calculations to explain the zoning, the probable physico-chemical conditions of the ore solutions, and the ore-forming environments. According to Sato's model, the temperature rose from $150^{o}C$ in the top black ore to $250^{o}C$ in the stockwork zone. Other parameters such as pH, log fS_2, and log fO_2 varied from 4.7, -15.0, and -49.2 in the top of the ore to 3.7, -13.6, and -38.6 in the lower stockwork zone, respectively.

Lambert and Sato (1974) suggested that the ore solutions may have been derived from the crystallizing felsic magmas within the magma chamber below. Another possibility is, of course, the leaching of the Green Tuff rocks by circulating brines. The hydrogen, oxygen, and sulphur isotope data

strongly suggest circulation of sea water during the Kuroko mineralization (Sheppard, 1976). The ascending ore fluids would discharge on the sea-floor and their density would rise above that of the sea water as it mixed with the latter (Sato, 1972). The resulting ore solution would then sink, and by flowing down the submarine slopes and depositing the sulphides, the result would be the observed mineral zoning in the Kuroko deposits.

The Co and Ni contents of the Kuroko ores are low, with a general increase of Co content from the black ore to the stockwork zone (Table 1.3).

The general characteristics of the Eastern Black Sea ore province massive sulphides have been summarized in Chapter 3. The following comparison of the latter with the Kuroko deposits of Japan can be made:

(i) Both are associated with the felsic calc-alkaline volcanics and pyroclastics and are overlain conformably by tuffs and clay beds

(ii) The mineralogy, texture, and mineral zoning of the ores in both provinces are similar. Both are associated with barite and gypsum ores. Trace amounts of pyrrhotite in the ores of the Eastern Black Sea province may be due to slightly higher temperature or lower sulphur fugacities.

(iii) The overall chemistry and minor element contents, including Co and Ni concentrations, of the ores in the two regions are similar (Table 1.3 and 1.4), the exception being the generally low Pb contents of the Eastern Black Sea massive sulphides.

Table 1.3 Cu, Zn, Pb, Co, and Ni contents of the Kuroko-type ores of Japan

Massive Sulphide Deposit	%Cu	%Zn	%Pb	Co	Ni	Co:Ni Ratio	Remarks
Kosaka and Hanaoka Mines							25 m.t. of volcanogenic massive sulphide ore at Kasaka mine: 35 m.t. of volcanogenic massive sulphide ore at Hanaoka mine, Hokuroku district, Japan (Lambert and Sato, 1974)
(a) Black ore (7 samples)	2.2	22.5	16.0	Traces	10	<0.2	
(b) Semi-black ore (5 samples)	4.5	7.0	0.6	10	20	0.5	
(c) Yellow ore (18 samples)	7.4	2.0	0.2	30	40	0.75	
(d) Pyrite ore (3 samples)	0.4	0.2	0.07	-	-	-	
(e) Siliceous ore (7 samples)	1.9	0.2	0.06	40	15	2.67	
Average of above types of ore	3.28	6.38	3.39	20	21	0.95	
Kamikita mine: Honko deposit	-	-	0.01	13	3	4.3	The ore body is yellow ore, 50 x 40 m in area and 130 m in depth (Ishikawa et al., 1962)

Table 1.4 Cu, Zn, Pb, Co, and Ni contents of some volcanogenic massive sulphides in the Eastern Black Sea Ore Province

Massive Sulphide Deposit and Location	%Cu	%Zn	%Pb	ppm Co	ppm Ni	Co:Ni Ratio	Remarks
Madenköy (Çayeli)	3.0	4.0	0.12	87	26	3.3	20 m.t. of massive and stockwork-impregnation. type ore. Analysis of 41 ore samples only 18 of which were analysed for Co and Ni (author's data)
Kutlular (Sürmene)	2.2	1.5	0.04	37	25	1.5	1.5 m.t. of massive and stockwork-impregnation type ore. Average of 6 samples of ore for Pb, Co, and Ni (author's data)
Tunca (Ardeşen)	1.5	1.0	0.02	7	48	0.15	300,000 t. of massive and stockwork-impregnation type ore. Average of 4 samples for Pb, Co, and Ni (author's data)
Lahanos (Espiye)	1.6	2.0	0.6	49	65	0.75	8 m.t. of massive and stockwork-impregnation type ore. Average of 84 pyritic ore samples for Co and Ni (Leitch, 1975)
Kizilkaya (Espiye)	1.0	1-2	0.02	35	85	0.4	10 m.t. of mainly stockwork-impregnation type ore. Average of 45 pyritic ore samples for Co and Ni (Leitch, 1975)
Israil (Tirebolu)	2.0	0.12	0.005	280	98	2.9	200,000 t of massive ore. Average of 5 samples. (Acar, 1974)
Harköy (Tirebolu)	8.0	10.0	7.5	trace	trace	-	100,000 t of massive and associated impregnation and stockwork ore (D. Egin, pers. comm., 1977)
Harşit-Köprübaşi (Tirebolu):							
a) rich massive	1.0	10.0	7.5	trace	trace	-	Analysis of rich massive ore (Analysis of pyritic and stockwork ore)
b) pyritic and stockwork ore	3.0	2.0	1.0	trace	trace	-	5 m.t. of proven ore reserve (D. Egin, pers. comm., 1977)
Sadegöre (Görele)	4.0	9.0	0.2	40	70	0.6	Reserve not known. Massive and associated stockwork and impregnation zone. Average of 5 samples (Acar, 1974)

There are, however, a few deposits such as Harşit-Köprübaşi and Harköy that are high in Pb-Zn.

(iv) Both the Kuroko deposits of Japan and the Eastern Black Sea province volcanogenic massive sulphide deposits are characterized by hydrothermal alteration halos of argillization, sericitization, and silicification. In addition to these, carbonitization and hematitization have also been important processes in the Eastern Black Sea deposits, resulting in the occurrence of siderite, dolomite, calcite, and hematite in the alteration zones. This may be due to differences in the composition of the altered rocks and physico-chemical conditions of the ore-forming solutions.

CHAPTER 2

REVIEW OF GEOCHEMICAL EXPLORATION FOR VOLCANOGENIC MASSIVE SULPHIDE DEPOSITS

Volcanogenic massive sulphide deposits are important producers of the world's base and precious metals. The deposits in the Canadian Shield alone produce half of Canada's production of zinc and copper and one-third of the lead, as well as important amounts of gold and silver (Cameron, 1975). The Kuroko deposits of Japan supply half of Japan's output of copper, one quarter of its zinc, one-third of its lead and silver, and one-fifth of its gold (Lambert and Sato, 1974). In Turkey, most of the copper production, together with considerable amounts of gold, are supplied by the volcanogenic sulphide deposits of Ergani, Murgul, and Küre.

Until recently, geochemical exploration has played a minor role in the discovery of volcanogenic massive sulphide deposits. However, in the last few years, geochemical exploration for these deposits has assumed a new initiative, and it is now more common for one to see reports in the literature of geochemical exploration techniques designed specifically for massive sulphides. This is for two reasons:

(a) We now know a great deal more about the mode of formation, associated rock types and type of volcanicity, and the tectonic environment of these deposits. This has been achieved as a result of intensive studies over the last 15 years.

(b) Gradual consumption of the present reserves of these deposits that usually occur near or at the earth's surface has brought about the need to search for blind

ore bodies of the same type under thick overburden. As a result, methods of geochemical exploration specific to these deposits have been intensively investigated over the last few years in order to "fingerprint" anomalous zones above, and peripheral to, hidden orebodies. These investigations, reviewed below, have been carried out in many parts of the world.

The relationship of volcanogenic massive sulphide mineralization to specific rock types has led a number of workers to study the chemistry and petrology of the associated rocks. Such regional studies narrow the target area from an entire orogenic belt to specific volcanic zones. Such a study was carried out by Descarreaux (1973) in the Abitibi volcanic belt of the Canadian Shield. He distinguished two types of volcanic rock suites, tholeiitic and calc-alkaline, and has shown that the sulphide deposits are associated with the calc-alkaline volcanic rock series. The association of the Kuroko deposits with the felsic members of the calc-alkaline suite is also now well established (Lambert and Sato, 1974). Other volcanogenic massive sulphide deposits occur in ophiolite complexes and basic lavas of variable type, as discussed earlier. Such knowledge is of immense help in organizing programs in geochemical exploration for these deposits.

Volcanogenic massive sulphide deposits are associated with endogenic hydrothermal alteration halos and more extensive primary geochemical halos of major and minor elements. These halos occur extensively in the footwall of most of these deposits, whereas the hanging walls are generally characterized by relatively weak or less extensive halos. The hydrothermal alteration halos of these deposits contain

propylitic and/or argillic assemblages which are commonly expressed as chloritization, kaolinization, sericitization and silicification. Such alteration zones are spatially and genetically related to the volcanogenic sulphide deposits. The shape, size, intensity, and mineralogical and chemical composition of the halos depend on many factors. The porosity, permeability, and chemical composition of wall-rocks, the physicochemical properties of ore-bearing solutions, and the physicochemical nature of the ore-forming environment are some of the major controlling factors. Descarreaux (1973), in a petrochemical study of the Abitibi volcanic belt, found high concentrations of Mg and K and a depletion in Na and Ca in the vicinity of Cu-Zn massive sulphide deposits in the Abitibi volcanic belt. The same trend was found, and its use in geochemical exploration has been outlined, by other workers, for example, Sakrison (1967) in the Lake Dufault deposit, Quebec, Canada; Nilsson (1968) in the Boliden deposit, Sweden; Tatsumi and Clark (1972) in the Kuroko deposits, Japan; Boyle (1974) in the Bathurst deposits, New Brunswick, Canada; Franklin et al. (1975) in the Mattagami deposits, Canada; and Goodfellow (1975) in the Brunswick No. 12 deposit, New Brunswick, Canada.

Primary dispersion of minor elements in the vicinity of massive sulphide deposits has also been investigated. Davenport and Nichol (1973), in the Birch-Uchi Lakes Belt of Ontario, Canada, showed that the upper felsic volcanic cycle with associated Zn-Cu-Ag sulphide deposits contained more Zn and less Cu, Co, and Ni than the barren, lower felsic volcanic cycle. Later, Cameron (1975), on a more regional scale, found S and Zn to be useful in distinguishing between

massive sulphide and barren volcanic provinces in the Canadian Shield. Whitehead and Govett (1974) studies the primary dispersion halos of some minor elements in the Heath Steele mine, New Brunswick, Canada, and found by discriminant analysis of the Pb-Zn data that an extensive Pb halo existed in the hanging wall.

An excellent study of the primary geochemical dispersion of base metals in the vicinity of many of the pyritic massive sulphide deposits in the Caucasus, Urals, and Rudnyy Altay regions of the U.S.S.R., was made by Ovchinikov and Baranov (1972). They demonstrated that the subvolcanic-hydrothermal deposits, such as the Gay, Madneuli and Leninogorsk, were associated with extensive alteration halos in their footwalls as well as in their hanging-walls; the hydrothermal-sedimentary deposits such as the Urup and Khudessia in the northern Caucasus, were associated with weak or absent alteration halos in their hanging-wall rocks. The deposits also exhibited an elemental zonation of Co-Cu-Bi enrichment in the footwalls, and a Zn-As-Pb-Ag-Ba enrichment in the hanging walls. Yelchev and Tokmachieva (1971) also found a similar zoning in the Radka sulphide deposit in Bulgaria.

Rock geochemical surveys in the vicinity of the massive sulphide deposits of Cyprus have been described by Govett (1972), and Pantazis and Govett (1973). These workers investigated the dispersion of Cu, Zn, Ni, and Co in pillow lavas, dykes, and sills. Their results did not give a definite indication of the deposits. However, a combination of statistical techniques somewhat distinguished the mine areas from the background.

The primary dispersion of Cu, Zn, Pb, and Ba around the Kuroko deposits, of Japan, has been studied by Ishikawa et al. (1962), and Shiikawa et al. (1975). The former authors mention the use of Cr, V, and Co dispersion in geochemical exploration and indicate that the Pb content in wall-rocks is the best indicator of several of these deposits. The latter workers, using factor analysis, distinguished three major factors of which the first, (Co-V-Cu-Ni), and the third (Cr-Ni), were related to the mudstone intercalations, with the first giving high negative scores over the mineralization. The second factor (Pb-Ag-Zn-Cu) was related to mineralization. In the overburden they obtained extensive enrichments of Ba and Ag. Trend surface analysis by the same authors outlined areas of mineralization.

In the Eastern Black Sea region of Turkey, Tugal (1969) studied the primary dispersion of several elements including Cu, Zn, Pb, Te, Mo, S and As, on a 100 m interval sampling grid over and around the Lahanos mine. The dispersions of these elements were very erratic, and his isoconcentration lines were usually centred around spuriously high values without any support from the surrounding samples.

Leitch (1975), analysing total sulphide concentrates for several elements, in the pyritic ore horizon of the Lahanos and Kizilkaya deposits, demonstrated weak zonations of Co, Sb-As, and Cu. During the drilling stages of exploration he suggests that increases in the ratios Co/Ni, As/Cu, As/Sb, increasing contents of base metals, and decreasing Se concentrations may be used to indicate the direction in which to search for ore.

Secondary elemental dispersions from volcanogenic massive sulphides have also been studied by many workers. These investigations involve more conventional geochemical methods such as stream sediment and soil surveying. Copper and zinc in soils have been used successfully to locate buried Kuroko deposits (Shiikawa et al., 1975). Lake sediment and glacial till surveys have been demonstrated to be effective in reconnaissance geochemical exploration in the Canadian Shield, a large part of which is covered by lakes and glacial drift (Allen, et al., 1973; Ridler and Shilts, 1974). Anomalous contents of Cu, Zn, Ni, Co, Mn, and As were obtained as a result of geochemical dispersion from a gossan zone in the Agricola area, N.W.T., Canada (Allen, et al., 1973). A follow-up lake sediment and soil sampling survey in this area outlined the mineralization. The most significant anomaly/background ratios in soils were indicated by Pb, Ag, Au, and As; mobile elements such as Zn and Cu gave relatively lower anomaly/background contrasts. Ridler and Shilts (1974) used till as a sampling medium in the Canadian Shield. Their technique involved the sampling and analysis of the <2 μ fraction of the till for Cu and Zn. This study was successful in outlining an exhalite horizon in the Kaminak Lake area within the Keewatin greenstone Belt of Northwest Territories.

Geochemical methods of exploration for volcanogenic massive sulphides, based on a sound knowledge of the general features of these deposits, are now playing a major part in their discovery. These methods are applicable at all stages of exploration. The anomalous areas of possible mineralization

can be outlined by regional reconnaissance surveys involving drainage, lake sediment, or till sampling, according to the type of the secondary environment present. These areas can then be assessed by more detailed pedogeochemical and lithogeochemical surveys, followed hopefully by successful drilling programs.

CHAPTER 3

PHYSIOGRAPHY, REGIONAL GEOLOGY, AND MINERALIZATION OF THE EASTERN BLACK SEA ORE PROVINCE

3.1 LOCATION OF STUDY AREA

The mineralized areas studied lie within the eastern part of the Eastern Black Sea (Eastern Pontus) Metallogenic Province (Figures 3.1 and 3.2). The metallogenic province itself extends from the river Kizilirmak in the west to the Russian border in the east. It has a length of about 480 km from east to west, and a width of about 75 km from north to south. The region consists of the eastern part of the Pontid mountains which rise from the Black Sea coast southwards reaching an elevation of 3937 m at Mount Kaçkar in the central part. The study area comprises mineralizations within the coastal band (except Murgul) that covers the area up to elevations of 600 m. It includes seven study areas of mineralization bound by longitudes 41° and 41°35' and latitudes 40°45' and 41°25' and extends from Sürmene in the west, a town to the east of Trabzon, to Hopa in the east, near the Russian border. From west to east the deposits studied are Kutlular, Kotarak dere, Madenköy, Sarisu, Sirtköy, Tunca, and Murgul (Figure 3.2).

The population is mainly concentrated along the coast. Tea, hazelnuts, maize, tobacco, and beans are the main agricultural products, and many tea processing plants occur along the coast. Fishing is an important industry.

As a result of the rugged topographic relief the roads leading inland from the coast are not well developed;

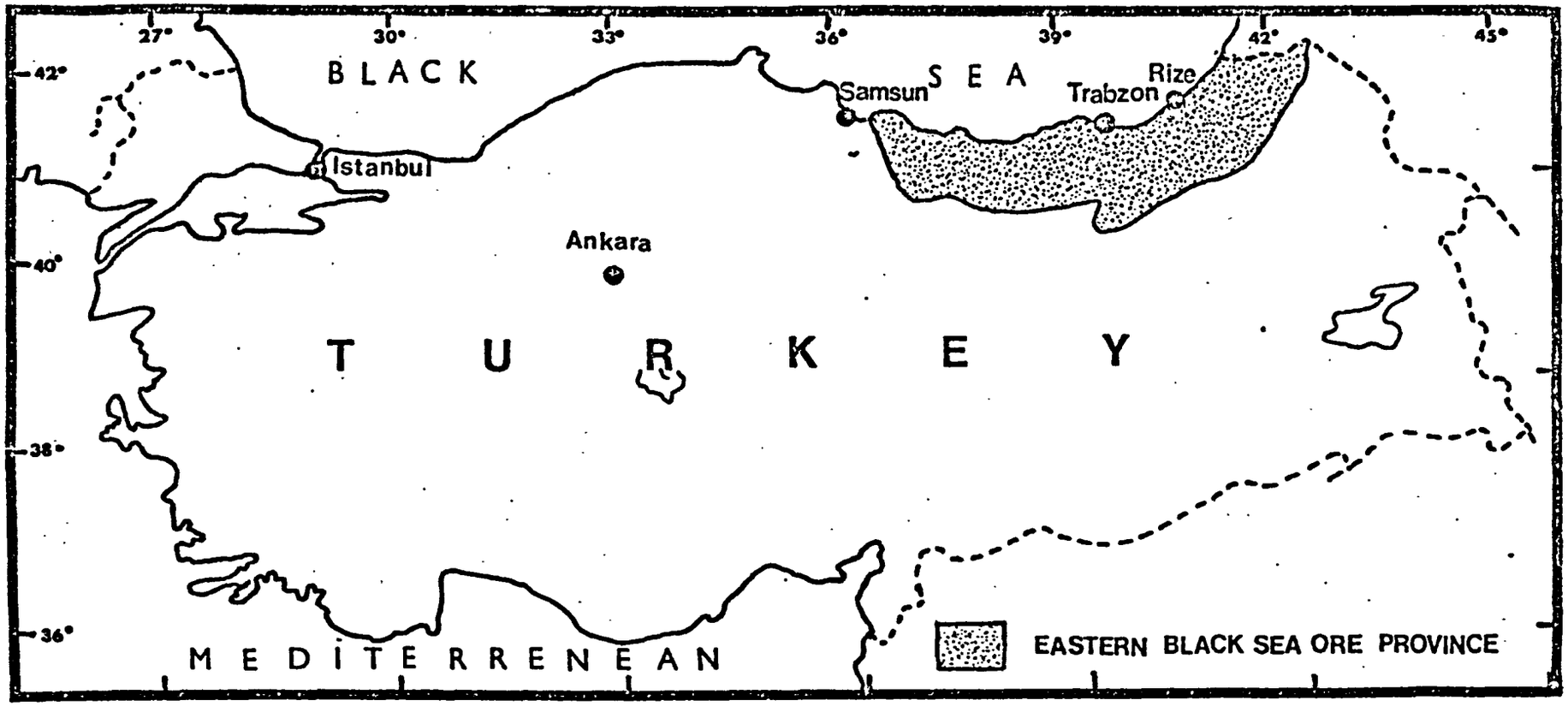


Figure 3.1 Location of the Eastern Black Sea Ore Province.

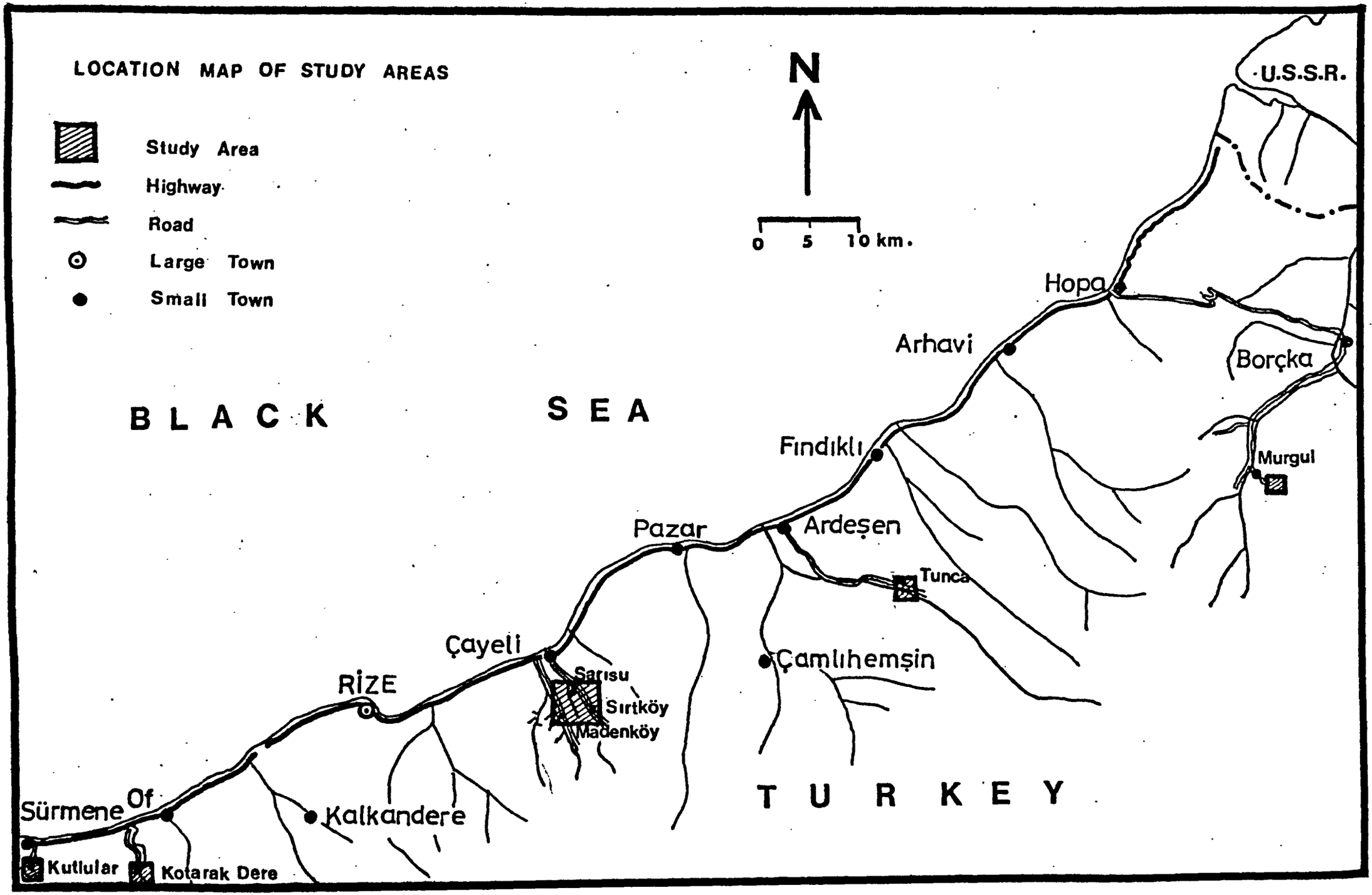


Figure 3.2 Location map of study areas.

all are rough earth roads on which travel is possible only by jeep. There is a good asphalt highway paralleling the coast.

3.2 CLIMATE

The coastal strip is the most humid and rainy part of Turkey. The rainfall reaches 2.5 m in many places and is due to two main factors - the meteorological depressions which originate in Europe and the northern winds that pass over the Black Sea picking up water vapor. The rainfall along the coast generally correlates with elevation. Figure 3.3 illustrates the distribution of rainfall for the year 1969. Generally the greatest amount of precipitation falls in the autumn with successively decreasing amounts in winter, spring, and summer.

The temperature is moderately warm with a 14°C isotherm passing through the area. The warmest month is August and the coolest is February with average temperatures of 20°C and 7°C respectively (Tanriverdi, 1973). According to the observations made between the years 1929 and 1965, Tanriverdi (1973) reports that in Rize the most extreme temperatures observed are in May and February with 40°C and -7°C respectively. However, proceeding inland from the coast the region increases in elevation and above 1000 m the winter is severe. None of the study areas, except Murgul at 1200 m, has an elevation above 600 m.

3.3 TOPOGRAPHY AND DRAINAGE

The coast forms a broad arc beginning at Arakli, 5 km east of Trabzon, and ending at the Russian border. The

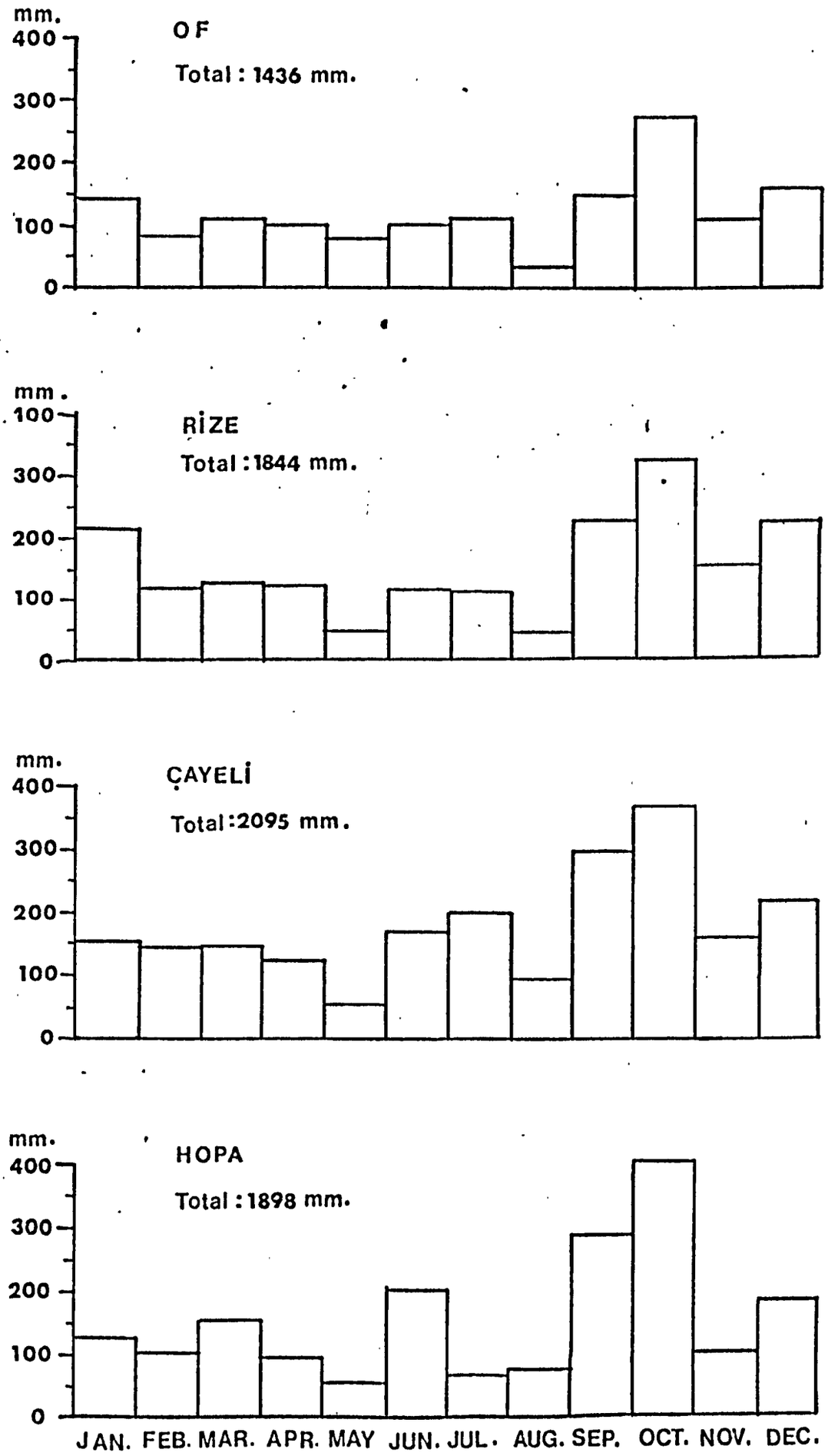


Figure 3.3 DISTRIBUTION OF ATMOSPHERIC PRECIPITATION FOR THE YEAR 1969.

coastal region rises steeply to the south, and topographic lows occur only where rivers enter the sea. These low areas are covered by alluvial soils and thus constitute the centres for agricultural activity and small towns. The general topography, with its steep hills, deeply incised valleys, and waterfalls, presents a high topographic relief.

The coastal strip is generally covered by a dense green vegetation comprising many species of shrubs and trees. In some parts the forest commences at the coast and continues inland. The vegetation cover over the coastal region as a whole is chiefly "Colchis Flora" which is closely related to the coniferous forests of the Caucacus (Tanriverdi, 1973).

Streams in the area form a well developed dentritic pattern with the headwaters originating in the high mountainous land to the south. They have a high velocity as a result of the high topographic relief, and, therefore, a high erosion capacity. The streams flow in deeply disected valleys and mainly follow tectonic lines. As they approach the sea, they deposit their load in wide stream beds near the coast.

The main rivers in the area are the Solakli deresi near Of; the Büyük (Lâtum) dere and Şairler deresi near Çayeli; the Furtuna deresi and Tunca deresi near Ardeşen; the Piskale deresi near Findikli; the Hopa deresi near Hopa; the Murgul deresi, and the river Çoruh near Murgul.

3.4 SOILS

The soils of the eastern Black Sea Region have been classified as a mountain type, red podzolic soil group formed under humid, subtropical climatic conditions (Oakes, 1958). However, in the opinion of the author the soils are not

sufficiently well developed to be called podzolic soils. The soils in the study areas are generally undifferentiated immature mountain soils. The thickness of the soils rarely exceeds 1 m, and as a result of the relief in the area they are well aerated and drained. The measurements of pH made on more than 100 soils show that they are strongly acidic with pH values ranging from 3.5 to 6.7, the most frequently observed pH being 4.5.

Soils, analyzed by X-ray diffraction for their clay mineralogy, were found to possess clays of illite and vermiculite type. The range of organic carbon contents for top soils in tea-planted and forested areas is 1.21% to 6.23% and 2.06 to 19.48% respectively (Tanriverdi, 1973).

Bedrock in the area is generally weathered. Fresh rocks are usually difficult to find for sampling.

3.5 HISTORY OF TECTONIC AND MAGMATIC DEVELOPMENT IN THE EASTERN BLACK SEA REGION

The Eastern Black Sea Region, in a strict sense, forms the eastern part of the Pontids, one of Ketin's four tectonic units of Turkey (Ketin, 1959, 1966). On its southern extension the region is bordered by the North Anatolian Fault, a right-lateral transform fault of major tectonic significance (Figure 3.4).

The Eastern Black Sea Region has been involved in the Caledonian, Hercynian, and Alpine Orogenies. The Mesozoic rocks involved in the Alpine Orogeny rest on the Paleozoic meta-sediments and meta-volcanics involved in the Hercynian Orogeny. Some of the crystalline rocks in the region are probably of Precambrian age. During Precambrian time a

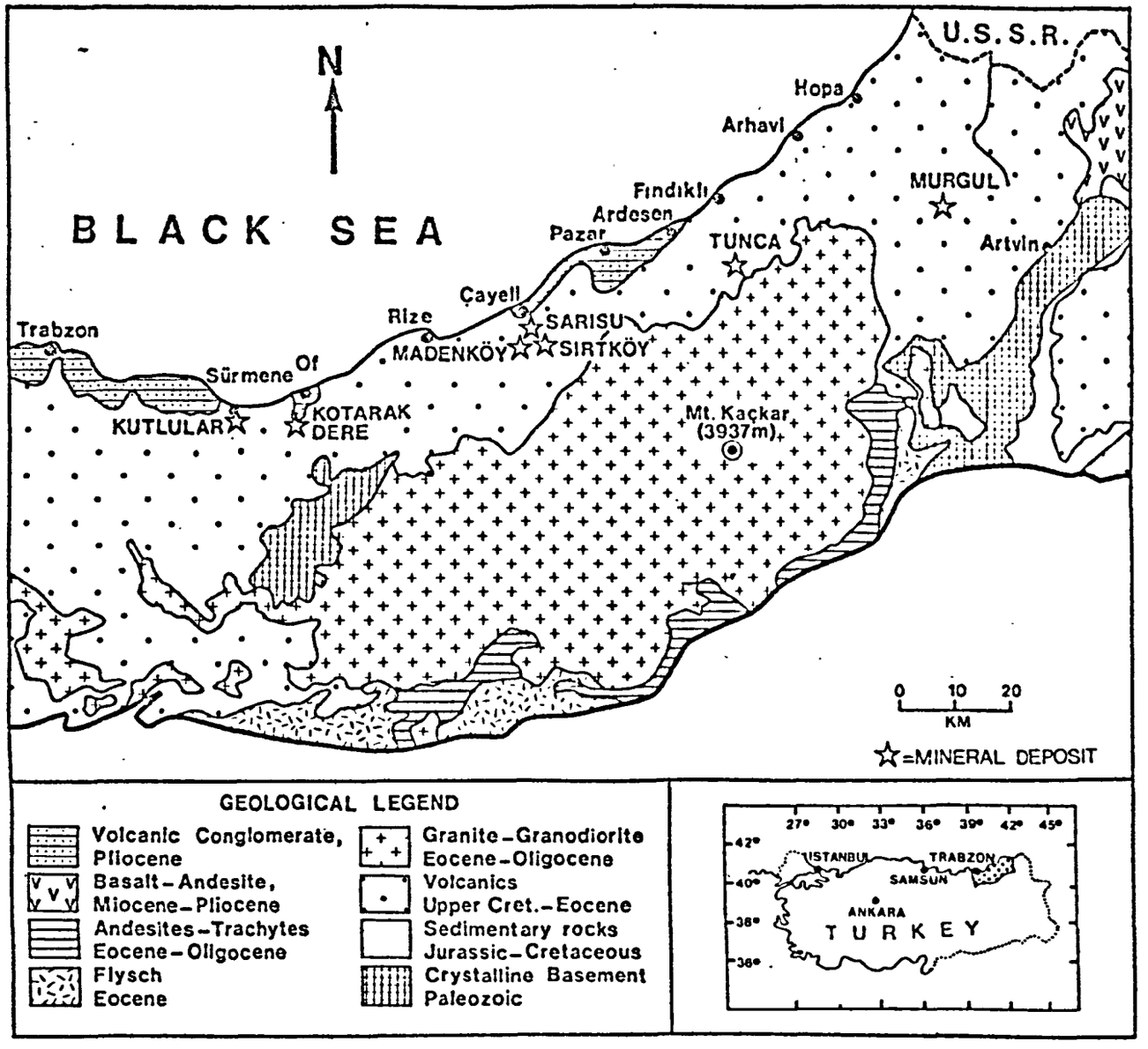


Figure 3.4 Geology of eastern part of Eastern Black Sea Region, Turkey.

synclinorium extended from the Ukraine in the U.S.S.R. to the southern part of the Black Sea Region in Anatolia. According to Brinkmann (1974) metamorphism of the rocks in this structure occurred before Cambrian time.

During the whole of the Paleozoic the present position of the Black Sea, and the coastal part of the Eastern Black Sea Region, was occupied by a landmass that provided clastic sediments to the shallow Silurian and Devonian seas to the south. The Hercynian orogeny occurred during the Permo-Carboniferous period, and folding and faulting were accompanied by granitic intrusions, dated at 300 m.y. in Gümüşhane province (Çoğulu, 1970).

The Alpine Orogeny began with an important transgression over the whole of Anatolia during Triassic and early Jurassic times. There is no record of Triassic rocks within the Eastern Black Sea Region, the period being marked by an unconformity between the Permo-Carboniferous and Jurassic. Muratov (1966) distinguished two major stages in the Alpine history of the region: a geosynclinal stage of basin formation and sediment deposition followed by a final stage of geosynclinal development and mountain building. The first stage covers the time span from the Triassic to the end of Oligocene; the final stage occurred during the Neogene and Quaternary.

In the Eastern Black Sea Region the early phase of geosynclinal development began with the formation of the Lias-Dogger trough of northern Anatolia. This trough was bordered by the Pontian Landmass in the north which long continued as the source of clastic sediments. After the Cimmerian tectogenesis the Lias-Dogger trough moved northwards

with time and developed to be what is now known as the Pontian geosyncline. To the south of the Pontian geosyncline, carbonates and clastic sediments were deposited during the Jurassic and Lower Cretaceous periods. During Middle Cretaceous time, an extensive eugeosyncline known as the North Anatolian Tethys containing radiolarite-ophiolite facies, formed along the present North Anatolian Fault. The rocks which evolved within this geosyncline clearly belong to a different tectonic unit. This tectonic unit has been called the "Anatolids", by Ketin (1959), and the "Northern Anatolian Tethys Ophiolite Nappe" by Horstink (1971, in Akinci, 1974). The ophiolites of the North Anatolian Tethys are of Upper Cretaceous age and consist of serpentinites, gabbro-diabases, spilites, radiolarites, and limestones mapped as "Mof" on the Samsun and Trabzon sheets of the geological map of Turkey (Gattinger et al., 1962; Göksu et al., 1974).

According to Dewey et al. (1973), the extensive Upper Cretaceous-Eocene volcanicity in the Eastern Pontids is related to subduction along the North Anatolian Fault. Tokel (1973) suggests that the North Anatolian Tethys closed at the end of the Cretaceous, but Ataman et al. (1975), believes the age of the completion of the closure to be Oligo-Miocene, which seems more reasonable.

During Middle Cretaceous time the Pontian landmass was submerged under the present Black Sea.

The volcanic activity in the eastern part of the Pontian geosyncline began during Jurassic time, becoming very extensive during Upper Cretaceous and Eocene times. It commenced with basaltic lavas, which were followed by andesites, dacites, and pyroclastics, all of which are particularly well developed along the coastal strip of the Eastern Black Sea Region.

The main tectogenesis and formation of the Pontian mountain chain took place at the end of the Eocene. The granitic, granodioritic, and porphyritic intrusions of the Eastern Pontids were emplaced during the Upper Eocene and Oligocene.

From Oligocene time onward the continuously subsiding Black Sea basin became the foredeep of the Pontids. The oceanic crustal structure of the Black Sea has been established on the basis of seismic reflection and gravimetric data (Neprochnov, 1959; Rezanov and Chamo, 1969). The formation of oceanic crust in the Black Sea basin is attributed to the denudation of the continental crust of the Pontian landmass.

3.6 STRATIGRAPHY

The stratigraphy of the region have been compiled and is shown in the explanatory texts of the geological map of Turkey for the Samsun and Trabzon sheets on a 1/500,000 scale (Gattinger et al., 1962; Göksu et al., 1974). More detailed work has been carried out in specific parts of the Eastern Black Sea Region, for example by Kräeff (1963b) in the Hopa Murgul district; by Sawamura and Yilmaz (1971) in the Sürmene-Of district; by De Geoffroy (1960) and Kawada and Engin (1973) in the Çayeli district; and by Tokel (1973) and Yilmaz (1973) around Gümüşhane.

Table 3.1 shows the general stratigraphy of the Eastern Black Sea Region at three locations from west to east. From the investigations mentioned above, a generalized stratigraphical succession has been compiled and is shown in Table 3.2. Descriptions of the formations follow.

TABLE 3.1 STRATIGRAPHY OF THE EASTERN BLACK SEA REGION, TURKEY

AGE PERIOD, EPOCH	GIRESUN-TRABZON REGION Schultze-Westrum (1961)	ÇAYELİ DISTRICT	MURGUL DISTRICT Kräeff (1963b)
PLEISTOCENE-RECENT	SEA and RIVER TERRACES	ALLUVIUM AND TERRACE DEPOSITS	ALLUVIAL, PLEISTOCENE, and DEBRIS DEPOSITS
MIOCENE-PLIOCENE	YOUNG BASIC SERIES (basalt dykes, trachy-andesite)	VOLCANIC CONGLOMERATE and ANDESITE BRECCIA: BASIC INTRUSIVE SERIES (basalt and andesite dykes)	ANDESITES AND BASALTS
EOCENE-OLIGOCENE	GRANODIORITE and MONZONITE INTRUSIONS	GRANITIC and DIORITIC INTRUSIONS	ALBITE TONALITE, GRANODIORITE, and GRANITE ALBITE DACITE III TUFF SERIES LIMESTONE-MARL SERIES HIPPURITIC LIMESTONE SERIES
UPPER CRETACEOUS-EOCENE	UPPER BASIC SERIES (spilite, agglomerate, andesitic and basaltic lavas and tuffs)	UPPER BASIC SERIES (basalt and tuff intercalations, andesite tuff-breccia, sandstone, and limestone)	SPILITIC SERIES (Spilite, sodium keratopyre, agglomerate, and tuff)
UPPER CRETACEOUS	DACITE II (rhyodacite, hypabyssal dacite) DACITE and ANDESITE MIXED SERIES	– –	ALBITE DACITE II (coarse and green to red-violet in colour)
UPPER CRETACEOUS	LOWER DACITIC SERIES (DACITE I)	DACITIC SERIES (dacite and dacitic tuff)	ALBITE DACITE I (albite dacite, partly silicified and silicified albite dacite; and dacitic tuff)
JURASSIC-CRETACEOUS	LOWER INOCERAMUS LIMESTONE LOWER BASIC SERIES (spilite, basalt, andesite, agglomerate, tuff, massive limestone, and phyllite)	LOWER BASIC SERIES (basalt, andesite, and volcanic breccia)	SPILITIC SERIES (sodium keratopyre-spillite with tuff and agglomerate)
PERMO-CARBONIFEROUS	CRYSTALLINE BASEMENT (sericitic quartzite and quartzite-conglomerate)	–	–

TABLE 3.2 GENERAL STRATIGRAPHY OF THE EASTERN BLACK SEA REGION, TURKEY

ERA OR EPOCH	FORMATION	LITHOLOGY
Quaternary	Glacial moraines, alluvial and terrace deposits	-
Pliocene	Young Basic Series	Volcanic conglomerate; sand, gravel, and clay
Miocene	Basic Dykes	Basalt and andesite dykes
Upper Eocene-Oligocene	Granitic intrusives	Granite, granodiorite and diorite
Eocene	Quartz-feldspar porphyries	Albite-granite-porphyrite and diorite porphyry
Eocene	Flysch and interbedded volcanics	Flysch (sandstone, shale, marl, and conglomerate) intercalated with andesite and tuff
Upper Cretaceous-Lower Eocene	Upper Basic Series	Spilitic basalt, keratopyre, and andesitic pyroclastics with intercalated limestones
Upper Cretaceous	Dacitic Series	Dacite and dacitic tuff
Jurassic-Cretaceous	Lower Basic Series	Basic volcanics and pyroclastics
Carboniferous (Westphalian) Permo-Carboniferous Paleozoic-Precambrian	Crystalline Basement	a) Hercynian granitic intrusions b) Meta-sediments c) Metamorphic Series

3.6.1 Crystalline Basement

The crystalline basement comprises mainly Paleozoic rocks of the Hercynian orogeny, divisible into three main series:

a) Metamorphic Series,

b) Permo-Carboniferous Metasedimentary Series,

c) Granitic Intrusions of the Hercynian orogeny.

The Metamorphic Series consists of mica-schist, quartzite, phyllite, and gneisses. On the basis of geomagnetic anomalies, and correlation with crystalline basement rocks in southern Russia, the gneisses are most probably Precambrian (Brinkmann, 1974). No fossils have been reported from any of the rock types of this series. The metamorphic series occurs as far north as the Soğanli mountains, 45 km south of the town of Of.

The Permo-Carboniferous Metasedimentary Series is typified by arkose, quartz sandy schist, and quartzite. There are also lavas and tuffs of andesitic nature occurring in the south of the region. This series contains fossils and is petrologically similar to the metamorphic series mentioned above. Thus, the two series could be synonomous.

The Hercynian granites were intruded into the mica schists and gneisses and in places caused melting of these rocks. These granites occur at a number of localities (eg. Gümüşhane, Kelkit Valley). In the Gümüşhane region the granites cover 250 km^2 and occur in contact with Upper Carboniferous quartzites; they have been dated at about 300 m.y. (Çoğulu, 1970).

3.6.2 Lower Basic Series

The Triassic is not marked by sedimentation or volcanism in the Eastern Black Sea Region. Instead the Lower Basic Series of Lower Jurassic to Upper Cretaceous age lies unconformably on the Permo-Carboniferous Series of the crystalline basement. The Lower Basic Series is composed of tholeiitic basalt, andesite, and volcanic breccia in the Çayeli area (De Geoffroy, 1960); spilites of a keratophyre nature and associated tuffs and agglomerates in the Murgul district (Kräeff, 1963b); and basaltic lava flows and associated dykes and plugs in the Gümüşhane area (Tokel, 1973).

3.6.3 Dacitic Series

The volcanogenic sulphide mineralization in the Eastern Black Sea Region is intimately related to the Dacitic Series of Upper Cretaceous age. This series consists of dacite and dacitic pyroclastics. The dacite varies in character from place to place; in some areas it is porphyritic whereas in other areas it is equigranular. The Dacitic Series has been divided into three units (Kräeff, 1963b) - Dacite I, Dacitic Tuffs, and Dacite II. Dacite I and the Dacitic Tuffs are commonly grouped together and called the Lower Dacitic Series or Dacite I (Schultze-Westrum, 1960; Kräeff, 1963b). Dacite II does not occur in the Madenköy area (Çayeli). However, around the Murgul area and Arhavi area Dacite II is of widespread occurrence. In the Murgul mine area it is coarse grained and hematitized. The sulphide ore deposits are generally found either between Dacite I and the overlying Dacitic Tuffs or within the Dacitic Tuffs.

For the first case most of the economic massive sulphide occurrences can be given as examples. The latter case is well represented by the Murgul sulphide deposits where the stockwork ore occurs within the Dacitic Tuffs and is overlain by hematitized Dacite II.

3.6.4 Upper Basic Series

This is an extensive formation which has a widespread occurrence especially along the coastal strip. The series consists mainly of spilitic basalt, keratophyre, and andesitic pyroclastics, with some limestone intercalations. The limestones in the Madenköy area are dated as Maestrictian (uppermost Cretaceous), but the age of the whole series is Upper Cretaceous to Eocene. In the Gümüşhane area the Upper Basic Series consists of rock types covering the range from olivine-dolerite through hornblende-andesite and trachy-andesite to trachyte (Tokel, 1973). In the Murgul area the series is made up of spilitic basalt, keratophyre spilite, and basic pyroclastics amounting to 1000 m in thickness (Kräeff, 1963b). As in the Çayeli area, the Upper Basic Series of the Kutlular, the Kotarak Dere, and the Tunca areas consist of basic rocks with pyroclastics and limestone intercalations.

3.6.5 Flysch and Interbedded Volcanics

The Upper Basic Series is unconformably overlain by a series consisting of flysch with intercalations of andesite, tuff, and porphyries. The flysch itself is comprised of sandstone, conglomerate, shale, marl, and limestone. It is fossiliferous, has been dated as Eocene (Gattinger et al., 1974), has a wide distribution, and occurs to the south of

the Tatos batholith as well as near the Black Sea Coast (e.g. in Pazar).

3.6.6 Quartz-feldspar Porphyries

These intrusive porphyries occur south of the Çayeli area. They are porphyritic with feldspar and quartz phenocrysts and some mafic minerals. In the Murgul area the porphyries are called Dacite III and in places they are associated with some pyritic and sulphidic mineralization (Kräeff, 1963b). In the vicinity of the Lahanos massive sulphide deposit (Tuğal, 1969), the Dacite III has intrusive as well as extrusive characters.

3.6.7 Tertiary Igneous Intrusives

The most important and voluminous intrusive rocks in the region are the synorogenic granitic intrusions that form the high plateau south of the coastal strip. The largest intrusive, exposed to the south of Rize, is called the Tatos batholith. The Tertiary intrusives occur along the major anticlinal axis of the eastern Pontids, and range in composition from tonalite and granodiorite to granite. Contact metamorphism of the country rocks has been induced by the intrusives, for example, the Upper Cretaceous limestones and lavas north of Gümüşhane have been highly metamorphosed and the Eocene flysch (Lutetian) east of the Soganli Mountains exhibits anatexis as a result of the intrusions. The age of the Tertiary intrusives is believed to be Eocene to Oligocene on geologic evidence. The batholith to the south of Rize was dated at 25 m.y. by Çoğulu (1970).

There are also a number of diorite-gabbro intrusions in the Çayeli area (Figure 4.1). These are believed to be of the same age as the granitic intrusives.

Basic dykes of basaltic and andesitic composition in the Çayeli area have been called "dolerite dykes" by Kawada and Şarman (1973). Andesitic dykes also occur near the Madenköy massive sulphide deposit. The age of these basic dykes is thought to be Miocene.

3.6.8 The Young Basic Series

The Young Basic Series unconformably overlies the Upper Basic series and consists of two units in the Çayeli area - andesite breccias, and volcanic conglomerates. This Pliocene Series is best seen along the coast between Çayeli and Pazar. The volcanic conglomerates along the coast contain rounded pebbles and boulders of up to 0.5 metres in diameter representing various rock types. The groundmass is basaltic in composition.

In the Murgul Region, between Murgul and Çoruh, the series consists of hornblende-augite andesite and augite-hornblende basalt sometimes with olivine (Kräeff, 1963b).

3.6.9 Glacial Moraines, Alluvial and Terrace Deposits

Towards the coastal region where the stream and river beds are broader, and the rate of flow is slower, alluvial deposits with many striated pebbles and boulders are extensively developed. The striated pebbles and boulders derive from glacial moraines which occur on the high plateau region south of the coastal strip. In addition, during Pleistocene

time glacial valleys were formed and boulder clays were deposited on the higher plateau parts of the region. Alluvial terrace deposits are widespread in the region and several levels can be observed. Sea terraces are well developed around Trabzon as well as at a number of other coastal locations.

3.7 STRUCTURAL GEOLOGY OF THE EASTERN PONTIDS

The Eastern Pontids, with its volcano-sedimentary complex of Mesozoic and Tertiary age, forms a distinct tectonic unit whose rocks generally strike in a NEE-SWW direction and dip northerly, the rocks becoming younger from south to north.

Geological mapping carried out in the region after 1960 has shown that the Eastern Pontids do not represent a typically Alpine folded region (Zankl, 1961; Schultze-Westrum, 1961; Kräeff, 1963a and 1963b). For instance, there are no tectonic elements such as nappes and overthrusts of the classic Alpine type. On the contrary the region has a germanotype (horsts and grabens) tectonic style with fault tectonics predominating (Kronberg, 1970), and folding is only gentle in some parts of the region. In the Çayeli area some folds are present within the Lower Dacitic Series, having a NE-SW trend. In the Sürmene district certain synclines and anticlines have E-W and NE-SW trends. Similarly, in the Hopa-Murgul region, folding is only gentle, with axial trends of NE-SW, and NE plunges. The work of Japanese geologists in the last few years has revealed frequent dome structures within the region. Sawamura and Yilmaz (1971), working

in the Sürmene district, mapped a large dome, with a core of Lower Basic Series (Kestel Dome). The presence of several dome structures with NW-SE trends in the Hopa-Murgul region has been postulated by Sawa et al. (1972).

Tectonic movements, which gave rise to block-faulting and dome structures, are old, beginning probably during the Lias and continuing throughout the Alpine Orogeny up to the present. These tectonic movements were not, however, continuous throughout the Alpine Orogeny; for example, one discontinuity, which resulted in the unconformity between the Dacitic Series and Upper Basic Series, is well illustrated in the Sürmene and Çayeli districts.

Tectonic lines, generally deep faults, which facilitated the intrusion of hypabyssal dacites of Upper Cretaceous age, as well as the granitic, basaltic, and andesitic rocks of Tertiary age, played an important role in the distribution of the volcanogenic sulphide deposits. Later faulting related to tectonic uplift followed the same tectonic lines and resulted in the exposure of dacitic windows beneath the basic cover.

The faults in the central part of the Eastern Pontids have two dominant trends, NW-SE and NE-SW (Kronberg, 1970). In the Sürmene district the fault trends are mainly in E-W, N-S, and NW-SE directions. In the Çayeli area, the faults affecting almost all the formations, generally have NE-SW, NW-SE, NNE-SSW, and NEE-SWW trends, the most common being those with NE-SW trends. In the Hopa-Murgul region faults are developed in NW-SE, NE-SW, N-S, and E-W directions (Kräef, 1963b). Faults trending NW-SE are the most common and oldest in most parts of the Eastern Pontids.

3.8 MINERALIZATION

3.8.1 Plate Tectonics and Mineralization in the Tethyan Region with Special Reference to Turkey

The general relationship of ores to specific magmatic rock suites has been known for many years. According to the plate tectonic hypothesis, calc-alkaline rock series and associated granitic and granodiorite intrusions mark the sites of compressive plate margins whereas ophiolite belts represent oceanic crust which have been generated at mid-ocean ridges and later obducted over the Benioff zones (Dietz, 1963; Isacks, Oliver and Sykes, 1968; Dewey and Bird, 1970). It thus follows that the plate boundaries, especially along the consuming margins, are locations of important metallogenic belts (Pereira and Dixon, 1971; Smith, 1971; Sillitoe, 1972; Guild, 1972; Mitchel and Bell, 1973).

Mineralization in the Tethyan region, in the light of the plate tectonics hypothesis, has recently been examined by Dixon and Pereira (1974), and Grant (1974). The opening of the Atlantic during Permian or early Triassic times resulted in movements in the Tethyan region which developed as a true ocean filled with islands or microcontinents. These microcontinents are now represented by the Rhodope massif in the Balkans, the Menderes, Anatolian and Bitlis massifs in Turkey, and the Lut massif in Iran. These massifs are important elements of the Alpine Orogeny, and although they were rigid blocks they were later intruded by Alpine igneous phases.

Ophiolite belts in the Tethyan region form the second tectonic element, ranging in age from Jurassic to Upper

Cretaceous. The ophiolite complexes in Cyprus, southeastern Turkey, Iran and Oman, are of Upper Cretaceous age. These are associated with important massive copper-pyrite and chromite deposits (e.g. the Ergani and Siirt-Madenköy massive copper-pyrite deposits and the Guleman chromite deposits in southeastern Turkey; and the Küre massive pyritic copper deposit in the western Pontids of Turkey). The Elburz and Zagros ophiolite belts in Iran are also known to contain pyritic copper deposits (Dixon and Pereira, 1970).

The compressional plate margins are marked by calc-alkaline volcanicity and granitic intrusions. This type of volcanicity, and related ore deposits, represents the third element in the Alpine orogenesis. Such volcanic activity of Lower Jurassic age occurred in the Carpathians of Romania, in the Crimea, and in the major Caucasus; all of these volcanic belts have associated massive copper-pyrite and porphyry copper deposits.

The time period from Jurassic to Eocene witnessed the development of two island arc systems and associated mineralized-belts in the central and eastern Tethyan region. The first belt is manifest within the Carpathians of western Czechoslovakia, passes through Romania, Yugoslavia, Bulgaria, and the Eastern Pontids (Black Sea), terminating in the Elburz mountains of Iran (Superceanu, 1971; Akinci, 1974). Important deposits associated with this belt are - the Kremnica, Banska, and Matra in Czechoslovakia; the Brad, Rodna, Boshia, Stara Zagora, and Burgas deposits in Romania; the Majdenpek and Bor deposits in Yugoslavia; the Medets deposit in Bulgaria; the Köprübaşi, Lahanos, Madenköy, Tunca, and Murgul deposits in the Eastern Pontids; and the Pambec-

Zangezur copper-molybdenum belt in the Minor Caucasus. The second mineralized belt is the Pelagonia-Taurus-Zagros island arc system (Dixon and Pereira, 1974). This belt is a part of the southern branch of the Alpine-Himalayan orogen. The Vardar zone of the Hellenides and the Zagros Mountains in Iran contain many polymetallic massive sulphide and porphyry copper deposits, associated with calc-alkaline volcanics and granitic and granodioritic intrusions.

3.8.2 Mineralization in the Eastern Black Sea Ore Province

Two genetic types of ore deposits occur in the Eastern Black Sea Ore Province:

a) deposits associated with the Upper Cretaceous-Eocene calc-alkaline volcanic suite,

b) deposits genetically related to the Eocene-Oligocene granitic and granodioritic intrusions.

The deposits of the first category include the volcanogenic, polymetallic sulphide, and exhalative-sedimentary manganese deposits. The deposits of the second category include copper and iron skarn deposits and copper-molybdenum type occurrences around the Tatos batholith and smaller granitic stocks in the region. Important occurrences of the above types of mineralizations are given in Figure 3.5.

3.8.2.1 Ore Deposits Associated with the Upper Cretaceous-Eocene Calc-alkaline Volcanic Suite

Five types of ore deposits of this genetic association occur in the province:

(a) Massive sulphide-type deposits

(b) Stockwork-type sulphide deposits

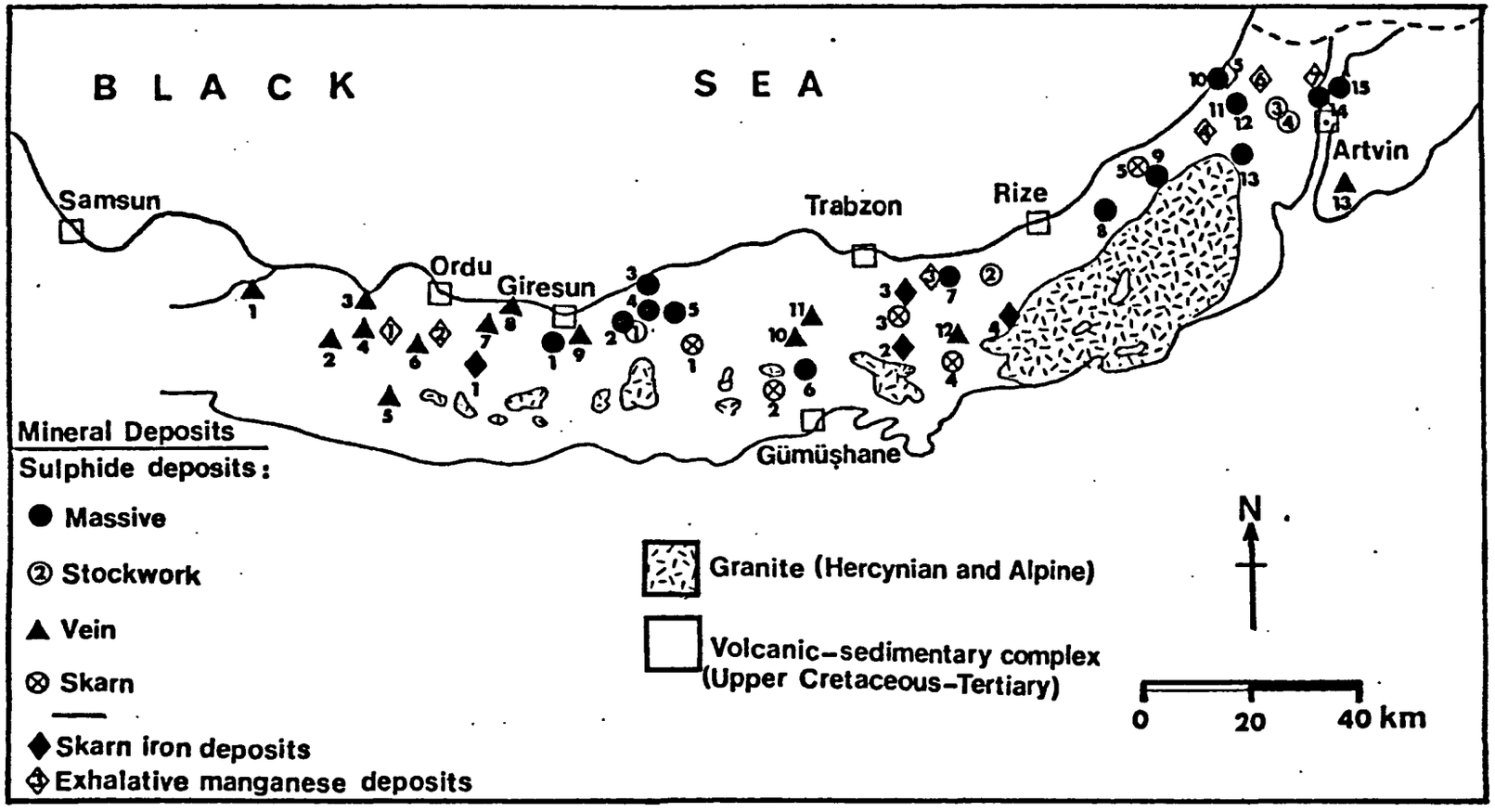


Figure 3.5 Principal mineral deposits of the Eastern Black Sea Ore Province, Turkey. (Massive sulphide deposits: 1-Akköy, 2-Lahanos, 3-Harşit-Köprübaşi, 4-Harköy-Köprübaşi, 5-Irail, 6-Zigana, 7-Kutlular, 8-Madenköy, 9-Tunca, 10-Peronit, 11-Kutonit, 12-Sivrikaya, 13-Akarşen, 14-Zinkot, 15-Kuvarshan. Stockwork sulphide deposits: 1-Kizilkaya, 2-Kotarak Dere, 3-Petek, 4-Murgul. Vein sulphide deposits: 1-Kumarli, 2-Zevli, 3-Gözevi-Basköy, 4-Arpalik, 5-Çatak, 6-Aytepe, 7-Bulancak, 8-Piraziz, 9-Dari, 10-Fol, 11-Alacadağ, 12-Derebaşi, 13-Hot. Skarn sulphide deposits: 1-Oyraca, 2-Torul, 3-Hozarak, 4-Ayman, 5-Pilarcivat. Iron deposits: 1-Çambaşi, 2-Kiran Maden, 3-Asoköy, 4-Cimildağ. Manganese deposits: 1-Geci, 2-Akoluk, 3-Pirki, 4-Abuhemşin, 5-Peronit, 6-Korucular, 7-Çavdarli).

(c) Impregnation-type sulphide deposits

(d) Vein-type sulphide deposits

(e) Exhalative-sedimentary manganese deposits

All four types of sulphide deposits are generally related to the Dacitic Series of Upper Cretaceous age. However, the vein type appear to range in age from Upper Cretaceous to Middle Tertiary. The sulphide deposits of the first three types either occur within the Upper part of the Dacitic Series (eg. Murgul), or at the top of the series, being covered by the Upper Basic Series (eg. Madenköy). The manganese deposits are of Upper Cretaceous age and occur at or near the base of the Upper Basic Series.

(a) The Volcanogenic massive sulphide deposits in the province are polymetallic, pyritic, copper-zinc-lead deposits displaying variable grade with respect to these elements. For example, the Madenköy, Lahanos, Kutlular and Tunca deposits are mainly Cu-Zn ore bodies whereas Harşit-Köprübaşi and Harköy are essentially Pb-Zn-Cu deposits. An abundance of the Cu-Zn association is characteristic of the eastern part of the Eastern Black Sea Ore Province.

The massive sulphides occur as conformable lenses having associated stockwork-impregnation zones in the footwall dacites. The massive ores are generally overlain by hematitized sedimentary pyroclastic rocks having a lateral extent exceeding the dimensions of the massive sulphide body in the order of a few hundred metres. The footwall dacites display widespread alteration halos represented by intense feldspar alteration and argillization accompanied by silicification and carbonatization. The alteration continues into the overlying rocks with a lesser intensity, often being most

prominent in the first 20 m or more of the hanging-wall pyroclastic rocks which may demonstrate argillization as well as carbonitization and hematitization (e.g. Madenköy deposit).

Thus, the massive sulphide deposits are essentially composed of two parts - massive ore which is considered to be syngenetic, and a stockwork-impregnation zone which is essentially hydrothermal and epigenetic in origin. The massive ore generally shows vertical zonation from a sphalerite-galena-chalcopyrite-rich zone at the top, through pyrite-chalcopyrite-rich zones into massive pyrite at the bottom. In most deposits, such as Lahanos (Tuğal, 1969; Leitch, 1975) and part of Madenköy, this zonation is well represented whereas in others, such as Kutular and Tunca, some of these zones may be missing.

The ores comprise varying amounts of pyrite, chalcopyrite, sphalerite, and galena as the main ore constituents, together with minor amounts of marcasite, pyrrhotite, tennantite-tetrahedrite, bournonite, enargite, electrum, and traces of Pb, Bi, Sb, Se, and Te minerals such as bismuthinite, tetradymite, and seligmannite (Table 3.3). Other minerals are quartz, barite, carbonates, and clay minerals.

The ore textures described by Tuğal (1969) and Leitch (1975) from Lahanos are in agreement with those observed by the author in Madenköy, Kutlular, Kotarak Dere, and Tunca. The top of the massive ore is characterized by fine framboidal, collomorphic and botryoidal textures generally shown by pyrite, which may be accompanied by chalcopyrite, sphalerite, and galena. This assemblage of minerals commonly forms banded collomorphic aggregates. Towards the bottom of the massive ore, and especially within the stockwork-

TABLE 3.3 Ore and gangue minerals in volcanogenic sulphide deposits in the Eastern Black Sea Ore Province, Turkey

Mineral	Theoretical formula	Massive Sulphide deposits	Stockwork deposits	Vein type deposits
Major minerals				
Pyrite	FeS_2	x	x	x
Chalcopyrite	$CuFeS_2$	x	x	x
Sphalerite	ZnS	x	x	x
Galena	PbS	x	x	x
Minor minerals				
Marcasite	FeS_2	x	x	x
Pyrrhotite	FeS	x	x	x
Bornite	Cu_5FeS_4	x	x	x
Fahlore	$(Cu,Fe)_{12}(Bi,As)_4S_{13}$	x	x	x
Enargite	Cu_3AsS_4	x	?	
Bournonite	$PbCuSbS_3$	x		x
Digenite	Cu_9S_5	x		x
Chalcocite	Cu_2S	x		x
Covellite	CuS	x		x
Rare minerals				
Seligmannite	$PbCuAsS_3$	x	?	
Bismuthinite	Bi_2S_3			
Tetradymite	$BiTe_2S$	x	?	
Hedleyite	Bi_7Te_3	x	?	
Electrum	(Au,Ag)	x	x	
Arsenopyrite	$FeAsS$			x
Betekhtinite	$Cu_{10}(Fe,Pb)S_6$			x
Idaite	Cu_3FeS_4			x
Boulangerite	$Pb_5Sb_4S_{11}$			x
Aikinite	$PbCuBiS_3$			x
Gangue minerals				
Barite	$BaSO_4$	x	x	x
Gypsum	$CaSO_4$	x	x	
Chalcedony	SiO_2	x		
Quartz	SiO_2	x	x	x
Illite-sericite	hydrous Al,Fe,Mg aluminosilicate	x	x	x
Kaolinite	$Al_2Si_2O_5(OH)_4$	x	x	?
Calcite	$CaCo_3$	x	x	x
Siderite	$FeCO_3$	x	x	x
Dolomite	$(Ca,Mg)CO_3$	x	x	x
Ankerite	$Ca(Fe,Mg,Mn)(CO_3)_2$	x	x	x

Note: x indicates occurrence of minerals

impregnation zone, this type of texture gives way to coarse, euhedral to subhedral pyrite and chalcopyrite together with zoned pyrite grains. This coarser granular pyrite and chalcopyrite generally shows cataclastic deformation. It is believed that this euhedral phase is earlier than the framboidal and collomorphic phase. A later hydrothermal phase manifests itself as chalcopyrite-sphalerite veining in the massive ore and also fills the cataclastic fractures within the pyrite-chalcopyrite euhedral phase. This vein filling phase has been interpreted by Aslaner (1971) to be the result of plastic deformation processes. Some of the massive sulphide bodies (eg. Madenköy) have associated gypsum ores which are usually interbedded with tuffaceous material.

The massive sulphide deposits of the Eastern Black Sea Ore Province, with their characteristic vertical zonation, mineralogy, texture, and minor element geochemistry, exhibit close similarities to the Japanese Kuroko deposits as discussed in the previous chapter. They were probably formed in a relatively shallow and quiet volcanic-exhalative submarine environment, being either deposited on the sea floor or within uncompacted pyroclastic material as result of the mixing of volcanic exhalations with sea water, probably towards the waning stages of the dacitic volcanism (see Chapter I).

Interesting features are apparent in the distribution of the volcanogenic massive sulphide deposits in the Eastern Black Sea Ore Province. Their tendency to occur along NE-SW zones is striking. For example, the six deposits and occurrences studied by the author fall along a linear extending from Kutlular in the southwest to Murgul in the northeast.

These zones are believed to be lineaments of deep structural significance which have been active during the whole of the Alpine Orogeny, thus controlling the location of dacitic magmatic activity and the distribution of the associated ore deposits.

The distribution and genesis of the Black Sea sulphide deposits has previously been discussed by a number of workers (Tuğal, 1969; Tuğal and Phillips, 1971; Hamamcioğlu and Sawa, 1971; Vujanovic, 1974; Popovic, 1975). It is believed by some that these deposits are hydrothermal in origin and are related to the Tertiary granitic intrusions. The occurrence of these deposits along linear zones led Popovic (1975) to consider these linear features to be thrust zones and channel-ways for hydrothermal solutions from granitic intrusive processes. He has proposed three such zones: a) Arhavi-Sivrikaya-Peronit thrust fault, b) Rize-Pilarcivat-Kutonit-Pehlivan köy-Maradit thrust fault, and c) Madenköy-Tunca-Akarşen thrust fault.

The well known massive sulphide deposits in this province from west to east are - the Akköy, Harşit-Köprübaşi, Harköy, Israil, Yarmaden, Hasköy and Lahanos deposits in the province of Giresun; the Kutlular, KOtarak Dere, and Baştimar deposits in the province of Trabzon; the Madenköy and Tunca deposits in the province of Rize; and the Peronit, Kutonit, Akarşen, Zinkot, Irsa, and Kuvarshan in the province of Artvin.

(b) Volcanogenic stockwork sulphide deposits commonly occur as an intricate network of veins and veinlets, the thickness of which vary from a few mm (e.g. Sirtköy) to 15 cm (e.g. Murgul). These stockwork deposits are invariably associated with the Dacitic series, which is silicified in

the proximity of the mineralization. The ore minerals are mainly pyrite and chalcopyrite with minor to trace amounts of pyrrhotite, sphalerite, galena, tetrahedrite-tennantite, and traces of telluride minerals, usually occurring as small inclusions (Table 3.3). The gangue minerals are quartz, barite, carbonates, and clay minerals. The mineralogy and textures of these deposits are similar to the stockwork and impregnation zones of the massive sulphides. Thus many of the stockwork sulphide deposits presently exposed at the surface may represent the stockwork zones of massive sulphides which have been removed by erosion or are concealed beneath the flanks of the overlying cover rocks. The best example of this is seen at the Kotarak Dere and Kizilkaya (near Giresun) where a very small amount of massive pyrite ore remains above the Stockwork zone.

Economic stockwork deposits are important for their copper, pyrite, and gold (eg. Anayatak, Çakmakkaya, and Çarkbaşi in the Murgul area; Kizilkaya near Espiye; Kotarak Dere near Of). A large number of uneconomic occurrences (eg. Sirtköy) occur in the region; in these the principle mineral is pyrite occurring as thin veinlets with minor amounts of chalcopyrite.

(c) Impregnation - type sulphide mineralizations are uneconomic and widely distributed in the Eastern Black Sea Ore Province. They occur as sulphide impregnations in the Dacitic Series. Pyrite is generally the only ore mineral, but occasionally traces of chalcopyrite and galena may also be present. For example, the Sarisu occurrence is pyrite-bearing only and displays similar hydrothermal alteration features to those observed in the footwall rocks of the

Madenköy deposit. Similar occurrences have been reported by Kawada and Engin (1972) in the Beyazsu area of the Çayeli district, and by Sawamura and Yilmaz (1971) in the Sürmene district.

(d) The vein-type sulphide deposits are polymetallic fissure fillings with ore minerals comprising galena, bournonite, tennantite-tetrahedrite, aikinite, pyrite, chalcopyrite, sphalerite, idaite, digenite, boulangerite, betekhtinite, arsenopyrite, and marcasite (Table 3.3). The gangue minerals are quartz, barite, calcite, and dolomite. These deposits are essentially subvolcanic hydrothermal mineralizations occurring generally in northwest trending fissures and fractures within the altered dacites, andesites, and pyroclastics. The age of these deposits appears to be variable from Upper Cretaceous to Middle Tertiary. The subvolcanic hydrothermal vein type deposits of the Sürmene district occur in the dacitic series within northeast-trending fracture zones (Sawamura and Yilmaz, 1971), whereas the veins of Bulancak have been genetically related to the Middle Eocene igneous activity. The latter resemble the Neogene subvolcanic hydrothermal veins of Japan (Akinci, 1974). The vein-type sulphide deposit of Piraziz in the province of Giresun occurs in fractures of andesitic breccia and is marked by wall rock alteration, mainly silicification and argillization (Aslaner and Çağatay, 1973).

These deposits show a wide distribution in the western part of the Eastern Black Sea Ore Province. The sulphide deposits in this group are Kumarli, Arpalik, Karakiraz, and Gözevi-Başköy in the province of Ordu; Kuşluvan, Dari, and Dereköy in the province of Giresun; Derebaşi in the province

of Trabzon; and Alacadağ and Fol in the province of Gümüşhane.

(e) Exhalative-sedimentary manganese deposits in this province are of the bedded nodular type. They are mainly associated with dacitic and andesitic tuffs of Upper Cretaceous age and are generally small in size, reserves being around 1000 t or less. Some of the manganese deposits have been worked in the past. In the Sürmene district the manganese deposits occur either at or near the base of the Upper Basic Series (Sawamura and Yilmaz, 1971). At Peronit, near Arhavi, the manganese ores occur as nodules within silicified dacitic tuffs, being covered by purple dacitic tuffs (Kräeff, 1963b). Other manganese deposits in the region include Geci, Akoluk, and Ilişar in the province of Ordu; Pirki, Galyan, and Gazlik in the province of Trabzon; Yukari Oturak and Abuhemşin in the province of Rize; and Korucular and Çavdarli in the province of Artvin (Gümüş, 1970; Uzkut, 1971).

3.8.2.2 Deposits Genetically Associated with Eocene-Oligocene Granitic and Granodioritic Intrusions

The deposits in this group comprise:

(a) Skarn-type deposits, and

(b) Copper-molybdenum vein-type occurrences.

Porphyry copper deposits have not yet been found in the region although a few showings are present in and around the large Tatos batholith. An Exploration program by M.T.A. is still in progress having as its aim the discovery of porphyry-type copper mineralization.

(a) Skarn-type deposits occur at the contacts between Tertiary quartz porphyries or granites and limestone, basalt,

or basic country rocks. Two phases of hydrothermal mineralization are present in these deposits (Vujanovic, 1974). The first is marked by the formation of contact silicates such as actinolite, diopside, garnet, epidote, and chlorite, together with magnetite and hematite. The second phase is characterized by the formation of sulphide ores consisting of pyrite, chalcopyrite, and minor sphalerite and galena, with a gangue of quartz and calcite. Where a low sulphur fugacity has prevailed hematite-magnetite bodies formed rather than sulphide bodies.

The skarn-type sulphide deposits are generally small and uneconomic, the most important being, Torul in the province of Gümüşhane; Hazarak, Ayman, and Kestel in the province of Trabzon; and Pilargilat near Ardeşen.

The iron deposits occur as lenses of hematite-magnetite and are usually small in size. The iron deposits in the region include: Çambaşi in the province of Ordu; Kiran Maden in the province of Giresun; Asoköy and Küsmer Yayla in the province of Trabzon; and Cimildağ in the province of Rize (Gümüş, 1970).

(b) Copper-molybdenum vein-type occurrences are closely associated with the granites. Popovic (1975) proposes a copper-molybdenum-zinc zone immediately surrounding the Tatos batholith. Copper-molybdenum mineralization of this type occurs at Kösedaği, Tiryal Dağ, Ispir, and Gümüşhane.

CHAPTER 4

LOCAL GEOLOGY AND MINERALIZATION

4.1 INTRODUCTION

The main geological features of the various types of volcanogenic sulphide mineralizations in the Eastern Black Sea region are summarized in Table 4.1. The deposits studied by the author comprise the Madenköy, Kutlular and Tunca massive sulphide deposits; the Kotarak Dere and Murgul pyritic copper stockwork deposits; the slightly mineralized Sirtköy stockwork-impregnation zone; and the Sarisu barren pyrite impregnation occurrence. The Murgul deposit was not, however, studied in detail mainly because of severe contamination problems in the area.

All the mineralized bodies are associated with the Dacitic Series which has been exposed in many areas by block faulting. For example, the Madenköy, and Kutlular deposits are concealed massive sulphide orebodies with exposed stockwork-impregnation zones and the Tunca massive sulphide deposit sub-outcrops on the edge of the down-faulted part of a dacite window.

Diamond drilling programs have been carried out by the M.T.A. at the Madenköy, Kutlular, Kotarak Dere, Tunca, and Murgul deposits; no drilling has been done at the Sirtköy and Sarisu occurrences (Figure 4.1).

Detailed descriptions of the geology and ore mineralogy of these mineralizations are given below. The chemistry of the ores is dealt with in Chapter 6, and the hydrothermal alteration and chemistry of the host rocks are described in Chapter 8.

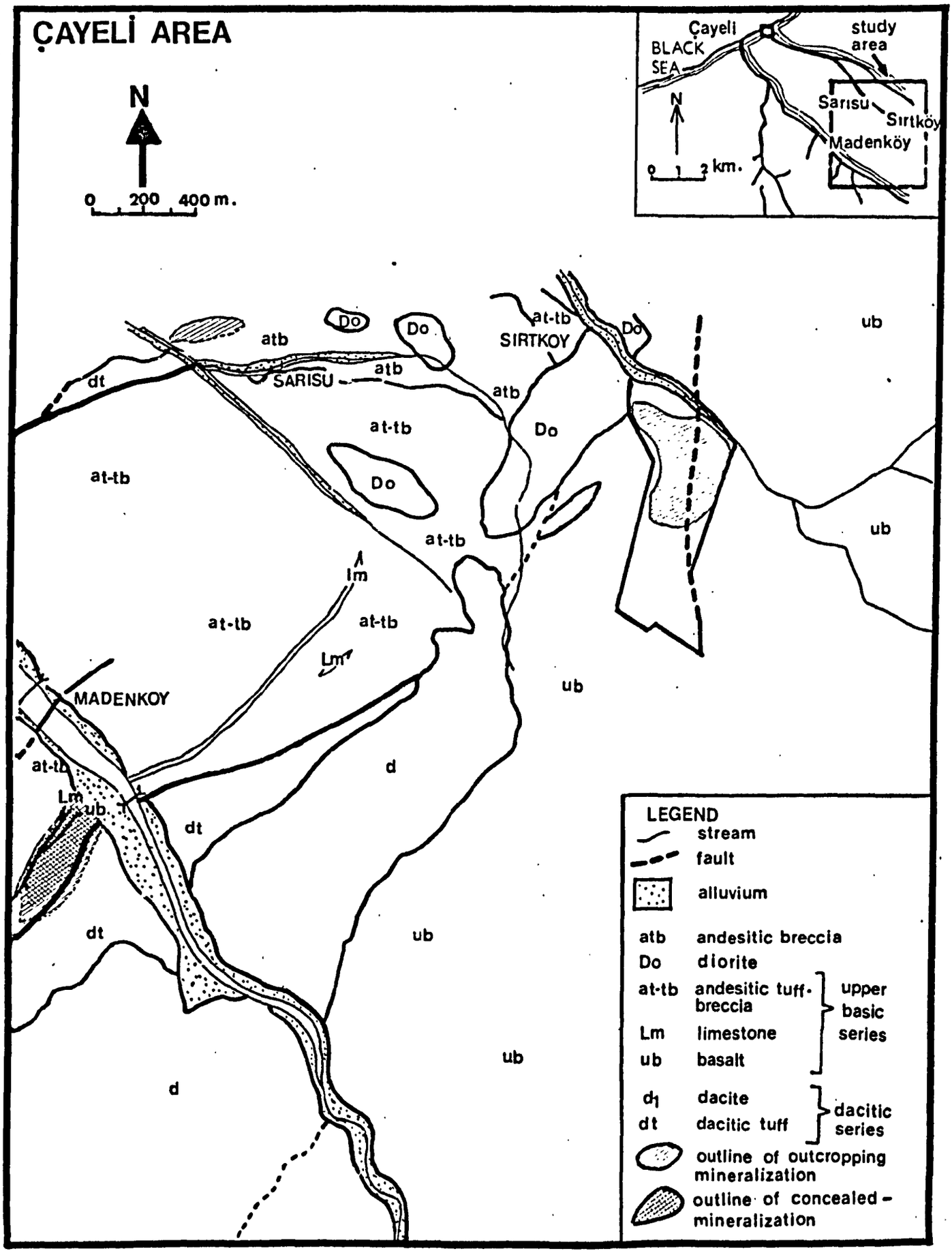


Figure 4.1 Geology of Çayeli area (revised and simplified after Kawada and Şarman, 1973).

Table 4.1 VOLCANOGENIC SULPHIDE MINERALIZATION, EASTERN BLACK SEA PROVINCE, TURKEY.

DEPOSIT (type)	RESERVES(in tons) and GRADE (in %)	MASSIVE ORE	FOOTWALL ZONE	HANGING-WALL ZONE	REMARKS
MADENKOY (Massive)	20m;4%Zn,3%Cu (Ag+Au)	Concealed;pyrite, sphalerite, chalcopyrite,minor galena,gypsum,barite	Post-ore andesite and chalcopyrite-pyrite stockwork and pyritic impregnation zone in dacitic tuffs	Hematitized pumice tuffs overlain by basalts and andesitic tuff breccias	Undisturbed;part of stockwork-impregnation zone exposed.
KUTLULAR (Massive)	1.5m;2.2%Cu, 0.4m;1.5%Zn	Concealed;pyrite, chalcopyrite, sphalerite,minor galena,barite.	Diabase and chalcopyrite-pyrite stockwork and pyrite impregnation zones in dacitic tuffs	Mineralized dacitic tuff breccia overlain by basalts.	Undisturbed;stockwork and impregnation zones exposed;post-ore hydrothermal activity.
TUNCA (Massive)	0.3m;1.5%Cu,1.0% Zn	Exposed;pyrite, chalcopyrite, sphalerite,galena.	Same as Madenkoy;no andesites.	Hematitized porphyritic dacites overlain by basalts.	Stockwork,impregnation, and massive ore zones exposed by steeply dipping fault zone.
KOTARAK DERE (Stockwork)	2.0m;0.4%Cu, 1.0%Zn	Small remnant of massive ore.	Chalcopyrite-pyrite stockwork (minor sphalerite) and pyritic impregnation zones in dacites.	Basalts	Most of stockwork and impregnation zones exposed.
MURGUL (Stockwork)	47m;1.4%Cu	Not formed	Chalcopyrite-pyrite-stockwork with minor sphalerite, galena,and barite in dacitic tuffs;peripheral gypsum.	Hematitized dacites and tuffs overlain by andesites, agglomerate,sandstone, limestone	Extensive mining activity since Medieval time.
SITRKOY (Stockwork)		Not formed	Pyrite and minor chalcopyrite stockwork (0.2% Cu) in porphyritic dacite.	Basalts	Basalts are locally pyritized.
SARISU (Pyrite impregnation)		Not formed	Pyrite impregnation zone in dacites.	Basalts and andesitic tuff breccias.	No associated stockwork.

4.2 MADENKÖY (1) AREA

4.2.1 Previous Work

Geological work in the Cayeli area was begun in 1940 by Atabek, and pursued later by De Geoffroy (1960). The Madenköy deposit has been known for a long time; closed and demolished galeries suggest that it was worked in Medieval times. Detailed exploration work in the area was initiated by M.T.A. in 1967. Mapping of the Madenköy, Sirtköy, Sarisu, and surrounding areas was done by Kawada and Sarman (1973) at a 1/10,000 scale. Detailed geological mapping of the Madenköy (I) deposit was carried out by Altun (1972) at a 1/1000 scale. Between 1967 and 1975, 45 diamond drill-holes, amounting to about 12,000 m of drill-core, were drilled over the deposit. On the bases of the drill-core data Nebioğlu (1975) has produced a revised geological interpretation of the Madenköy mine area.

4.2.2 Geology of Madenköy (I) Area

The stratigraphy in the Cayeli Area has been summarized in Table 3.1, and the distribution of the various rock types is given in Figure 4.1. In the vicinity of the Madenköy deposit (Figure 4.2) the following formations are observed (in stratigraphically descending order):

4. Alluvium
3. Basic Dykes (andesitic dykes)
2. Upper Basic Series (pumice tuffs, basalts, andesitic breccia, intercalated limestones and sandstones)
1. Dacitic Series (dacite and dacitic pyroclastics)

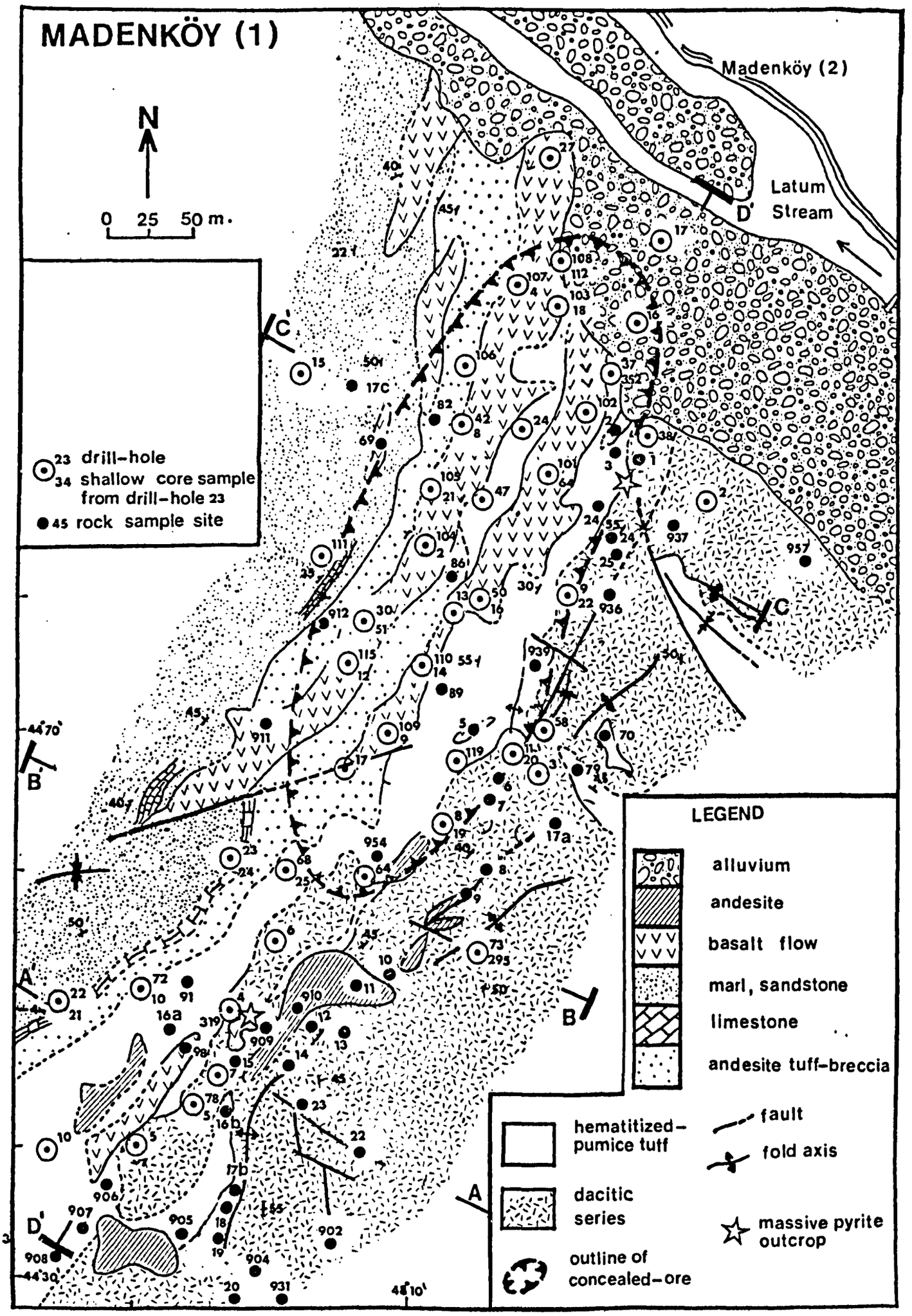


Figure 4.2 Geology of Madenköy (1) area with rock sample and drill-hole locations (geology modified after Nebioğlu, 1975).

The existence of volcanic breccias and pumice tuffs in this area strongly suggests the presence of a nearby volcanic centre.

In the Madenköy area there was an important orogenic event at the end of the dacitic vulcanism that resulted in the folding of the Dacitic Series. This series, as a result, generally dips to the NE at about 45°. There is also a distinct unconformity developed between the Dacitic series and the northwesterly dipping Upper Basic Series (Figure 4.3). The latter series also plunges towards the NE (Figure 4.4). Determining whether this plunge is due to an original submarine slope or to a later tectonic tilting requires further detailed structural analyses. Nevertheless, the plunge and the observed lines of evidence outlined below suggest the presence of a volcanic centre to the SW of the Madenköy area. Evidence for this is based on: (a) thickening of the pumice tuff units towards the SW of the Madenköy map area; (b) coarsening of the pumice fragments towards the SW; and (c) increase in the intensity and extent of the hydrothermal alteration from NE to SW (see Chapter 8). These features suggest that this volcanic centre is the source of the Dacitic and Upper Basic Series as well as the sulphide ores.

Faults with NNE and NW trends occur in the Madenköy area; these are steeply dipping and usually reverse faults.

A description of the lithologies occurring in the Madenköy area follows.

4.2.2.1 Dacitic Series

The Dacitic Series in the Madenköy area is composed mainly of dacitic tuffs and lavas. However, in drill cores 4,

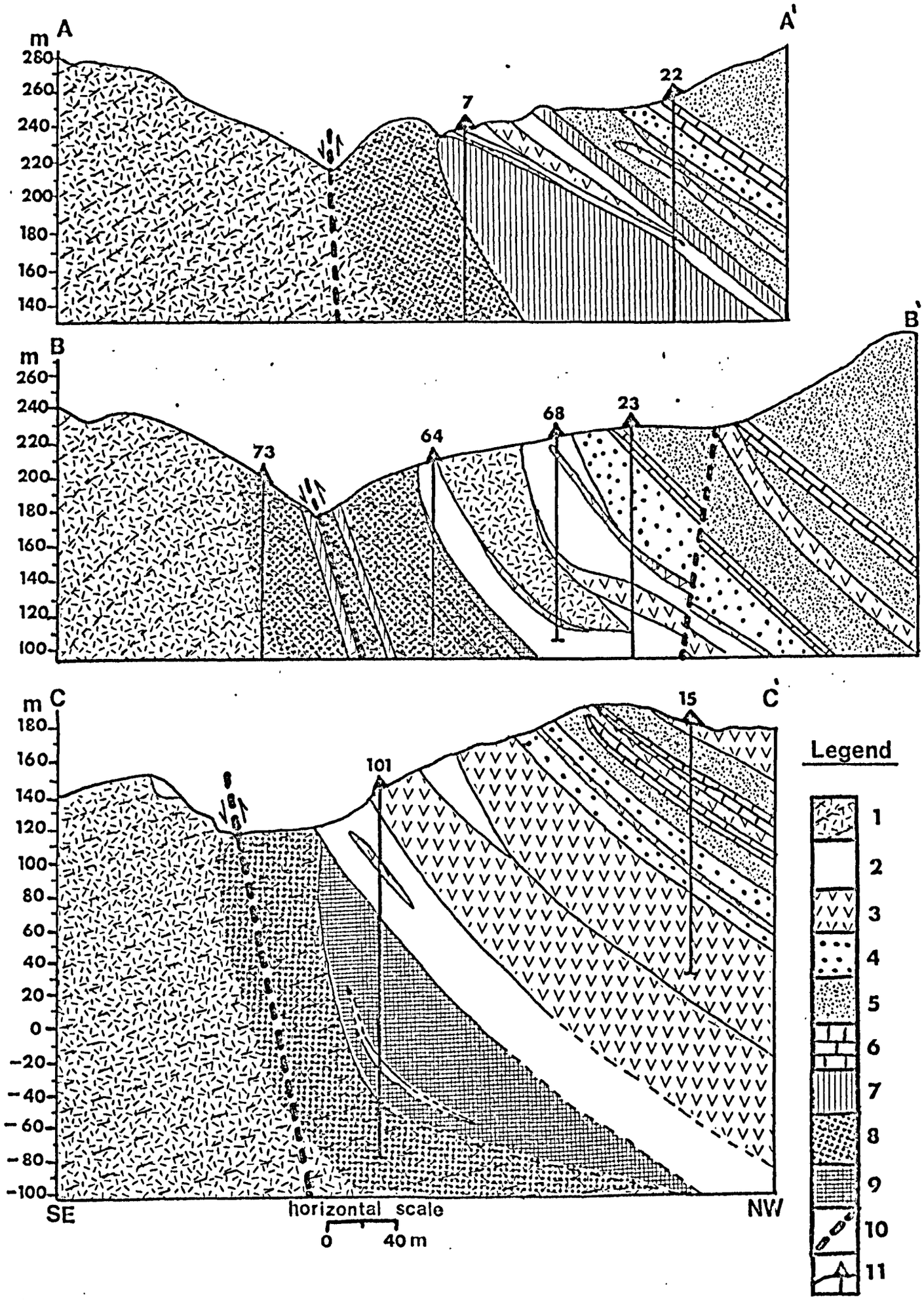


Figure 4.3 Geological cross sections, Madenköy massive sulphide deposit (1- Dacitic Series, 2- Pumice Tuffs, 3- Basalts, 4- Andesitic Tuff-breccia, 5- Sandstone, 6- Limestone, 7- Andesite, 8- Stockwork-impregnation zone, 9- Massive ore, 10- Fault, 11- Drilling site).

For locations of cross sections see Figure 4.2. Vertical scale is equal to horizontal scale.

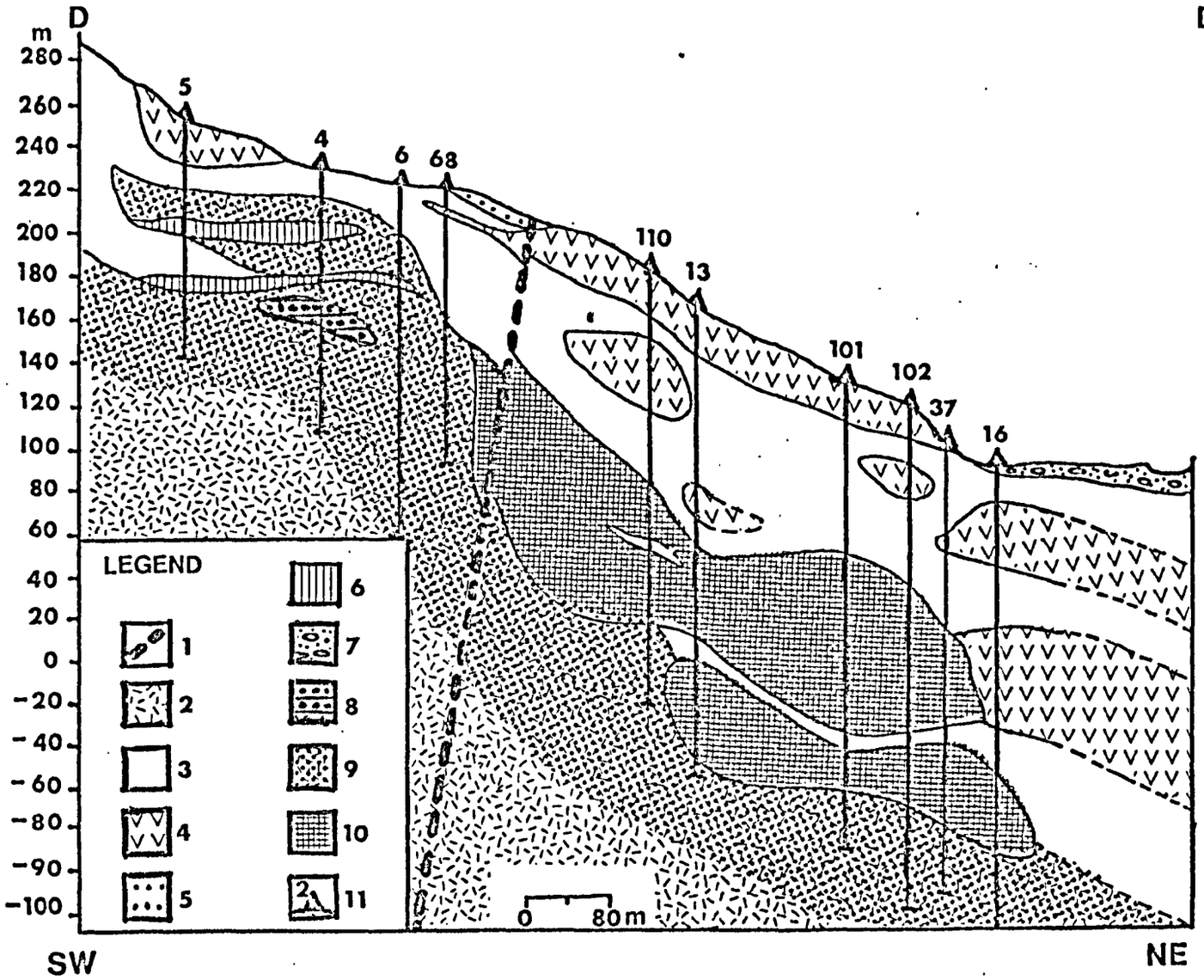


Figure 4.4 Geological cross section along strike, Madenköy massive sulphide deposit (1- Fault, 2- Dacitic Series, 3- Pumice Tuffs, 4- Basalts, 5- Andesite Tuff-breccia, 6- Andesite, 7- Sandstone, 8- Gypsum ore, 9- Stockwork-impregnation zone, 10- Massive ore, 11- Drilling site). For location of cross section see Figure 4.2. Vertical scale is twice the horizontal scale.

30, and 110 which have been sampled and studied by the author, there is evidence of the presence of a shallow intrusive dacite body. The hydrothermal alteration is so intense, however, that the intrusive character of the rock is only suggested by the relict textural relationships. This rock has a porphyritic texture with large quartz phenocrysts. The feldspars are completely altered. The alteration consists mainly of argillization, carbonitization, and silicification. The carbonates are dolomite and siderite with well developed large crystals. There is considerable sericite and kaolinite after alteration of the feldspars. The matrix consists mainly of clay minerals and fine-grained quartz. The dacite underlies the ore or occurs under altered dacitic tuffs. It usually contains some well developed pyrite crystals.

The dacitic tuffs are also hydrothermally altered in the vicinity of the Madenköy massive sulphide deposit. The hydrothermal alteration near the massive ore body is generally in the form of sericitization (including illite) kaolinitization, carbonitization, and some silicification. The colour of the tuffs may be yellow, gray, or white according to the type of alteration. Red to purple colours due to hematitization are also observed to the south of the detailed survey area (Figure 4.2). These rocks consist of quartz phenocrysts and phenocrysts of andesine to oligoclase composition in a fine matrix of the same composition. Pumice fragments are also common in some of the dacitic tuff samples. In the vicinity of the ore deposit there is an extensive silicification and some pyrite impregnation of these rocks; this is represented by fine hydrothermal quartz and globular aggregates of pyrite respectively. The feldspars of the dacitic tuffs are altered

to kaolinite and illite-sericite clays with some carbonates, and the quartz phenocrysts are usually corroded. Relatively less altered tuffs occur to the north east of the ore deposit, near the Latum Bridge in Madenköy (II) area. These tuffs present good flow structures and contain plagioclase and quartz phenocrysts in a fine-grained matrix consisting of quartz, plagioclase, and clays of montmorillonite and kaolinite.

In the central part of the Madenköy mine area (Figure 4.2) dacitic tuffs are tectonically brecciated. This can be especially well observed in road cuttings where a strong silicification and fine pyrite dissemination and veining can be seen.

In places the dacitic tuffs demonstrate good laminations and bedding, and are intercalated with pelitic tuffs as observed in drill-hole 4.

4.2.2.2 Upper Basic Series

This formation includes the pumice tuffs, andesitic tuff-breccias, and a marl-sandstone unit which is interbedded with limestone. All the above mentioned pyroclastic rocks are intercalated with at least four basalt flows in the area.

4.2.2.2.1 Pumice Tuffs

These rocks have been studied by the author in some detail because of their close association with the Madenköy deposit. Their occurrence and petrology are described below. For a detailed X-ray diffraction study of their hydrothermal alteration and chemistry the reader is referred to Chapter 8.

The pumice tuffs unconformably overlie the Dacitic Series and appear to occur at two stratigraphic horizons (Figures 4.3 and 4.4). Each of the pumice tuff units varies in thickness from 25 m to 40 m; their thicknesses increases towards the SW of the map area (Figure 4.2). The massive ore is almost always overlain and sometimes intercalated with the pumice tuffs, the boundaries between the two being sharp. However, the pumice tuffs extend far beyond the limits of the sulphide deposit along the general strike of the rocks. They are intercalated with friable, gray to brown tuffaceous sandstones which are in places impregnated with fine sulphide grains. Occasionally the pumice tuffs also possess red limestone intercalations which are not laterally continuous.

The pumice tuffs demonstrate a colour variation from violet to greenish gray. However, they usually have a violet to brick red colour in the vicinity of the ore body. As a result of this colouring they have previously been called violet tuffs (Altun, 1972).

Megascopically these rocks are soft, finely foliated, and banded. They contain euhedral to subhedral quartz crystals and pumice fragments in a fine-grained quartz and clay-rich matrix. In the southwest of the map area these tuffs demonstrate fine, alternating hematite and quartz-carbonate-rich layers with a thickness of about 1 mm. This greenish grey and brown banding and fine foliation is particularly characteristic of the pumice tuffs in the Madenköy area. In places one colour may dominate over another and the whole rock becomes either greenish-gray or violet to reddish-brown in colour. In drill holes, such as 101, 106, 108, and 110, it

is possible to see the gradual passage between the two. Quartz and carbonate veining are common in hand specimens of the pumice tuffs.

Thin section examination of the pumice tuffs reveals that they consist of quartz, altered feldspar crystals, and variable sized altered pumice fragments in a fine quartz, carbonate, and clay matrix: These pumice fragments are oriented parallel to the laminations and banding, and occasionally show microfolding. The hematite occurs as very fine amorphous grains, forming hematite-rich layers, and in places fills microfractures. Manganese oxides and occasionally manganese carbonate (rhodochrosite) may also be present; the pumice tuffs in drill-hole 117 are considerably enriched in manganese (T.Y. Nebioglu, pers. comm., 1975). The pumice tuffs may also be impregnated with various sulphides such as pyrite, sphalerite, galena, and sulphosalts. In addition native copper and specularite have been observed (T.Y. Nebioglu, pers. comm., 1975).

The pumice tuffs display a strong hydrothermal alteration. The feldspars and pumice fragments are usually completely altered leaving ghost crystal outlines and structures generally filled with clay minerals. The matrix contains a high proportion of carbonate in the form of dolomite. Dolomite veining is also a common phenomenon. Silicification is also widespread, being represented by fine, mozaic textures of hydrothermal quartz. This secondary quartz replaces some feldspars and primary quartz crystals and occasionally occurs as veins. The corrosion of primary quartz, and the deposition of mozaic textured, fine hydrothermal quartz, are well demonstrated in some thin sections of these rocks.

In conclusion, the nature of the occurrence and petrochemistry (see also Chapter 8) of the pumice tuffs strongly suggests a pyroclastic-sedimentary origin for these rocks. At least part of the hematitization was contemporaneous with the sedimentary bedding. Later ascending iron-rich solutions resulted in hematite enrichment and veining, the process taking place towards the end of the sulphide deposition in a sulphur deficient, oxidizing environment. During the deposition of these rocks the environment was alkaline; the pH probably being between 8 and 9.

4.2.2.2.2 Basalt Flows

These rocks are intercalated within the pumice tuffs, andesite tuff-breccias, and the limestone-marl-sandstone series. They are fine-grained, dark green rocks with pronounced flow and onion-shaped exfoliation structures. Thin section studies show that they have an ophitic texture and contain amygdales that are filled with calcite. Phenocrysts of augite and olivine are altered, and the feldspars which are of labradorite composition are altered to clay minerals around the grain boundaries. Calcite, and occasionally dolomite veinlets are common especially in the lower members of the basalt flow units. The matrix consists of needle shaped plagioclase microlites and altered pyroxenes.

A plot of the ratio FeO (total Fe expressed as FeO) /MgO against SiO_2 content for 40 basalt samples from the Madenköy area is shown in Figure 4.5. The results indicate considerable variation from calc-alkaline to tholeiitic composition for these rocks. Similar results were obtained by Akinci (1974) in the Giresun area.

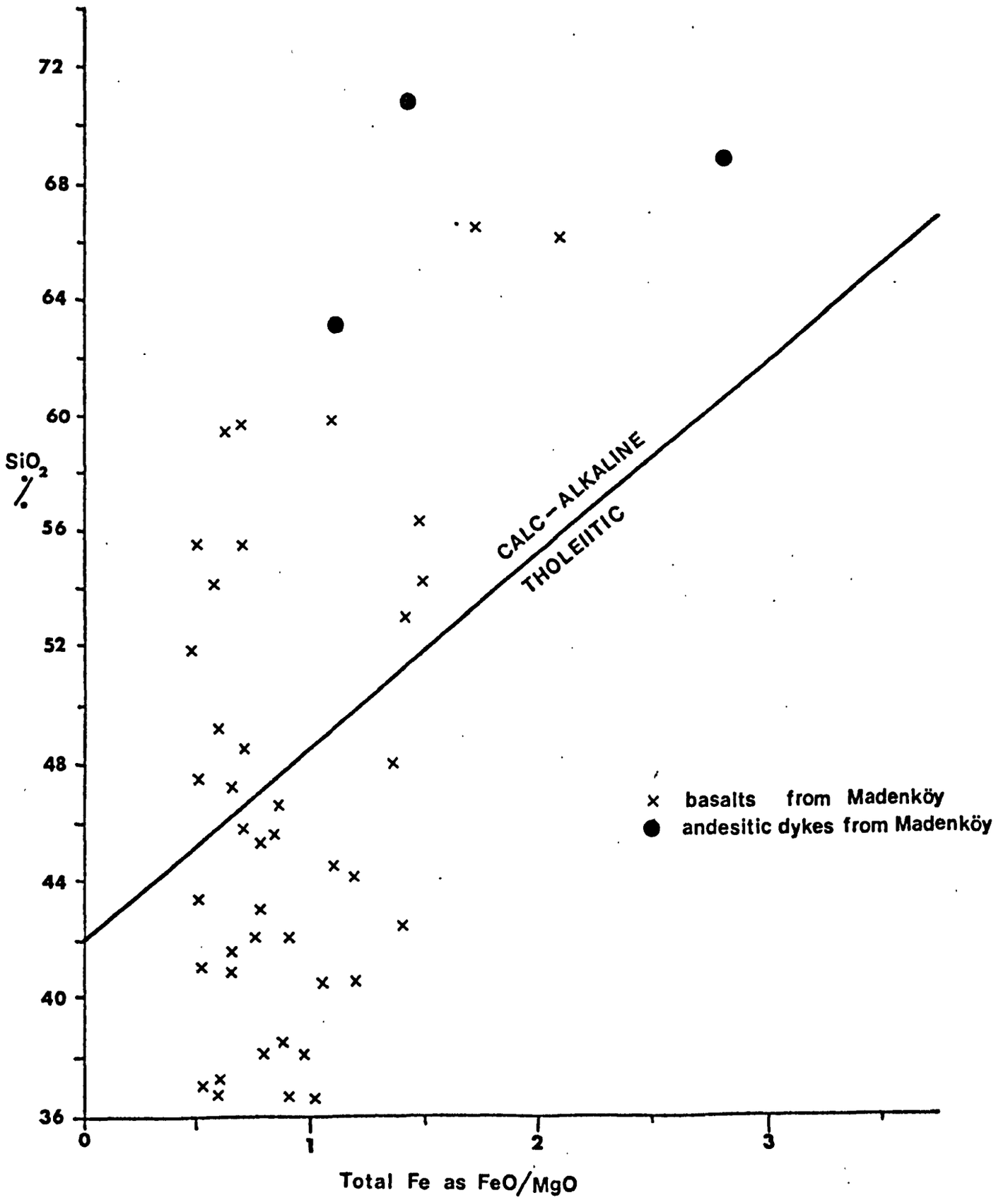


Figure 4.5 Plot of FeO (total Fe expressed as FeO)/MgO vs. SiO_2 for Madenköy basalts and andesitic dykes on variation diagram of Miyashiro (1974).

4.2.2.2.3 Andesitic Tuff-Breccias

The andesitic tuff-breccias are green in colour and contain angular and subrounded pebbles of dacite, andesite, and basalt. The groundmass is fine grained and has been argillitized. Although the green colour has been attributed to chloritization, microscopic and X-ray powder diffraction studies did not reveal the presence of chlorite. Instead, the clays in the matrix were found to be mainly montmorillinite with some kaolinite. These rocks also contain a significant amount of calcite, and when in contact with the hematitized pumice tuffs, the lower parts of the breccia are usually hematitized.

4.2.2.2.4 Limestone - Marl - Sandstone Series

The limestone - marl - sandstone series lies unconformably on the andesite tuff-breccias and pumice tuffs. The limestone can be classified as a marly limestone varying in colour from red to gray and containing abundant Globotruncana and Globogerina fossils. It has been dated as Senonian (Upper Cretaceous) on the basis of these fossils (Altun, 1972).

The sandstone is fine-grained and arkosic in composition.

4.2.2.3 Basic Dykes

These dykes are of andesitic composition and of Miocene age. In the Madenköy (I) area they are generally fresh in appearance, containing occasional calcite veinlets, and large hornblende phenocrysts and amygdales filled with calcite in places. Columnar jointing is a distinctive feature. The variation in the FeO (total Fe expressed as FeO) with SiO_2 content for a limited number of samples suggests a calc-alkaline affinity (Figure 4.5).

4.2.3 Mineralization

4.2.3.1 Occurrence

The Madenköy sulphide deposit is a pyritic, Zn-Cu volcanogenic massive sulphide deposit associated with dacitic volcanism. It occurs in the uppermost levels of the Dacitic Series and is covered by the Upper Basic Series. The mineralization took place during the final stages of the Dacitic stage of volcanism and consists of two parts:

(a) a massive ore body which is totally under rocks of the Upper Basic Series, and

(b) stockwork and impregnation sulphide zones which are partly exposed.

The massive ore is lens-shaped, dips at about 50^{o} NNW (Figure 4.3), and occurs as a conformable body underlying the pumice tuffs. The length of the massive ore along its strike is about 420 m (Figure 4.4). The limit of its western extension is not known, and deep drilling is required to outline the western boundary. The massive ore thickens in a NNW direction, reaching vertical thicknesses of 106 and 84 m in drill-holes 30 and 105 respectively. In a NNW-SSE direction its surface projection is at least 180 m wide.

To the SW of the massive ore body a 15 m thick section of gypsum ore was observed in drill-hole 4 (Figure 4.4). The gypsum is interbedded with sedimentary dacitic material.

The stockwork and impregnation zones, occur within the upper levels of the Dacitic Series and have a combined lateral width of about 100 m in an easterly direction from the massive ore and a much wider lateral distribution to the south of some 350 m as evidenced from drill-hole logs.

The stockwork zone which extends for approximately 20 m beneath the massive ore consists of veins, mainly of chalcopyrite and pyrite, having a thickness of about 1 cm with occasional local thickening. This zone passes both vertically and laterally into the more extensive impregnation zone.

4.2.3.2 Ore Mineralogy

Vertical core sections of the Madenköy massive sulphide deposit were studied in drill-holes 30, 37, 101, 105, 106, 108, and 110 (see Figure 4.2 for locations). Megascopic examination of the massive sulphide ore generally suggests a division of the massive ore into a sphalerite-chalcopyrite-pyrite-rich black ore and a chalcopyrite-pyrite-rich yellow ore, a zoning similar to that observed in the Japanese Kuroko deposits, with the exception that the Madenköy black ore is poor in Pb and is more like the sub-black ore of the Japanese deposits. In drill-holes 37, 101, and 110 the top of the massive sulphide sections are represented by black-ore which is friable, fine-grained and rich in sphalerite and barite; most of the galena present is concentrated in this zone. Chalcopyrite and pyrite also occur in major quantities as "blebs" and pebbles giving the ore horizon a brecciated appearance; chalcopyrite veining is also a common feature of this zone. This type of ore gradually passes into a yellow, fine-grained, friable ore consisting mainly of pyrite and chalcopyrite with some bornite. Sphalerite is always present and may exist in considerable quantities at some levels, occurring mainly as veins associated with chalcopyrite. The deposition of yellow ore appears to have been interrupted in

some core sections (e.g. 101 and 110) by deposition of pumice tuffs and gray to brown tuffaceous sandstone layers which are often disseminated with sulphides.

In drill-holes 30, 105, and 106 the massive ore section begins with a predominantly pyrite-chalcopyrite mineralogy. Sphalerite is, however, a major constituent and at some levels increases considerably in quantity. Since these three drill-holes cut the western part of the massive sulphide ore it may be presumed that the black ore is confined only to the eastern and central parts of the ore body.

The yellow ore zone generally passes into a pyrite, chalcopyrite and quartz-rich stockwork zone which in turn grades into a pyrite-rich impregnation zone. The contacts between the last two zones are gradational and, therefore, difficult to place.

The distinction between the black and yellow ores is also by no means easy and simple. This becomes especially apparent when the sulphide samples are studied microscopically. Polished sections of ore specimens from drill-holes 101 and 110 were examined under the microscope to determine the detailed mineralogy and textural relationships which could shed light on the genesis of the deposit. The ore minerals present are pyrite, sphalerite, chalcopyrite with minor amounts of galena, bornite, and tetrahedrite. The gangue minerals are barite and quartz. Specimens from the massive part of the ore body show the pyrite, chalcopyrite, sphalerite, bornite, and galena to have a colloform texture (Plates 4.1(a), (b), (c), and (d)). The colloidal intergrowth between these minerals, giving globules and spheroidal aggregates, is typical of ore at the top of the massive sulphide body. It is

this fine intergrowth that makes the distinction between the black ore and yellow ore difficult under the microscope as well as causing considerable technological problems in concentrating these ores.

The pyrite occurs as either collomorphic intergrowths and spheroids or euhedral to subhedral crystals. In places subhedral crystals have cataclastic texture which becomes more common towards the base of the massive ore and continues into the stockwork zone (Plate 4.1(f) and 4.1(g)). In some sections the cataclastic pyrite exhibits magnetite, ilmenite, and hematite in its fractures and may contain pyrrhotite and rutile inclusions (Plate 4.1(h)). Pyrite at the top of the massive ore commonly contains marcasite which becomes rare in the stockwork zone. The pyrite also displays a zonation, suggesting at least two stages of growth (Plate 4.1(g)).

Chalcopyrite and sphalerite exhibit either a collomorphic texture or occur as fracture fillings and veinlets (Plate 4.1(e) and 4.1(f)). Sphalerite occasionally has a cataclastic texture and may contain tetrahedrite and bornite inclusions in places. The vein-type sphalerite commonly contains chalcopyrite exsolutions. In the pyrite-rich yellow ore and stockwork ore the chalcopyrite contains rare inclusions of native gold.

Relatively small amounts of galena occur in the upper levels of the massive ore body. It has as collomorphic as well as euhedral to subhedral texture and is closely associated with sphalerite.

Bornite is usually present in minor amounts forming colloidal growth structures with pyrite, chalcopyrite, and

PLATE 4.1

Ore Textures, Madenköy massive sulphide deposit

Plate 4.1(a) Collomorphic intergrowth of pyrite and chalcopyrite. Top of orebody; drill-hole 110 (Specimen KC-5 -220X-Oil).

Plate 4.1(b) Collomorphic banding and collomorphic spherulites of pyrite, chalcopyrite, and bornite. Note the cataclastic pyrite on the left hand side of the photomicrograph. Top of orebody; drill-hole 110 (Specimen KC-8 -220X-Oil).

Plate 4.1(c) Collomorphic spherulites of pyrite and chalcopyrite, together with sphalerite and galena. Note the porous and vuggy nature of the sphalerite. Top of orebody; drill-hole 110 (Specimen KC-5 -220X-Oil).

Plate 4.1(d) Sphalerite-chalcopyrite-pyrite-bornite collomorphic banding. A few euhedral pyrite crystals can also be seen. Top of orebody; drill-hole 110 (Specimen KC-8 -110X-Air).

Plate 4.1(e) Veinlets of chalcopyrite infilling fractures in pyrite, probably a 'radial bomb' texture. Top of orebody; drill-hole 110 (Specimen KC-8 -220X-Oil).

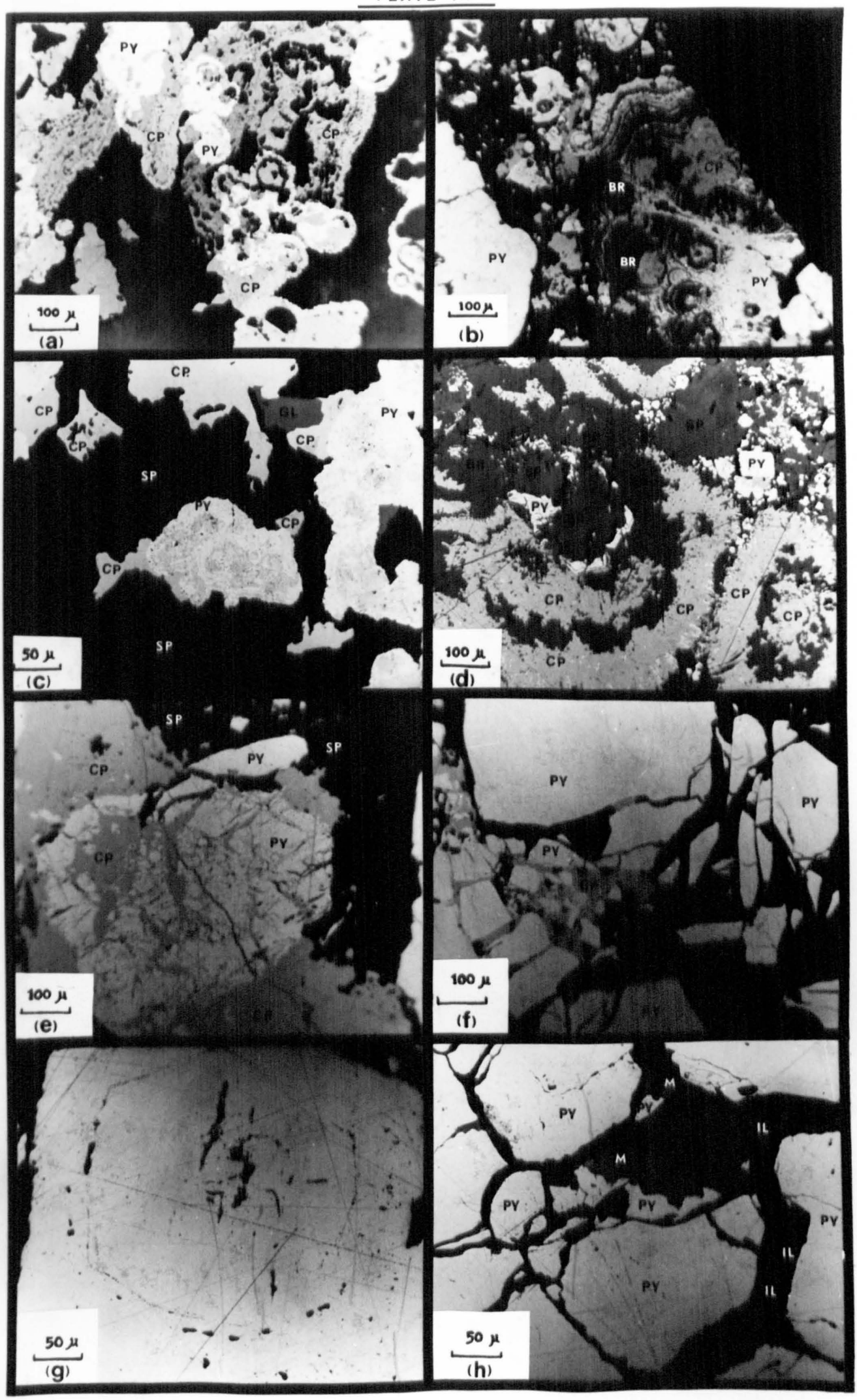
Plate 4.1(f) Cataclastic pyrite, with chalcopyrite infilling fractures. Yellow ore; drill-hole 110 (Specimen KC-7 -220X-Oil).

Plate 4.1(g) A zoned pyrite crystal. Stockwork zone; drill-hole 110 (Specimen KC-10 -110X-Air).

Plate 4.1(h) Cataclastic pyrite containing magnetite, ilmentie, and sphalerite in fractures. Stockwork zone; drill-hole 110 (Specimen KC-10 -110X-Air).

Note: PY pyrite GL galena M magnetite
CP chalcopyrite BR bornite IL ilmenite
SP sphalerite

PLATE 4.1


PY
CP
PY
CP
CP
100 µ
(a)
BR
CP
PY
BR
PY
100 µ
(b)
CP
CP
GL
PY
CP
CP
SP
PY
CP
CP
SP
50 µ
(C)
SP
BR
SP
PY
PY
CP
CP
CP
CP
CP
100 µ
(d)
SP
PY
SP
CP
CP
PY
100 µ
(e)
PY
PY
PY
100 µ
(f)
50 µ
(g)
M
PY
IL
M
PY
PY
PY
IL
PY
IL
50 µ
(h)

sphalerite (Plate 4.1(b) and 4.1(d)). It also occurs as small inclusions in sphalerite and pyrite. In a few sections it has been altered to covellite.

Tetrahedrite-tennantite occurs as small grains in minor quantities and is usually associated with chalcopyrite, and sometimes with sphalerite. It is concentrated towards the upper part of the massive ore.

Electrum (an Ag-Au alloy) was occasionally observed in polished sections from the top of massive ore, occurring as small highly reflective dots.

The polished section studies indicate three phases of sulphide mineralization in the Madenköy massive sulphide deposit. These phases, in chronologic order are:

(i) an early pyrite (chalcopyrite and minor sphalerite) phase displaying a cataclastic texture and euhedral to subhedral crystals.

(ii) a pyrite, chalcopyrite, sphalerite and minor bornite mineral paragenesis which exhibits colloform intergrowth, and

(iii) a vein and fracture filling hydrothermal phase of chalcopyrite, sphalerite, and minor bornite which fill the fractures and interstices of phases (i) and (ii).

The first phase is particularly characteristic of the stockwork and impregnation zones as well as the lower half of the massive ore (Table 4.2). The second phase is thought to be of volcanic-sedimentary origin, the textures being those which typically occur in a low-temperature

aqueous environment. As can be seen from Table 4.2 this phase is more common in the upper part of the massive ore body. The third phase (hydrothermal chalcopyrite-sphalerite veining stage) generally occurs within the massive ore body. It is characterized by exsolution of chalcopyrite within sphalerite.

Table 4.2 Vertical distribution of three ore-forming phases in ore samples from drill-hole 110

Sample No.	Level (m)	Type of ore	Euhedral, subhedral, cataclastic phase	Colloform sedimentary phase	Hydrothermal chalcopyrite-sphalerite veining phase
KC-5	102.34-107.70	Black ore		X	X
KC-8	107.70-111.75	Black ore	X	X	X
KC-12	111.75-114.90	Black ore		X	
KC-11	114.90-119.70	Black ore	X	X	X
KC-7	150.20-155.55	Yellow ore	X		X
KC-6	155.55-158.6	Yellow ore	X		
KC-10	161.65-165.35	Stockwork-impregnation			
KC-3	170.00-175.50	"	X		X
KC-22	185.20-190.10	"	X		
KC-13	190.10-196.65	"	X		

Note: X signifies presence of phase.
Marcasite is present only in the first four samples.

4.3 SIRTKÖY STOCKWORK MINERALIZATION

The Sirtköy occurrence is situated 9 km southeast of the coastal town of Cayeli (Figure 4.1). The stockwork and associated impregnation mineralization at Sirtköy is associated with the Dacitic Series and have been exposed as a result of block faulting in NE and NW directions (Figure 4.6; see also Figure 9.15 for cross section).

At Sirtköy the mineralized rocks contain from 0.04 to 0.18% Cu together with minor amounts of Zn and Pb (see Table 6.6). The main mineral is pyrite which occurs as veinlets and impregnations and is usually present as euhedral to subhedral grains, some of which exhibit an intergrowth with quartz. Chalcopyrite occurs in minor quantities. An iron-capping (gossan) developed on oxidised veins of a stockwork nature occurs in the Gümüşdere stream. Small amounts of secondary copper minerals, such as covellite, occur in this gossan.

The dacite containing the mineralization is light gray to greenish in colour, locally shows a holocrystalline-porphyritic texture, and is commonly autobrecciated, containing pebbles and boulders of the dacitic rock. Extensive alteration is present in the form of chloritization and sericitization in and around the mineralization. The Dacitic Series is unconformably overlain by spilites of the Upper Basic Series which have also been chloritized and pyritized. These rocks exhibit distinctive onion-shaped exfoliation structures and contain amygdales which are filled with quartz, sericite, and occasionally pyrite.

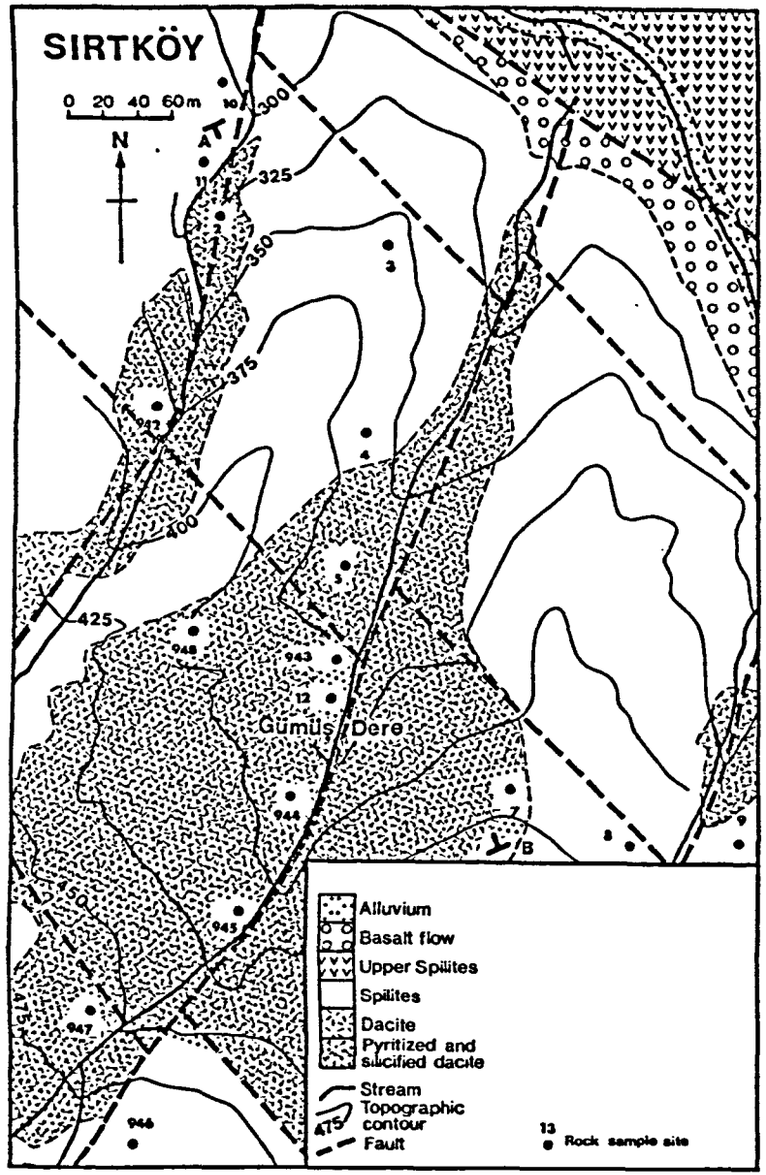


Figure 4.6 Geology of Sirtköy area (geology after Turhan, 1968).

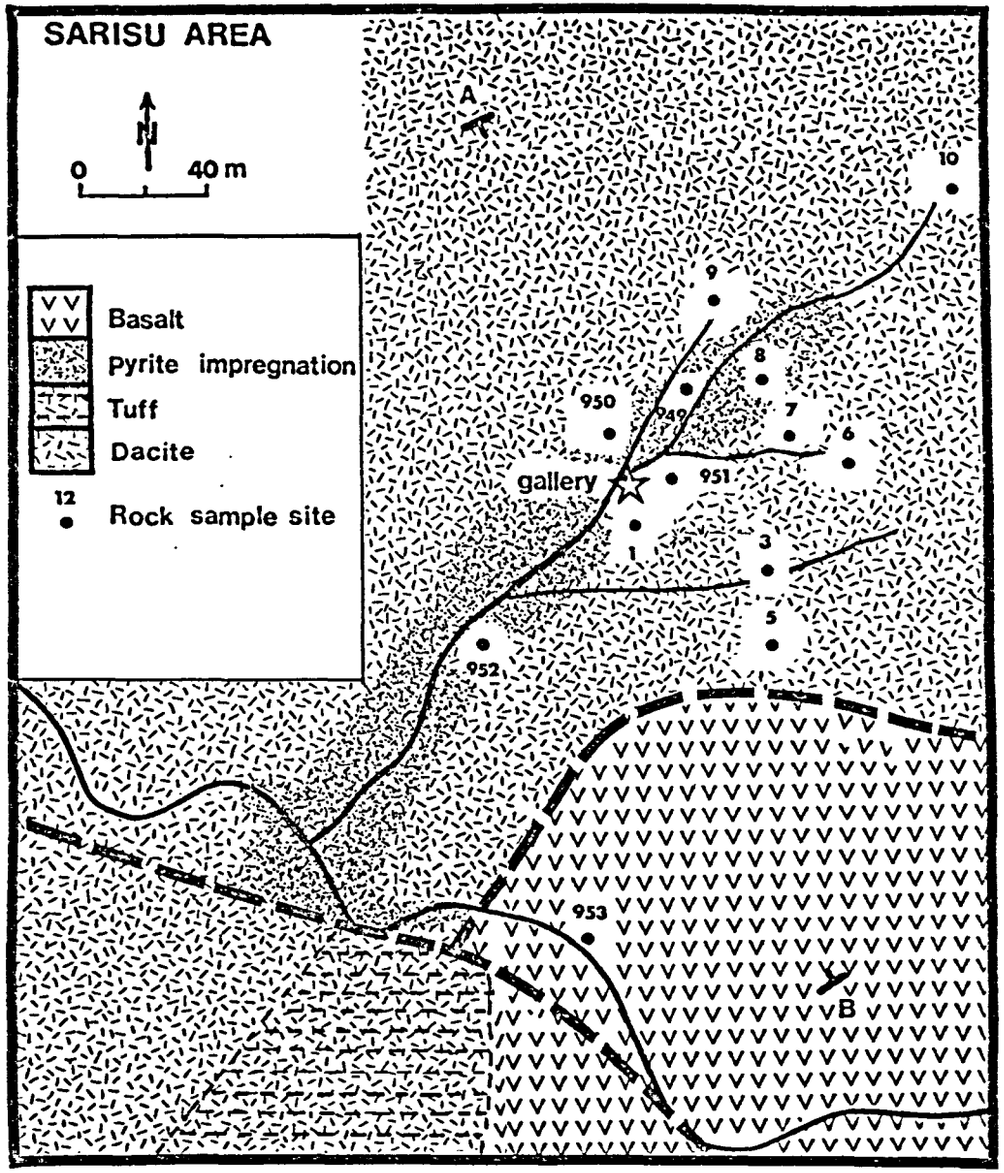


Figure 4.7 Geology of Sarisu area (geology after Aydinöz, 1971).

4.4 SARISU BARREN PYRITIC IMPREGNATION OCCURRENCE

The Sarisu occurrence is located 7 km south of Çayeli (Figure 4.1).

At Sarisu the barren pyritic impregnation zone is confined to a fault bound porphyritic dacite window (Figure 4.7; see also Figure 9.16 for cross section). The geological setting at this locality is somewhat similar to that at Madenköy. The dacite is stratigraphically overlain by dacitic tuffs which are in turn followed by basalt flows. Pyrite is the only sulphide mineral and occurs as fine subhedral to anhedral grains exhibiting a common intergrowth with quartz. The mean Cu, Zn, and Pb contents of mineralised samples are 24, 29, and 15 ppm respectively (See Table 6.7). The dacites exhibit argillic hydrothermal alteration with kaolinite and montmorillonite clay minerals predominating. An exploration gallery opened by a private mining company in the altered dacite has collapsed, but the rubble around the opening of the gallery is similar to the pyrite impregnated dacite observed at the surface.

4.5 KUTLULAR MASSIVE SULPHIDE DEPOSIT

The Kutlular massive sulphide deposit occurs within the Sürmene district of Trabzon province.

Block-faulting with a NW trend has played an important role in exposing dacites associated with the orebody (Figure 4.8; see also Figures 4.10 and 9.12 for cross section). The deposit is a Cu-Zn volcanogenic sulphide deposit with a reserve of 1,500,000 tons assaying 2.2% Cu. The northern part of the orebody contains 400,000 tons of the massive ore averaging 1.5% Zn. The deposit was found by drilling subsequent

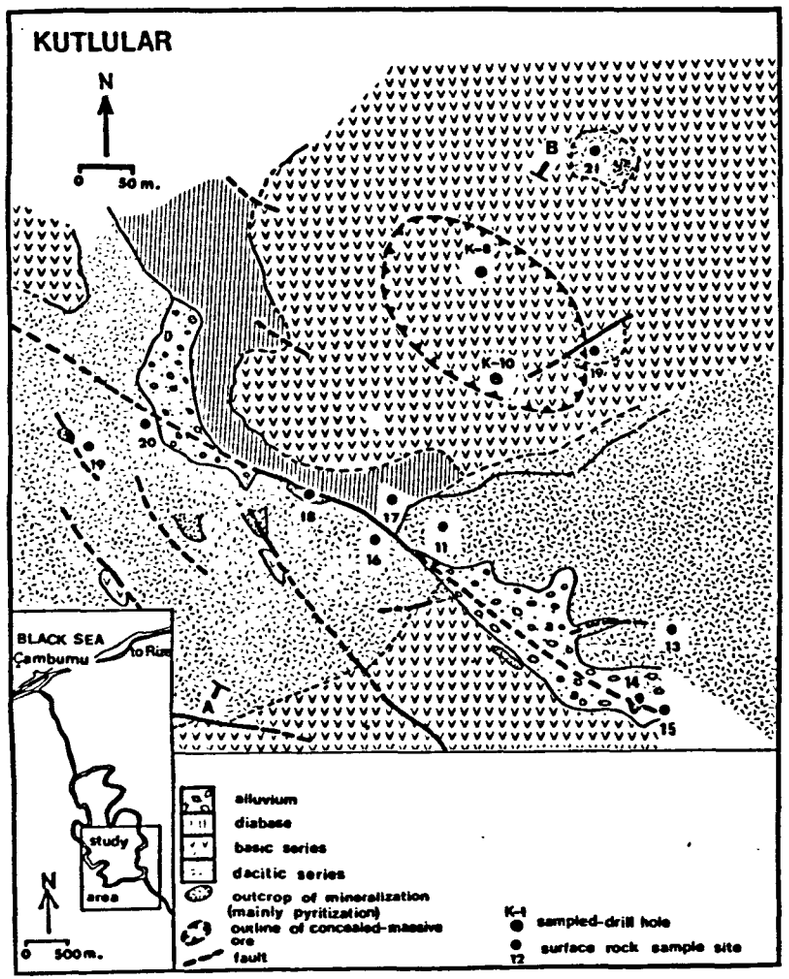


Figure 4.8 Geology of Kutlular area (geology modified after Gümrükçü, 1973).

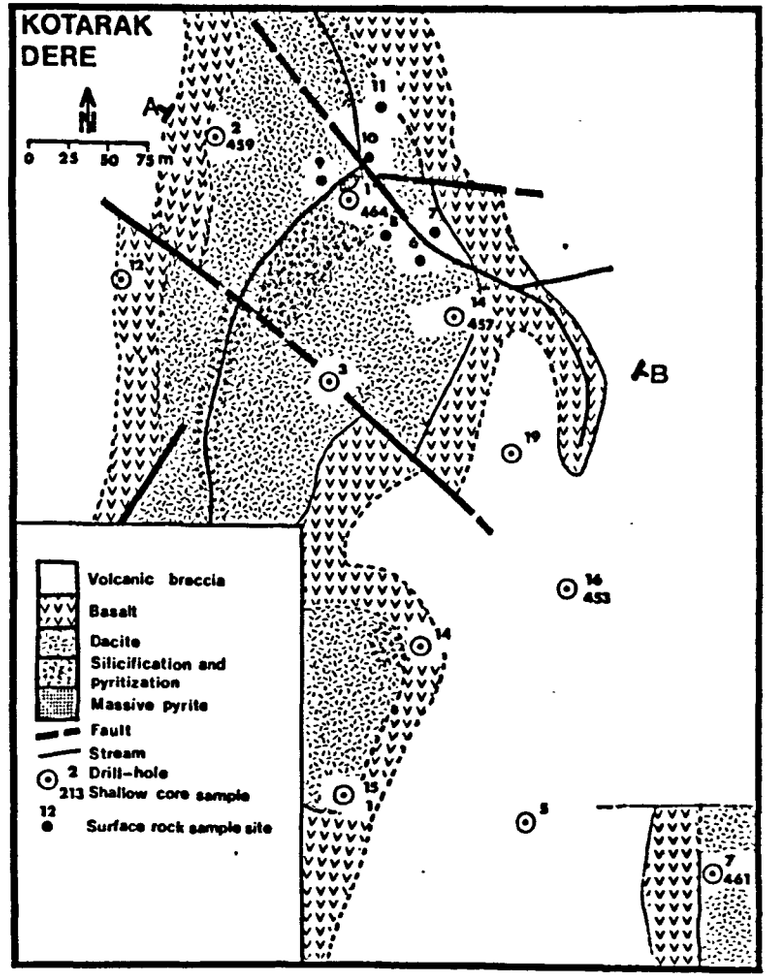


Figure 4.9 Geology of Kotarak Dere area (geology modified after Gümrükçü and Takaoğlu, 1974).

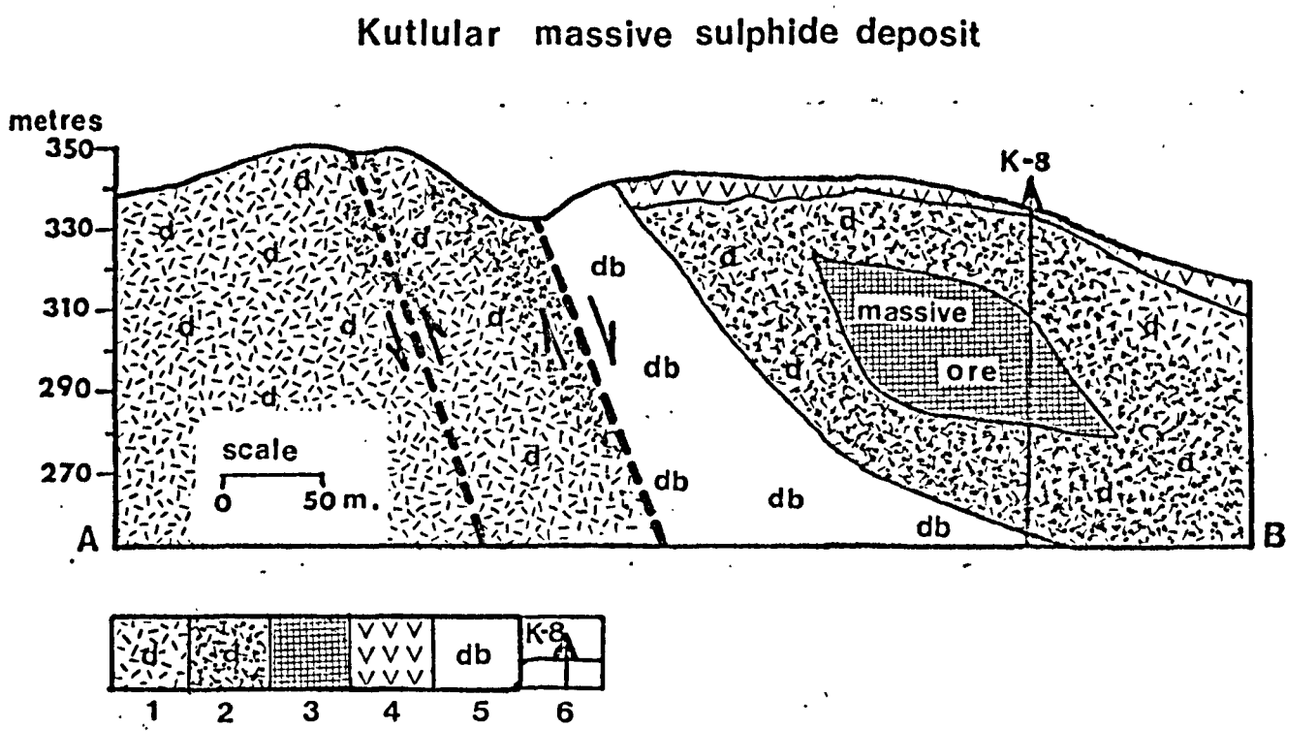


Figure 4.10 Geological cross section of the Kutlular massive sulphide deposit (1- Dacitic Series, 2- sulphide impregnation and silicification, 3- massive sulphide, 4- basalt, 5- diabase, 6- drill-hole). For location of cross section see Figure 4.8.

to detailed geological mapping. Twenty five drill-holes amounting to 3855 m have been drilled by M.T.A. The massive sulphide ore is completely concealed and occurs between the Dacitic Series and the overlying Upper Basic Series (Figure 4.8). It is ellipsoid in shape, elongated in a N35°W direction with a length of about 230 m. The projected width of the deposit on the surface is 140 m, and the thickness varies from a few metres to 30 m. The ore minerals and ore textures are similar to those at Madenköy, with the exception that at Kutlular the massive ore consists entirely of yellow and pyrite ore containing pyrite and chalcopyrite. Sphalerite occurs in relatively small amounts, and galena is present only in minor quantities. Polished section studies of ore samples collected from drill-hole K-8 indicate that the massive ore is brecciated and is somewhat more enriched in sphalerite at the top. Massive pyrite occurs at the base of the massive ore where it passes into the stockwork and dissemination zones. The three mineralised phases observed at the Madenköy deposit are also observed here, but the hydrothermal phase appears to be considerably more pronounced in this deposit. The occurrence of chalcopyrite exsolution in sphalerite suggests relatively high formation temperatures of the order of 350°C for the deposit. The ore minerals, in order of abundance, are pyrite, chalcopyrite, sphalerite, galena, and tetrahedrite-tennantite. Barite and quartz are the main gangue minerals.

The Dacitic Series is extensively altered and displays an extensive pyritic dissemination zone. The massive ore is overlain by a dacitic tuff-breccia consisting of poorly sorted dacitic pebbles in a matrix of mainly clay and quartz. This

cover rock is hydrothermally altered and contains veinlets of pyrite and chalcopyrite, as well as small pockets of gypsum. The dacitic tuff-breccia is in turn unconformably overlain by basalts of the Upper Basic Series. The basalts have a porphyritic texture and contain amygdales that are usually filled with calcite. The basalts are thin in the vicinity of the deposit and in places have been eroded allowing the Dacitic Series to outcrop. The two series have been intruded by a diabase dyke of possibly Tertiary age.

4.6 KOTARAK DERE STOCKWORK DEPOSIT

The Kotarak Dere stockwork sulphide deposit is situated in the Sürmene district west of Trabzon province.

This deposit is also associated with a block-faulted dacitic window (Figure 4.9). Seventeen drill-holes amounting to 2052 m of diamond drill-core has been drilled by M.T.A. in the vicinity of this deposit. The reserves are estimated to be about 2 m.t. assaying 0.4% Cu. Analysis by the M.T.A. laboratories of sub-surface ore samples indicate the presence of high amounts (up to 12%) of Zn in a few samples. The surface exposures suggest that the deposit is of the stockwork type, associated with an extensive pyritic impregnation zone in the Dacitic series. In addition, a small pocket of massive pyrite near the Kotarak Stream is present (Figure 4.9, see also Figure 9.14 for cross-section).

It would appear from both the above description and the subsequent geochemical studies (See the section on Regional Assessment of Mineralized zones in Chapter 8) that the stockwork exposure at Kotarak Dere was once associated with a massive sulphide orebody now eroded away.

The ore minerals and their textures are similar to those observed at the Madenköy and Kutlular deposits. Pyrite, sphalerite, and chalcopyrite are the more common ore minerals. A massive pyrite orebody outcrops in the vicinity of drill-hole D-1. The stockwork and impregnation mineralization occur within the dacite and dacitic tuffs of the Lower Dacitic Series where they are strongly altered. Basalt and volcanic breccia of the Upper Basic Series overlie rocks of the Dacitic Series which have been exposed as a result of NE and NW block faulting that elevated and exposed the Upper Basic Series to erosion in this area. The limestone intercalations in the volcanic breccia have been dated as Upper Cretaceous (A. Gümrükçü, pers. comm., 1975).

4.7 Tunca Massive Sulphide Deposit

The Tunca massive sulphide body is located in the eastern part of the province, south of the coastal town of Ardeşen (Figure 3.1 and 3.3).

The orebody outcrops on the steep, northern bank of the Tunca River near the village of Tunca (Figure 4.11 and 4.13). It was found by M.T.A. in 1972 and mapped by Todorovic and Nebioğlu (1972) with later revisions by Can (1976). Exploratory drilling was carried out by M.T.A. between 1973 and 1975. The reserves in the deposit are about 300,000 tons of sulphide ore assaying about 1.5% Cu and 1.0% Zn with only minor amounts of Pb.

The geological setting, ore-mineral paragenesis, and ore textures are similar to those at the Madenköy deposit. The massive ore has a mean thickness of 5 m and outcrops for about 70 m in an E-W direction. At its western boundary,

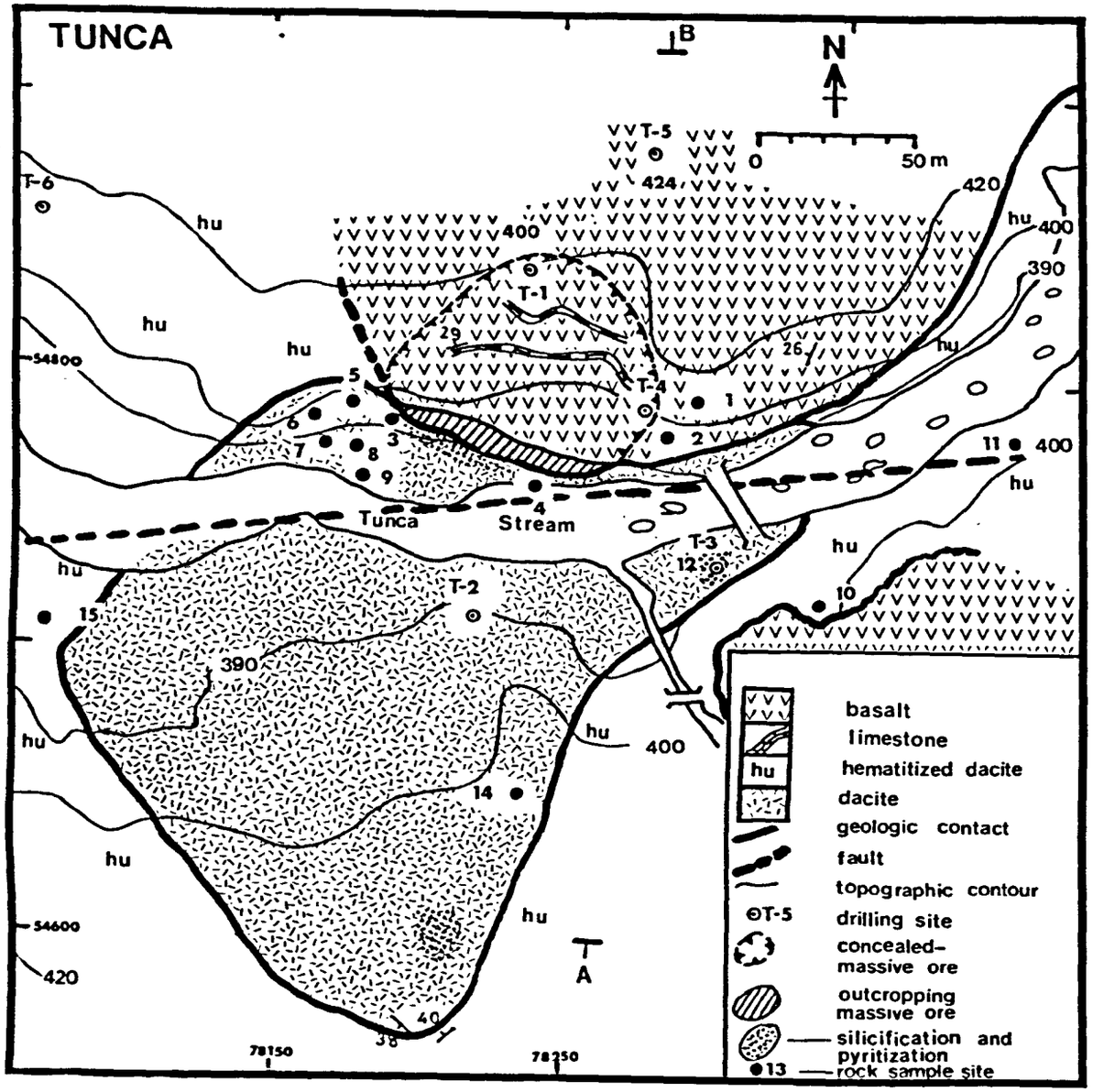


Figure 4.11 Geology of Tunca area (geology modified after Can, 1975).

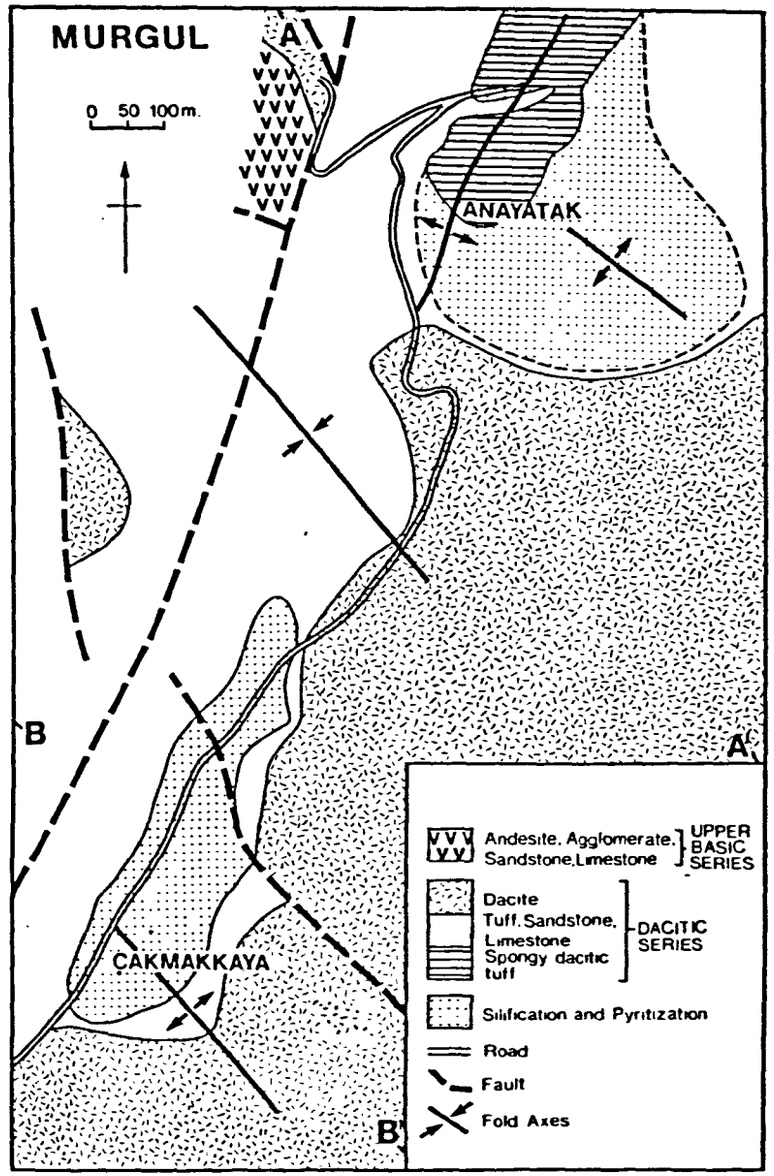


Figure 4.12 Geology of Murgul area (geology after Sawamura, 1970, in Sawa et al., 1972).

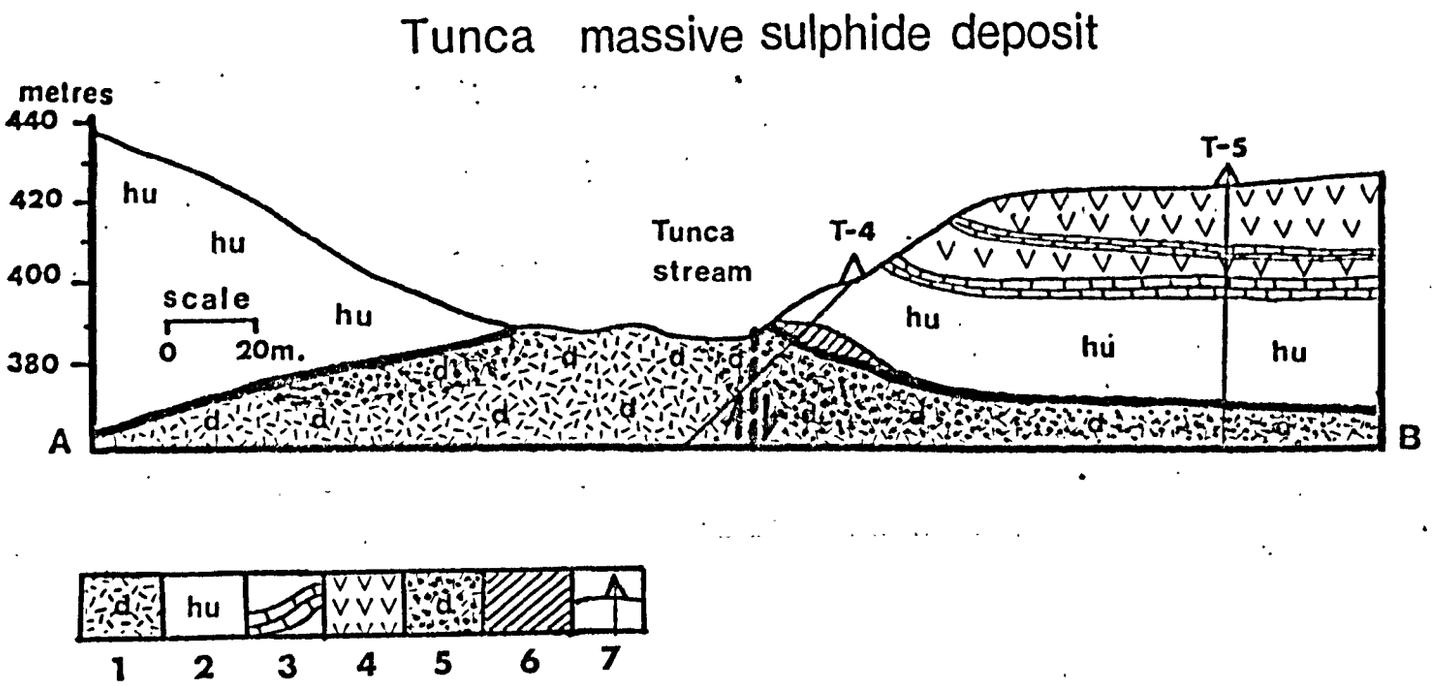


Figure 4.13 Geological cross section of the Tunca massive sulphide deposit (1- dacite, 2- hematitized dacite, 3- limestone, 4- basalt, 5- pyritization and silicification, 6- massive sulphide, 7- drill-hole). For location of cross section see Figure 4.11.

there is a 1.5 m thick clay bed containing boulders of the massive ore (20 to 30 cm in diameter), a feature that probably represents submarine reworking of the massive ore.

The ore minerals are mainly pyrite, chalcopyrite and sphalerite, with minor quantities of galena and tetrahedrite-tennantite. The gangue minerals are quartz and barite. The massive ore is underlain by stockwork and dissemination zones within the exposed dacite window. The massive ore in the exposed southern part the dacite window has been eroded away as a result of uplift along a fault which follows the Tunca river; only remnants of the stockwork and disseminated zones occur in this dacitic block.

The ore body is overlain by a hematitized porphyritic dacite that displays a strong localized foliation. This unit is in turn overlain by a basalt that has been brecciated and hydrothermally altered, the fractures being filled with hematite and carbonates (calcite and dolomite).

4.8 MURGUL STOCKWORK DEPOSIT

The Murgul stockwork deposit is located near Artvin in the eastern part of the region (Figure 3.1 and 3.3). The deposit comprises two orebodies (Anayatak and Çakmakkaya) about 800 m apart (Figure 4.12 and 4.14). The oldest mining activity is believed to date from Medieval times. At present, Anayatak and Çakmakkaya with reserves of 21 and 22 million tons assaying 1.6% and 1.2% Cu respectively, are the largest copper mines in operation in Turkey. The blister copper contains 0.8% Ag and 0.2% Au. The area has been described in detail by many geologists (Kraeff, 1963(b); Mado, 1972; Sawa et al., 1972; and Buser and Cvetic, 1973).

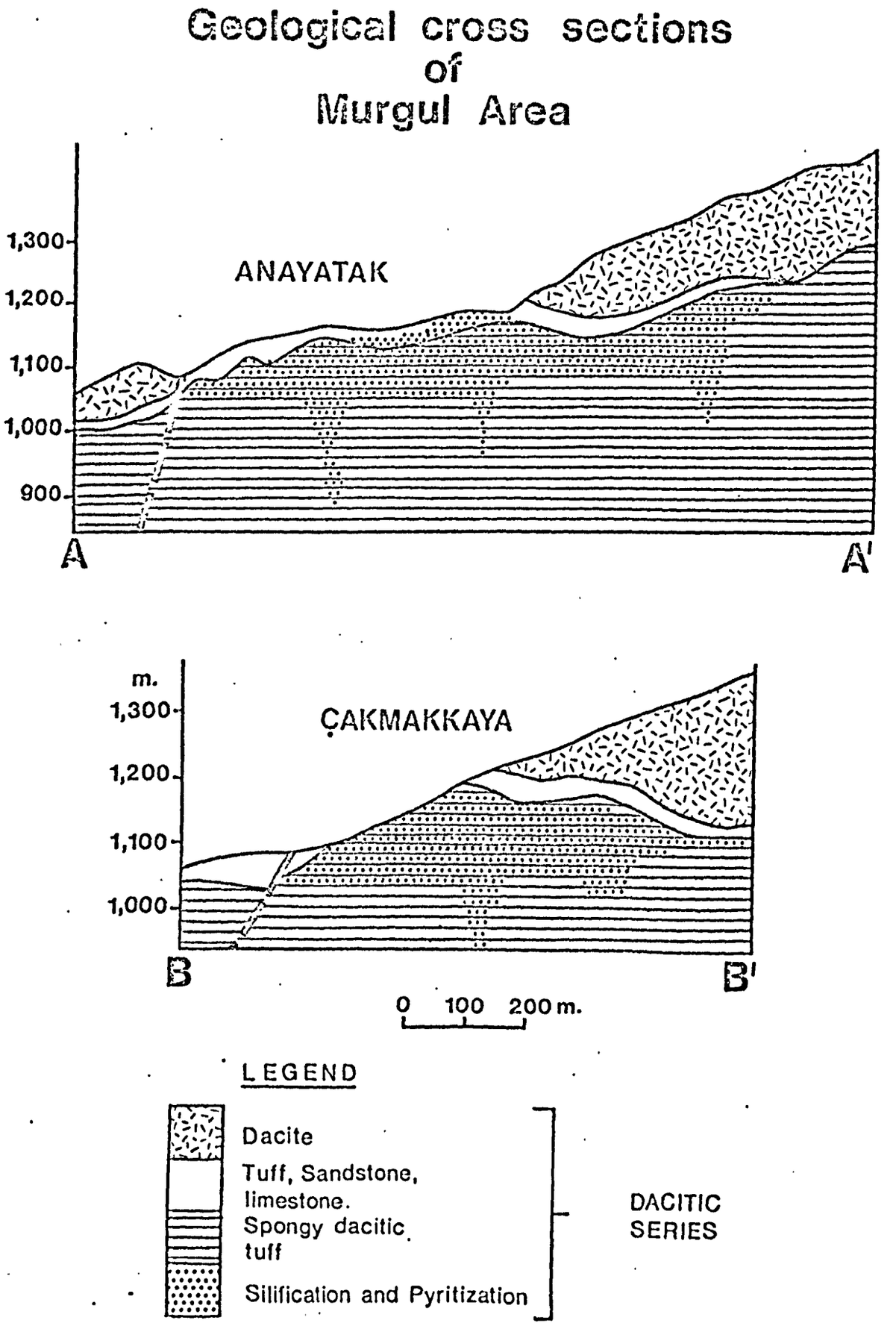


Figure 4.14. Geological cross sections of Murgul mine area (Geology after Sawamura, 1970, in Sawa et al., 1972).

The mineralization occurs within dacitic tuffs of the Dacitic Series. The stockwork veins are comprised mainly of pyrite and chalcopyrite with a quartz gangue. On the upper stratigraphic levels, the stockwork veins contain minor sphalerite and galena with a barite gangue. Silver and gold tellurides have also been found in this deposit (B. Arman, pers. comm., 1976). The thickness of the veins varies considerably, the average being of the order of 10 cm. The mineralized zones in both deposits are ellipsoidal with their long axes having a NW trend. Both these zones pass laterally into soft, kaolinized horizons which contain an abundance of large pyrite crystals exhibiting many variations of the cubic system. Pockets of gypsum occur adjacent to the sulphide bodies in a tuff-sandstone unit of the Dacitic Series.

The mineralization is confined to spongy dacitic tuffs and overlying dacitic tuffs. The spongy dacitic tuffs are mainly submarine tuff flows interbedded with sandstones and conglomerates of the same composition. This unit generally contains pumice fragments in its lower levels and is often foliated in places (Sawa et al., 1972). On the upper levels of the deposit the spongy tuff unit passes into dacitic tuffs which are intercalated with sandstone, red limestone, marl, and siltstone. These rocks contain pumice fragments at some levels and are usually hematitized.

The ore bodies are overlain by a hematitized dacite unit which in turn is covered by an andesite-agglomerate-sandstone-limestone unit of the Upper Basic Series.

CHAPTER 5

ANALYTICAL METHODS

5.1 INTRODUCTION

The methods of analyses used in the present research together with the elements concerned are outlined below:

(a) atomic absorption spectrometry for Cu, Zn, Pb, Cd, Fe, and Mn in all samples and for Ag, Ni, and Co in selected samples.

(b) direct reading optical spectrography for Fe, Mn, Cu, Pb, Zn, Cd, Ag, Mo, V, Co, Ni, Cr, Ga, Sn, Ti, Be, Mg, Ca, Sr, Ba, K, Li, Al, Sc and Si.

(c) colorimetry for As and Mo.

(d) specific ion electrode and ionanalyser (Orion) for F.

(h) flameless atomic absorption spectrometry for total and differential thermal phase analysis of Hg.

(f) selective extraction techniques for Fe, Cu, Zn, and Pb in soils and in selected pumice tuff samples.

(g) pH electrode and millivolt meter for soil pH and universal indicator (BDH) with compatible color chart for stream water pH.

(h) X-ray diffraction for feldspar, quartz, and clay minerals.

(i) microwave-induced argon plasma for selenium analysis.

Detailed descriptions of the various methods are given, and a comparison is made of the atomic absorption and direct

reading spectrographic methods for Cu, Pb., Zn, Fe, and Mn. A comparison is also made of the colorimetric and spectrographic methods for As and Mo. Some factors affecting the colorimetric determinations of As and Mo were investigated. Various methods of Se analysis are discussed and a microwave-induced argon plasma system was investigated with the aim of developing a fast and precise method for Se analysis.

5.2 ATOMIC ABSORPTION SPECTROMETRY

Cu, Ni, Co, Pb, Zn, Ag, Cd, Fe, and Mn were analysed by atomic absorption spectrophotometry. Nitric acid and nitric/perchloric acid digestion procedures were employed for rocks, soils, stream sediments, ores, and separated pyrite samples. All of the samples were attacked by using the nitric acid procedure to obtain a higher total extraction. For the ore samples a combined bromine-nitric acid attack was used. These three sample digestion procedures are described in Appendix B.1.

Samples prepared by procedures noted above were analysed using a Perkin Elmer 403 atomic absorption spectrophotometer. An air/acetylene (ratio: 57/27) flame was used with operating conditions shown on Table 5.1.

The bromine-nitric acid digestion is satisfactory if the galena content of the samples is less than 3%. In all the samples analysed the lead content did not exceed 1%. At the end of the procedure nitric acid in place of hydrochloric acid was employed for leaching (Appendix B.3) to avoid the precipitation of silver as silver chloride when this element is present in high quantities (i.e. 150 ppm).

TABLE 5.1

Analytical characteristics of the elements analysed by atomic absorption spectrophotometry.

Element	Wavelength nm	Slit width	detection limit µg/ml
Cu	324.7	4	0.01
Pb	283.3	4	0.5
Zn	213.8	4	0.01
Cd	228.8	4	0.01
Ag	328.0	4	0.01
Ni	232.0	3	0.1
Co	240.7	3	0.1
Fe	371.9	3	0.1
Mn	279.5 201.5	3 3	0.1 1.0

Comparison of the nitric and the nitric/perchloric acid digestions were made by analysing a number of rock, soil, and stream sediment samples. The results for iron, manganese, copper, lead, and zinc are presented in Table 5.2, from which it is evident that as far as the extractability is concerned, the nitric acid digestion is adequate for all the elements except iron in the rock and stream sediment samples. This is due to the form in which the iron occurs; in the soil samples iron is present mainly as iron hydroxides whereas in hematitized-pumice tuff rock samples and stream sediments the element occurs as more chemically resistant oxides. In the cases where the lead is above 600 ppm the extractability of the element, using the nitric acid digestion, is up to 2.4 times higher in some rock, soil, and stream sediment samples when compared with the nitric/perchloric procedures. This is thought to be due to the precipitation of lead chloride ($PbCl_2$) in the presence of perchloric acid. Thus, when lead is to be determined, and the element is present in high concentrations (above 600 ppm), the nitric acid digestion should be the preferred method. The latter procedure also has the advantage of being faster and less costly.

5.3 DIRECT READING OPTICAL SPECTROGRAPHIC ANALYSIS

All of the rock and ignited-soil samples (at 450°C) and some sulphide samples were analysed for Fe, Mn, Cu, Pb, Zn, Mo, Cd, Ag, Co, Ni, Cr, Ti, V, Mg, Ca, K, Be, Sr, Ba, Li, Sc, Al, and Si, and in some samples As, by using a combination of direct reading spectrographic techniques and a computer program which processes the raw data into elemental

Table 5.2 Extractability of metals with nitric acid and nitric acid/perchloric acid digestions. Number of samples for rocks, soils and stream sediments are 23, 16, and 10 respectively.

Element	Sample Type	Extractability (Nitric acid/Nitric+perchloric acid)x100 Mean	Range
Fe	Rock	43.3	18.3-103.2
	Soil	82.7	57.5-100.0
	Stream sediment	42.9	29.8- 54.4
Mn	Rock	98.0	90.0-110.9
	Soil	95.4	57.5-111.8
	Stream sediment	73.2	60.3- 87.7
Cu	Rock	81.5	71.3- 85.7
	Soil	91.8	78.6- 96.5
	Stream sediment	74.4	62.4- 89.0
Pb	Rock	64.8	33.7-127.7
	Soil	69.9	32.0-240.0
	Stream sediment	80.0	80.0-113.3
Zn	Rock	77.0	40.6- 92.8
	Soil	76.9	43.2- 95.7
	Stream sediment	79.5	72.1- 84.2

concentrations. A detailed description of the system is given in Applied Geochemistry Research Group Technical Communication Report No. 59 (1973). The sample preparation and operating conditions are given in Appendix B.2. The analytical characteristics of the above-mentioned elements for this system are given on Table 5.3.

5.4 COMPARISON OF RESULTS OBTAINED BY ATOMIC ABSORPTION ANALYSIS AND DIRECT READING SPECTROGRAPHIC ANALYSIS

A comparison, by means of linear correlation analysis, of the atomic absorption and direct reading spectrographic methods for Cu, Zn, Pb, Fe, and Mn, is presented in Table 5.4. The table shows good correlations between the two techniques except in the case of iron in rocks and copper in soils. The poor correlation for iron is due to the low iron extraction by the nitric acid digestion (see Table 5.2). The poor correlation for copper is partly due to self absorption of the 327.39 nm line at high concentrations (Ahrens and Taylor, 1961), and partly due to the weight loss of soils as a result of ignition before the direct reading spectrographic analysis were done.

A number of ore samples were analysed after dilution with specpure silica. The results obtained by the atomic absorption and the direct reading spectrographic methods indicate reasonably good agreement except in the cases of copper and lead (Table 5.5). The former is due to the self absorption at high concentrations of copper as mentioned earlier, and the latter is thought to be due to matrix effects which give elevated signals during determination by the direct reading spectrographic procedure.

Table 5.3 Analytical characteristics of the elements determined by the direct reading spectrographic system.

Element	Wavelength nm	Detection Limit *	Upper Limit	Precision ** %
Fe	273.96	0.1%	15.0%	N.D.
Mn (I)	279.83	20	500	40 at 1000 ppm
Mn (II)	293.31	500	10000	N.D.
Cu	327.39	4	1000	24 at 1000 ppm
Pb	283.31	4	1000	48 at 20 ppm
Zn	328.23	10	1000	N.D.
Mo	317.03	0.6	100	N.D.
Cd	228.80	1.5	100	N.D.
Ag	338.29	0.4	100	35 at 2 ppm
Co	345.35	2	1000	10 at 38 ppm
Ni	341.47	2	1000	10 at 42 ppm
Cr	425.44	4	1000	20 at 38 ppm
Ti	365.35	20	20000	42 at 1000 ppm
V	437.92	10	1000	29 at 100 ppm
Mg	277.98	0.06%	5.0%	32 at 0.5%
Ca	315.89	0.1%	25.0%	45 at 2%
K	404.40	0.2%	10.0%	24 at 2%
Be	313.03	0.8	100	38 at 3 ppm
Sr	460.73	8	1000	40 at 200 ppm
Ba	455.40	10	1000	34 at 150 ppm
Li	610.36	6	1000	64 at 20 ppm
Sc	390.75	6	100	100 at 10 ppm
Al	237.84	0.7%	15.0%	N.D.
Si	243.52	4%	46.0%	N.D.
As	234.93	20	1000	N.D.

Note: all values in ppm unless mentioned.

*Detection limit is defined as twice the standard deviation at zero concentration.

** Precision is defined as $P_c = 100 \times C_L/C + K'$ where P_c is precision; C_L is detection limit, C is the concentration at which precision is required and k' is a constant of the system for each element (N.D.- constant k' not available for these elements therefore precision was not determined).

Table 5.4 Comparison of atomic absorption (nitric acid digestion) and direct reading spectrographic methods of analysis.

Element	Rocks		Soils	
	Number of samples	Correlation coefficient	Number of samples	Correlation coefficient
Cu	198	0.81	222	0.57
Zn	198	0.94	222	0.95
Pb	198	0.90	222	0.98
Fe	126	0.85	222	0.33
Mn	126	0.81	222	0.92

Table 5.5 Comparison of atomic absorption and direct reading spectrographic methods for ore samples. Atomic absorption determinations of Cu, Pb, Zn were made after a bromine/nitric acid digestion; Fe, Mn and Ag were analysed after a nitric acid digestion.

Sample	Fe%		Mn(ppm)		Cu(ppm)		Pb(ppm)		Zn(ppm)		Ag(ppm)	
	A.A	D.R.	A.A.	D.R.	A.A.	D.R.	A.A.	D.R.	A.A.	D.R.	A.A.	D.R.
M-1	34.4	47.0	1930	2902	7800	6795	2350	3355	6600	*	109	162
M-2	26.0	37.0	130	N.D.	75000	6293	1900	5979	31000	*	128	154
M-3	31.6	40.0	130	N.D.	45000	5784	1900	2997	144000	*	119	135
M-4	43.2	43.0	150	N.D.	33000	5208	1050	1371	39000	*	76	85
M-5	5.3	4.6	4000	2191	8270	2312	620	451	20500	*	17	20
M-7	29.6	42.0	2200	4105	14700	5304	505	747	11400	9406	14	17
M-8	42.8	56.0	340	293	63000	6275	185	214	14000	*	21	26
M-9	44.8	40.0	280	313	3150	6996	145	75	1110	816	5	8
M-10	41.6	57.0	180	N.D.	1160	1307	310	368	2100	1698	6	N.D.
3127	27.6	42.0	120	N.D.	54800	6193	480	1085	3880	3741	26	28
3131	4.2	15.0	430	817	208	289	32	87	62	320	2	N.D.

Note: N.D.: not detected
* above calibration range

For the reasons explained above atomic absorption analysis are better suited for the sulphide analysis.

5.5 COLORIMETRIC ANALYSIS

5.5.1 Arsenic Analysis

Arsenic analyses of rocks, soils, and stream sediments were carried out by the "Gutzeit method" after a potassium bisulphate fusion. The method involves leaching with 6M hydrochloric acid after the fusion, followed by generation of arsine (AsH_3) and hydrogen by adding stannous chloride and zinc pellets. The evolved arsine reacts with mercuric chloride paper to give coloured-spots ranging from yellow to brown. These spots are compared with prepared standards. The method has been described by Stanton (1968) and in an Applied Geochemistry Research Group Technical Communication Report - 1971. A detailed description of the method is given in Appendix B.3.1.

Work was carried out by the author to determine the effect of certain parameters on this method.

It is generally believed that the potassium bisulphate fusion technique is not a good method of sulphide digestion. To check this a number of sulphide samples were digested by the sodium hydroxide fusion method. The effect of the two digestion procedure on arsenic determinations were not significantly different (Table 5.6). The sodium hydroxide fusion technique has a disadvantage in giving a high dilution factor of 250. The potassium bisulphate fusion was found to be adequate and much more rapid for sulphide digestion.

Table 5.6 Effect of the $KHSO_4$ and NaOH fusion techniques on the analysis of arsenic in sulphide samples

Sample	$KHSO_4$ fusion As (ppm)	NaOH fusion As (ppm)
M-2	4500	4250
M-3	1750	1625
M-5	225	344
M-7	850	1000
M-11	110	125
M-13	750	758
M-18	10	N.D.
3123	25	40
3127	3500	3250
3133	95	110

The effects of solution acidity on the sensitivity of arsenic analysis was investigated by taking 1 ml aliquots containing relatively large quantities of arsenic into three test tubes and then making them up to 5 ml with 2M, 4M, and 6M hydrochloric acid. The results suggested a significant improvement of sensitivity with lower acidities (Table 5.7). The reaction time between arsine (AsH_3) and the mercuric chloride paper depends considerably on the acid strength of the solution. The rush of hydrogen, carrying the arsine, will shorten the time of the reaction. This, therefore, results in lower sensitivity with lower pH. The size of the zinc pellets are also important as far as the sensitivity and the precision are concerned. Finer zinc particles present a larger surface area and cause a greater rate of hydrogen and arsine generation. It is, therefore, important to keep these parameters constant for good precision. Although better sensitivity is obtained with low molarity hydrochloric acid solution, for faster and better leaching, and in the case of Mo analysis (see following section), 6M hydrochloric acid was used throughout the analyses.

The method described above has a precision better than ±20% at the 95% confidence level over the concentration range 5-30 ppm (Table 5.8). About 100 samples can be analysed per man day. The detection limit of the method is 4 ppm with a dilution factor of 8. The detection limit can be lowered by using lower dilution factors.

5.5.2 Molybdenum Analysis

The colorimetric method used for Mo analysis is described in an Applied Geochemistry Research Group Technical

Table 5.7 Effects of solution acidity on arsenic determinations

I : made up to 5 ml with 4 ml of 2M HCl

II : made up to 5 ml with 4 ml of 4M HCl

III : made up to 5 ml with 4 ml of 6M HCl

I As (ppm)	II As (ppm)	III As (ppm)
5500	5000	4500
2100	1600	1400
1100	800	750
325	300	225
140	130	110
12.5	10	10

Table 5.8 Precision at 95% confidence level of the Gutzeit method as determined by replicate analyses of two rock samples

Rock sample No.	Number of analysis	Mean As (ppm)	Coefficient of variation (%)	Precision (2 x coefficient of variation) (%)
446	11	30.4	3.5	7.0
78	10	4.9	9.7	19.4

Communication Report - 1971. The potassium bisulphate fusion was used for the digestion of rock, soil, and stream sediment samples. Sodium hydroxide fusion/hydrogen peroxide oxidation was used for the dissolution of ore samples. Molybdenum was also determined in rock and soil samples by the direct reading spectrographic technique. A detailed description of the colorimetric method is given in Appendix B.3.2.

Many problems are associated with the method when analysing siliceous, carbonaceous, and sulphide-rich samples. In these cases after the addition of zinc dithiol solution a greenish gelatinous precipitate was usually formed. This precipitate passed into the toluene layer. A longer and more vigorous shaking appeared to settle the precipitate such that reasonable absorbance measurements could be made. Also, the acetone-washing procedure of Hoffman and Waskett-Myers (1974) gave improved clarity to the toluene layer in such cases.

The effect of the acidity of the sample solution on molybdenum analysis was examined by preparing two sets of standard solutions in 6M HCl and 7M HCl. The calibration graphs obtained from these two sets of standards are shown in Figure 5.1. The graphs suggest that higher absorbance and therefore higher sensitivities are obtained at higher acidities. Because As and Mo were determined from aliquots of the same solution, and higher sensitivities were obtained at lower acidities for As analysis (see preceding section), a compromise was made and 6M HCl was used for the leaching.

With a dilution factor of 8 the detection limit was 0.3 ppm. The precision (2 x coefficient of variation at a particular concentration) of the method was ± 15% at 4 ppm.

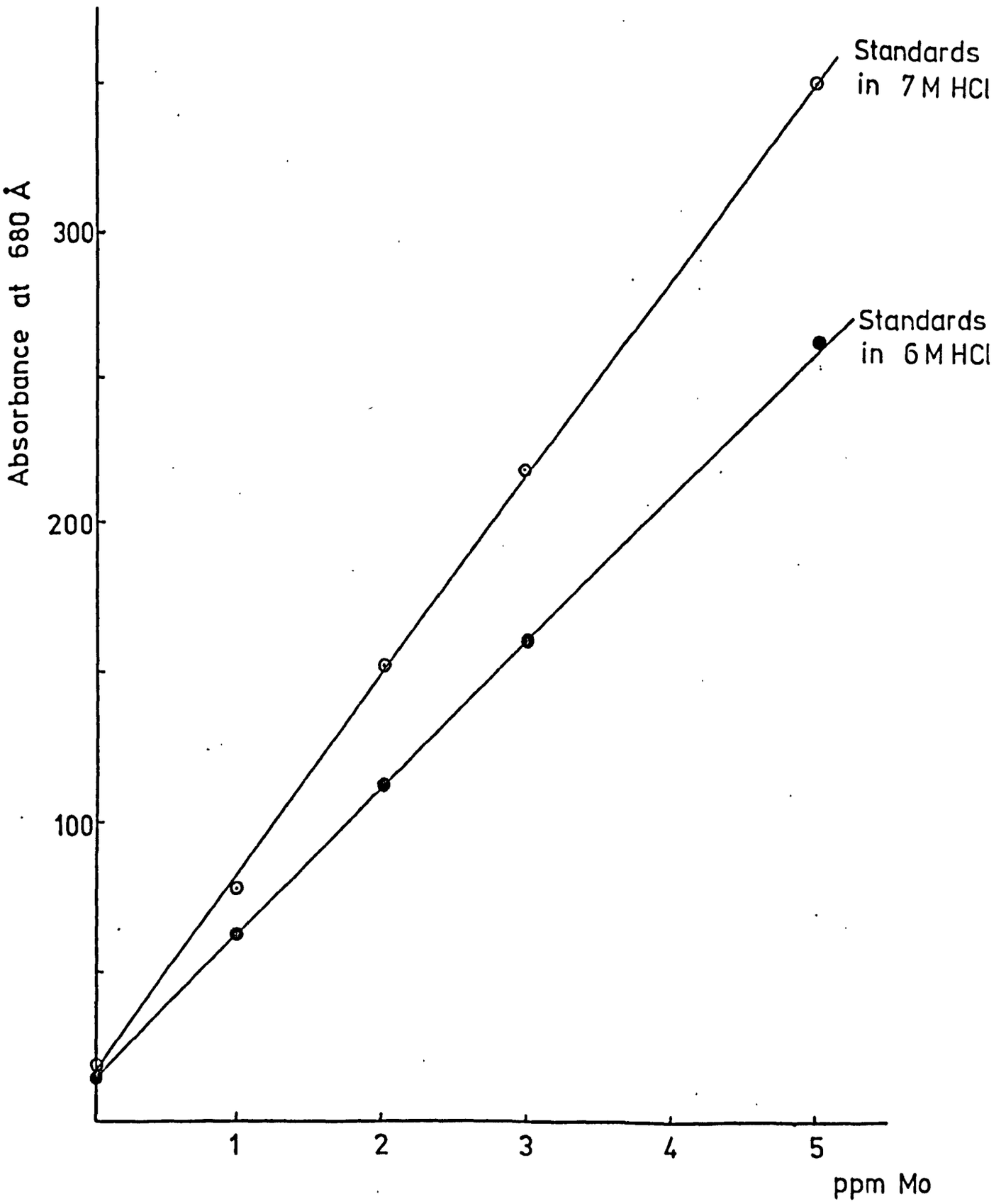


Figure 5.1 Effect of acidity on molybdenum determination.

Molybdenum in rocks and soils was also analysed by the direct reading spectrographic method. A good correlation was obtained between the two methods. The correlation coefficients (r) were found to be 0.82 and 0.71 for rocks and soils respectively. The number of rock and soil samples included in the calculations were 143 and 195.

5.6 FLUORINE ANALYSIS BY ION-SELECTIVE ELECTRODE

Fluorine analyses of rocks were carried out by the method of Boyle (1976). Details of this method are given in Appendix B.4. The method involves fusion of the sample with concentrated NaOH solution first at 200°C and then 420°C and leaching of the fused sample in a citrate-acetate buffer. The final pH is tested to ensure a pH of 7.0 to 7.5. The fluorine content of the final solution is measured with a fluoride specific ion electrode, reference electrode, and ionanalyser (Orion) or millivolt meter.

The dilution factor was 400 during the analysis that give a range of 8-4000 ppm which was adequate for the author's purposes. The method is easy and fast with a production of about 150 samples per man day being possible. From rock samples, the precision of the method was calculated to be ± 8.6% at 814 ppm and ± 30% at 40 ppm.

5.7 MERCURY ANALYSIS - FLAMELESS ATOMIC ABSORPTION METHOD

Quantitative total mercury analysis and qualitative thermal evolution profiles of mercury were made using a method of flameless atomic absorption spectrophotometry. The mercurometer used is essentially the same as that used by James and Webb (1964) with modifications by Halenko (in prep.).

The apparatus is schematically illustrated in Figure 5.2. It consists of three parts: a sample introduction system, a mercurometer, and a read-out system.

The sample introduction system, in the case of total mercury analysis, consists of a charcoal containing-tube, a wash bottle containing sample solution and 2 ml of 10% stannous chloride that can be fitted with a sinta glass bubbler for generation of mercury, a tube containing magnesium sulphate connected to the wash bottle by tubing in the manner shown in Figure 5.2. The charcoal and magnesium sulphate ($MgSO_4$) are used respectively to clean the nitrogen carrier gas and absorb any water vapor generated during bubbling of the sample solution. Stoppers were used to direct the flow of the carrier gas.

In the case of mercury vapor phase analysis the wash bottle is replaced by a Stanton-Redcroft furnace (100 volts and max. temperature: 1050°C) connected to a linear programmer (Stanton-Redcroft, model LVP-C).

The mercurometer has two flow meters (1100 Rotameter Mfg. Co. Ltd. England) to regulate and divide the nitrogen mercury mixture into two equal parts. The mercury in one channel is absorbed by palladium chloride-impregnated glass wool. The light emitted from a mercury lamp is absorbed by the two cells connected to the two channels. The signal is the difference in absorbance between the two cells measured by two photometers.

The read-out system is made up of a voltmeter (Philips PM 2440) and a two channel Servescribe recorder, one channel of which records the temperature in the case of thermal evolution mercury analysis.

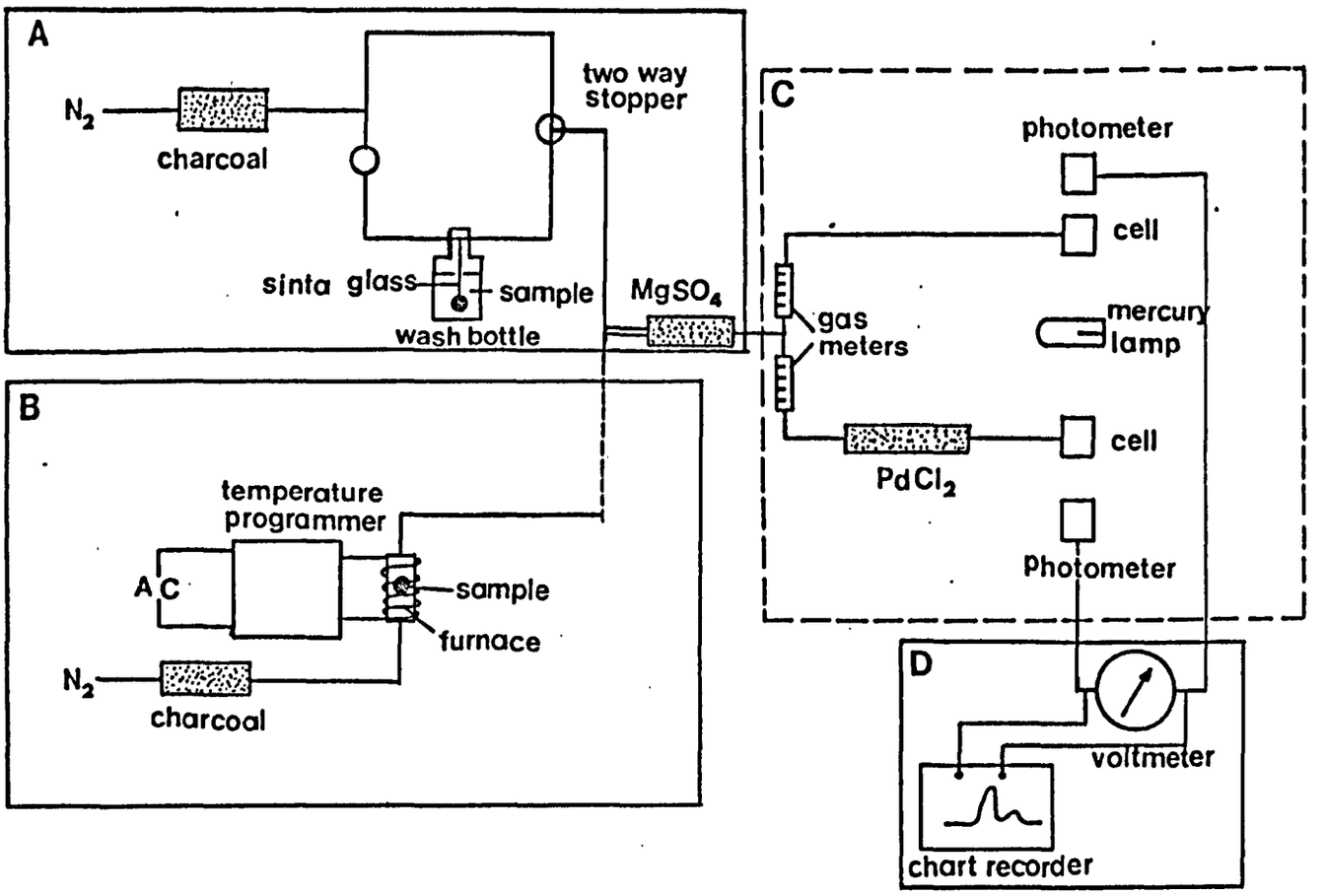


Figure 5.2 Apparatus for mercury analysis:

A: Sample Introduction Unit for total mercury analysis
B: Sample Introduction Unit for mercury vapor evolution analysis
C: Mercurometer
D: Read out unit

A warm-up time of 30 minutes is required for the apparatus. Details of the analytical procedure for the total and vapor evolution profile mercury analysis are given in Appendix B.5.

Solution standards and U.S.G.S. rock standards were run and a calibration graph was obtained for each batch of samples. About one standard for every ten samples was included to check the drift frequently observed for the instrument. The detection limit of the method was found to be 10 ppb. Precision of the method is 15% at a concentration of 200 ppb at the 95% confidence level.

The mercury evolution profiles were compared with those of the artifically prepared standards of Halenko (in prep.) and the previous results of Watling, et al. (1973).

5.8 SELECTIVE EXTRACTION METHODS

Soil, rock, and stream sediment samples were leached using three reagents - 0.05 M ammonium EDTA (pH:4.65), acidified 1M hydroxylamine hydrochloride ($NH_2OH.HCl$) solution (pH:1.3), and ammonium oxalate in oxalic acid (pH:3.3). Details of the analytical procedures of these methods are given in Appendix B.6. The residues left after extractions were washed twice with deionized water and kept for further analysis after drying at 50°C. The elements investigated by these methods were Fe, Mn, Cu, Zn, and Pb.

5.8.1 EDTA Extraction

A one-hour EDTA extraction was used to leach the geochemical samples. The 0.05M ammonium EDTA solution has the advantage of being sprayed directly into the flame of

the atomic absorption spectrophotometer. A more concentrated EDTA solution would be too heavy and, therefore, a dilution step would be necessary in the procedure.

During sample leaching and standard preparation care was taken to prevent hydrolysis. At low pH values precipitation of metals occur in the EDTA solution. The pH had to be controlled during the preparation of samples and standards using small quantities of concentrated ammonia, as the pH of the extractant solutions could be changed considerably by the occurrence of organic acids and hydroxides in the geochemical samples (Table 5.9).

Details of the method are given in Appendix B.6.1.

5.8.2 Acidified Hydroxylamine Hydrochloride Extraction

The method used by Chester and Hughes (1967) was modified to permit a more practical leaching. A more acidic solution (pH:1.3) than that used by Chester and Hughes (1967) was employed to obtain

(a) a stronger extraction and,

(b) a more effective solution matrix to keep the extracted metals in solution.

A sixteen-hour period was used with the hydroxylamine hydrochloride extraction. The sample solution was analysed instead of analysing the residue. The latter procedure would have involved the total analysis of the extracted as well as non-extracted samples and a weight correction.

Details of the method are given in Appendix B.6.2.

TABLE 5.9

Modification of the pH of the EDTA solution (pH: 4.65) by soil and hematitized pumice tuff samples

Sample number	Sample Type	pH of Sample Solution
MS-46	Soil	3.9
MS-50	Soil	4.0
K-23	Soil	4.2
K-25	Soil	4.3
2	Rock	5.2
64	Rock	4.6
74	Rock	5.0

5.8.3 Ammonium Oxalate Extraction

0.157M ammonium oxalate in oxalic acid (pH:3.3) was used for iron-manganese oxide extraction of rock and soil samples. The method is that described by Le Riche and Weir (1963). The samples were emersed in the ammonium oxalate solution for five days and then stirred under ultra-violet light for one hour. Total analysis of the attacked residues and unattacked samples was carried out, and the ammonium oxalate extractable metals were calculated after the necessary weight corrections.

Details of the method is given in Appendix B.6.3.

5.9 pH DETERMINATIONS

The pH of soils was determined in the laboratory. A field test was used to determine the pH of stream waters.

5.9.1 Determination of Soil pH

10 g of -2 mesh (B.S.S.) soil sample was treated with 20 ml of 0.01M calcium chloride solution for 30 minutes with occasional stirring. The pH of the solution was determined using a pH meter (Pye, Model 605). The sensitivity of the meter is 0.05. The method has good precision.

5.9.2 Determination of the pH in Stream Waters

5 ml of stream water in a calibrated test tube was mixed with 0.1 ml of BDH (British Drug House) universal indicator. The colour of the solution was compared with the colours on the BDH colour chart. This method covers a pH range of 4.0 to 11.0 and has a sensitivity of 0.5 of a division.

5.10 X-RAY DIFFRACTION ANALYSIS

Hydrothermal alteration minerals in rock samples were determined by X-ray diffraction analysis using a Phillips X-ray diffractometer. The samples were ground to -250 mesh (B.S.S.) and packed in aluminum metal holders of fixed area. Special care was taken to produce the same close packing and smooth flat surfaces for all samples. The constant grain size, packing, and flatness of sample surfaces are important in obtaining reproducible results.

The rock samples were scanned from 4 degrees to 40 degrees with a scanning speed of 1 degree per minute, using CoKα radiation. The chart recorder speed was 600 mm/hour with a time constant of 2. The X-ray diffractometer was operated at 34 kv and 24 ma at a sensitivity of 400 cps.

Feldspar, quartz, clay minerals, carbonates (calcite, dolomite, siderite), and hematite peak intensities at particular 2θ angles (Table 5.10) were measured and recorded for each rock sample. The peak intensities depend on several characteristics of the sample which can be summarized as follows: (a) crystallinity; (b) grain size; (c) packing and, therefore, orientation a feature that is especially true in the case of minerals with tabular and platy habits (e.g. carbonates, clay minerals, micas and to a lesser extent quartz), resulting in the strengthening of basal reflections; (d) matrix effects such as the occurrence of other reflections at the same 2θ value which could enhance the signal.

For the above variables, grain size and packing can be controlled to some extent, and the other variables should be roughly constant as long as one is dealing with a single rock type. The peak height (intensities) recorded under

TABLE 5.10

Characteristic reflections of minerals at which peak intensities were measured by X-ray diffraction

Mineral	2θ values (Co Kα radiation)
Feldspar	32.4 - 32.7
Quartz	31.1
Kaolinite	14.5
Montmorillonite	~7
Illite-sericite	~10.3
Chlorite	14.4
Calcite	34.3
Dolomite	36.1
Siderite	37.8
Hematite	38.9

TABLE 5.11

Identification of clay minerals by X-ray powder diffraction (after Shaw, 1971)

Air dry basal spacing	Glycerated sample	Heated at 400°C for one hour	Heated at 550°C for one hour	Boiled in 10% HCl	MINERAL
~26-29A	Expands to 31-32A with rational sequence of higher orders	May disappear or give 24A spacing	Increase in intensity of 24A spacing	-	Regular interstratified CHLORITE-MONTMORILLONITE or CHLORITE-VERMICULITE
~26-29A	Expands but gives irrational sequence of reflections	May give irrational sequence of reflections	May give irrational sequence of reflections and increase in intensity of 12-14A peaks	-	Randonly interstratified CHLORITE-VERMICULITE
~14A	No change	No change	Increase in intensity	All reflections vanish	CHLORITE
~14A	No change or slight increase	Collapses to 10A	No change or slight additional collapse	No change	VERMICULITE
~14A	No change or slight increase	Collapses to ~ 12A	Additional collapse to 11A	No change	DIOCTAHEDRAL VERMICULITE
~14A	Expands to 18A	Collapses to ~ 10A	No change or slight additional collapse	May dissolve in HCl	MONTMORILLONITE
>10-14A	No change	Collapses to ~ 10A	No additional collapse	No change	Regular interstratified ILLITE-VERMICULITE
>10-14A	No change	No change	No change or slight increase in intensity	No change	Regular interstratified ILLITE-CHLORITE
>10-14A	No change	Collapses to ~ 10A	No additional collapse	No change	Randonly interstratified ILLITE-VERMICULITE
>10-14A	No change	No change	No change	May dissolve in HCl	Randonly interstratified ILLITE-CHLORITE
>10-14A	Expands to higher spacing	Collapses to ~ 10A	No additional collapse	No change	ILLITE-MONTMORILLONITE
12-12.5A	No change	Destroyed or intensity reduced	Destroyed	Destroyed	SEPIOLITE
10.5A	No change	Destroyed	Destroyed	No change	ATTAPULGITE or PALYGORSKITE
10A	Unsymmetrical peak with perhaps a slight shift	No change	No change except for a slight sharpening of reflection	No change	ILLITE (MUSCOVITE)
~7A	No change	No change	No change	No change	CHRYSOTILE or ANTIGORITE
~7A	Increase in spacing of possibly no change	Collapses to 7A again	Destroyed	No change	HALLOYSITE
~7A	No change	No change	Destroyed	No change	KAOLINITE (DICKITE, NACRITE)

the above-specified conditions are, therefore, related semi-quantitatively to the mineral concentration.

From the recorded peak intensities the ratio of clay (kaolinite - montmorillonite - illite - sericite)/feldspar was calculated for the rock samples.

Clay minerals were identified using tests summarized in Table 5.11. In some cases the clay fraction had to be separated (see Appendix A.5). From this fraction, disc mounts and loosely packed mounts were prepared to obtain the basal and random orientations needed for identification.

5.11 SELENIUM ANALYSIS

5.11.1 Purpose of Selenium Analysis

The hydrothermal phase of ore formation is the major phase in which selenium is concentrated. The element occurs in a wide variety of deposits, either in a dispersed state, isomorphously substituting for sulphur, or more rarely, forming its own minerals. The silver and gold veins of Mexico and Chile contain high concentrations of selenium (Sindeeva, 1964). Other deposits with a high selenium concentration include pyrite and copper-pyrite deposits, polymetallic sulphide deposits with sulfarsenide and arsenide minerals, sandstone-type uranium deposits, and certain skarn and greisen deposits. Selenium is also reported to be concentrated in the massive sulphide orebodies of the Noranda, Flin Flon, Normetal, and Aldemac mines (Hawley and Nichol, 1959), with average concentrations up to a few hundred ppm.

The widespread occurrence of selenium in ore deposits makes it a good pathfinder, but difficulties encountered in

the analysis of the element have largely prevented its application in mineral exploration. The need for a fast, practical, and economic method for selenium analysis has, therefore, always been present.

5.11.2 Review of Present Methods of Selenium Analysis

Earlier methods of selenium analysis consisted mainly of a distillation technique from selenium tetrabromide, the detection limit being about 10 ppm, a value which is too high for normal geochemical samples (Robinson, et al., 1973; and Lakin, 1959). The more sophisticated methods of neutron activation used by Brunfelt and Steinnes (1967) and Kiesl, et. al. (1970), and the spectrofluorometric method employed by Schnepfe and Flanagan (1973) are too slow and expensive to be used in exploration geochemistry. The recent and a more feasible method appears to be the atomic absorption method by hydride generation. The first account of this method was given by Holak (1969), and this was followed by a series of reports by Madsen (1971), Dalton and Malanoski (1971), Fernandez and Manning (1971), Pollock and West (1972, 1973) and Thompson and Thomerson (1974). The principle of the method depends on the generation of covalent hydrides of Groups IV, V, and VI elements where the number of valency electrons are equal or greater than the number of orbitals, these include Ti, Ge, Sn, B, Si, Al, Bi, Te, Pb, and P, as well as As, Se, and Sb. Sodium borohydride ($NaBH_4$) has been found to be the best reducing agent and generator of hydrogen. The generated hydrides are measured by an atomic absorption spectrophotometer. A detection limit of 0.15 ug/litre selenium has been reported by Fernandez (1973).

A method similar to that of Thompson and Thomerson (1974) was investigated by S. Walton (pers. comm., 1975) a member of the Applied Geochemistry Research Group; this gave a detection limit of 4.1 ng/ml using 1 ml aliquots of standard solution. A precision of ± 12% at 50 ng/ml using 1 ml concentration and a working range of 5 ng/ml to 70 ng/ml was obtained.

The atomic absorption method of selenium analysis by the hydride generation technique appears to be particularly promising.

Two methods of selenium analyses were investigated by the author. These were the conventional colorimetric method and the microwave-induced argon plasma method.

5.11.3 Colorimetric Method of Selenium Analysis

Cheng (1956) used 3,3'-diaminobenzidine to determine selenium colorimetrically. Later Luke (1959) applied the separation of selenium by co-precipitation with arsenic. Mabuchi and Nakahara (1963) used a dithizone procedure for selenium determinations. However, investigations by Stanton and McDonald (1965) indicated copper interference and instability of the selenium complex for the latter procedure.

The method used by the author is essentially that of Stanton and McDonald (1965) who used a 3,3'-diaminobenzidine as the complex forming reagent. Details of the method are given in Appendix B.7. It should be noted that there are serious problems associated with this method as discussed below.

5.11.3.1 Discussion

As can be seen from the procedure (Appendix B.7), the method is long and tedious, involving two separations and two evaporation stages. The average productivity is about 15 samples per man-day. The linear calibration range is 0.5-30 ppm and the detection limit is about 0.5 ppm using a 1g sample. The precision was found to be bad and the results for batch analyses of the same sample set indicated a poor correlation (Table 5.12).

This poor correlation is probably related to the loss of selenium during the two evaporation stages. To evaluate the loss during the whole procedure, solutions containing 1, 5, and 10 µg selenium were treated in the same way as the samples. Care was teken not to over-dry and not to evaporate the acids vigorously. At the end of the procedure, the selenium contents of the solutions were found to be not detectable for the solutions originally containing 1 and 10 µg selenium, and 2.75 µg Se for the solution originally containing 5 µg Se.

These results suggest that considerable loss of selenium occurs during the evaporation stages and possibly some during the filtration stage.

The other problems with the method are the occasional formation of a white precipitate of ammonium perchlorate and the formation of white, brown, and purple gelatinous precipitates within the toluene phase. The former did not affect the readings. The latter problem, however, had a considerable effect on the spectrophotometric readings, a feature that is probably due to silica which had to be filtered off before the spectrophotometric determinations.

TABLE 5.12

Comparison of duplicate selenium analyses obtained for two different batch analyses

Rock sample number	First batch determination Se (ppm)	Second batch determination Se (ppm)
DR-2	0.5	0.5
DR-7	5.4	N.D
DR-18	1.6	2.1
DR-19	2.3	11.0
DR-27	3.0	2.9
DR-29	1.2	0.8
DR-38	N.D.	0.7
DR-48	N.D.	N.D

Because of poor precision and low productivity, this method was thought to be unsuitable for the author's investigations.

5.11.4 Microwave Induced Argon Plasma Analysis

5.11.4.1 Introduction

Plasma is an ionized gas with the concentration of electrons and ions being in equilibrium. It has the important property of sustaining large quantities of electrical energy which can then be used to obtain high temperatures. A plasma can be formed by dissociating and then ionizing gas molecules at atmospheric pressure by applying a high frequency electromagnetic field.

Analytical use of plasma has become important as a source of atomic vapor for absorption and emission spectroscopy. The atomization is achieved at temperatures above 5,000 K. For analytical purposes an inert gas is necessary to prevent the formation of ion-plasma complexes.

No attempt will be made here to give a complete review of plasma sources for emission spectrography. The interested reader is referred to review articles by Greenfield et al. (1975 a, b).

The use of plasma as an excitation source has become important because of the high electronic temperatures (as high as 10,000 K) attained by the plasma sources. This enables this type of source:

(a) to excite analytically useful spectral lines of a large number of elements,

(b) to reduce chemical and spectroscopic interferences, and self.absorption,

(c) to yield high sensitivities.

These three characteristics are all interrelated.

Three types of plasma emission sources are employed in the analytical field.

(i) Plasma jets. These operate on a d.c. power supply and are capable of being operated up to 100 kw (Greenfield et al., 1975a).

(ii) Microwave plasma generators. These are operated at frequencies greater than 300 MHz, the most common frequency being 2450 MHz. These are operated at lower power (up to about 120 watts).

(iii) High-frequency (radio-frequency) plasma generators operating at frequencies between 1-300 MHz. The high-frequency plasmas operate at relatively high powers (0.4-15 kw).

The low-powered microwave plasmas have been used for the determination of sulphur, phosphorus, and the halogens and certain other elements in solution (Murayama et al., 1968; Aldous et al., 1971 and Fallgatter et al., 1971).

Meyer and Lam Shang Leen (1973) and Meyer (1973) described an induction-coupled, microwave plasma system for the analysis of geochemical samples. This system was designed to analyse metal vapors evolved from solid samples through a temperature range of 20 to 1000°C. Solutions could also be used by vaporization of the residue after a solvent evaporation procedure.

The use of high-frequency plasma generators as excitation sources in optical spectroscopy have recently become more common than the low-powered microwave plasma generators. This is due to the following reasons:

(i) a plasma of any inert gas can be formed at atmospheric pressure with the radio-frequency plasma generators,

(ii) more stability and fewer problems of the extinguishing of radio-frequency plasmas,

(iii) better sensitivity and less interference due to the higher temperatures attained with the radio-frequency type of plasmas,

(iv) inexpensive and easy operation of the radio-frequency plasma generators.

Inductively coupled radio-frequency plasma sources have been used to determine sulphur and phosphorus (Kirkbright et al., 1972) and iodine, arsenic, mercury, and selenium in aqueous solutions (Kirkbright et al., 1973). Recently, there have been a number of successful attempts at using the induction coupled radio-frequency plasma generators as sources for multi-element atomic emission spectrophotometric analysis (Kirkbright and Ward, 1974; Greenfield, et al., 1975c; Scott and Kokot, 1975).

Among the attempts at selenium determination three can be mentioned. Aldous et al. (1971) determined selenium with a detection limit of 3.24 ppm using the 203.9 nm selenium line employing a microwave plasma generator operating at 2450 Mhz and 100 watts. Lichte and Skogerboe (1973) analysed selenium with a detection limit of 0.04 ppm using the 196 nm selenium line and employing the same type of plasma generator as that used by Aldous et al. (1971). And finally Kirkbright et al. (1973) determined selenium with detection limits of 0.11 and 0.16 using the 196.1 and 203.4 nm selenium lines by

employing a radio-frequency plasma generator operating at 36 MHz and 5kw.

5.11.4.2 Research and Development on an Inductively Coupled Microwave Plasma System for Selenium Analysis

5.11.4.2.1 Introduction

The aim of the present research in this field was to develop a fast and precise method of selenium analysis, and provided the method was applicable, to investigate the different forms of selenium in the primary and secondary geochemical environments by studying vapor evolution profiles. A better understanding of the geochemistry of selenium in the vicinity of volcanogenic sulphide environments could, therefore, be outlined. However, the author's research in this field failed to produce a useful method. Nevertheless, an account of this research points out several problems associated with low-powered microwave plasmas and sample introduction systems that may be of interest to future investigators in this field. The system used is essentially the one described by Meyer and Lam Shang Leen (1973) and Meyer (1973) with some modifications. The present research described here is the first real application of this system to the quantitative analysis of geochemical samples. The apparatus is fully described by Meyer and Lam Shang Leen (1973) and Meyer (1973), but, a short description will serve to orient the reader at this point.

5.11.4.2.2 Instrumentation

The microwave-induced argon plasma system used in present research consists of three parts: (a) sample

introduction, (b) vapor excitation, and (c) signal detection units (Figure 5.3).

(a) Sample Introduction: a Leco induction furnace operating at 14.6 MHz and 1500 w, was used to heat micro-crucibles (electrodes) of graphite, carbon and steel within a combustion tube (35 mm in internal diameter) placed concentrically in the coil of the furnace. The combustion tube extends into a 5 cm long and 2 mm internal diameter quartz tube heated by a coil to prevent condensation on the walls of the tube. The argon gas is introduced into the base of the combustion tube through a sample changer. The flow rate is read on a flow meter. The flow of argon forms the plasma as well as acting as a carrier gas for the evolved vapors. The iron, graphite, carbon, and gold-foil electrodes prepared were capable of holding 10, 10, 50, and 10 mg of sample. The temperature of the crucibles was controlled by a variable transformer attached to the induction furnace. Temperatures of 1100°C for the graphite crucible and 840°C for the iron crucible were obtained with full power. By heating the sample using full power a total analysis could be made and by slowly heating the sample vapor evolution profiles could be obtained.

(b) Vapor Excitation: the excitation of the vapor evolved was achieved by a Microtone 200 microwave generator operating at 2450 MHz. An alumel

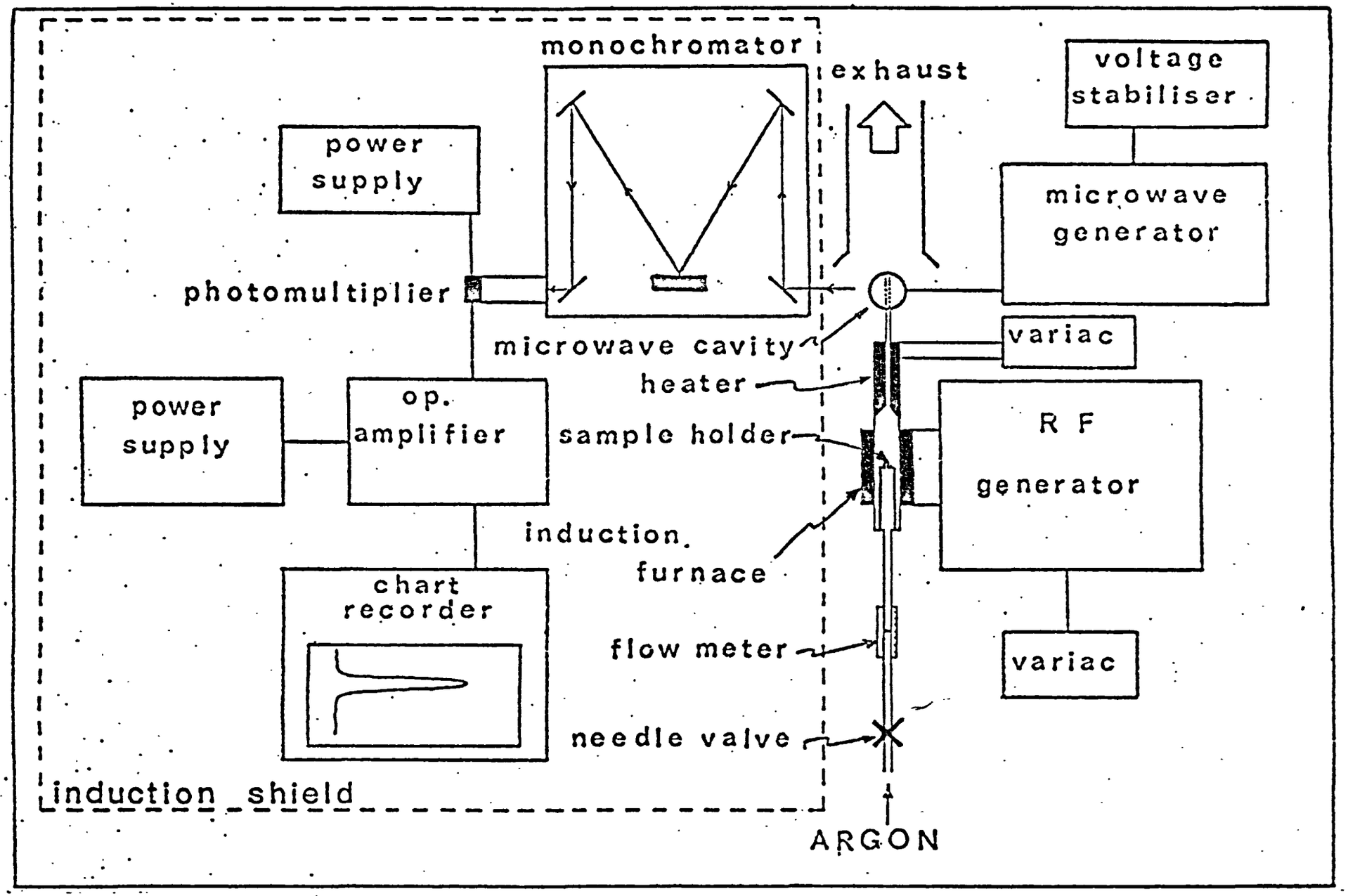


Figure 5.3 Schematic diagram of microwave-induced argon plasma emission system (after Meyer, 1973).

wire was attached to the quartz tube to ensure plasma stability.

(c) Detection System: radiation from the plasma was dispersed by a Czerny-Turner 0.3 - m monochromator with bilaterally adjustable slits. A photomultiplier connected to a negative EHT supply of 1.0 kV was used to detect the light at a particular wavelength. The signals were amplified by a chopper stabilized operational amplifier and displayed by a Servoscribe recorder. The whole detection unit was placed in an aluminum cage to reduce the effect of radio- and microwave - frequency interference.

A period of at least 30 minutes was necessary for the warm-up of the apparatus, especially the microwave generator. A particular spectral line of selenium (e.g. 196.1 nm) was located on the monochromator-detector system by adjusting the monochromator so that the maximum signal was obtained from the light emitted from the electrodeless discharge lamp of selenium.

5.11.4.2.3 Preparation of Standards

Two sets of solid standards were prepared by two different procedures. The first set of standards was prepared by weighing out 10g of specpure Johnson-Matthey rock base into a 100ml beaker and adding adequate amounts of selenium solution (i.e. for 1 ppm add 1 ml of 10 µg/ml solution of Se). Twenty ml of absolute alcohol were added and the whole stirred throughly to make a slurry which was then evaporated to dryness on a hot plate at 55°C. The material was ground

in an agate mortar, another 20 ml of absolute alcohol was added, and the mixture was stirred and evaporated as before. When dry, the standards were homogenized in a shaker mill for 15 minutes.

The second set of standards was prepared from an ignited tuff used as the rock base. Adequate amounts of selenium solutions were added to a 4g portion of the rock base, dried under an infra red lamp, and then homogenized thoroughly in a mechanical mortar for six hours.

The first set of standards gave a better calibration curve. This was probably due to better homogenization.

Liquid standards were analysed after adding aliquots of selenium standard solutions to a blank rock base in an iron electrode.

5.11.4.2.4 Investigations

The spectral lines of selenium, 203.9 nm and 196.1 nm, were investigated to find the most sensitive line. It was found that the 196.1 nm line gave the greatest sensitivity.

The argon plasma is formed by sparking a tesla coil at the tip of a quartz tube while the argon is flowing. The plasma generator was usually operated at about 80 W. Increases in power resulted in slight increases in sensitivity (Table 5.13).

Greater flow rates reduced the sensitivity due to dilution of the element vapor by large quantities of argon (Table 5.14 and Figure 5.4). High flow rates of argon also reduce the plasma temperature thus decreasing the number of excited atoms and lowering the sensitivity. The power and the argon flow rate are interrelated as far as plasma stability

Table 5.13 The effect of microwave generator power on the signal obtained by running a solid standard containing 5 ppm selenium

Power in watts	Signal intensity (Arbitrary divisions)
75	20
100	22
120	23

Table 4.14 The effect of argon flow rate on the sensitivity of the signal obtained by running a 5 ppm selenium solid standard

Flow Rate litres/minute	Signal intensity (Arbitrary divisions)
7	20
8	18
9	12

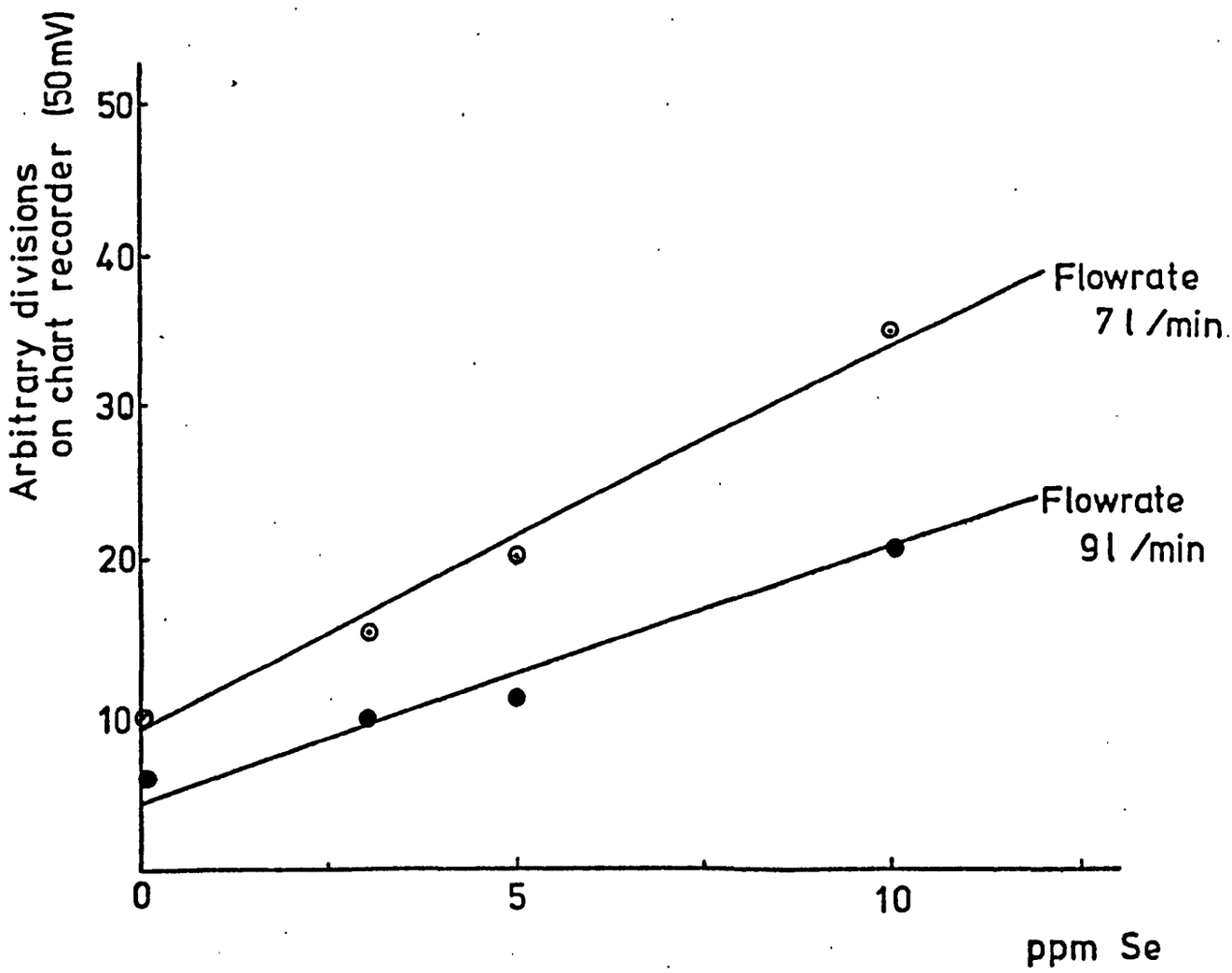


Figure 5.4 Effect of argon flow rate on calibration. The curves have been obtained with the solid standards.

is concerned. The best conditions for stability were obtained at a flow rate of 8 litres/min and a power of 80 watts.

It was found that the sensitivity changed considerably depending on which part of the plasma was being observed. The original viewing position of below the tip of the quartz tube was not used. Instead, the portion just above the tip of the quartz tube was viewed. Thus, the absorption by the quartz tube at the low wavelength range was avoided. Further absorbance was caused by the frosting of the quartz tube. The new viewing position above the tip of the quartz tube increased the sensitivity by a factor of two. A 50 ppm Se solid standard gave signal heights of 40 and 78 arbitrary divisions at the two referred positions.

The slits and the height on the monochromator were set to 0.05/0.05 and 6 respectively to obtain better signals at the 196 nm selenium line.

The effects of different electrodes on the release of selenium from the solid samples and standards were examined. The electrodes were made of iron, carbon, graphite, and gold foil.

Better results were obtained with the iron electrodes which gave much sharper peaks and less background interference (Figure 5.5). With the gold foil electrode an unstable plasma was obtained. This was thought to be due to the small mass of the crucible which caused a sudden evolution of vapors, and this in turn greatly diluted the plasma and at times resulted in an extinguished-plasma. The carbon crucible held about 50 mg sample from which the evolved vapors were usually too great for the low power plasma. The

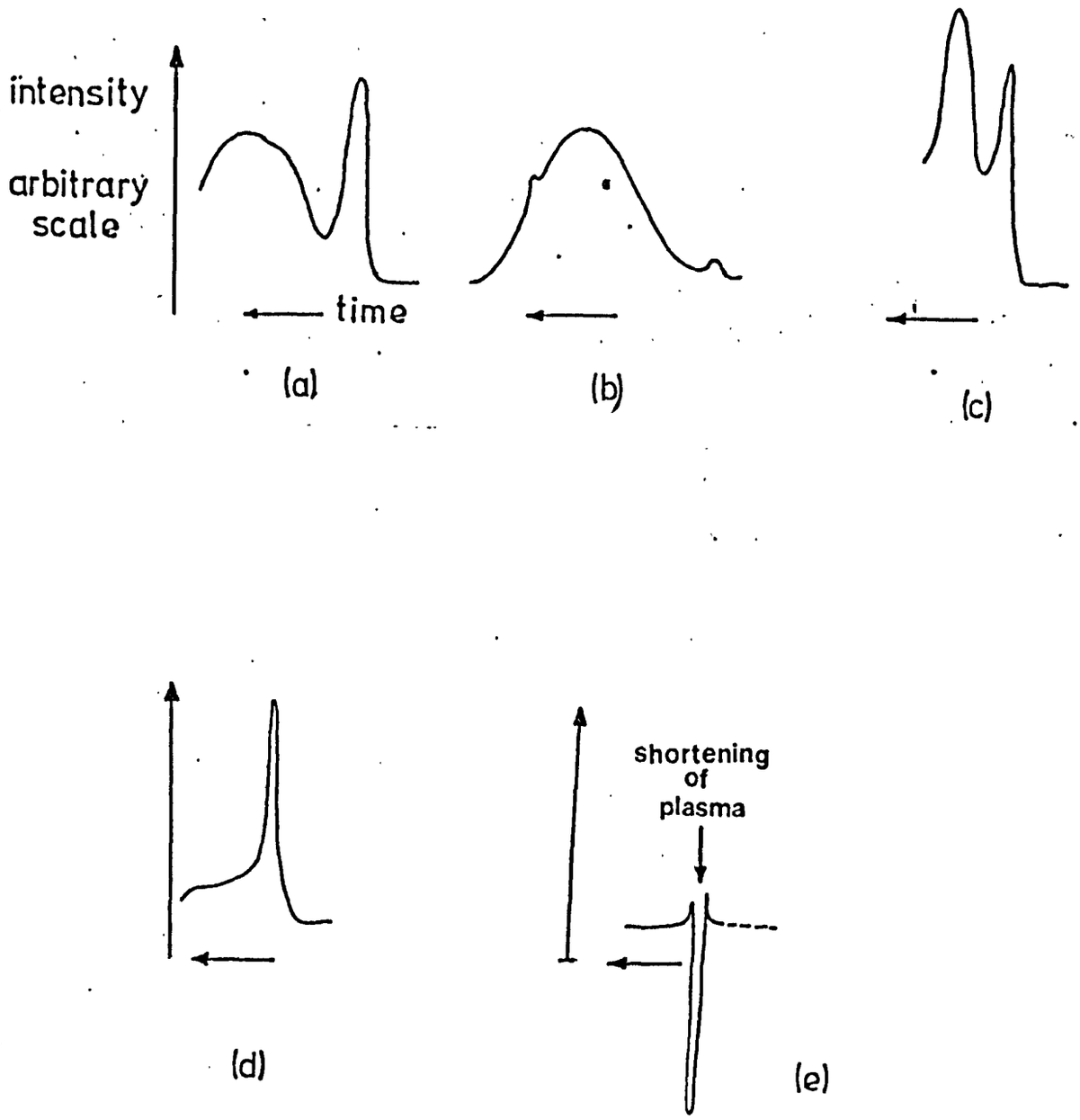


Figure 5.5 Typical signals obtained with different crucibles:

(a) carbon crucible containing 50 ppm Se standard heated at 600°C;
(b) blank solid standard heated in a carbon crucible heated to 600°C;
(c) graphite crucible containing 50 ppm solid Se standard heated to 600°C;
(d) empty iron crucible heated to 600°C after being left in air overnight;
(e) empty gold crucible heated to 500°C. Note the shortening of plasma.

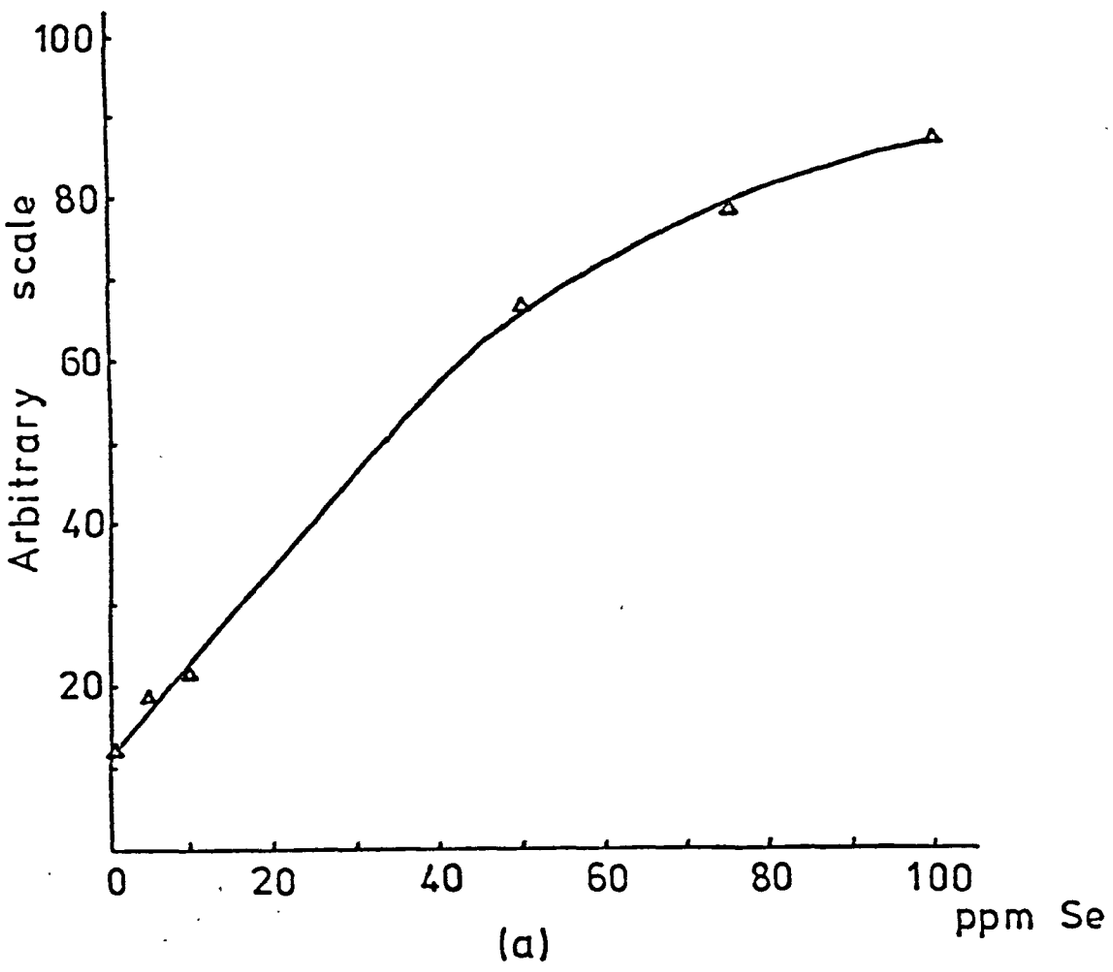
calibration curve obtained using solid Se standards and iron electrodes is presented by Figure 5.6a.

Aliquots of known amounts of selenium solutions were transferred to iron electrodes filled with a blank rock base. The standards prepared in this way gave a better calibration (Figure 5.6b). A dissolution procedure of preheating at 130°C was necessary before the final heating to 600°C.

5.11.4.2.5 Discussion

Many problems are associated with this type of sample introduction. Even when using solid samples of 10 mg in weight, the quantities of vapor evolved were more than the low power plasma could cope with. As a result an unstable plasma was obtained in most cases, often producing negative signals (Figure 5.5e). The vapors evolved are mainly water vapor, sulphur dioxide, and carbon dioxide. The water vapor evolved from the structure of different minerals at different temperatures caused problems by giving false signals due to the establishment of an unstable plasma. Even samples which were left in the open air for 15 minutes after being run at 600°C produced significantly strong signals which were thought to be related to adsorbed moisture from the atmosphere. Since different samples contained different amounts of constituent vapors, different backgrounds and matrix interferences were, therefore, present.

Because of background interference, calibration with the solid standards was not possible below 5 ppm Se. The calibration graph became flat above 50 ppm. With the solution standards in the blank rock base, concentrations down to 1 ppm could be measured, but much stronger signals were



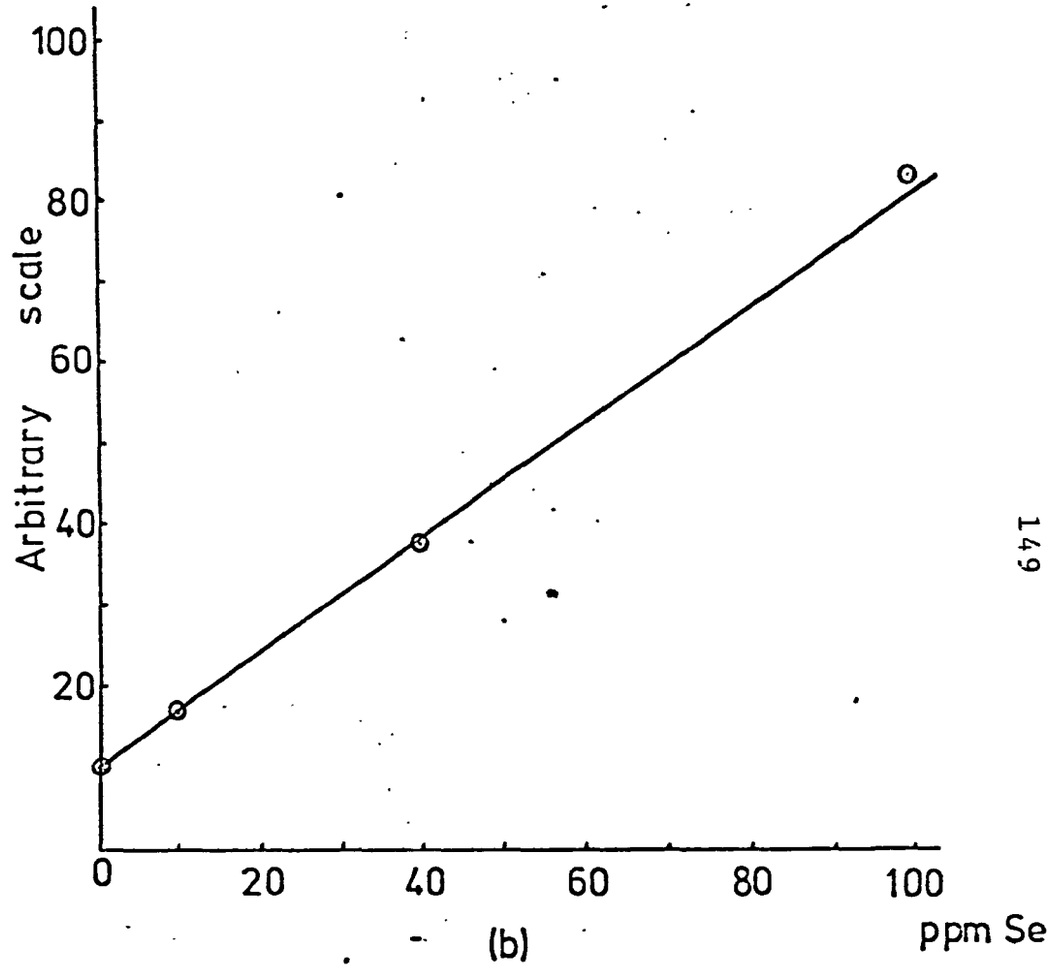


Figure 5.6 Calibration curves for selenium;

(a) Calibration curve obtained from solid standards prepared by using aliquots of Selenium solutions
(b) Calibration curve obtained by using aliquots of standard selenium solutions on blank rock base

obtained with the solid standards. This was thought to be due to the higher background contribution from the latter type of standards. The sources of interferences were investigated. The interferences are believed to have been caused by molecular bands of N_2 (Pearse and Graydon, 1950) and possibly OH.

Because of the high detection limits no attempt was made at quantitative analysis of samples. Initial analysis gave results which were higher than expected. Some qualitative vapor evolution studies were carried out, from which it was found that selenium in the elemental form was vaporized at 320°C using iron crucibles (Figure 5.7a). Selenium in the selenite (SeO_3) form was evolved from solid standards at 430°C. About 15 samples were slowly heated to obtain their selenium vapor evolution profiles. The most common peaks were obtained at 320°C, 370°C, and 430°C corresponding to selenium, structural selenium in pyrite, and selenite respectively (Figure 5.7).

5.11.4.2.6 Conclusions and Recommendations

The solid sample introduction system described here was unsuitable for the low power microwave plasma. Introduction of samples in solutions followed by evaporation of the solvent appeared to be more promising. A nebulising system involving a solvent evaporation procedure of the type used by Fallgatter et al. (1971) seems to be a feasible way of sample introduction.

More work needs to be done on the analysis of vapor evolution profiles to determine the different forms of

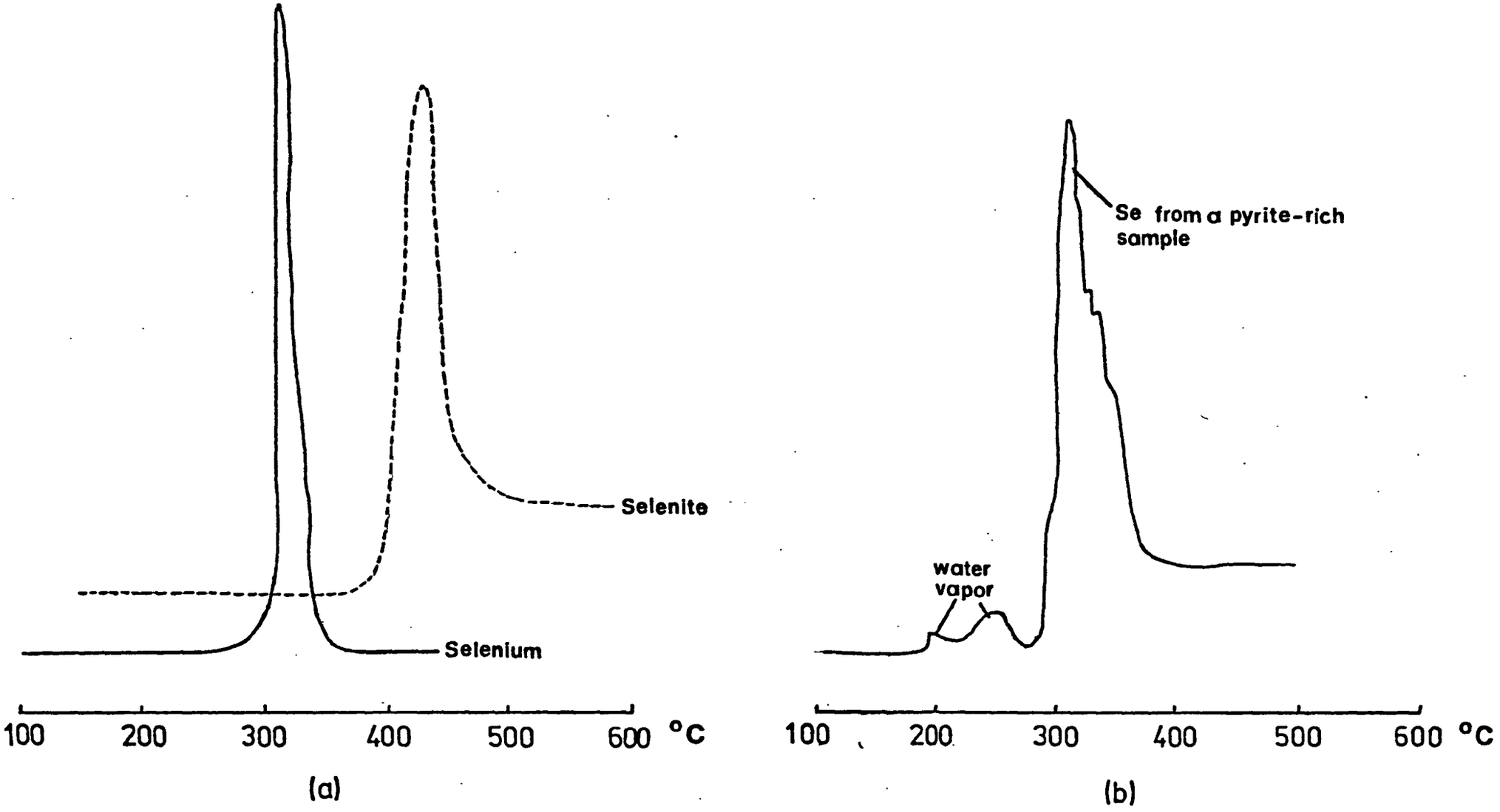


Figure 5.7 Vapor evolution profiles for different forms of selenium.

selenium in geochemical samples. This type of work could contribute considerably to an understanding of the geochemistry of this element.

CHAPTER 6

CHEMISTRY OF THE SULPHIDES

6.1 INTRODUCTION

Geochemical exploration for a particular type of deposit, requires data on the chemistry of the typical ore to ascertain the effective indicator and pathfinder elements. A good knowledge of the chemistry of the ores, combined with their ore mineralogy can also help in solving many questions about the primary and secondary dispersion of their constituent elements.

Ore samples from Madenköy, Kutlular, Tunca, Kotarak Dere, Sirtköy and Sarisu were analysed for Cu, Zn, Pb, Cd, Ag, As, Mo, Ba, Co, and Ni. Mercury was only determined in the Madenköy and the Kutlular ore samples, and fluorine only in the Madenköy drill-hole 110 ore samples. The analytical methods are described in Chapter 5.

Several samples of pyrite were separated from the ores of all the sulphide bodies. The techniques of separation used are summarized in Appendix A.2.6. The pyrite samples were analysed for Cu, Zn, Pb, As, Mo, Co, and Ni. The main purpose of these analyses was to investigate any differences present between the minor element chemistry of the pyrite from different types of sulphide bodies.

6.2 CHEMISTRY OF THE ORES

In common with most volcanogenic massive sulphide deposits of calc-alkaline rock association the economic sulphide bodies studied in this thesis are polymetallic in nature. All are enriched in base metals (with the exception of lead which occurs only in minor amounts), gold and silver,

as well as in many other elements such as Ba, Hg, As, and Cd. The contents of base metals and minor elements in each of the ore samples are controlled by the type and relative amounts of ore and gangue minerals in the particular sample.

At the Madenköy massive sulphide deposit the vertical mineral zoning observed and described in Chapter 4 is indicated by the chemical analysis (Tables 6.1 and 6.2). In this deposit the ore samples from drill-hole 110 represents the full range of zones present, the zoning being exemplified clearly by the Hg and As distributions (Figure 6.1). The contents of Pb, Zn, Cu, Cd, Ag, Ba, As, and Hg increase sharply towards the top of the ore; Mo is more concentrated in the black ore and remains constant in the other zones. Cobalt, and to a very large extent F, are enriched in the stockwork and impregnation zones. The Ni content decreases slightly towards the stockwork-impregnation zone of the deposit. The distribution of most elements such as Zn, Pb, Cd, Ag, Ba, As, and Hg are controlled to a large extent by the occurrence and abundance of sphalerite, galena, barite, and sulphosalts. For example, the As and Hg concentrations are mainly dependent on the content of sulphosalts, galena, and sphalerite which have their highest modal abundance in the black ore.

Tin was also analysed in a few ore samples from the Madenköy deposit, the content of which ranged from a few ppm to 945 ppm. The highest Sn content was found in a pyrite-sphalerite-rich ore sample. The Sb, Bi, Ge, and Au analyses carried out at the M.T.A. laboratories in Ankara gave ranges of N.D. (not detected) - 520 ppm; N.D. - 150 ppm, N.D.- 40 ppm; and N.D. - 2.6 ppm respectively for these elements. The

Table 6.1 Analysis of Samples from different zones of the Madenköy massive sulphide deposit in drill-hole 110. Element concentrations are in ppm unless otherwise stated (Location of drill-hole 110 is given in Figure 4.2).

Type of Zone	Sample Number	Cu	Zn	Pb	Cd	Ag	As	Mo	Hg (ppb)	Ba	Co	Ni	F
BLACK ORE	M-1	78000	66000	2350	260	109	1165	133	1723	32704	24	20	48
	M-2	75000	310000	1900	1200	128	4500	90	5830	2930	10	14	64
	M-3	45000	144000	1900	500	119	1750	79	7160	5547	21	24	104
	M-4	33000	59000	1050	180	76	1400	67	-	2398	16	12	70
Mean	4 Samples	57600	144800	1800	535	108	2072	106	3904	12280	18	18	
Disseminations in gray tuffaceous sandstone	M-5	8400	21000	620	80	17	225	83	598	5334	13	16	2030
	M-6	6200	13500	580	43	13	325	12.5	1550	2394	10	16	2030
YELLOW ORE	M-7	14700	11400	505	34	14	850	29	1395	2255	27	20	1040
	M-8	56800	14000	185	27	21	375	50	1395	1975	39	12	53
	M-9	3200	1120	145	8	5	380	25	1195	932	304*	10	97
Mean	3 Samples	28200	6810	197	23	13	667	35	1328	1721	33	17	
SILICEOUS-STOCKWORK ORE	M-10	1160	2100	310	10	6	650	50	1990	622	128	3	185
	M-11	340	3700	145	11	5	110	25	30	1082	188	6	248
	M-12	340	3000	50	10	5	75	5	155	105	103	17	650
	M-13	1200	1370	90	5	5	750	58	372	428	163	10	416
	M-14	13700	56000*	70	200*	7	275	50	1660	6459*	301*	19	510
Mean	5 Samples	3348	2543	133	9	6	372	38	841	559	146	11	
IMPREGNATION ORE	M-15	2000	270	40	3	3	33	29	86	64	64	4	780
	M-16	30000	470	185	4	4	75	20	66	712	77	8	864
	M-17	10100	2600	100	9	5	38	62	73	219	25	15	1200
	M-18	2700	3600	30	4	2	10	16	60	196	51	5	1320
Mean	4 Samples	13058	1630	71	5	4	40	32	71	298	54	8	

* Figures not included in calculation of means.

detection limits were respectively 100, 10, 10 and 1.5 ppm. All four elements are concentrated at the top of the massive ore and are undetectable in the stockwork and dissemination zones. Germanium has its highest concentration in zinc-rich

Table 6.2. Analysis of samples from different zones of the Madenköy massive sulphide deposit in drill-hole 101. All concentrations are in ppm.

Type of Zone	Number of Samples	Cu	Zn	Pb	Cd	Ag
BLACK ORE	7 samples	40400	167860	2840	615	22
YELLOW ORE	6 samples	37720	45430	1390	157	10
STOCKWORK AND IMPREGNATION ORE	4 samples	57350	6075	460	10	5

samples (about 25% Zn), and Au is more highly concentrated in Ag-rich samples (about 130 ppm Ag), the latter feature suggesting that the occurrence of electrum is the main controlling factor in the distribution of gold. Gold also occurs as rare inclusions in chalcopyrite in the lower levels of the massive ore.

Ore samples from drill-holes at the Kutlular, Kotarak Dere, and Tunca deposits were also analysed, and results are given in Tables 6.3, 6.4, and 6.5. Samples from the Kutlular deposit are mainly from the yellow ore; at Kotarak Dere only the massive pyrite and underlying stockwork and impregnation zones were sampled; and at Tunca only the stockwork-impregnation zone was sampled. The available samples from all of these deposits are probably too few to be representative.

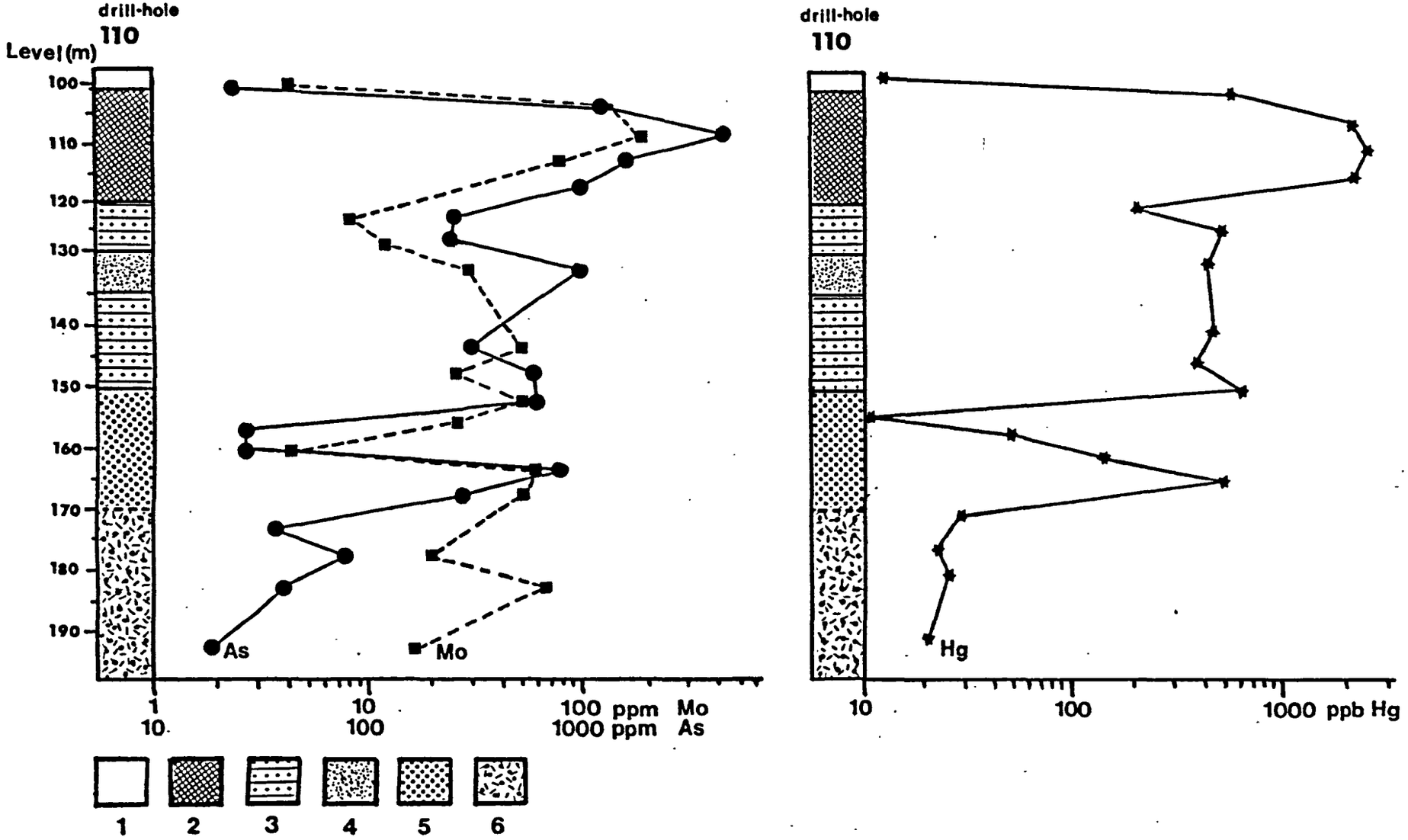


Figure 6.1 Vertical distribution of As, Mo, and Hg in the Madenköy sulphide ores (drill-hole 110) (1- pumice tuffs, 2- black ore, 3- yellow ore, 4- tuffaceous sandstone and pumice-tuff, 5- stockwork ore, 6- impregnation ore).

Table 6.3 Analysis of ore samples from drill-hole K-10 of the Kutlular massive sulphide deposit. Element concentrations are in ppm except for Hg which is in ppb.

Sample No.	Position of sample	Type of zone	Cu	Zn	Pb	Cd	Ag	As	Mo	Hg	Ba	Co	Ni
3123	22-23 m	Impregnations and veins in hanging-wall	25000	2300	200	29	7	40	25	60	685	33	13
3125	24-25.5 m	" "	34600	760	800	7	29	2200	65	374	273	59	45
3127	26-27 m	" "	68500	760	480	23	26	3500	220	136	23912	76	26
3130	30-31 m	" "	2640	1040	92	8	5	600	220	61	45170	30	18
3133	34-36.5 m	" "	36000	900	1200	-	-	300	95	-	23912	76	26
3136	39.5-41 m	Stockwork	409	147	67	3	16	113	5	36	655	5	8
3138	43-45 m	"	208	62	32	2	2	100	40	12	460	21	37

Table 6.4 Analysis of ore samples from the Kotarak Dere sulphide deposit.

All element concentrations are in ppm.

Sample No.	Position of sample	Type of zone	Cu	Zn	Pb	Cd	Ag	As	Mo	Ba	Co	Ni
Core-1												
D-1	2-2.5 m	Massive pyrite	1200	970	296	7	15	650	30	8969	3	27
D-2	7-8 m	Massive pyrite	320	220	92	5	4	450	29	-	20	16
466	6-6.5 m	Stockwork-	530	310	136	2	6	-	8	2598	3	44
462	10.5-11 m	"	1300	30000	32	110	5	-	19	1322	5	56
463	18-18.50 m	"	130	1800	32	7	2	-	1	900	2	60

Table 6.5 Analysis of surface ore samples from the Tunca ore deposit.

All concentrations are in ppm.

Sample No.	Type of zone	Cu	Zn	Pb	Cd	Ag	As	Mo	Ba	Co	Ni
TO-1	Stockwork-impregnation	230	300	52	1	1	58	7	746	4	53
TO-2	" "	4200	1070	320	6	43	650	15	2439	2	74
TO-3	" "	710	29000	280	79	8	150	1	11122	5	46
405	" "	280	370	140	1	3	60	3	353	3	52
406	" "	73	1800	36	5	2	11	1	2191	3	30

The general decrease of base metals and other minor elements from the top of the massive ore into the stockwork and dissemination zones observed in the Madenköy deposit is present in the Kutlular and Kotarak Dere orebodies. However, in the last deposit the Cu and Zn contents in the stockwork and dissemination zones are higher than in the massive pyrite. The decreasing trends shown by As and Hg in the Kutlular ore are more regular than those of the other elements.

Ore samples from the stockwork and impregnation zones of the Tunca deposit have comparable amounts of base metals, Ag, As, Mo, and Ba with those of the Madenköy, Kutlular, and Kotarak Dere deposits. The Co contents in the Kutlular, and especially in the Tunca and Kotarak Dere ores, are considerably lower than those in the Madenköy ores. For the Kutlular ores, Co > Ni; for the Kotarak Dere and Tunca ores Co < Ni.

Mineralized samples from the Sirtköy and Sarisu occurrences contain lower contents of As, Mo, Ag, and Ba (Tables 6.6 and 6.7), especially Sarisu which contains very low quantities of Cu, Zn, Pb, and Cd as well as As, Mo, Ag, and Ba. The Co content of the ores from these two occurrences are higher than all the other deposits except the Madenköy deposit. The average Co/Ni ratio for both the occurrences is about 1.5.

Ores from the Lahanos, Kizilkaya, and other deposits were analysed by Tuğal (1969). The results are within the range encountered in the deposits studied in this thesis. The mean contents were 0.42% Cu, 0.30% Zn, 0.69% Pb, 150 ppm As, 93 ppm Mo, 25 ppm Mo, 4 ppm Ag, and 15 ppm Ni. Leitch (1975) analysed ore concentrates from the pyritic ore zones

Table 6.6 Analysis of surface ore samples from the Sirtköy barren stockwork-impregnation mineralization. All concentrations are in ppm.

Sample No.	Type of zone	Cu	Zn	Pb	Cd	Ag	As	Mo	Ba	Co	Ni
SO-1	Stockwork-impregnation	660	202	172	1	1	12	1	393	70	20
SO-2	" "	1060	430	28	2	1	7	2	61	34	33
SO-3	" "	1760	116	10	2	1	18	4	74	34	33
SO-4	" "	350	147	10	1	1	<4	1	56	19	21

Table 6.7 Analysis of mineralized surface samples from the Sarisu barren pyrite-impregnation mineralization. All concentrations are in ppm.

Sample No.	Type of zones	Cu	Zn	Pb	Cd	Ag	As	Mo	Ba	Co	Ni
SSO-1	Impregnation	10	24	10	1	<1	<4	15	-	48	20
SSO-2	Impregnation	38	38	10	3	1	<4	1	41	16	21
SSO-3	Impregnation	28	29	15	3	1	<4	2	48	12	15
SSO-4	Impregnation	28	23	24	1	1	<4	3	74	24	14

of the Lahanos and the Kizilkaya deposits and found logarithmic mean contents of 280 ppm Cu, 55 ppm Zn, 155 ppm Pb, 400 ppm As, 9 ppm Ag, 23 ppm Co, and an arithmetic mean of 82 ppm Ni for the Lahanos deposit; and logarithmic means of 490 ppm Cu, 180 ppm Zn, 130 ppm Pb, 250 ppm As, 7 ppm Ag, 29 ppm Co, and an arithmetic mean of 65 ppm Ni were calculated for the Kizilkaya deposit. Gold assays performed by the Black Sea Copper Company (K.B.I.) gave 1.7 and 1.1 ppm for the black and yellow ores of the Lahanos deposit, and 0.15 ppm for the Kizilkaya ores.

From the ore chemistry studies it is clear that As, Hg, Ag, Cd, Pb, Zn, and Ba are concentrated in the massive ore. It is probable, therefore, that the secondary dispersion of these elements can be useful in distinguishing between the different types of sulphide deposits. Copper and Mo in the secondary environment could be good indicators of the mineralization in general, but their use in discriminating between the different types appears to be inadequate.

6.3 MINOR ELEMENT CHEMISTRY OF THE PYRITE

6.3.1 Previous Work and Objectives of the Study

As far as the ore genesis is concerned considerable emphasis has been placed on Co and Ni, and to some extent S, Se, and As in pyrite and coexisting sulphides (Loftus-Hills and Solomon, 1967; Bethke and Barton, 1971).

Auger (1941) and Hawley (1952) studied the distribution of several minor elements in the pyrite of Canadian gold deposits. No discernible regularities in the distribution of As with depth, temperature of formation, or grain

size was found by these workers. Cobalt followed a similar pattern to As except that it was more abundant in the high temperature pyrite, thus giving rise to higher Co/Ni ratios in this phase of pyrite. Carstens (1941 and 1942, in Fleischer, 1955, p. 999 and 1004), analysed hydrothermal and sedimentary pyrite and found that the Co contents of the hydrothermal pyrite were considerably higher (mean of 500 ppm) than those of the sedimentary pyrite (usually less than 100 ppm). Furthermore the Co contents were higher than the Ni contents in the hydrothermal type whereas the reverse was true for the sedimentary type. Similar results were obtained by Hawley and Nichol (1961) who found higher Co and Ni contents and Co/Ni ratios for hydrothermal pyrite. Sinclair (1971) analysed pyrite from the No. 5 and H ore bodies of the Horne mine at Noranda, Quebec. His results indicated that the pyrite from the H ore body contained significantly higher contents of Co and Se, both of which decreased with depth. As a result he suggested that the two ore bodies were formed independent of each other. Tuğal (1969) analysed four pyrite samples from the Lahanos mine and several pyrite concentrates from a number of deposits in the Eastern Black Sea Region. He could not detect Co in any of the pyrite samples and could only detect As in one pyrite sample (487 ppm As), whereas Ni ranged between 21 and 75 ppm with a mean of 39 ppm. However, pyrite concentrates from several deposits gave Co/Ni ratios within the range of 0.52 and 102.10, most ratios being generally greater than one.

Following the observation that pyrite-rich samples in the Madenköy deposit contained more As than similar samples from the Sirtköy and Sarisu areas and the above studies,

emphasising the relationship between trace element content or pyrite and ore genesis, the author decided to analyse pyrite samples from the various types of mineralization in the Eastern Black Sea Province in an attempt (a) to shed light on the genesis of the deposits under consideration, and (b) to determine any diagnostic differences between pyrite from the stockwork and dissemination zones of economic and noneconomic deposits, differences which hopefully would have a practical use in geochemical exploration.

Ideally, such a study should be carried out by electron microprobe analysis which would eliminate the factors (e.g. exsolution and occluded material) affecting the distribution of As and other minor elements in the pyrite-rich samples. Attempts by the author to analyse pyrite for Cu, Co, Ni, and As by a Cambridge electron micro analyser and Geoscan were, however, negated by the high detection limits of both these instruments for these elements. Consequently the author had to resort to the less efficient method of wet-chemical analysis. The technique for separating pyrite from other sulphides and gangue minerals is a long and tedius one (Appendix B.6). It was difficult to obtain pure pyrite samples due to the fine intergrowth of various ore minerals, especially in the case of massive sulphide samples. For example, pyrite sample CONC-1, separated from the top of the Madenköy massive ore, contained 7% Zn and 6% Cu (Table 6.8). However, some of the pyrite samples from the Murgul and Kutlular deposits were coarse grained enough to minimize impurities. Polished section and binocular microscope examinations of all the pyrite samples were made to ensure a good separation.

Only a limited number of pyrite samples could be obtained due to the small number of mineralized samples available, particularly from the Sirtköy and Sarisu areas. The data are, therefore, too limited to draw any statistically valid conclusions. Nevertheless, the study yielded some tentative results as regards the minor element chemistry of the pyrite and its bearing on the genesis and exploration of these deposits.

Copper, Cu, Zn, Pb, Ag, and Cd were also analysed in addition to Co, Ni, and As in order to determine the presence of any impurities in the samples.

6.3.2 Results

Pyrite samples separated from core samples obtained from drill-holes 110 and 101 in the Madenköy deposit were analysed, and the results are tabulated in Table 6.8. The results suggest that As is higher in the upper levels of the orebody and decreases gradually downwards. However, at the top of the orebody the presence of chalcopyrite, sphalerite, galena, and tetrahedrite-tennantite is indicated by the high concentrations of Cu, Zn, Cd, Pb, and Ag. In these samples it is difficult to determine how much of the As is due to the above mentioned impurities and how much of the element occurs as an isomorphous substitute. Co and Ni show no systematic variation with depth, and except for the first impure pyrite sample the Co contents are considerably higher than the Ni contents for the Madenköy pyrite.

The trace element contents of pyrite from the other deposits and occurrences are presented in Table 6.9. In the economic deposits - Kutlular, Kotarak Dere, and Tunca - the

TABLE 6.8 Trace element contents of pyrite from the Madenköy massive sulphide deposit. Elemental concentrations are in ppm.

Sample No.	Drill Hole	Level M.	Cu	Zn	Pb	Mn	Ag	Cd	As	Co	Ni	Remarks-Type of Zone
CONC-1	110	102.34-107.70	63600	70400	256	340	105	340	2000	36	40	Top of black ore, impurities present in sample.
CONC-2	110	145.00-150.20	10100	800	128	32	5	7	1300	188	16	Yellow ore
CONC-3	110	161.65-165.35	12000	920	144	44	5	7	1450	200	16	Stockwork zone
CONC-4	110	165.35-170.00	11300	46000	84	32	8	240	200	116	16	Stockwork-impregnation zone
CONC-5	110	170.00-175.50	850	2520	100	32	4	15	130	116	14	Stockwork-impregnation zone; pure pyrite
CONC-6	110	185.20-190.10	248	168	40	-	3	7	30	192	40	Stockwork-impregnation zone
CONC-14	101	198.50-204.95	27600	1272	104	30	8	7	180	200	28	Yellow ore
CONC-15	101	204.95-209.15	15000	2080	72	48	7	5	120	192	36	Stockwork-impregnation zone

Table 6.9 Trace element contents of pyrite from Murgul, Kutlular, Tunca, Kotarak Dere, Sirtköy, and Sarisu. All elemental concentrations are in ppm.

Mineralization	Sample No.	Remarks-Type of Zone	Cu	Zn	Pb	Mn	Ag	Cd	As	Co	Ni
MURGUL	A-1	Dissemination zone (hand-picked pyrite)	2600	17	36	12	4	5	80	40	16
	A-2	Dissemination zone (hand-picked pyrite)	750	11	32	12	4	5	80	56	16
	C-1	Dissemination zone (hand-picked pyrite)	590	84	98	12	3	5	1400	20	12
	C-2	Stockwork zone	250	312	36	8	3	6	130	40	12
	Mean	4 Samples	1048	106	51	11	4	5	97*	39	14
KUTLULAR	K-1	Dissemination zone (hand-picked pyrite)	310	176	48	28	3	6	250	76	56
	K-3	Massive yellow ore (chalcopyrite impurity present)	14700	188	92	36	9	5	75	128	56
	K-4	Stockwork zone	170	320	64	4	3	5	240	56	12
	Mean	3 Samples	240*	248	56	16	5	5	188	66	34
TUNCA	T-1	Stockwork zone	1300	136	52	28	5	5	42	84	60
	T-2	Massive ore; impurities present	430	900	220	20	6	6	400	20	30
	Mean	2 Samples	865	518	52*	24	6	6	42*	52	45
KOTARAK DERE	D-1	Stockwork zone	520	440	140	20	3	5	550	20	16
	D-2	Massive pyrite zone	250	256	108	24	3	4	450	24	16
	Mean	2 Samples	385	348	124	22	3	5	500	22	16
SIRTKÖY	S-1	Stockwork-impregnation	590	400	40	2	2	4	65	416	124
SARISU	SS-1	Stockwork-impregnation	24	2	32	2	2	4	6	184	100

* Maximum concentrations of elements not included in the calculation of the mean

As contents of pyrite are similar to those of the Madenköy deposit and relatively higher than those of the Sarisu and Sirtköy occurrences. The As content for the Sirtköy pyrite is, however, within the range observed for a number of economic deposits. Pyrite from the Sarisu impregnation occurrence is distinctly lower in As, and although only one pyrite sample was analysed from this occurrence it is believed to be representative; analyses of a few mineralized samples containing pyrite from this occurrence also gave very low As concentrations (Table 6.7).

The contents of Ni and Co in the pyrite from the Sirtköy and Sarisu area are higher than those of the economic deposits. The exception being the Co content of the Madenköy pyrite which is comparable with that of the Sarisu pyrite, but still considerably lower than that of the Sirtköy pyrites.

Following from the results discussed above, an attempt was made to find a simple factor which could discriminate between economic and barren mineralization. The ratio As/(Co + Ni) ratios for pyrite from the stockwork-impregnation zones was found to be the best diagnostic parameter for this purpose.

The As/(Co + Ni) ratios for pyrite from the stockwork-impregnation zones of the various deposits studied are presented in Table 6.10. The results suggest that this ratio is a good discriminator between economic and barren mineralization. Only one sample from the Madenköy deposit has a similar ratio to that of the Sirtköy mineralization.

Pyrite is a common and widely distributed mineral in areas of different types of sulphide mineralization. Thus, sampling of exposed mineralization and subsequent pyrite

Table 6.10. The As/(Co + Ni) ratio of pyrite samples from the stockwork and dissemination zones of various types of mineralization.

Sample Number	Deposit (Mineralization)	As/(Co + Ni) ratio
CONC-4	MADENKÖY (Massive)	1.5
CONC-5		1.0
CONC-6		0.1
CONC-15		0.5
A-1	MURGUL (Stockwork)	1.4
A-2		1.1
C-1		43.8
C-2		2.5
K-1	KUTLULAR (Massive)	1.9
K-4		3.5
T-1	TUNCA (Massive)	0.3
D-1	KOTARAK DERE (Stockwork-eroded massive sulphide)	15.3
S-1	SIRTKÖY (Stockwork-impregnation)	0.1
SS-2	SARISU (Impregnation)	0.02

analysis provides a useful approach for regional assessment of mineralized zones. However, the problems of representative sampling and efficient separation of pyrite free of impurities severely limits this technique as an exploration tool. There is a need for more data and further investigation before any firm conclusions can be drawn about the use of this method in geochemical exploration for massive sulphides.

CHAPTER 7

HYDROGEOCHEMICAL EXPLORATION

7.1 INTRODUCTION

The presence of a well developed dentritic drainage pattern fed by a year round active ground water flow makes hydrogeochemical surveying a practical exploration tool in the Eastern Black Sea Region. The streams in the area have steep gradients and high erosive capacities with considerable material being introduced from unstable slopes.

The stream waters are clear, except after heavy rainfalls, and they generally have a near neutral pH. Oxidation processes, in the vicinity of sulphide bodies are generally expressed in the stream waters by pH values as low as 4 or less.

A regional drainage survey was carried out by M.T.A. in part of the region between Rize and Findikli using Cu, Zn, Pb, and Mo in stream sediments with a sample density of one sample per square km (Yegülalp et al., 1972). This survey delineated all of the major mineralized zones in that part of the region, except the Tunca deposit. In the Tunca area the anomalies were probably masked to a considerable degree by high dilution in the Tunca river which is the only drainage channel associated with this deposit.

In the present study the pH of stream waters was determined in conjunction with D.R. Boyle using the method of Boyle and Troup (1976) (See Chapter 5.9.2). A reconnaissance stream sediment survey in the Çayeli area, and more detailed drainage sampling in the Madenköy, Sirtköy, Sarisu, and Kutlular areas, were carried out with the following objectives in mind:

(a) To investigate the efficiency of regional geochemical stream sediment surveys in exploration,

(b) To determine useful indicator and pathfinder elements and to study the factors controlling their dispersion,

(c) To determine the regional and local background and threshold values for (b), and

(d) To investigate the possible use of these indicator and pathfinder elements in distinguishing between different types of sulphide mineralizations.

During the field work 205 spring and stream sediments were collected from the Çayeli and Kutlular areas. The reader is referred to Appendix A for sample collection and preparation methods. The samples were analyzed for Cu, Zn, Pb, Ag, Cd, Mo, Fe, and Mn. Barium was only analysed in selected samples from the Madenköy and Sirtköy areas. All of the analytical methods used are described in detail in Chapter 5. The sample sites were plotted on maps and are presented in Figures 7.1, 7.2 and 7.3.

7.2 DATA PROCESSING AND INTERPRETATION

All the elemental values were entered on punched cards, and routine statistical parameters such as means, standard deviations, ranges, and correlation coefficients were computed. During the data processing some highly anomalous samples were excluded from the data to prevent a bias in the results. A summary of the results is given on Table 7.1.

A second program was used to plot normal and lognormal histograms and cumulative probability distributions. It was found that all elemental distributions were best approximated

by a lognormal distribution. From the lognormal cumulative plots, estimates of the mean, the mean plus one standard deviation, and the mean plus two standard deviations were calculated; the limits of the class intervals were set at these levels. Because of the poor precision of the analytical method for Mo at low concentrations, the first two classes were combined in order to avoid a high background variation for this element.

Estimates of the regional background values for the various elements were made by using the stream sediments collected to the east and south of the Madenköy deposit where no mineralization is known to occur. The average regional background contents for the elements studied correspond to the geometric means for the total data. The geometric means and the other parameters for the background data are presented in Table 6.2.

A comparison of Table 7.1 (total data) and Table 7.2 (selected background data) suggests that when estimating the average regional background contents of elements from the total (background and mineralized) data it is best to take the geometric mean or 50th percentile value from the logarithmic cumulative curve.

7.3 pH OF SPRING AND STREAM WATERS

The pH values for spring and stream waters in the Çayeli (Sirtköy, Sarisu), Madenköy (also includes drill-hole waters), and Kutlular areas are presented in Figures 7.1, 7.2 and 7.3 respectively. The pH values obtained from 70 measurements range from less than 4 to as high as 8.5. The regional background is about 7.

Table 7.1 Statistical summary of total stream sediment data (total number of samples is 205)*.

Element (in ppm unless stated)	Number of samples	Range of values	Means		50th percentile	Standard deviations		Correlation coefficients								
			Arith.	Geom.	(Log_{10} distrn)	Arith.	Geom.	As	Cu	Zn	Pb	Ag	Cd	Mo	Mn	Fe
As	199	1.5 - 175	14	4.7	3	27	3.9	1.00								
Cu	197	2 - 4600	127	40	33	362	4.6	0.38								
Zn	197	16 - 9900	346	115	69	1110	3.3	0.41	0.73							
Pb	197	4 - 2640	56	25	17	203	2.8	0.49	0.91	0.87						
Ag	146	0.5 - 80	1.8	0.9	0.7	6.7	3.1	0.40	0.95	0.76	0.98					
Cd	197	0.5 - 190	3.3	1.6	1.8	14.7	2.4	0.50	0.93	0.95	0.99	0.99				
Mo	170	0.5 - 14.1	2.4	1.3	1.4	1.7	2.5	0.52	0.50	0.41	0.48	0.48	0.67			
Mn	178	112 - 7000	1121	775	785	825	1.5	-0.08	-0.03	-0.11	-0.07	-0.07	-0.03	-0.01		
Fe%	178	0.6 - 11.2	3.7	2.6	2.4	2.2	1.7	0.08	0.16	-0.08	-0.05	-0.05	-0.02	0.25	0.39	1.00

* Not all the samples were analysed for all elements and very highly anomalous samples were excluded from the computations.

Table 7.2 Statistical summary of Stream sediment data from background areas.

Element (in ppm unless stated)	Number of samples	Range of values	Means		Standard deviations		Correlation coefficients								
			Arith.	Geom.	Arith.	Geom.	As	Cu	Zn	Pb	Ag	Cd	Mo	Mn	Fe
As	51	1.5- 8	2.6	1.9	1.9	3.4	1.00								
Cu	51	2 - 106	28	15	27	3.4	0.18								
Zn	51	25 - 280	95	88	42	1.5	-0.09	0.09							
Pb	51	4 - 60	17	15	9	1.7	0.43	0.49	0.11						
Ag	51	0.5- 1	0.9	0.9	0.2	1.3	0.07	0.29	0.15	0.34					
Cd	51	0.5- 2	1.3	1.1	0.6	1.6	0.13	0.66	0.20	0.34	0.18				
Mo	51	0.5- 3.5	1.3	1.1	0.6	2.1	0.16	-0.10	-0.27	0.14	0.04	-0.27			
Mn	51	280 -3440	1329	1133	681	1.9	0.26	0.55	0.36	0.85	0.37	0.47	-0.05		
Fe%	51	0.6- 6.0	2.9	2.5	1.3	1.5	0.13	0.61	0.53	0.44	0.51	0.60	-0.13	0.63	1.00

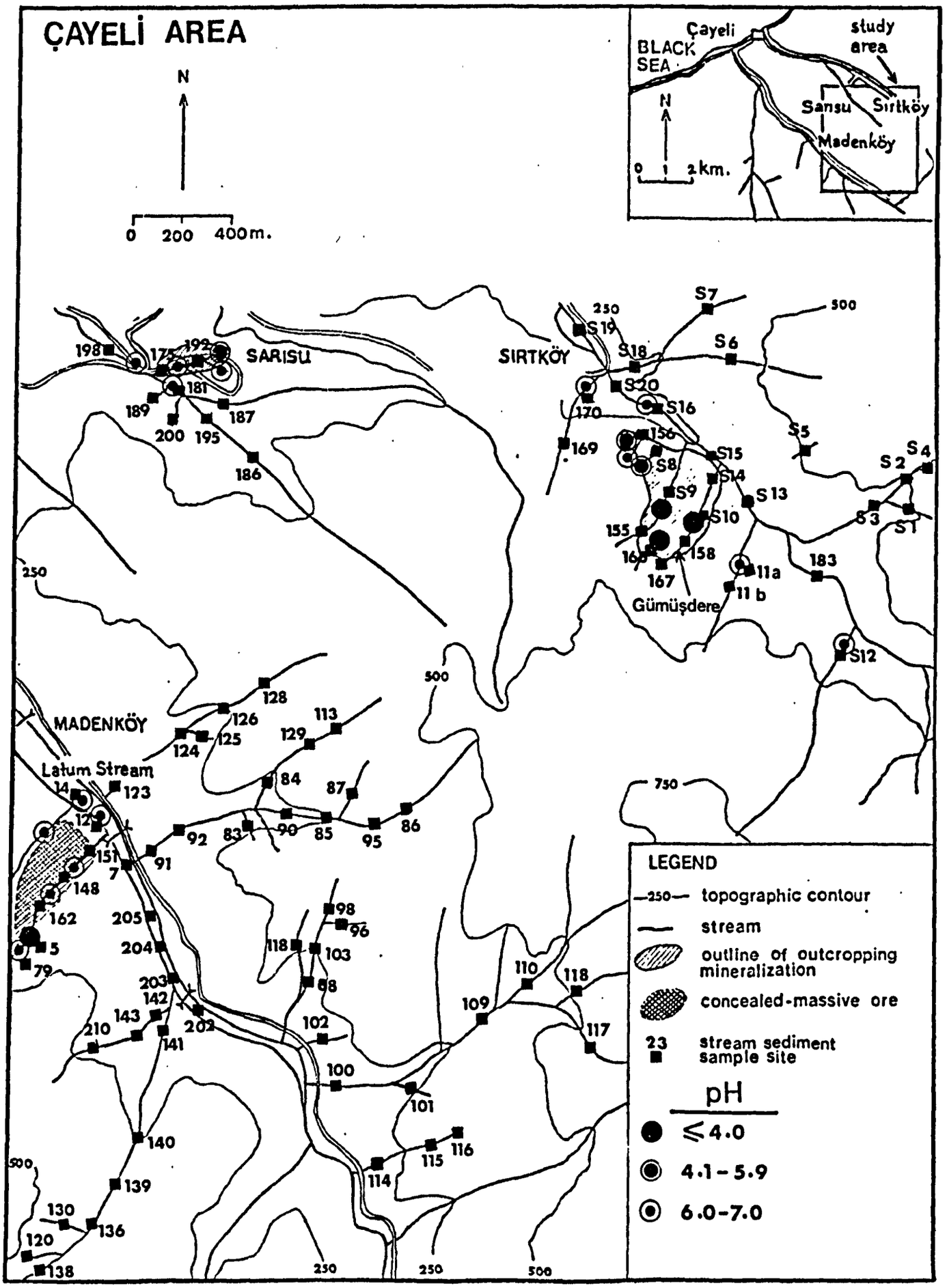


Figure 7.1 Stream sediment sample sites and the pH of stream and spring waters, Çayeli area.

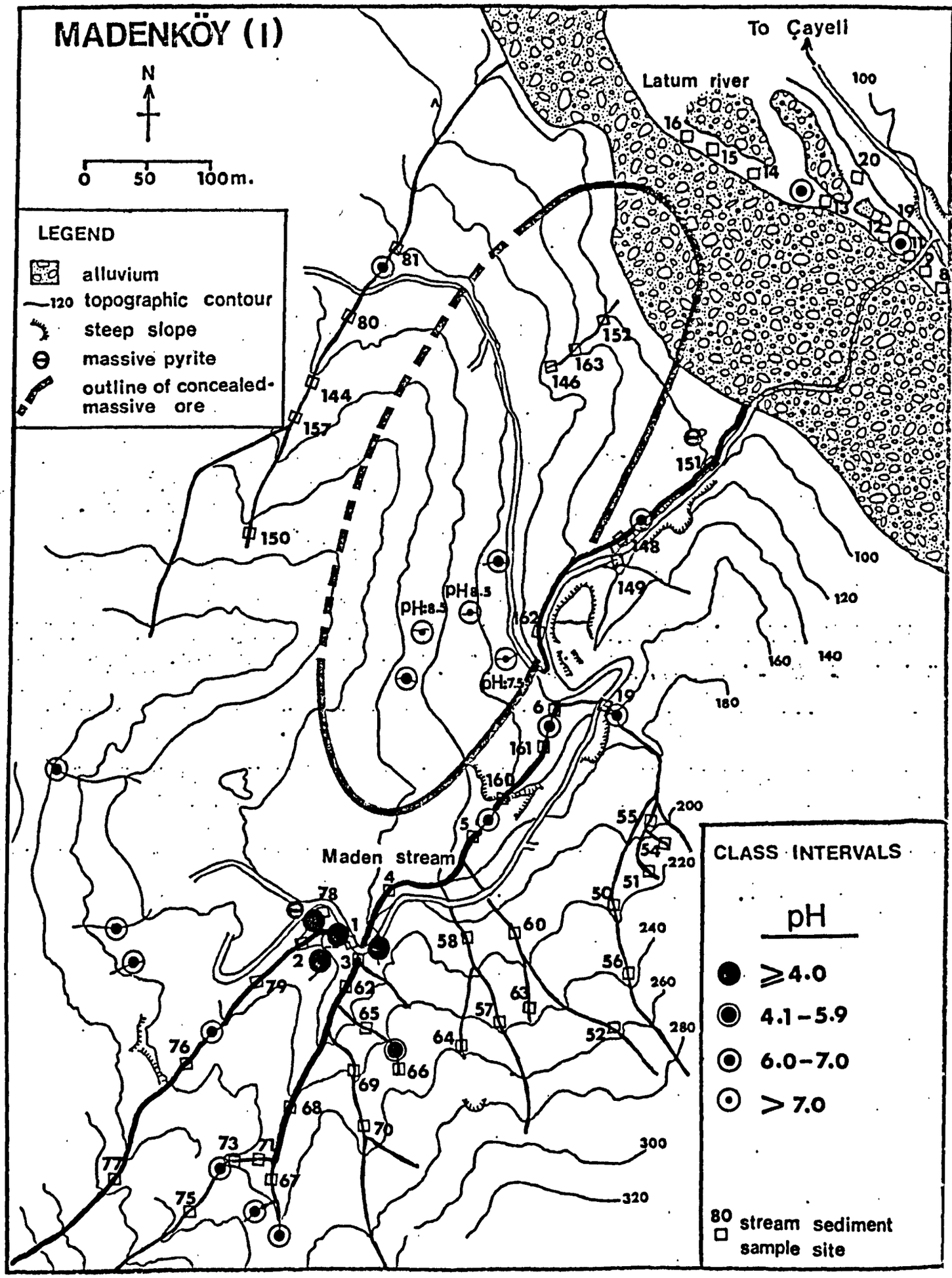


Figure 7.2 Stream sediment sample sites and the pH of stream and spring waters, Madenköy area.

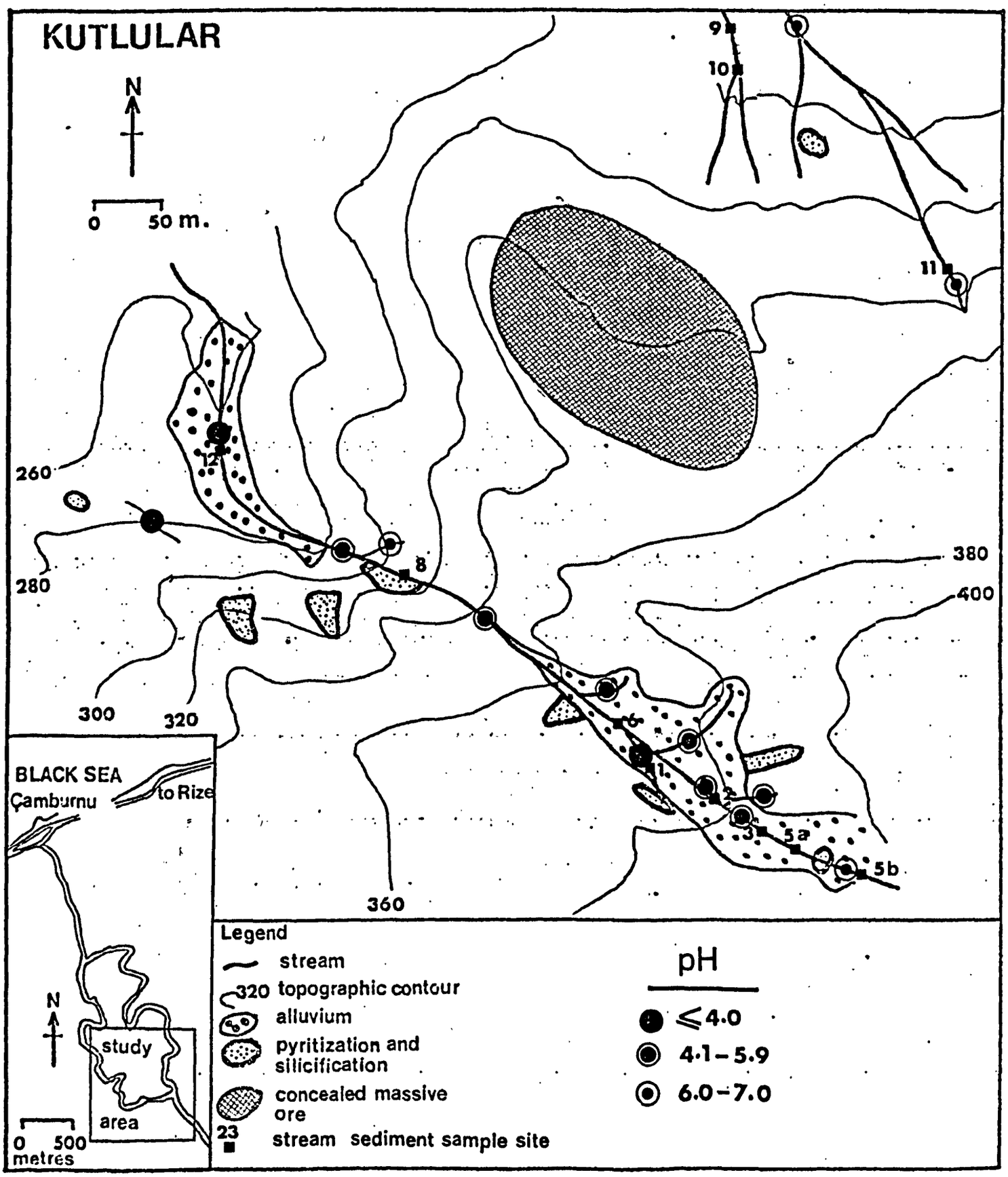


Figure 7.3 Stream sediment sample sites and the pH of stream and spring waters, Kutlular area.

The third order streams traversing the impregnation zone of the Madenköy deposit usually have pH values within the range 4 to 5 (Figure 7.2). These acid waters are neutralized as soon as they join a lower order stream. For instance, Maden stream, a second order stream traversing the stockwork and impregnation zone of the Madenköy deposit, had an acid pH only at one point on its course. The general pH values in the Maden stream and the Latum river are constant at 7. Three alkaline pH measurements were encountered over the concealed massive sulphide deposit. Two of them were drill-hole waters having pH values of 8.5, and the third was a seepage giving a pH measurement of 7.5. These waters are believed to have come in contact with or were in equilibrium with the pumice tuffs and carbonate rocks.

The pH values for the spring and stream waters near the mineralized Sirtköy area range from 4 to 6.5. The pH is about 4 for waters in Gümüşdere stream draining the gossan (Figure 7.1).

In the Sarisu area, the pH of spring and stream waters ranges from 5.5 near the mineralization, to 7.0 in the immediate surroundings (Figure 7.1).

In the Kutlular area the pH values range from less than 4 to 7. The strongly acidic pH values draining the deposit can be attributed to low stream gradients and a more extensive outcropping of the stockwork and impregnation zones (Figure 7.3).

In the Tunca area the pH values of spring and stream waters range from 4 to 7. Those values lower than 5.5 were indicative of sulphide oxidation in this area.

The acid pH values in the region are generally associated with zones of sulphide oxidation in the exposed dacite window, there being an absence of pyritic black shales in the region and a general lack of considerable organic matter in the streams. Thus, the pH measurements of spring and stream waters appear to have a useful application in exploration for sulphide mineralization in the Eastern Black Sea ore province. This application is limited, the acid waters generated as a result of the oxidation of the sulphides being, in some cases, neutralized in less than ten metres. Nevertheless, pH measurements are a practical in-field technique during geochemical surveys and routine geological mapping since they serve to direct attention to possible areas of mineralization. Furthermore pH measurements are invaluable additional information in interpreting geochemical data from the secondary environment.

7.4 ANALYSIS OF SIZE FRACTIONS

Stream sediments from the Maden and Latum streams in the vicinity of the Madenköy deposit were separated into -20-60 mesh (-750-250 μ), -60-80 mesh (-250-200 μ), -80-100 mesh (-200-150 μ), and -100 mesh (-15 μ) size fractions and analysed for Cu, Zn, Pb, Cd, Ag, and As. The metal contents of each of the stream sediment size fractions, together with the frequency each size fraction displayed maximum elemental concentrations, are presented in Tables 7.3 and 7.4. The first table indicates that the metals in the Maden stream sediments are concentrated mainly in the coarser fractions (-60-80 and -80-100 mesh sizes). On the other hand the metals

Table 7.3 Analysis of size fractions of stream sediments from Maden stream draining Madenköy deposit (contents in ppm).

Sample:	1					2					4					6					Frequency size fractions display max. elemental contents				
Size Fraction (mesh) / Element:	Cu	Zn	Pb	Cd	Ag	Cu	Zn	Pb	Cd	Ag	Cu	Zn	Pb	Cd	Ag	Cu	Zn	Pb	Cd	Ag	Cu	Zn	Pb	Cd	Ag
-20 - 60	2500	41000	3960	240	43	6200	42000	4640	210	5	2400	3400	508	19	5	2700	21000	600	110	5	2	1	0	1	0
-60 - 80	5000	45000	5200	250	33	5200	5240	5240	300	10	1220	9400	648	52	10	1430	21000	1040	110	8	0	3	1	3	3
-80 - 100	5800	47000	5280	280	50	5500	4440	4440	300	10	810	6900	680	32	10	1320	12200	960	70	6	2	1	3	2	2
-100	4900	38000	5280	230	31	3000	4040	4040	140	5	410	3800	440	18	5	550	5000	560	28	7	0	0	1	0	0

Table 7.4 Analysis of size fractions of stream sediments from Latum River near Madenköy deposit (contents in ppm).

Sample:	9					13					15					16					Frequency size fractions display max. elemental contents				
Size Fraction (mesh) / Element:	Cu	Zn	Pb	Cd	Ag	Cu	Zn	Pb	Cd	Ag	Cu	Zn	Pb	Cd	Ag	Cu	Zn	Pb	Cd	Ag	Cu	Zn	Pb	Cd	
-20 - 60	20	32	8	1	1	31	83	16	2	1	25	51	20	2	1	63	170	32	3	1	0	0	0	1	
-60 - 80	20	40	12	1	1	69	860	32	4	1	120	200	16	1	1	71	190	28	3	1	0	1	1	1	
-80 - 100	30	58	8	2	2	109	400	28	4	1	88	550	28	5	1	73	240	36	4	1	0	2	1	4	
-100	37	12	12	1	2	121	470	44	4	1	141	570	40	5	1	79	220	32	4	1	4	1	2	4	

in the sediments of the Latum stream, into which the Maden stream drains, are enriched in the finer fractions, especially in the -100 mesh fraction (Table 7.4).

The dispersion of arsenic follows a somewhat different pattern. In the stream sediments from the Maden stream the element is concentrated in the finest fractions analysed; in the Latum stream sediments arsenic consistently increases with decreasing grain size (Table 7.5). In order to eliminate any doubts about the variation in elemental concentration due to the effect of grain size on the efficiency of the sample digestion, selected size fractions were ground to -100 mesh and re-analysed. Comparison with results obtained from the original unground samples indicates that the differences are small and within the limits of the analytical error (Table 7.6).

A binocular microscopic examination of the size fractions of several stream sediments from the Maden stream revealed the presence of composite sulphide grains in the coarse fractions, the sulphides becoming more and more liberated as individual minerals in the finer fractions. Distant from the orebody, in the Latum stream, the sulphides usually occur in the finer fractions as a result of the breakdown of the composite sulphide grains during transport.

The above evidence suggests that the predominant type of elemental dispersion from the sulphide mineralization in this region is mechanical.

7.5 SELECTIVE EXTRACTION ANALYSIS

The mode of dispersion of trace metals in stream sediments from the Madenköy area was further investigated by

Table 7.5 Arsenic contents (in ppm) of size fractions of sediments from the Maden stream and Latum River, Madenköy area.

Size Fraction (mesh)	Samples from Maden Stream						Samples from Latum River	
	1	2	4	6	162	148	10	13
-20 - 60	115	205	38	68	38	29	N.D.	4
-60 - 80	188	213	66	94	38	40	N.D.	5
-80 - 100	200	250	78	88	43	40	4	8
-100	225	250	51	63	46	45	5	15
-80	115	250	44	66	45	41	4	13

Table 7.6 Arsenic content of ground (-100 mesh) and unground stream sediment samples from the Madenköy area.

Sample	Size Fraction (mesh)	Ground As ppm	Unground As ppm
1	-20 - 60	110	115
	-60 - 80	163	188
4	-20 - 60	41	38
	-60 - 80	68	66
148	-20 - 60	29	29
	-60 - 80	38	40
13	-60 - 80	8	8

selective extraction procedures involving 0.05 M ammonium EDTA (pH:4.65) and acidified 1M hydroxylamine hydrochloride (pH:1.3) solutions. These extraction procedures are described in detail in section 5.8 in Chapter 5 and in Appendix A.6.

The EDTA extraction desorbs exchangeable metal ions from clays and possibly from some colloidal organic particles and from iron- and manganese-oxides and hydroxides. The hydroxylamine hydrochloride solution, in addition to extracting the above forms of the metals, dissolves the common carbonates, manganese oxides and hydroxides, and clays. These two solutions have little effect on sulphides, except galena for which the solubility was found to be 0.01 and 5.0 per cent by the EDTA and hydroxylamine hydrochloride solutions respectively (Table 9.3). More information about the nature of the dissolution of geological materials by the two solutions is given in Chapter 9.

The percentages of the various metals extracted by the two solutions, as compared with the nitric/perchloric acid digestion, are given in Tables 7.7 and 7.8. The average percentages for exchangeable Cu, Zn, and Pb by the EDTA are 13.5, 5.3, and 38.5 respectively. Some of the base metals dissolved may be associated with Mn-oxides and hydroxides represented by 20% of total Mn extracted (Table 7.7).

The amounts of Cu, Zn, Pb, and Mn extracted by hydroxylamine hydrochloride (27%, 10%, 69%, and 51% respectively) are about twice, and for Fe about 20 times greater than that by EDTA. Therefore, approximately 13% and 5% of Cu and Zn respectively are structurally bound in Mn-oxides and hydroxides, and to a lesser extent in Fe-oxides and clay minerals. The high extractabilities of Pb are in part due to the

Table 7.7 Percentage of extractability* of various metals from Madenköy stream sediments using 0.05 M EDTA solution.

Sample+ Number	Percentage of metals extracted by EDTA				
	Fe	Mn	Cu	Zn	Pb
1 (M)	0.22	24.0	5.8	2.5	66.7
5 (M)	0.17	12.6	11.7	6.3	46.2
6 (M)	0.25	21.8	8.0	6.4	47.2
10 (L)	0.29	24.4	11.4	3.5	6.7
13 (L)	0.13	10.4	30.4	7.9	25.5
Mean	0.21	19.8	13.5	5.3	38.5
Std. dev.	0.06	3.35	9.8	2.2	23.0

*Extractability is expressed as "(EDTA extractable metal in ppm/HNO_3 + $HClO_4$ extractable metal) x 100".

+(M)-stream sediment from Maden stream.

(L)-stream sediment from Latum River.

Table 7.8 Percentage of extractability* of various metals from Madenköy stream sediments using 1M acidified hydroxylamine hydrochloride solution

Sample+ Number	Percentage of metals extracted by hydroxylamine hydrochloride				
	Fe	Mn	Cu	Zn	Pb
1 (M)	4.4	65.9	9.7	3.6	88.2
2 (M)	10.0	75.6	30.0	7.4	86.2
4 (M)	5.1	45.2	18.7	8.1	74.0
5 (M)	5.1	62.9	28.8	14.4	60.7
6 (M)	6.2	70.2	28.0	10.4	55.2
162 (M)	1.8	16.9	23.3	14.3	65.5
148 (M)	4.9	66.7	22.1	8.5	64.3
10 (L)	1.3	22.0	36.4	14.0	62.5
13 (L)	2.9	31.8	41.1	12.9	65.5
Mean	4.6	50.8	50.8	10.4	69.1
Std. dev.	2.6	22.3	22.3	3.8	11.4

*Extractability is expressed as "(hydroxylamine hydrochloride extracted metal in ppm/HNO_3 + $HClO_4$ extracted metal) x 100".

+(M) stream sediment from Maden stream.

(L) stream sediment from Latum river.

relatively higher solubility of galena in hydroxylamine hydrochloride solutions.

Extrapolation of the results obtained by the hydroxylamine hydrochloride extraction suggests that about 70% of the Cu and 90% of the Zn in stream sediments near the Madenköy deposit occurs in sulphides, Fe-oxides, and in clay minerals. Evidence cited above on the size fraction analysis and microscopic examination of the samples, verify the above results.

In regional geochemical programs a hot nitric acid attack for stream sediments appears to be the best digestion procedure in this region for detecting mechanical dispersion trains. However, weaker attacks such as the EDTA and hydroxylamine hydrochloride extraction procedures should be useful in detecting hydromorphic anomalies during detailed follow-up work.

7.6 HYDROGEOCHEMICAL DISPERSION OF METALS

7.6.1 Introduction

The elemental distribution in the stream sediments of Fe, Mn, Cu, Zn, Pb, As, Ag, Mo, and Ba in the Cayeli area; Cu, Zn, Pb, As, and Ag in the Madenköy area; and Cu, Zn, Pb, and As in the Kutlular area are presented in Figures 7.4 to 7.21. Cadmium values were not plotted for any of the areas, but its dispersion is briefly dealt with in the following text. Barium was only determined in selected stream sediments from the Madenköy and Sirtköy areas; values for this element have been plotted on the Çayeli base map. Silver and Mo were not determined in stream sediments from the Kutlular area.

The correlation matrices for the stream sediment data for the Madenköy, Sirtköy, and Sarisu areas have been computed

and are given in Table 7.9. The correlation matrix was not calculated for the Kutlular area stream sediment data as the number of samples from this area is too small. For the range and average background contents of the various elements the reader is referred to Tables 7.1 and 7.2.

7.6.2 Dispersion of Metals

A study of the dispersion of As, Cu, Zn, Pb, Ag, Mo, and Ba in the Çayeli area drainage sediments is a valuable aid in delineating mineralized zones in general and differentiating the three types of mineralization in this area (Figures 7.4, 7.5, 7.6, 7.7, 7.8, 7.9, and 7.10). Only Cu and to a lesser extent Mo and As are anomalous in the vicinity of all three types of mineralization (Madenköy massive sulphide deposit, Sirtköy pyritic stockwork, and Sarisu pyritic impregnation occurrences). The strongest anomalies of As and Cu were observed in the vicinity of the Madenköy deposit (Figures 7.4 and 7.5), and Zn, Pb, and Ag occur in significantly anomalous concentrations only near the Madenköy deposit (Figures 7.6, 7.7, and 7.8). Near the Sirtköy and Sarisu occurrences the contents of As, Cu, Zn, Pb, and Ag are almost within the regional background variation. Arsenic, Cu, Zn, and Pb also display high concentrations in the Kutlular area (Figures 7.11, 7.12, 7.13, and 7.14). From these data it is evident that high contents of As together with elevated levels of elements such as Zn, Pb, and Ag are specific to the sediments of streams draining stockwork and impregnation zones associated with massive sulphide bodies. It is also significant that the above listed elements are generally intercorrelated in the vicinity of massive sulphide deposits (e.g. Madenköy), whereas

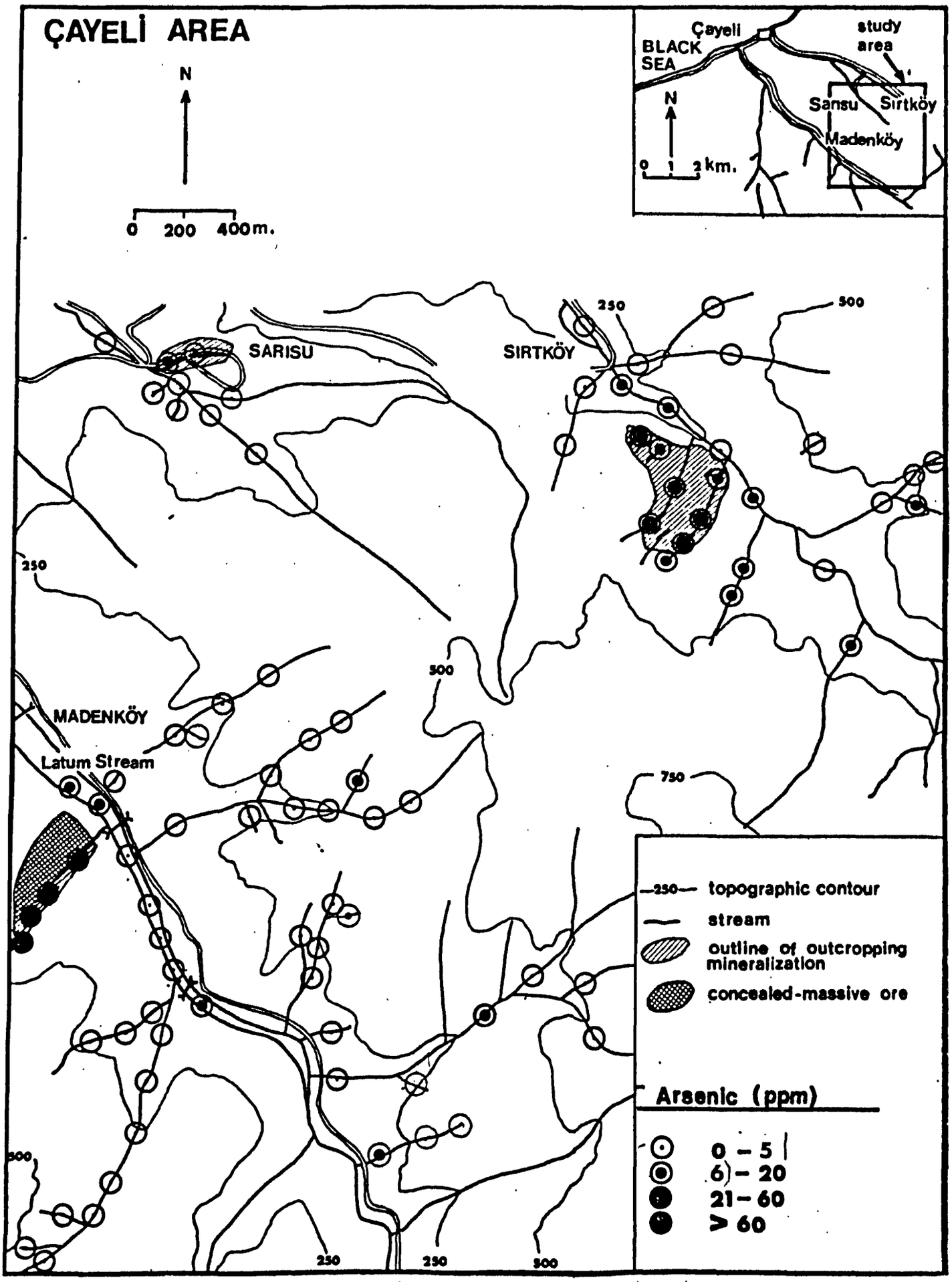


Figure 7.4 Dispersion of arsenic in stream sediments, Çayeli area.

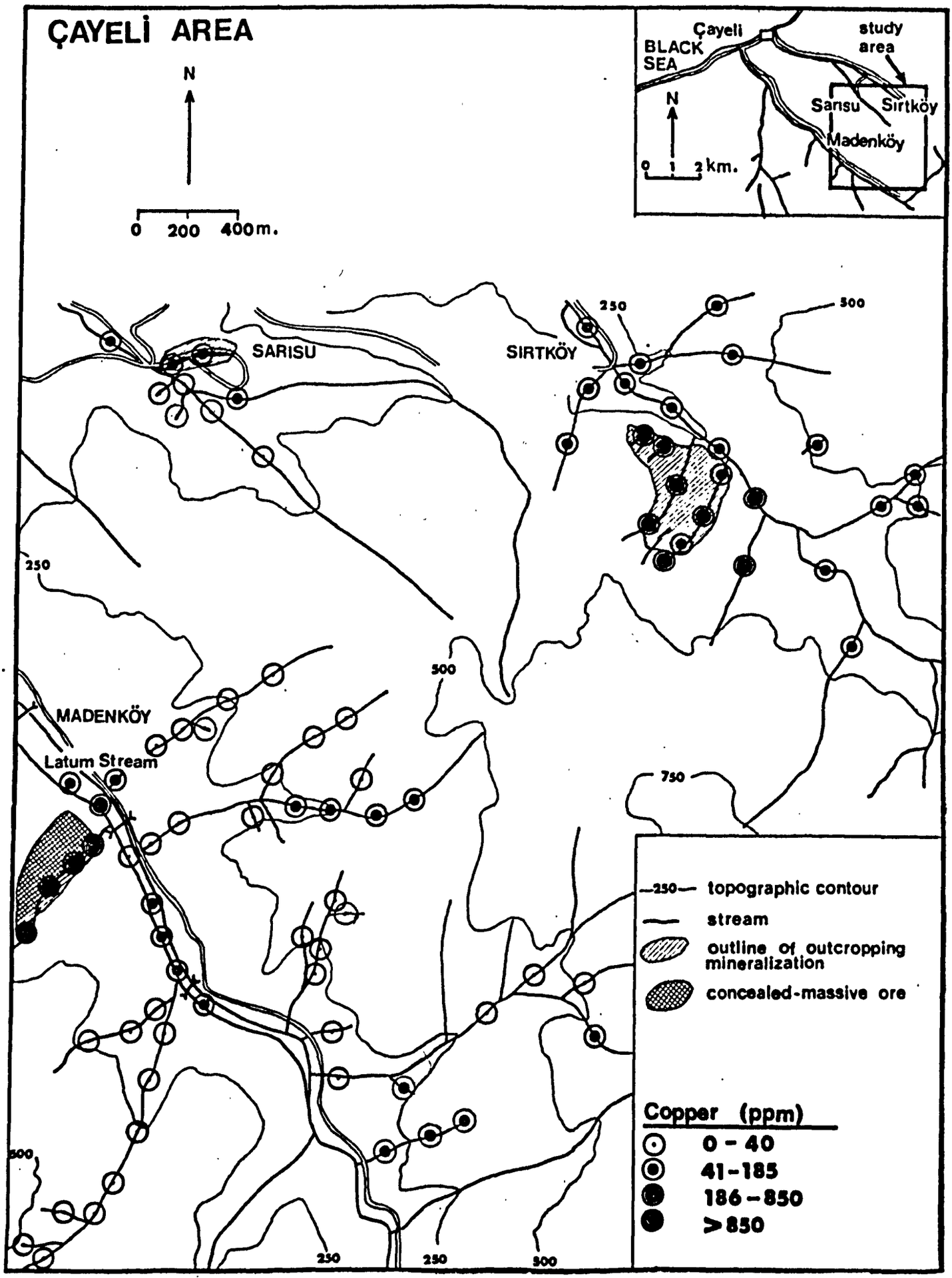


Figure 7.5 Dispersion of copper in stream sediments, Çayeli area.

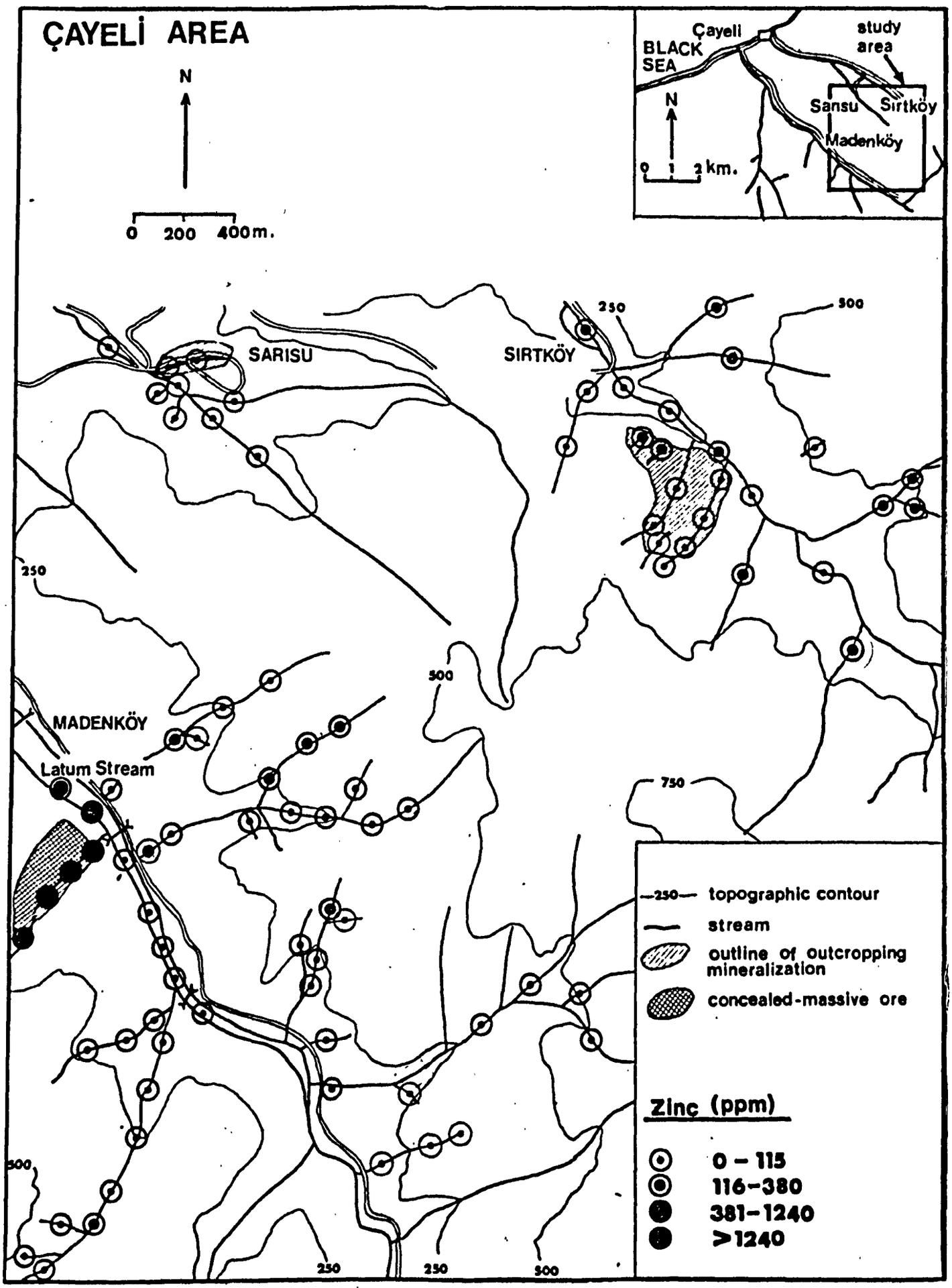


Figure 7.6 Dispersion of zinc in stream sediments, Çayeli area.

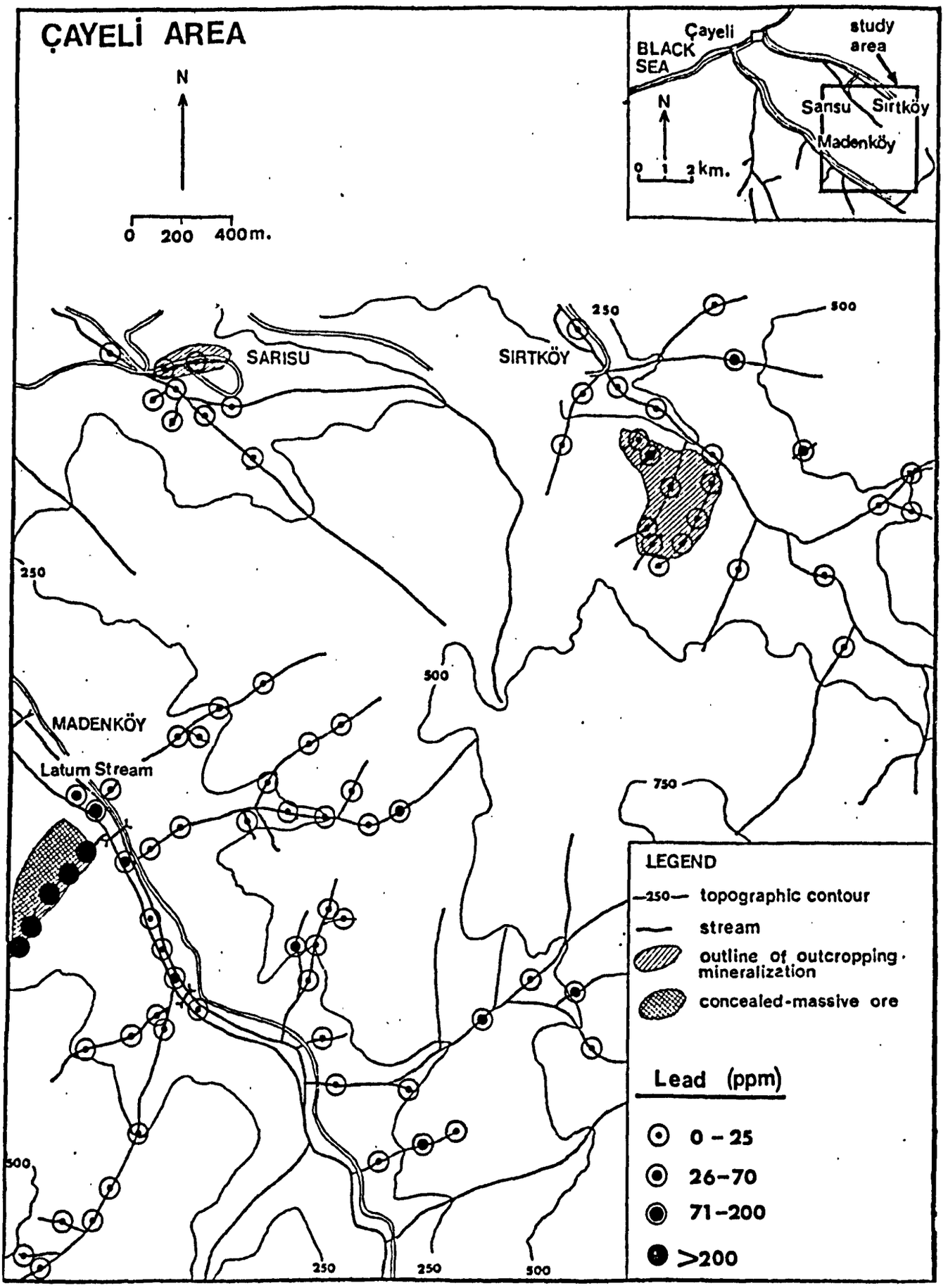


Figure 7.7 Dispersion of lead in stream sediments, Cayeli area.

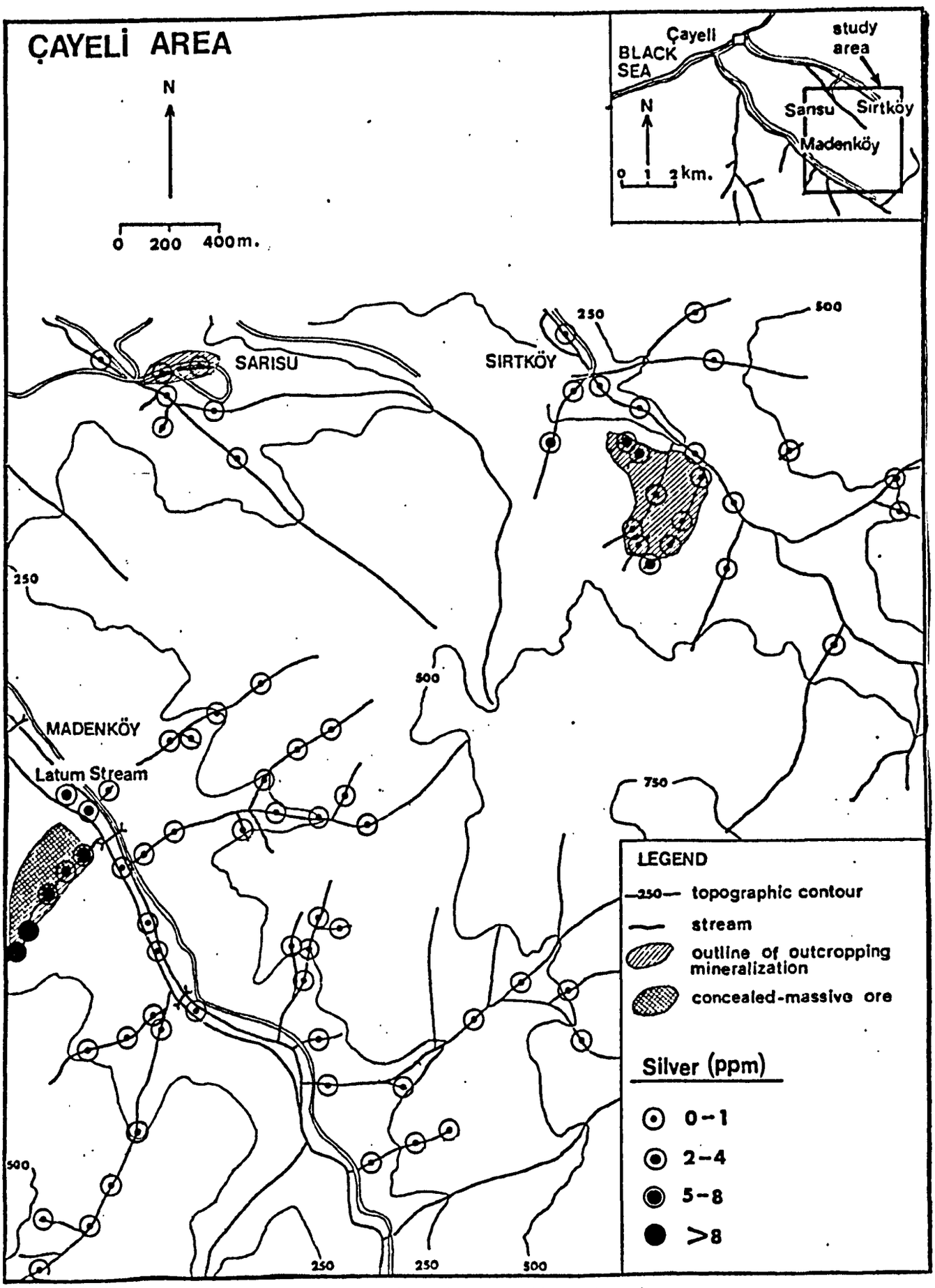


Figure 7.8 Dispersion of silver in stream sediments, Cayeli area.

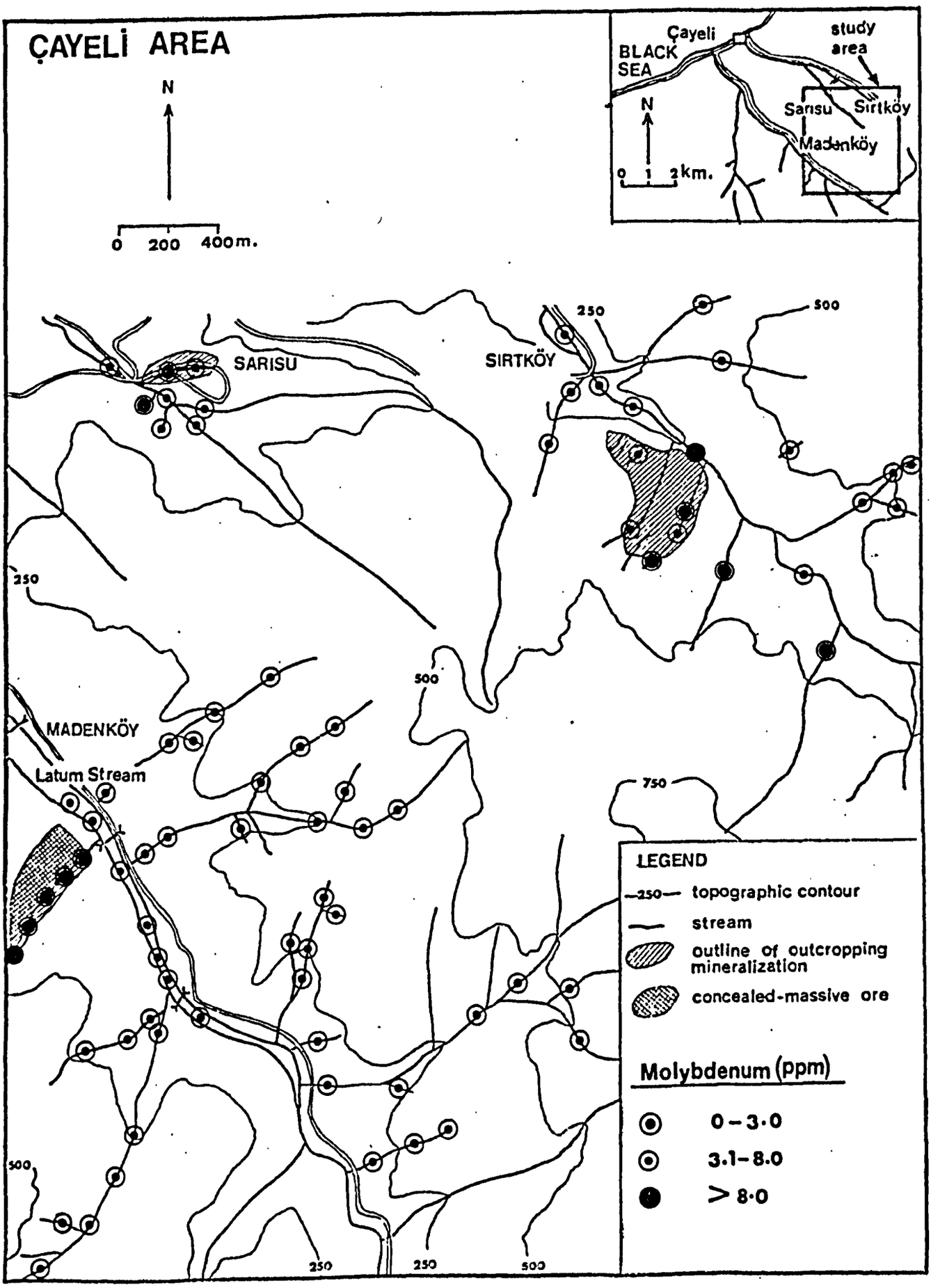


Figure 7.9 Dispersion of molybdenum in stream sediments, Çayeli area.

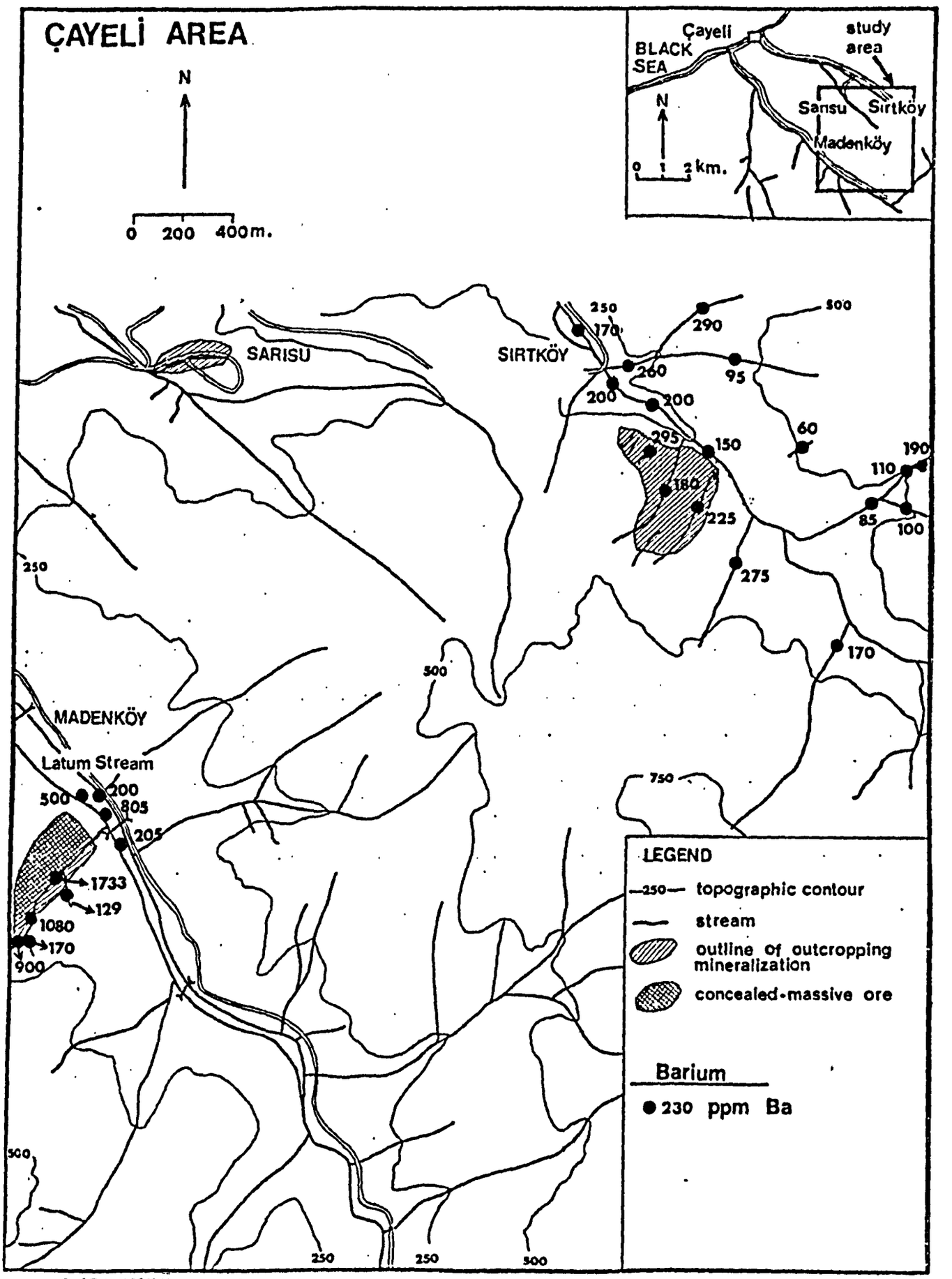


Figure 7.10 Dispersion of barium in stream sediments, Madenköy and Sirtköy areas, Cayeli.

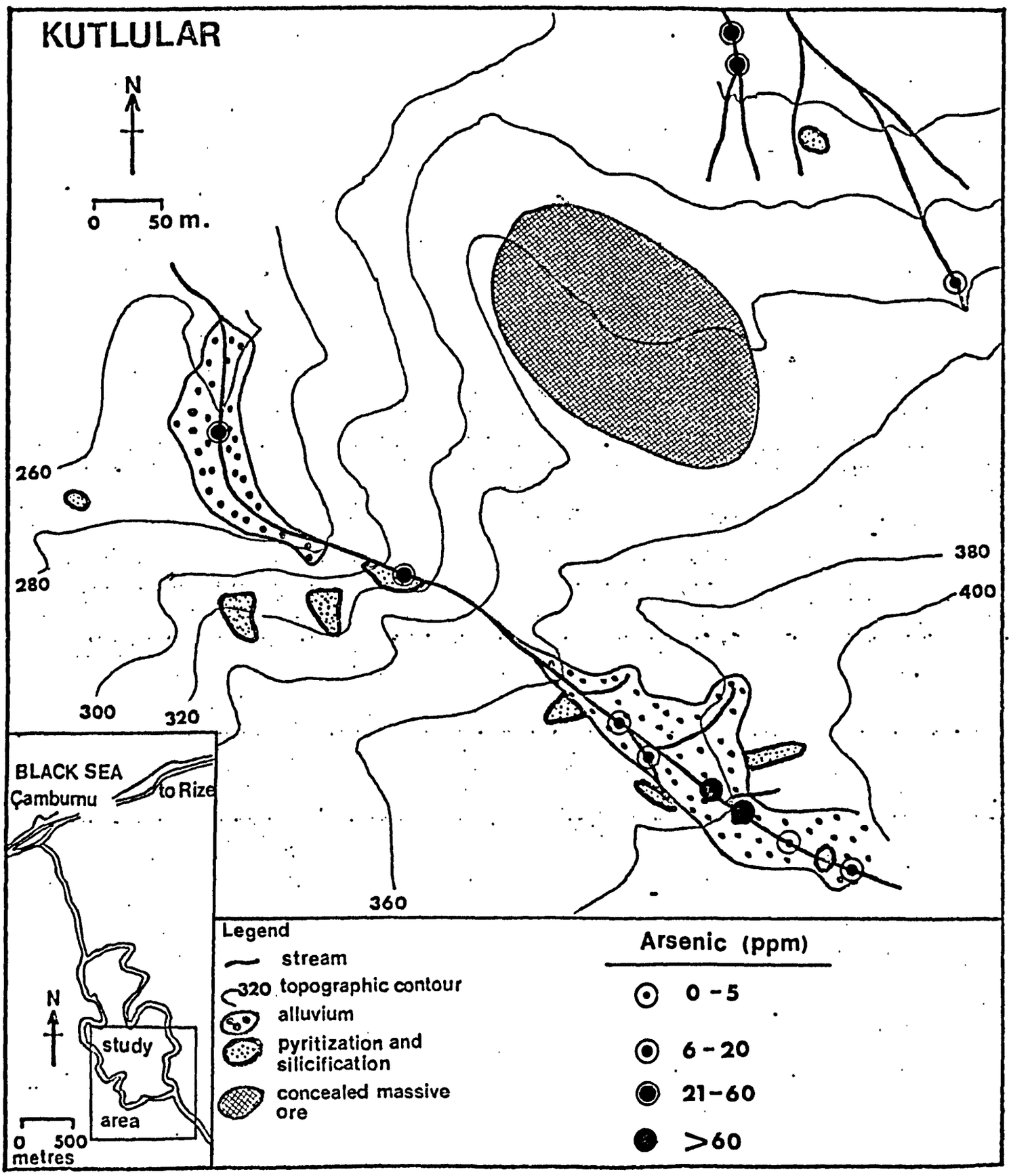


Figure 7.11 Dispersion of arsenic in stream sediments, Kutlular area.

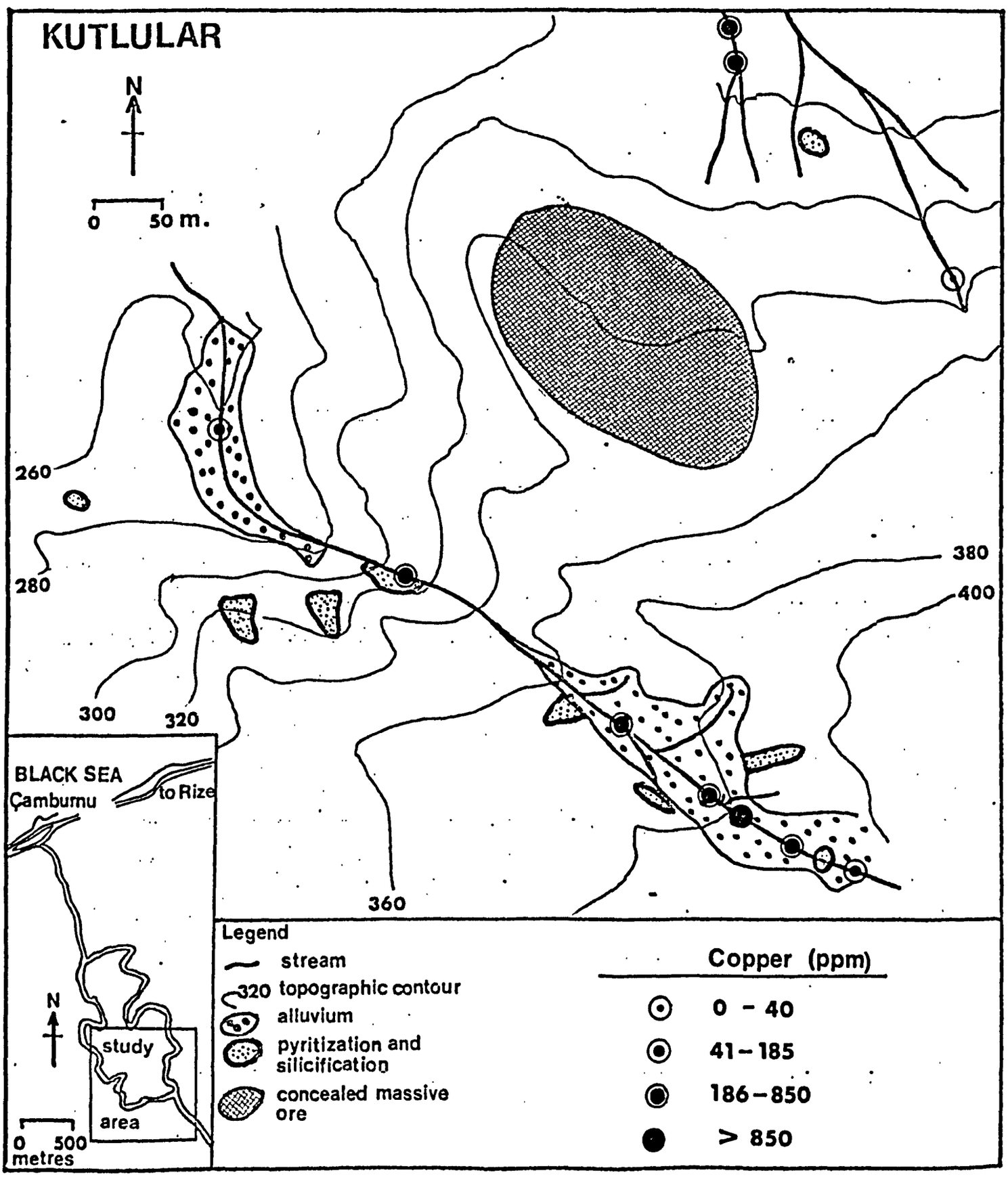


Figure 7.12 Dispersion of copper in stream sediments, Kutlular area.

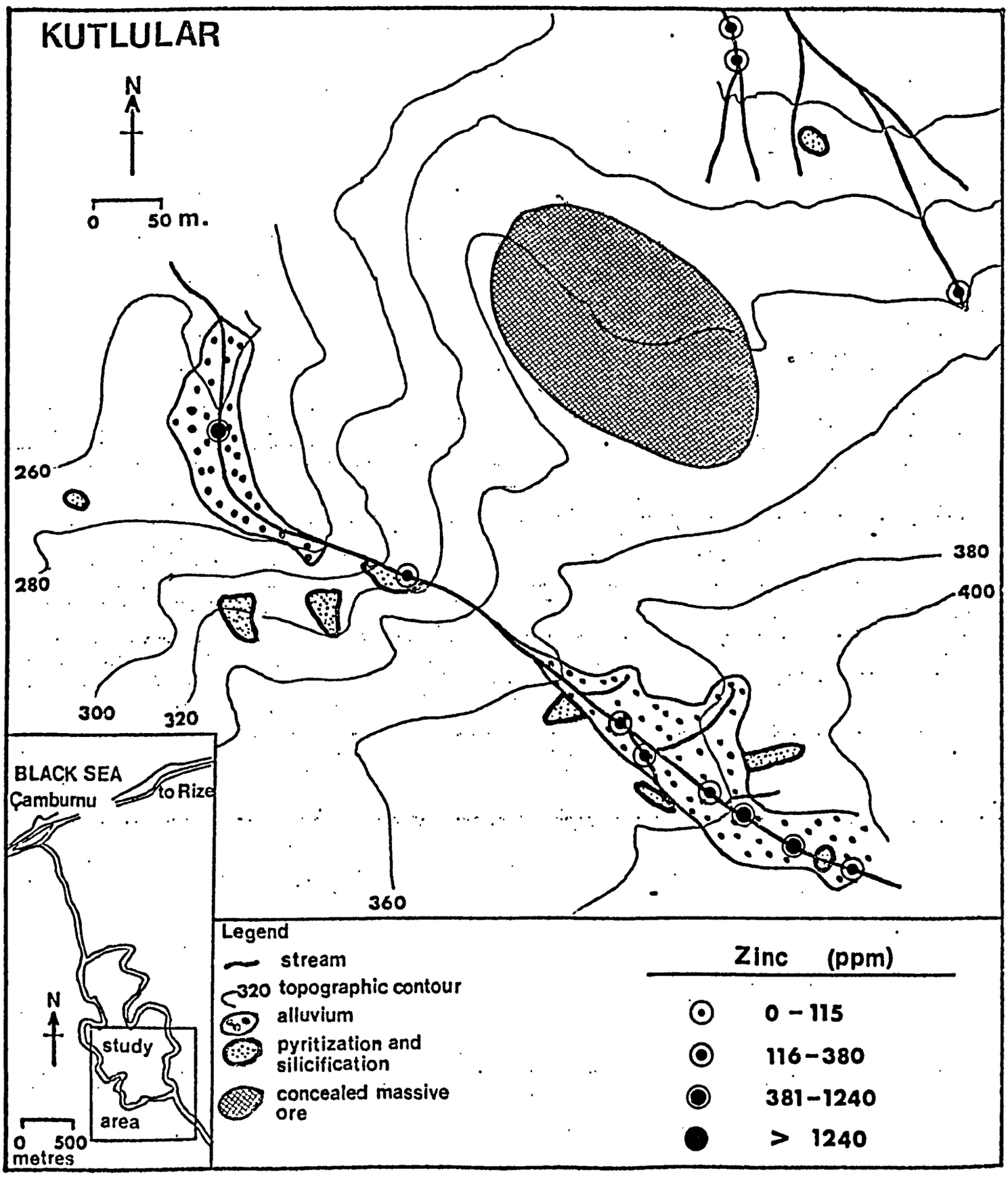


Figure 7.13 Dispersion of zinc in stream sediments, Kutlular area.

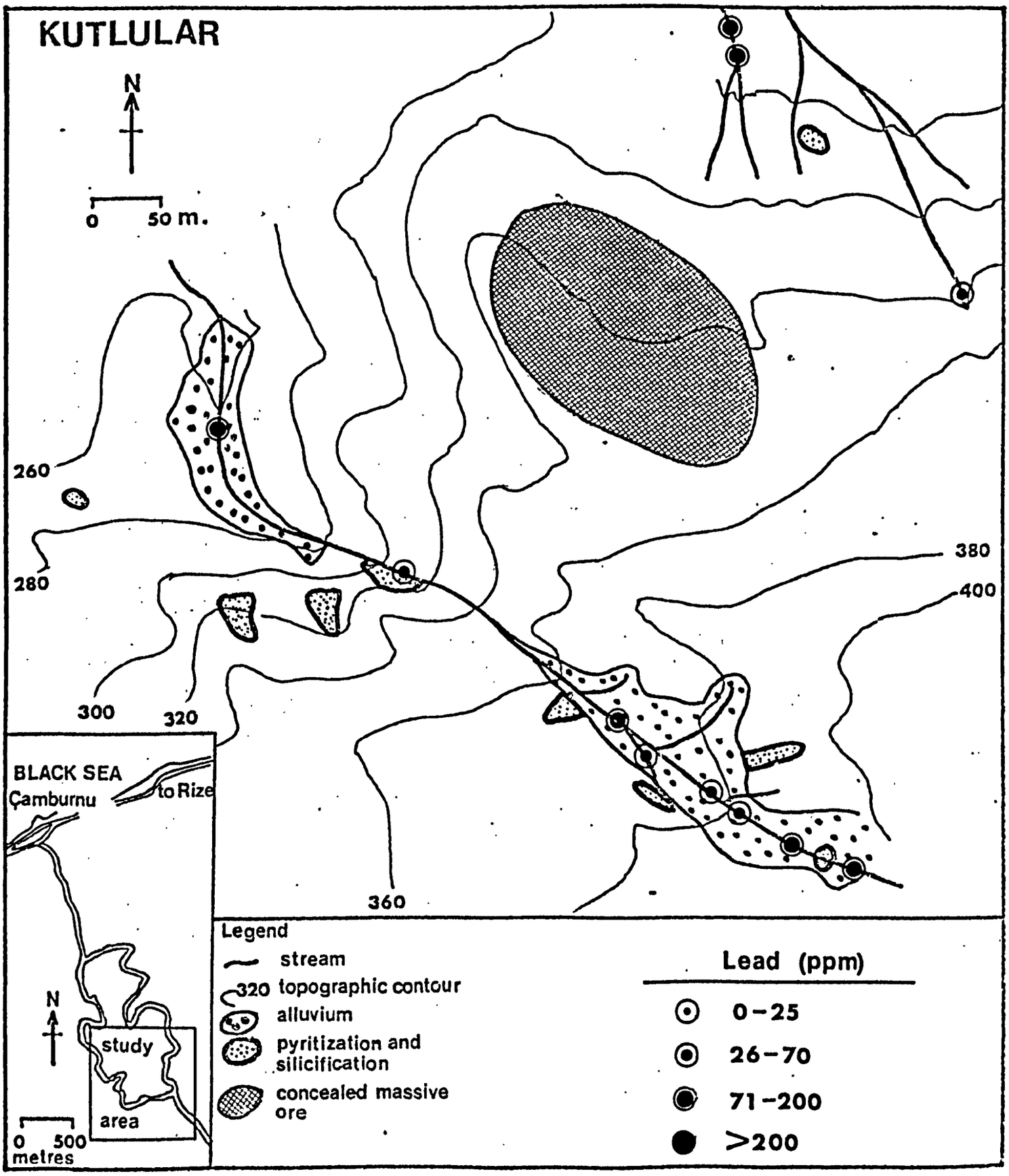


Figure 7.14 Dispersion of lead in stream sediments, Kutlular area.

no, or very little correlation, was observed between these elements in the Sirtköy, Sarisu, and general background areas (Tables 7.2 and 7.9). This is in accordance with the sulphide chemistry of mineralized samples from these various areas, As, Zn, Pb, and Ag being more enriched in massive sulphides with respect to the other types of deposits (see Chapter 6 for contents of these elements in mineralized samples from the various deposits).

Among the elements As, Cu, Zn, Pb, Ag, and Cd the most extensive dispersion trains were displayed by Zn and to a lesser extent by As and Cu. This is especially clear in the detailed survey of the Madenköy area (Figures 7.15, 7.16, 7.17, 7.18, and 7.19). The extent of the dispersion of Zn, Cu, and Pb follows the order of solubility of their sulphates (smithsonite ($ZnSO_4$) being the most and anglesite ($PbSO_4$) the least soluble of the three). For example, the anomalous Cu and Pb contents in Latum Stream do not extend to the eastern side of this stream bed whereas Zn occurs in anomalous concentrations on both sides (Figures 7.5, 7.6, and 7.8). The background variations in the Cu, and to a lesser extent Zn contents, in the Çayeli area are related to bedrock geochemistry. Lead displays a somewhat uniform background in the Çayeli area. Silver and Cd exhibit dispersion behaviours similar to those of Pb and Zn respectively as would be expected from the geochemistry of these four elements. Silver and Cd, however, have restricted dispersion patterns and display low background variations, mainly due to the high detection limits and low sensitivity of the analytical methods used. In the vicinity of the Madenköy deposit, Ag occurs in

Table 7.9 Correlation coefficients for stream sediment data from the Madenköy, Sirtköy, and Sarisu areas

	MADENKÖY (78 Samples)									SIRTKÖY (34 Samples)								
	As	Cu	Zn	Pb	Ag	Cd	Mo	Mn	Fe	As	Cu	Zn	Pb	Ag	Cd	Mo	Mn	Fe
As	1.00									1.00								
Cu	0.45									0.02								
Zn	0.47	0.76								-0.23	0.37							
Pb	0.55	0.95	0.86							-0.29	0.46	0.52						
Ag	0.46	0.97	0.76	0.98						-0.04	0.56	0.14	-0.27					
Cd	0.73	0.97	0.96	0.99	0.99					-0.07	-0.13	0.03	0.43	-0.24				
Mo	0.58	0.61	0.53	0.64	0.65	0.82				-0.23	-0.12	0.28	-0.04	-0.25	-0.15			
Mn	-0.01	0.08	-0.74	-0.02	0.01	0.01	0.16			-0.12	0.79	0.81	0.49	0.59	0.07	0.28		
Fe	0.06	0.18	0.07	0.06	0.09	0.05	0.35	0.53	1.00	0.05	0.36	0.20	0.43	0.24	-0.54	0.24	0.19	1.00

Table 7.9 (continued)

	SARISU (28 Samples)								
	As	Cu	Zn	Pb	Ag	Cd	Mo	Mn	Fe
As	1.00								
Cu	0.33								
Zn	0.51	-0.01							
Pb	0.01	-0.14	0.27						
Ag	0.02	0.01	0.15	0.11					
Cd	0.22	-0.18	0.37	0.20	0.01				
Mo	-0.22	-0.23	0.13	-0.8	-0.03	0.07			
Mn	-0.06	0.09	0.11	-0.16	0.16	0.24	-0.03		
Fe	0.29	0.78	0.08	-0.01	0.01	-0.16	0.09	0.13	1.00

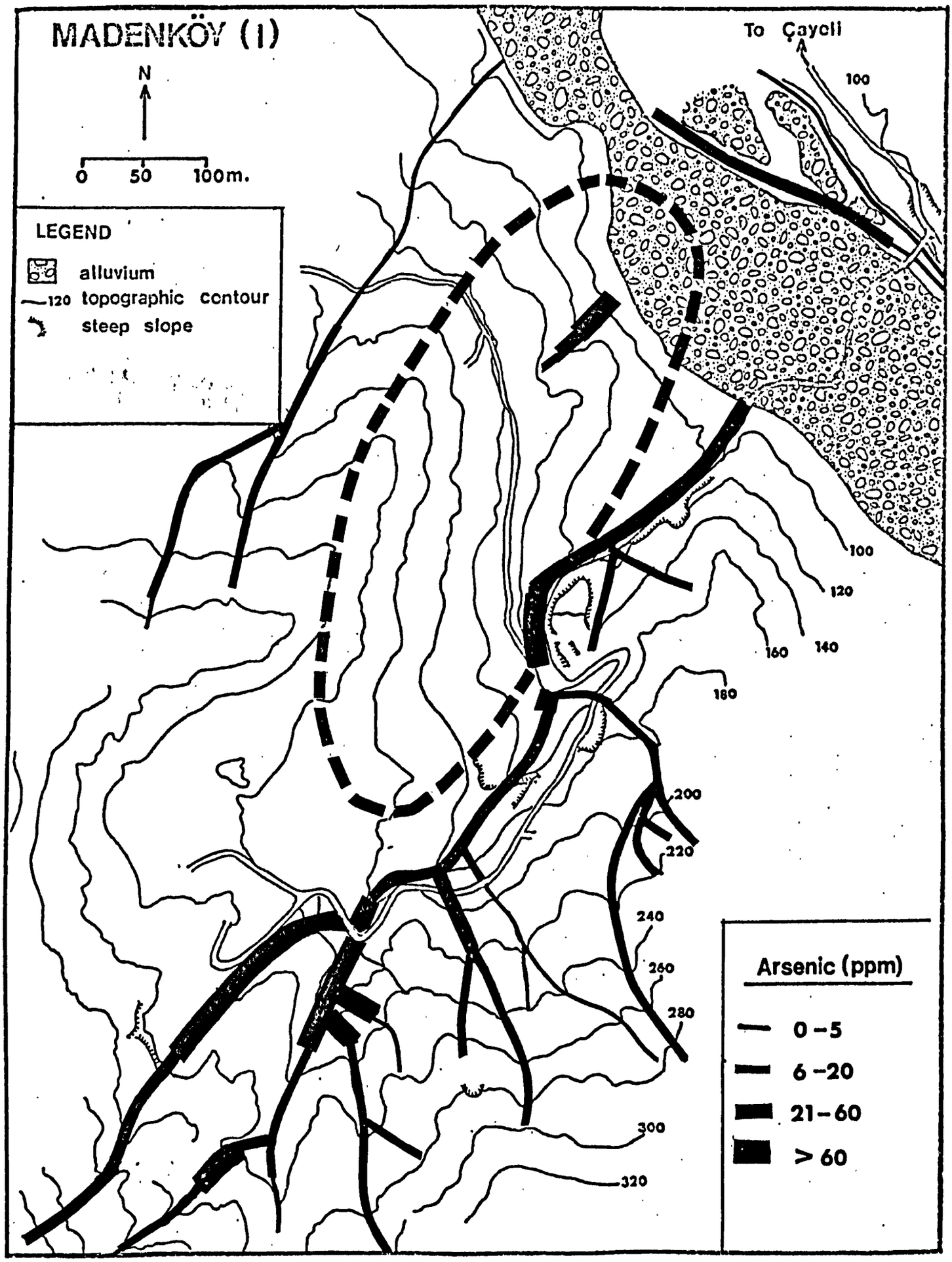


Figure 7.15 Dispersion of arsenic in stream sediments, Madenköy area.

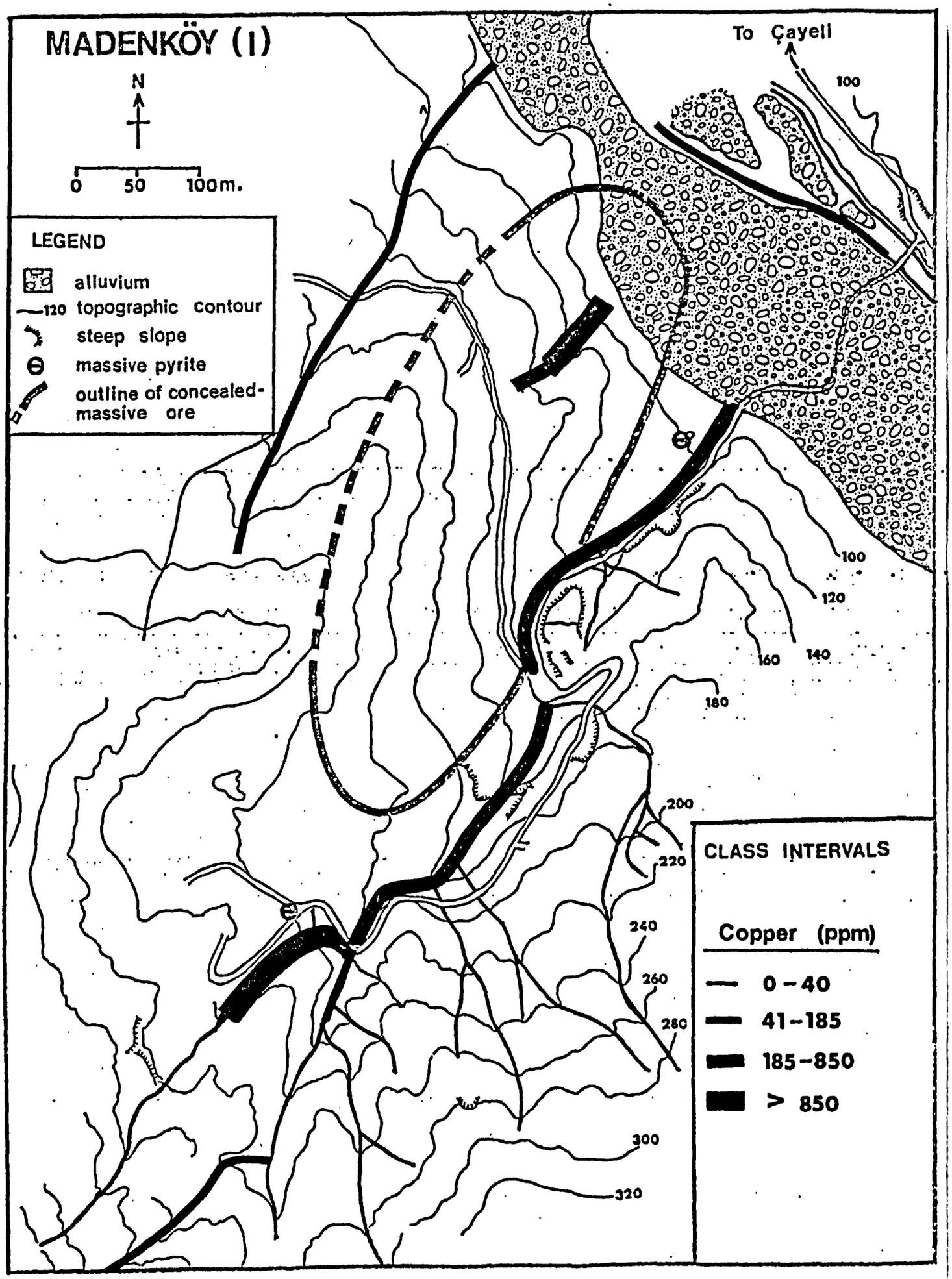


Figure 7.16 Dispersion of copper in stream sediments, Madenköy area.

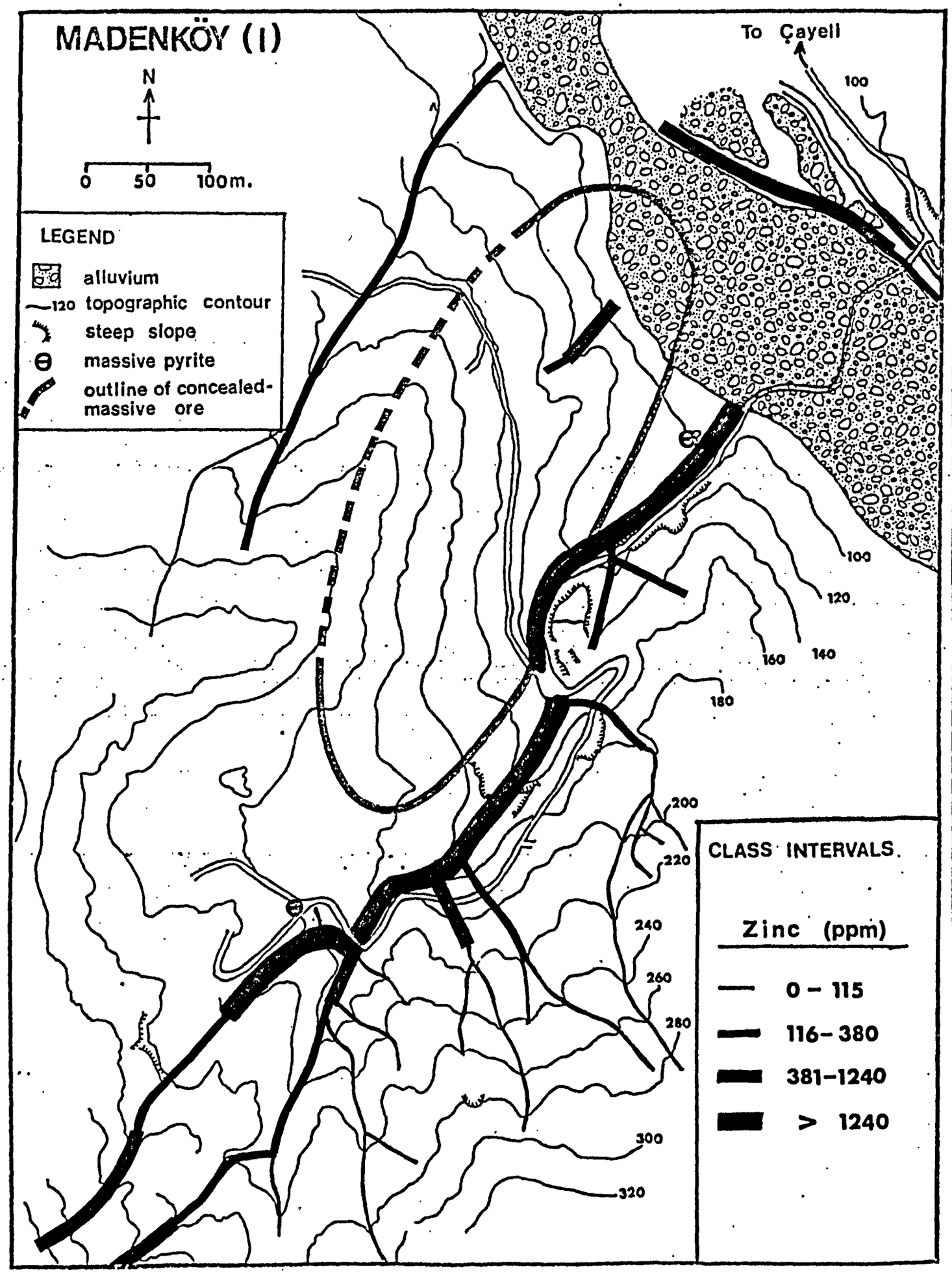


Figure 7.17 Dispersion of zinc in stream sediments, Madenköy area.

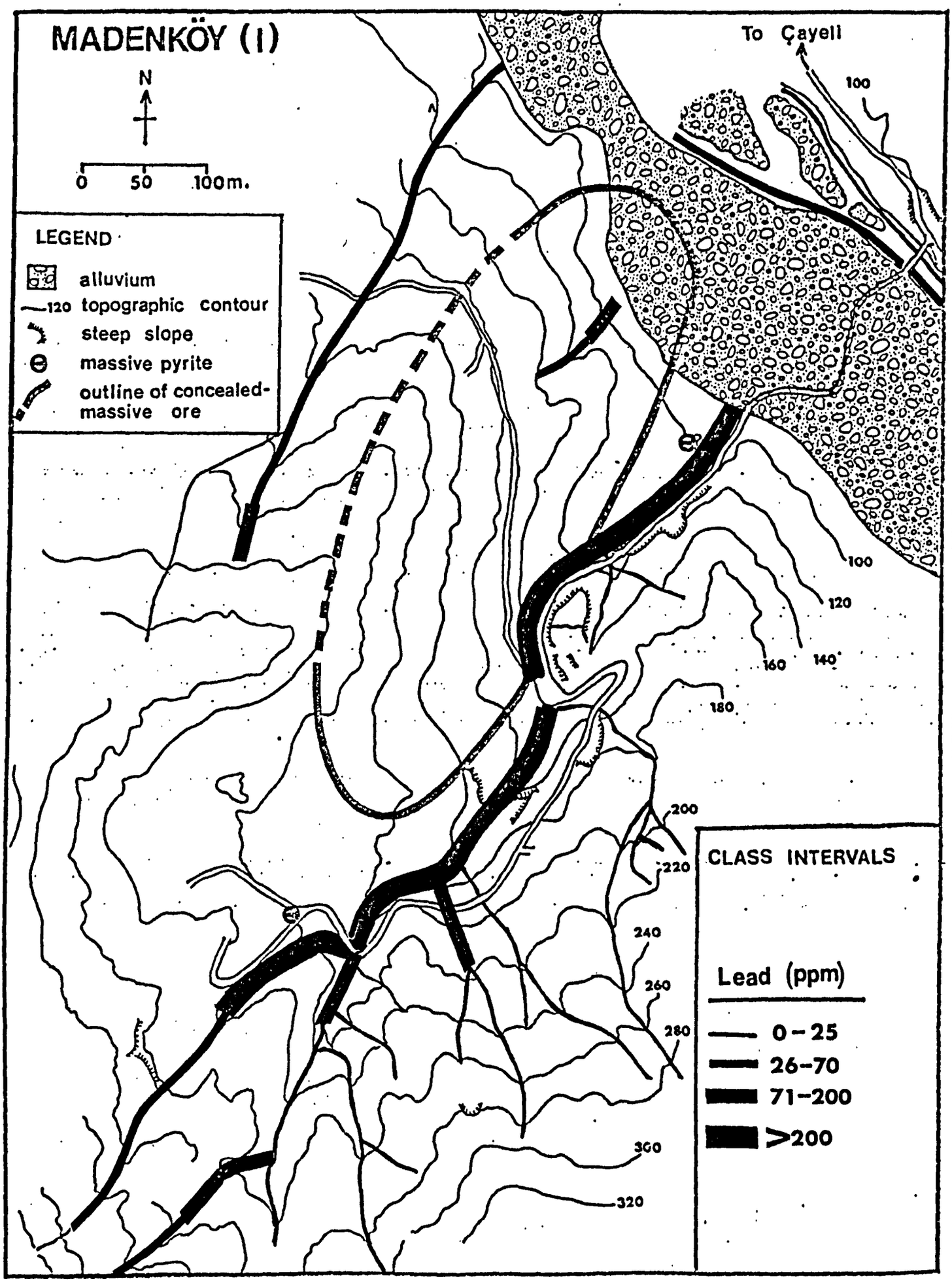


Figure 7.18 Dispersion of lead in stream sediments, Madenköy area.

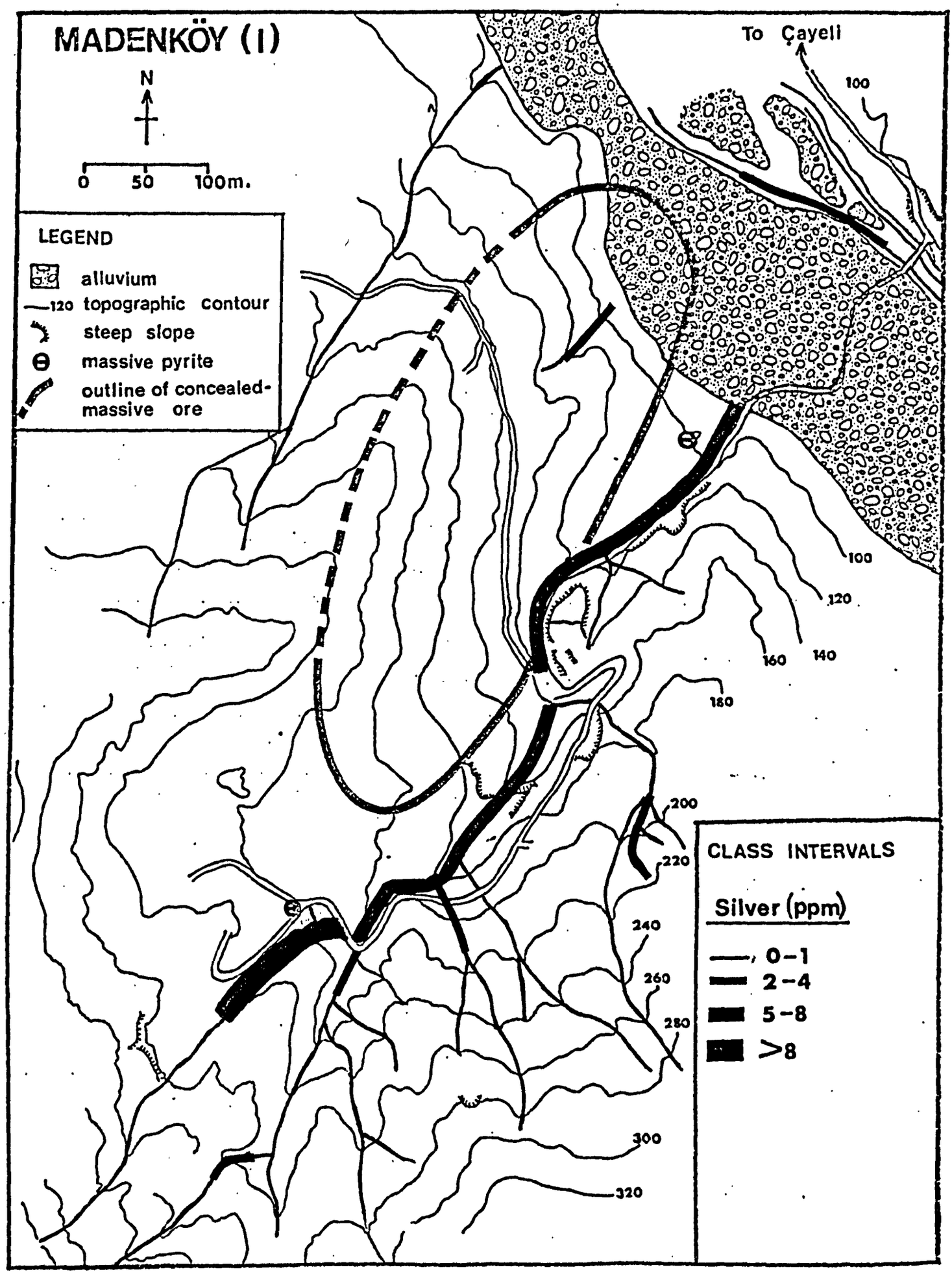


Figure 7.19 Dispersion of silver in stream sediments, Madenköy area.

high concentrations, but its concentration diminishes away from the deposit and anomalous contents die out at Latum stream (Figure 7.19).

Molybdenum exhibits an erratic dispersion with a noisy background in the Çayeli area (Figure 7.9). Part of the background variation below the 5 ppm level can be attributed to the relatively poor precision of the analytical method. However, the values greater than 8 ppm are related to sulphide mineralization in the area. The anomalous occurrence of Mo in stream sediments draining all types of sulphide mineralization makes it an ideal indicator of sulphide mineralization in general; it has, however, no discriminating properties with regard to type of mineralization in the Eastern Black Sea Region.

Barium in the form of barite is an important indicator element of massive sulphide deposits in the region. Its concentration in the Madenköy ore samples range from 100 ppm to 3.3 per cent; the Sirtköy and Sarisu occurrences have considerably lower contents, ranging from tens of ppm to a few hundred ppm (see Tables 6.1, 6.6, and 6.7). Despite its potential as a good indicator Ba demonstrates a restricted dispersion in the vicinity of mineralization due to its immobile character, barite being one of the most insoluble of sulphates (Figure 7.10). The contents of the element in the two stream sediments draining the stockwork impregnation zones of the Madenköy deposit are at the background levels of 170 and 129 respectively. High contents of Ba in the Maden stream sediments diminish in the Latum stream. The element is present at background levels in the spring and stream sediments in the Sirtköy area.

The dispersions of Fe and Mn in the Çayeli area reflect to a large degree the bedrock geochemistry; streams draining basic rocks have considerably higher Fe and Mn contents than those draining acid volcanic rocks (Figures 7.20 and 7.21). In the Sirtköy area, and to a lesser extent in the Sarisu area, the stream sediments draining the mineralized zones are much higher in Fe and Mn than those draining the Madenköy deposit. The high Fe and Mn contents in the Sirtköy and Sarisu areas are partly due to the predominance of basic rocks in these areas. These elements in the Sirtköy area are also enriched in the gossan zones which provide considerable material to the Gümüşdere stream. Iron oxide (limonite) precipitation was observed locally in seepages at Madenköy, Sirtköy, and Kutlular; the dissolved Fe in the acid seepage waters (pH:4) precipitates as soon as the pH rises to less acid values (i.e. 5.6). Apart from the above forms Fe also occurs as iron sulphides (mainly pyrite) in the mineralized areas. There is little or no correlation between Fe and Mn and other elements in stream sediments draining the Madenköy and Sarisu mineralized zones (except between Fe and As in the Sarisu area). This suggests that the scavenging effects of the oxides and hydroxides of Fe and Mn in these areas are minimal (Table 7.9). The correlation between As and Fe in the Sarisu area is indicative of the association of both these elements with pyrite. In contrast to Madenköy and Sarisu, there is a moderate correlation between Fe and Mn, and Cu, Pb, Zn, Ag, and Cd in the Sirtköy and non-mineralized areas (Table 7.2 and 7.9). In and near the gossan at Sirtköy the metal cations are absorbed by Fe- and Mn-oxides and hydroxides during the formation of the gossan before

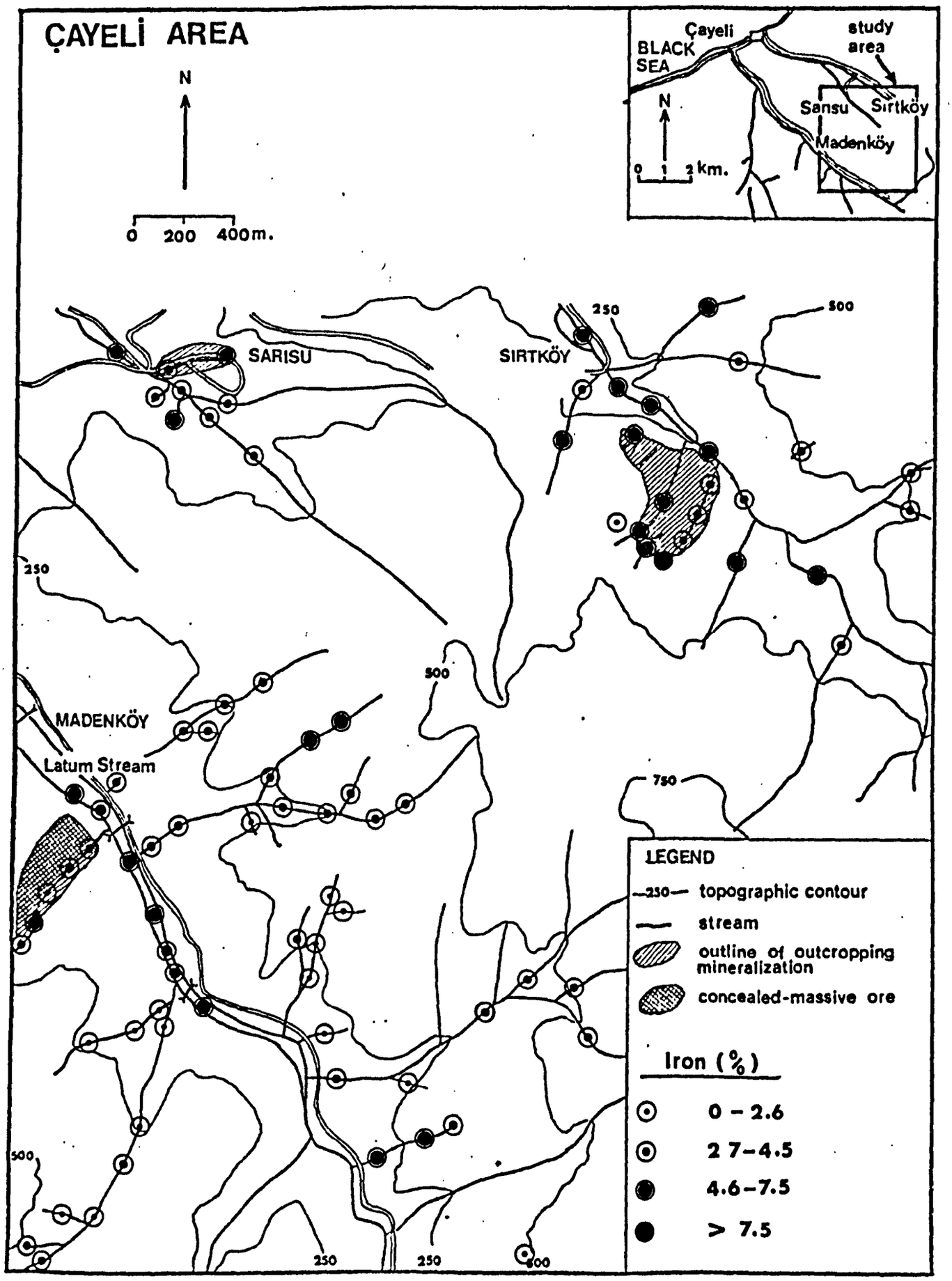


Figure 7.20 Dispersion of iron in stream sediments, Çayeli area.

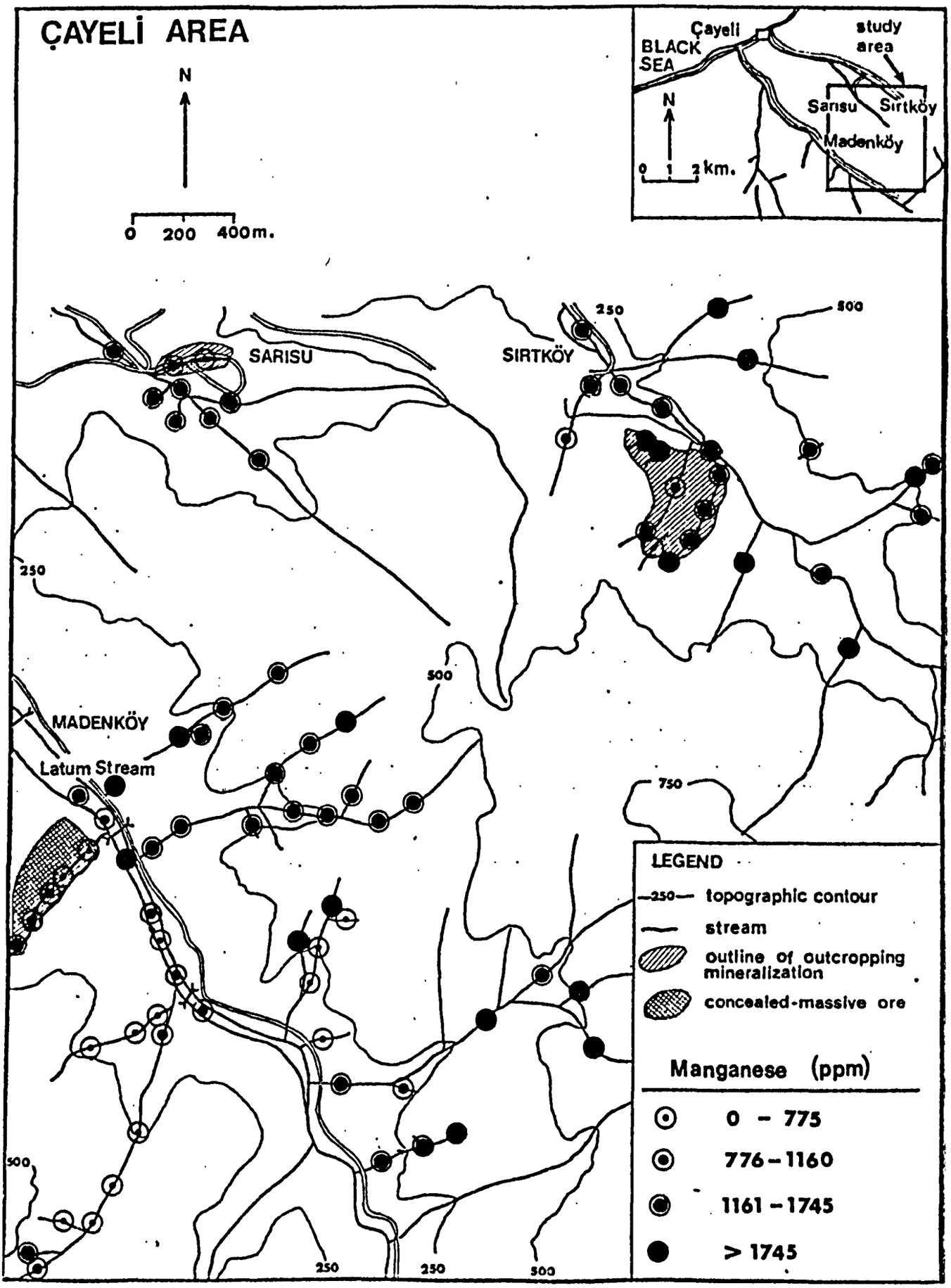


Figure 7.21 Dispersion of manganese in stream sediments, Cayeli area.

they can be freely transported into the stream. The element association of the original gossan is, therefore, reflected in the nearby stream sediments as a result of mechanical transport of the gossanous material.

7.7 SUMMARY AND CONCLUSIONS

Melt-waters from the snow-capped granitic massif in the south of the area, together with a high annual rainfall (up to 2.5 m) and a high topographic relief give rise to fast flowing, all year-active streams. Thus, the stability of hydromorphic anomalies in first and even second order streams is severely affected by flooding during periods of high rainfall or warm upland temperatures. In some mineralized areas such as Tunca there is no tributary drainage; the large streams flowing through these areas have no anomalous expression.

In the Çayeli and Kutlular areas the patterns for As, Cu, Zn, Pb, Ag, Cd, and Mo in the drainage net reveal the differences between the three types of mineralization. Arsenic is an excellent pathfinder for outlining the types of deposits, the strength and size of the drainage anomaly being related to the type and tenor of mineralization. The strongest As anomalies were observed in the vicinity of concealed massive sulphide deposits with partly exposed stockwork and impregnation zones (Madenköy and Kutlular). Zinc, Cu, Pb, and Ag exhibit stream sediment anomalies which are chiefly dependent on the type of mineralization; the strongest anomalies are associated with massive sulphide deposits whereas weaker and more specific anomalies (mainly Cu) are related to stockwork and impregnation deposits. Molybdenum

is not a good indicator of deposit type since strong anomalies are developed in stream sediments associated with both massive and stockwork deposits.

The constant flushing and youthful drainage pattern in the area retards the scavenging abilities of Fe, Mn, and organic precipitates thus reducing problems of interpretation due to these substances.

Sulphide mineralization is also indicated by the pH of spring and stream waters, values ranging from less than 4 to 5 being characteristic of waters leaching sulphide mineralization.

CHAPTER 8

LITHOGEOCHEMICAL EXPLORATION

8.1 Introduction

An investigation of the bedrock geochemistry in the vicinity of the six mineral deposits and occurrences in the Black Sea Ore Province was mounted with a view towards developing the following diagnostic parameters: (a) the detection of primary halos and alteration zones in hanging-wall and footwall formations of blind ore deposits, (b) indications of the position (with directional vectors) of concealed massive sulphide deposits, features that could aid the siting of exploratory drill-holes, and (c) discriminating features to differentiate barren stockwork and impregnation zones from their more productive counterparts associated with concealed massive sulphide bodies.

Part of the research on lithogeochemical exploration in the Eastern Black Sea Region has been described in a paper by Çağatay and Boyle (in press).

8.2 HYDROTHERMAL ALTERATION

8.2.1 Introduction

Hydrothermal alteration involves the mineralogical and chemical changes which occur as a result of the interaction between hydrothermal fluids and rocks. The type of alteration and subsequent mineral paragenesis depends on the mineralogy and chemistry of the initial rocks, the chemical composition of the hydrothermal solutions, and the temperature and pressure of the hydrothermal environment. The shape

and size of the altered zones are determined largely by the physical features of the host rocks such as porosity and permeability.

Many different types of hydrothermal alteration have been recognized. Chloritization, kaolinitization, sericitization, greisenization, argillization, and propilitization are terms to describe typical mineralogical assemblages. Potassium, sodium, or magnesium metasomatism are general terms that indicate specific chemical changes. Several attempts have been made to group hydrothermal alteration mineral phases into type assemblages which are formed under similar conditions of temperature, pressure, and pH. Creasey (1959 and 1966) distinguished three types: propylitic, argillic, and potassium silicate hydrothermal alteration assemblages. Burnham (1962) classified hydrothermally altered rocks into two facies, argillic and phyllic, his argillic facies being the equivalent of Creasey's propylitic and argillic types. Meyer and Hemley (1967) grouped hydrothermal alteration into five mineral assemblage types, in order of decreasing hydrogen metasomatism, as follows: (a) advanced argillic, (b) sericitic, (c) intermediate argillic, (d) propylitic, and (e) potassium silicate assemblages.

Three types of wall rock alteration, similar to the assemblages of Creasey (1959) are generally adequate for practical purposes. Subfacies, such as montmorillonite, kaolinite, and sericite within the argillic type, can be distinguished during detailed studies. It is important to recognize that the term "assemblage" does not mean a group of minerals found in equilibrium with one another. In most

cases equilibrium among alteration minerals and hydrothermal solutions may not have been attained (Meyer and Hemley, 1967).

The data for the above classifications were obtained mainly from three sources: (i) field data, predominantly from the hydrothermal alteration studies in porphyry copper deposits (Stringham, 1952; Creasey, 1959, 1966; Kent, 1963), (ii) laboratory stability field studies of feldspars and clays (Gruner, 1944; O'Neill, 1948; Hemley et al., 1971), (iii) present day hydrothermal alteration in geothermal areas such as Wairakei, New Zealand and the Salton Sea, California (Kerr, 1955; White, 1955, 1968).

The formation of certain hydrothermal alteration mineral species under weathering conditions has been known for a long time (Penrose, 1894). Clay minerals such as illite, montmorillonite, halloysite, and kaolinite can form by supergene processes especially under intense acid leaching tropical conditions (Kerr, 1955). On this account certain difficulties may arise in distinguishing between the products of hypogene and supergene alterations. However, some minerals such as dickite, nacrite, and sericite have been established as being strictly hypogene in origin. It is also generally believed that montmorillonite cannot form in rocks which have already been hydrothermally argillized since its formation requires some MgO.

The two main objectives of hydrothermal alteration studies in the Eastern Black Sea Region are firstly, to obtain a better understanding of the ore forming environments and secondly, to establish favourable criteria for discovering ore bodies. The spatial association of hydrothermal alteration with ore deposits has led many workers to study

the alteration zones with the aim of determining guidelines in the search for ore (Hewett, 1928; Lovering, 1949; Schwartz, 1955, 1956; and Creasey, 1959).

For the alteration studies in the mineralized study areas, 229 carefully collected fresh surface rock and drill-hole samples were analysed by X-ray diffraction analysis, and about 50 thin sections were examined under the petrographic microscope. A description of lateral and vertical zonation of the hydrothermally altered rocks in the study areas is given and the mode of formation of these different zones are discussed.

The relative abundance of the alteration minerals has been assessed by the intensity of their particular X-ray reflections (Table 5.11). For a more detailed account of the X-ray diffraction techniques used for clay mineral recognition and for estimating the relative abundance of alteration minerals the reader is referred to section 5.10.

8.2.2 Hydrothermal Alteration in the Madenköy Deposit

The Madenköy ore body is enveloped by an extensive zone of argillized host rocks, which in turn is probably surrounded by a zeolite zone. Zeolites could not be detected by X-ray diffraction analysis due to their small amounts, but their presence in the dacitic pyroclastics in the north bank of the Latum stream, about 300 m north east of the Madenköy deposit has been revealed by thin section studies. In these rocks radial aggregates of mordenite usually replace the volcanic glass shards.

The lateral distribution of clay and carbonate minerals are given in Figures 8.1 and 8.2, and their vertical

distribution in drill-holes 101, 108, and 110 is illustrated in Figure 8.3. Three distinct hydrothermal alteration zones can be distinguished in the Madenköy deposit. These zones are characterized by montmorillonite, kaolinite (-mixed-layer sericite-montmorillonite) and sericite. Their features and distribution can be summarized as follows:

Zone (1) Montmorillonite + calcite ± chlorite ± kaolinite[1] ± illite[2] zone. This zone occurs principally at the upper stratigraphic levels within the cover rocks where the basalts are usually carbonated. Chlorite and illite are occasionally present. The feldspars are partly altered in the pumice tuffs; in basalts they are relatively fresh. This zone grades imperceptively into Zone 2 with the appearance of kaolinite.

Zone (2) Kaolinite + mixed-layer sericite-montmorillonite + dolomite ± montmorillonite zone. This zone is generally restricted to the hanging wall rocks and occurs in closer proximity to the massive ore body than Zone 1. The pumice tuffs contain kaolinite, montmorillonite, and occasionally mixed-layer sericite-montmorillonite. The dominant carbonate mineral in this zone is dolomite. The occurrence of dolomite rather than ankerite is suggested by the relative intensity of X-ray reflection peaks for this mineral. The feldspars

---

[1]The term "kaolinite" includes all the kaolin group of minerals; dickite, nacrite, and kaolinite probably are present in most cases, but their specific presence was not authenticated except for nacrite which was determined in a few pumice tuff samples.

[2]Illite is used here to indicate clay minerals with a relatively broad basal X-ray reflection at about 10 A. This suggests the presence of expandable mixed-layering. In contrast, sericite does not contain any expandable mixed-layering and give sharp peaks at 10 A.

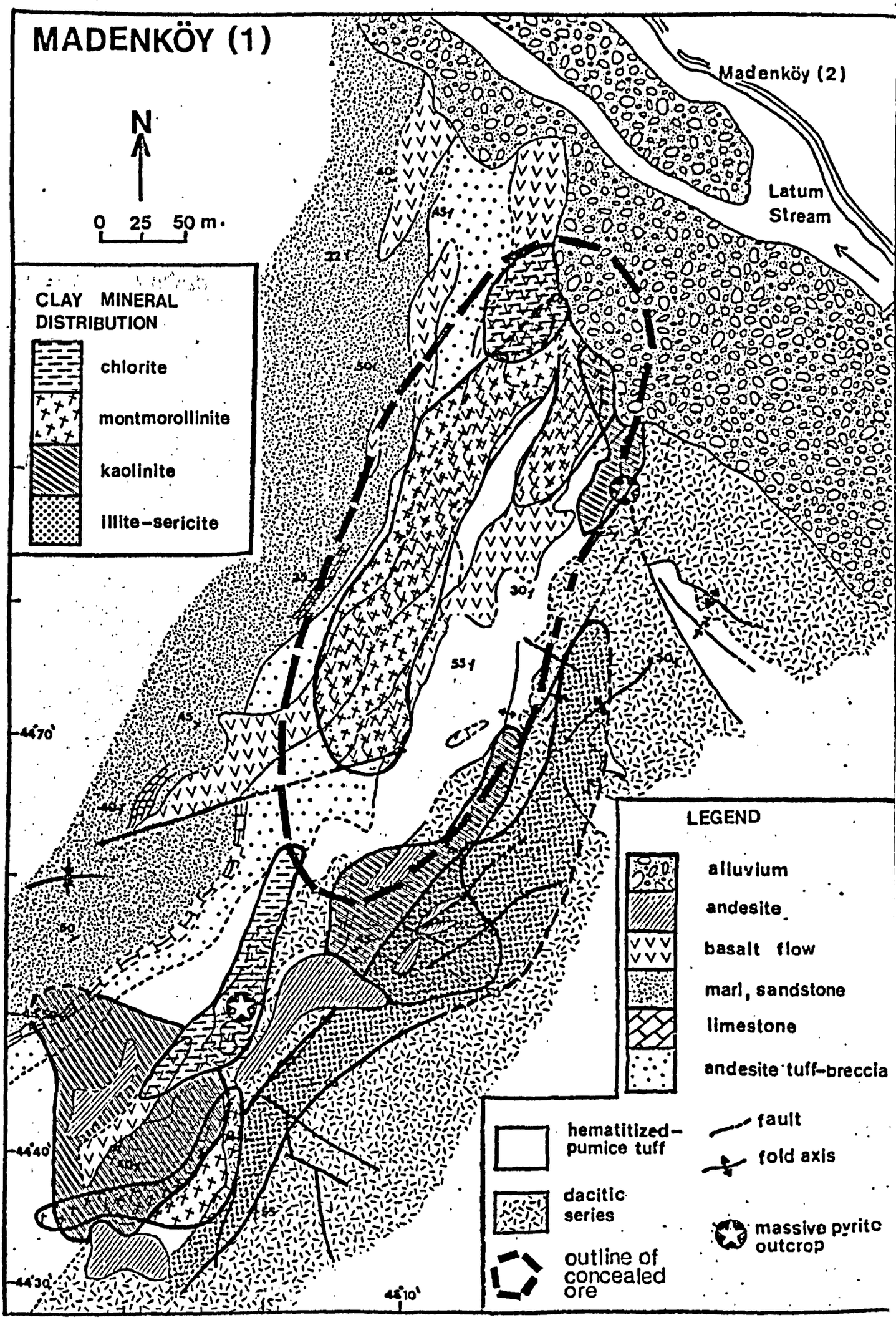


Figure 8.1 The most abundant zones of occurrence of clay minerals at the Madenköy massive sulphide deposit.

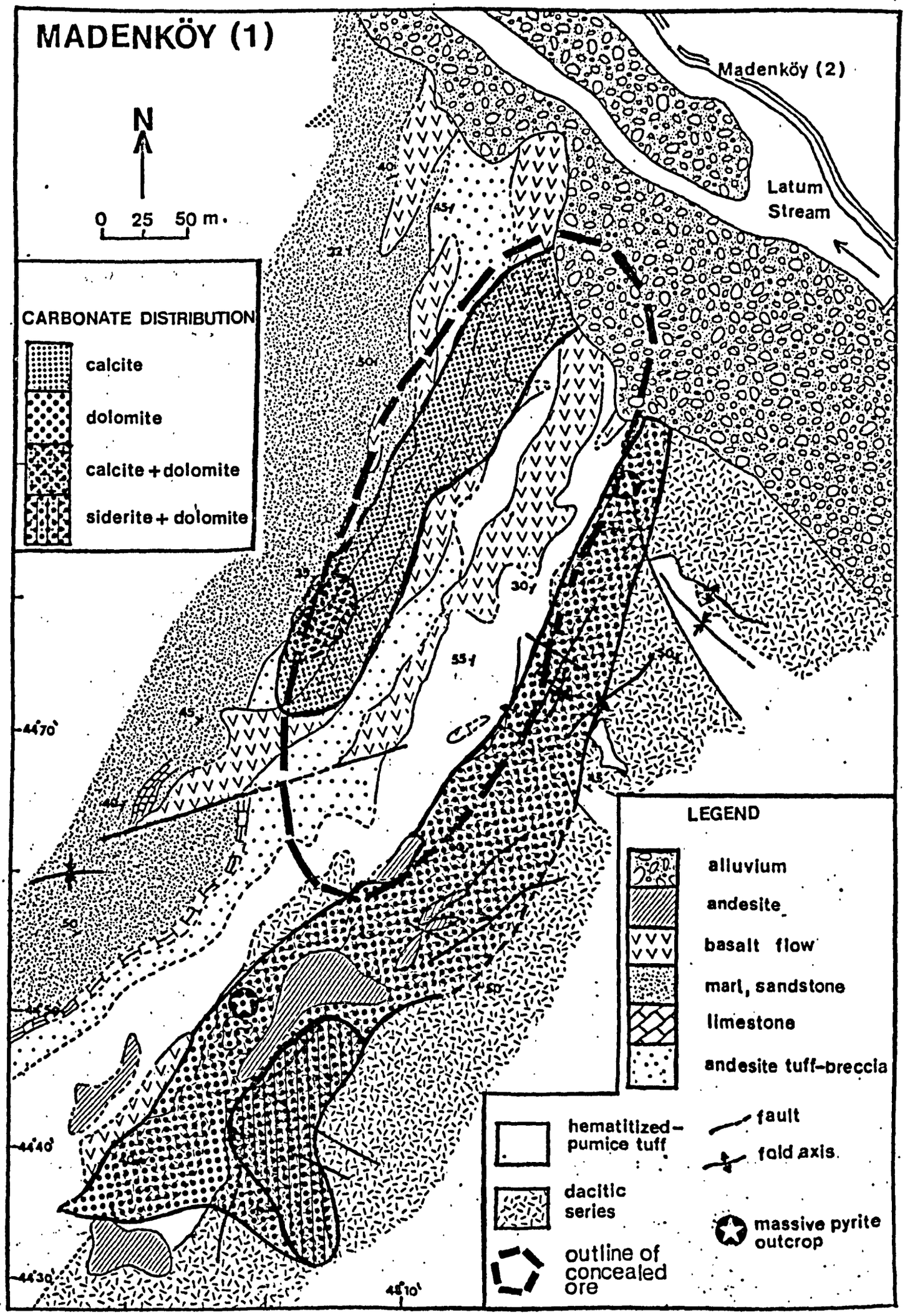


Figure 8.2 The most abundant zones of occurrence of carbonate minerals at the Madenköy massive sulphide deposit.

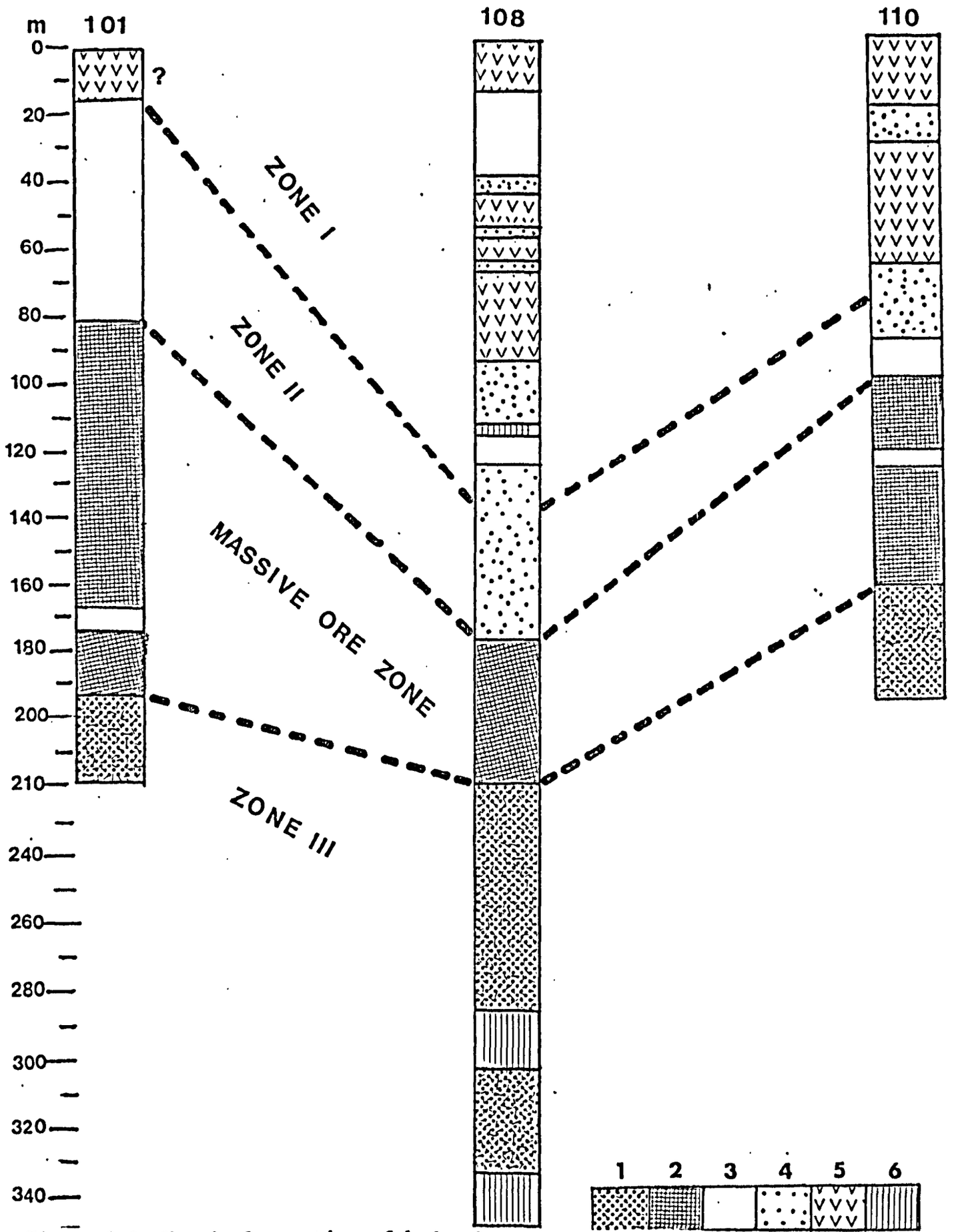


Figure 8.3 Vertical zonation of hydrothermal alteration halo at the Madenköy massive sulphide deposit (Zone I: Montmorillonite - calcite ± chlorite ± kaolinite ± illite; Zone II: Kaolinite - mixed-layer sericite-montmorillonite - dolomite ± montmorillonite; Zone III: Illite or sericite - kaolinite - dolomite - siderite - pyrite. Geological legend: 1- stockwork-impregnation ore, 2- massive ore, 3- pumice tuff, 4- pumaceous sandstone, 5- basalt, 6- andesite.

in the basalts are more altered in this zone than they are in Zone 1; in the pumice tuff samples the feldspars are usually completely altered.

Zone (3) Illite or sericite + kaolinite + dolomite + siderite + pyrite zone. This zone is confined to the dacitic rocks below the massive ore and encloses the stockwork and impregnation zones of the deposit. The rocks in this zone are silicified, the feldspars are almost completely altered, and dolomite and siderite generally occur in major quantities. The distribution of the illite-sericite group of clay minerals in this zone is irregular. In the stockwork-impregnation zone in drill-hole 110 the dominant clay mineral is sericite; in drill-hole 108 illite is abundant for about 50 m below the massive ore giving way to sericite at depth. As far as the lateral distributions of the two minerals are concerned, illite occurs more extensively and in greater quantities than sericite.

In addition to the above alterations, the pumice tuffs are generally hematitized. The hematite largely occurs as very fine amorphous grains impregnating the tuffs and occasionally forming thin layers or veins within them.

The distributions of clay and carbonate minerals in the altered host rocks of the Madenköy deposit are summarized in Table 8.1. The mineralogy of kaolinite and sericite-montmorillonite minerals in the clay fractions of the pumice tuffs were studied by X-ray diffraction and are described below:

Kaolinite: The mineral is highly crystalline, well ordered, and gives basal reflections at 7.085, 3.560, and 2.377 A with

Table 8.1

Clay and carbonate mineral distribution in the Madenköy massive sulphide deposit.

Mineral	Dissemination zone	Stockwork zone		HANGING-WALL ROCKS	
				Pumice Tuffs	Basalts
Illite					
Chlorite					
Montmorillonite					
Mixed-layer illite-montmorillonite			MASSIVE ORE		
Kaolinite					
Sericite					
Calcite					
Dolomite					
Siderite					

relative intensities of 10, 6.5, and 3 respectively. Its gradual collapse between 400°C and 550°C agrees with the general properties of the kaolinite group of clay minerals. The relative intensities of the X-ray reflections obtained with loosely packed cavity mounts of the mineral indicates that the kaolinite is present in the form of nacrite (Table 8.2).

Table 8.2 X-ray reflections of nacrite in pumice tuffs (loosely packed cavity mount).

d-spacing Å	7.085	4.44	4.33	4.14	3.93	2.85	3.56
Relative intensity (maximum 10)	10	4	2.5	1	0.5	0.5	6.5

Mixed-layer illite-montmorillonite: This is an unusually regular, highly ordered mixed-layer clay which is generally confined to the pumice tuffs. It is present in sparse amounts in the dacitic rocks of the impregnation zones, and less ordered varieties may occur in the basalts within the altered zone 2. The basal spacings, the results of heating, and the glycerol tests on this clay are given in Table 8.3. The data in this table compare well with that of bravaisite described by Millot (1970, p. 17).

8.2.3 Hydrothermal Alteration in the Sirtköy Pyritic Stockwork Occurrence

The dacite and the overlying basic rocks in the vicinity of the Gümüşdere stream are hydrothermally altered. The hydrothermal assemblage consists of - chlorite + sericite + quartz + pyrite ± calcite ± dolomite. The basic rocks are

Table 8.3

X-ray diffraction properties of mixed-layer illite-montmorillonite clay (in all tests oriented disc mounts were used).

Air dried		Glycerol treatment		Heated at 400°C		Heated at 550°C	
d-spacing	Intensity*	d-spacing	Intensity	d-spacing	Intensity	d-spacing	Intensity
27.50	10	29.75	10	45.00	10	46.5	10
12.00	9	13.70	3	9.87	4	9.78	5
4.91	1	9.34	2	4.90	1	4.89	1
3.70	½	5.39	¼	3.26	2		
		4.69	½				

* The basal reflection with highest intensity is given the value 10. Intensities of other reflections were calculated relative to the highest intensity.

strongly chloritized and in most cases pyritized. The dacitic rocks around the gossan near Gümüşdere stream have been sericitized and to a less extent chloritized. Feldspars in the dacites and to a lesser extent in the basic rocks are altered mainly to sericite.

8.2.4 Hydrothermal Alteration in the Sarisu Pyritic Impregnation Occurrence

The typical hydrothermal alteration assemblage in this area is - kaolinite + montmorillonite + quartz + pyrite + dolomite ± calcite ± illite. Kaolinite is widely distributed in the dacites and is occasionally present in the basic rocks. Montmorillonite occurs in both the basalts and dacites, especially where the latter are pyritized. Dolomite is also widely distributed in large quantities in the dacites and the feldspars in the dacite are partly altered.

8.2.5 Hydrothermal Alteration in the Kutlular Massive Sulphide Deposit

The hydrothermal alteration in the Kutlular area is represented by an - illite + quartz + pyrite ± montmorillonite ± sericite ± chlorite ± calcite - mineral assemblage. No obvious zonation was observed, but a vertical distribution of the alteration minerals in drill-hole K-8 suggests that the massive yellow ore body is enveloped by an illite - pyrite zone (Figure 8.4). In this alteration envelope feldspars are almost totally altered to clay minerals. Calcite and chlorite occasionally occur in the footwall and hanging-wall dacitic

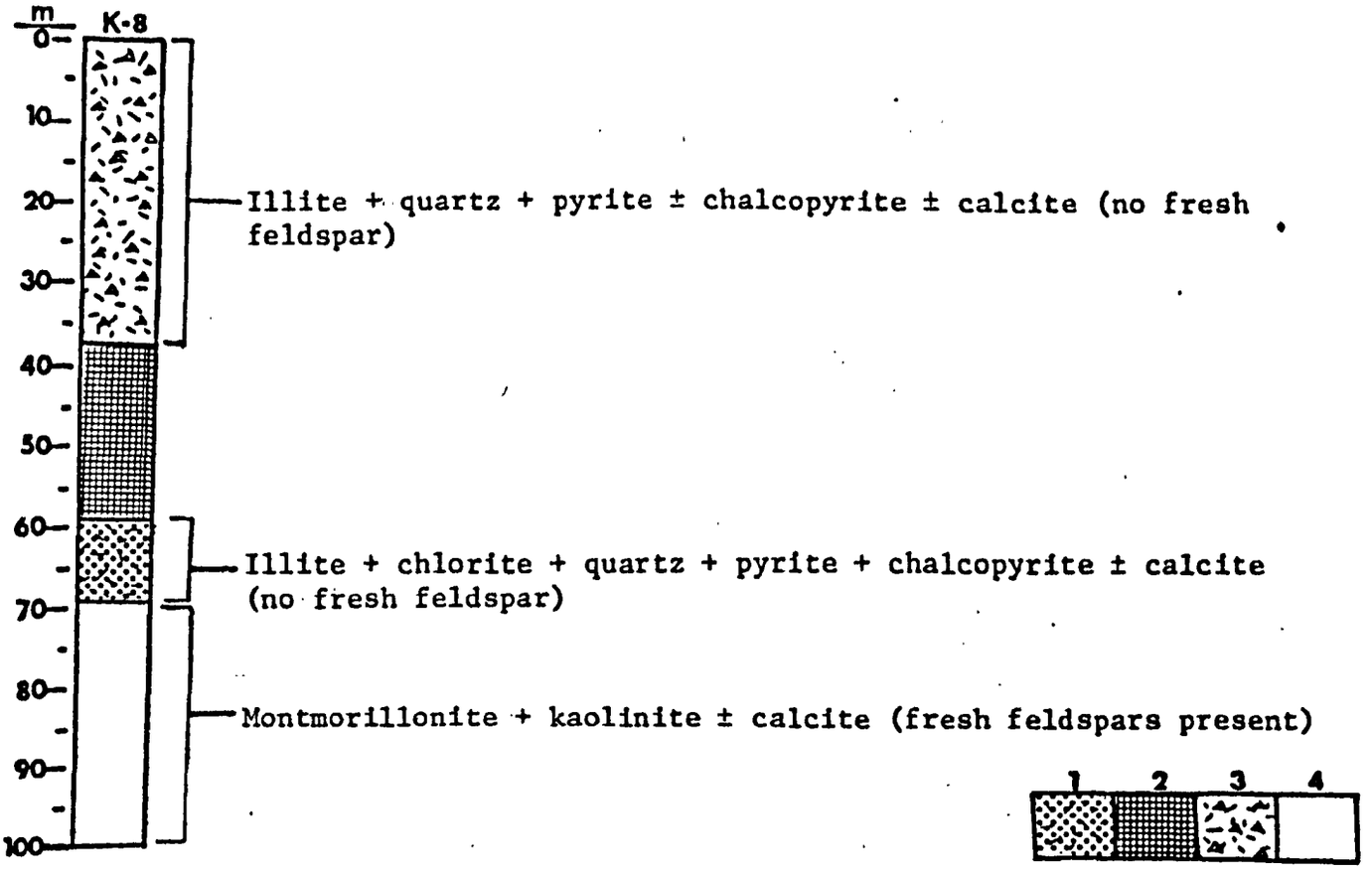


Figure 8.4 Vertical distribution of minerals in the Kutlular massive sulphide deposit (1- stockwork-impregnation zone, 2- massive ore, 3- dacitic tuff-breccia, 4- diabase).

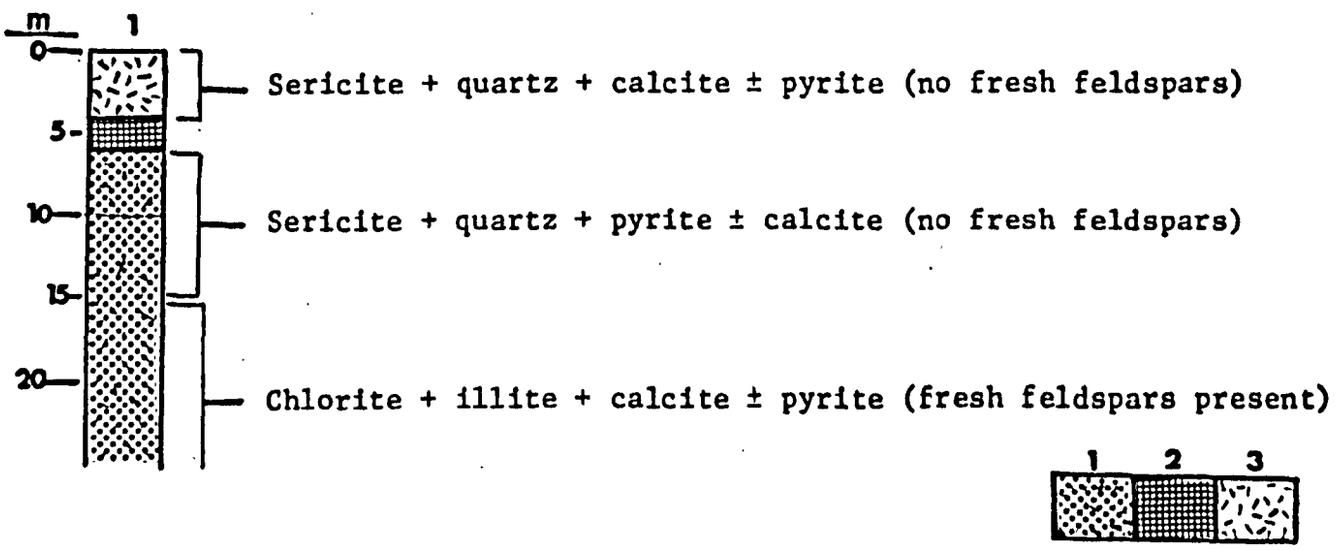


Figure 8.5 Vertical distribution of minerals in the Kotarak Dere deposit (1- stockwork-impregnation deposit, 2- massive pyrite, 3- dacitic tuff).

rocks and in the diabase. Montmorillonite occurs in the diabase and is only sparsely present in the hanging-wall of the deposit. Sericite was recognized in one drill-core (K-8) sample in the footwall which is silicified.

8.2.6 Hydrothermal Alteration in the Kotarak Dere Stockwork Deposit

The hydrothermal mineral assemblage in this deposit is similar to that observed in the Kutlular deposit. The mineral assemblage in the Kotarak Dere deposit consists of sericite, illite, quartz, chlorite, and pyrite. Compared with the surrounding dacitic rocks, sericite occurs in relatively greater amounts around the remnant of massive pyritic ore and the pyrite impregnation zone near drill hole 1. Sericite generally predominates over illite. Chlorite is present in large amounts surrounding the sericite-rich zone although both chlorite and sericite occur together in the dacites as well as in the overlying basalts. The closer spatial association of sericite with mineralization rather than chlorite is also suggested by the vertical distribution of these two minerals. For example, in drill-hole 1 sericite is present whereas chlorite and feldspar are absent in a 10 m thick zone enveloping the massive pyrite ore (Figure 8.5), the last two minerals being generally present remote from the strongly mineralized zones (e.g. in drill-hole 15 where there is only occasional pyrite impregnation).

The footwall rocks are generally silicified.

8.2.7 Hydrothermal Alteration in the Tunca Massive Sulphide Deposit

The distribution of hydrothermal alteration minerals was determined in surface rocks of this deposit and in drill-holes T-1 and T-5. Three distinct hydrothermal alteration assemblages can be distinguished (Figure 8.6). These zones to some extent conform to the lithology and display the following features:

(1) Chlorite zone: This zone generally contains chlorite, calcite, and rarely dolomite as alteration minerals. It is confined to the basic hanging wall rocks, the feldspars in these rocks being only slightly altered.

(2) Sericite or illite - chlorite zone: This zone occurs mainly in the hanging wall hematitized dacite and in the footwall dacites remote from the mineralization. Illite occurs in the upper, and sericite is present in the lower stratigraphic levels in the footwall dacites (Figure 8.6). The hanging wall dacites are impregnated and veined by hematite and contain calcite in places. The feldspars in this zone are more altered than in Zone 2.

(3) Sericite or illite zone: This zone is confined mainly to parts of the footwall dacites. As observed in drill core T-1 the only clay mineral is sericite or illite. The former mineral occurs in the lower levels of the footwall dacite and increases in amount with depth. Illite is generally confined to the upper levels of the footwall dacite. This zone is marked by an extensive feldspar alteration and some silicification.

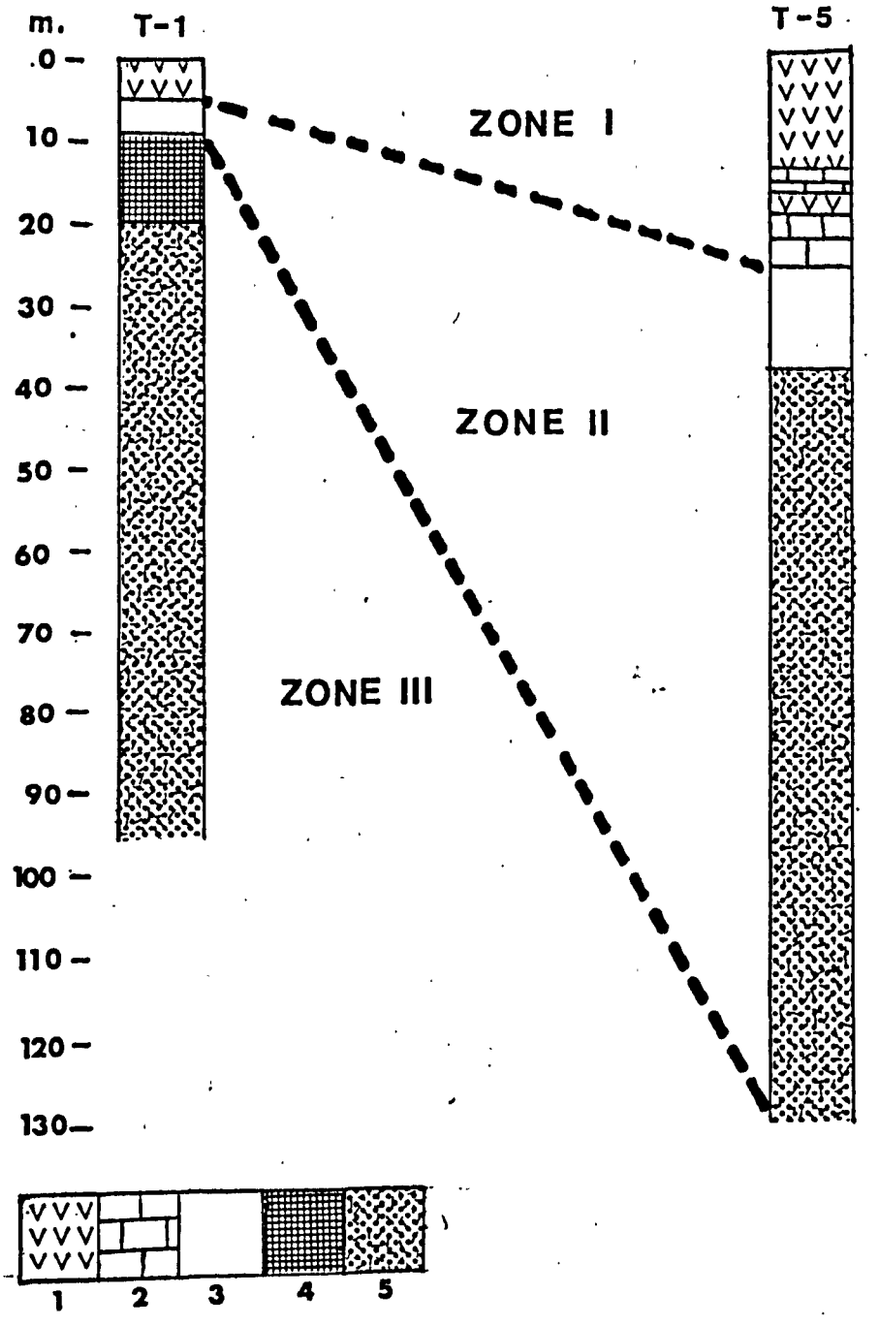


Figure 8.6 Vertical zonation of hydrothermal alteration halo at the Tunca massive sulphide deposit (Zone I: Chlorite - calcite, Zone II: Illite-sericite - chlorite ± hematite, and Zone III: Sericite. Legend: 1- basalt, 2- limestone, 3- hematized dacite, 4- massive sulphide, 5- stockwork and impregnation zone in dacite.

8.2.8 Discussion

From the preceeding descriptions it is evident that the hydrothermal alteration features in different study areas have similarities as well as differences. The main similarity is that the common form of alteration spatially associated with ore deposition is sericitization (including the presence of illite) of the dacitic footwall rocks. This alteration type involves hydrogen metasomatism including replacement of ions such as Na^+, Ca^{2+} and Mg^{2+} from the feldspars and mafic minerals of the wall rocks by H^+, the H^+ activity increasing with temperature.

The fields of formation of the alteration and sulphide assemblages at 250°C in the Madenköy deposit are given in Figure 8.7. The temperature of formation of these various alteration zones are evidently different. However, the effect of higher temperature is to lower the pH and to increase the H_2S partial pressure (Meyer and Hemley, 1967, p. 220).

As noted earlier, alteration Zones 2 and 3 in the Madenköy deposit contain kaolinite, dolomite, and siderite. In addition, the Zone 3 has illite-sericite clay minerals. The formation of kaolinite and illite-sericite in the same suite generally requires at least moderately high temperatures (250-350°C) and acid conditions (pH:3 to 5), although sericite can form under neutral to slightly alkaline conditions and kaolinite may form at lower temperatures. In general carbonates cannot be precipitated by simple cooling of hydrothermal solutions. Their deposition requires one or more of the following conditions: (1) rise in temperature, (2) boiling of hydrothermal solutions, (3) mixing, and (4) reduction

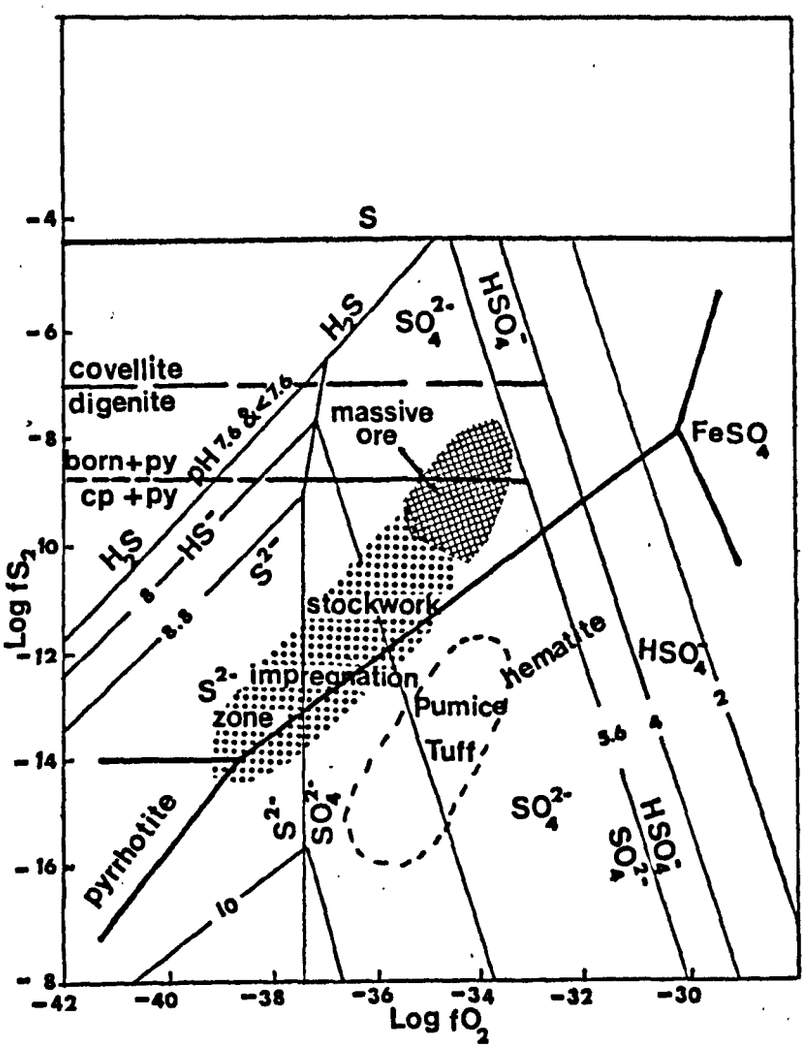


Figure 8.7 Field of formation of ore and hydrothermal mineral assemblages within massive ore, stockwork and impregnation zones, and pumice tuffs at the Madenköy massive sulphide deposit in the Cu-Fe-S-O system at 250°C and 0.1 molar total sulphur. Base diagram redrafted after Meyer and Hemley (1967, p. 220).

in H^+ activity. In most cases of silicate alteration associated with mineralization the last factor and to a lesser extent the third are responsible for carbonate deposition. The occurrence of clays and carbonates together at the Madenköy deposit can best be explained by the changing nature of the hydrothermal solutions. It is believed that the hydrothermal solutions which precipitated the massive ore and the stockwork ore were also responsible for the formation of the illite-sericite and kaolinite. These solutions were low in pH and high in temperature and sulphur fugacity. The solutions, however, become more alkaline with declining temperature towards the end of ore deposition. The hydrothermal activity would appear to have continued with less intensity after the formation of the pumice tuffs and basalt flows. Later movement of compaction fluids evolved as a result of diagenesis, and later deformation probably modified the alteration patterns surrounding the deposit. The pH of the pumice tuffs (average of 8.5 as determined by measuring the pH of a 0.01 $CaCl_2$ solution after it was equilibriated with powdered pumice tuff samples), their hematitized nature, and the occurrence of native copper in these rocks suggests that the hydrothermal solutions were considerably alkaline with low sulphur and high oxygen fugacities (Figure 8.7). As a result of the increased CO_3^{2-} activity, dolomite (± siderite) and calcite (± dolomite) were deposited in the pumice tuffs and basalts respectively. The presence of kaolinite suggests that either the hydrothermal solutions were acid during the earlier stages of the formation of Zone 2 or the kaolinite has a detrital origin.

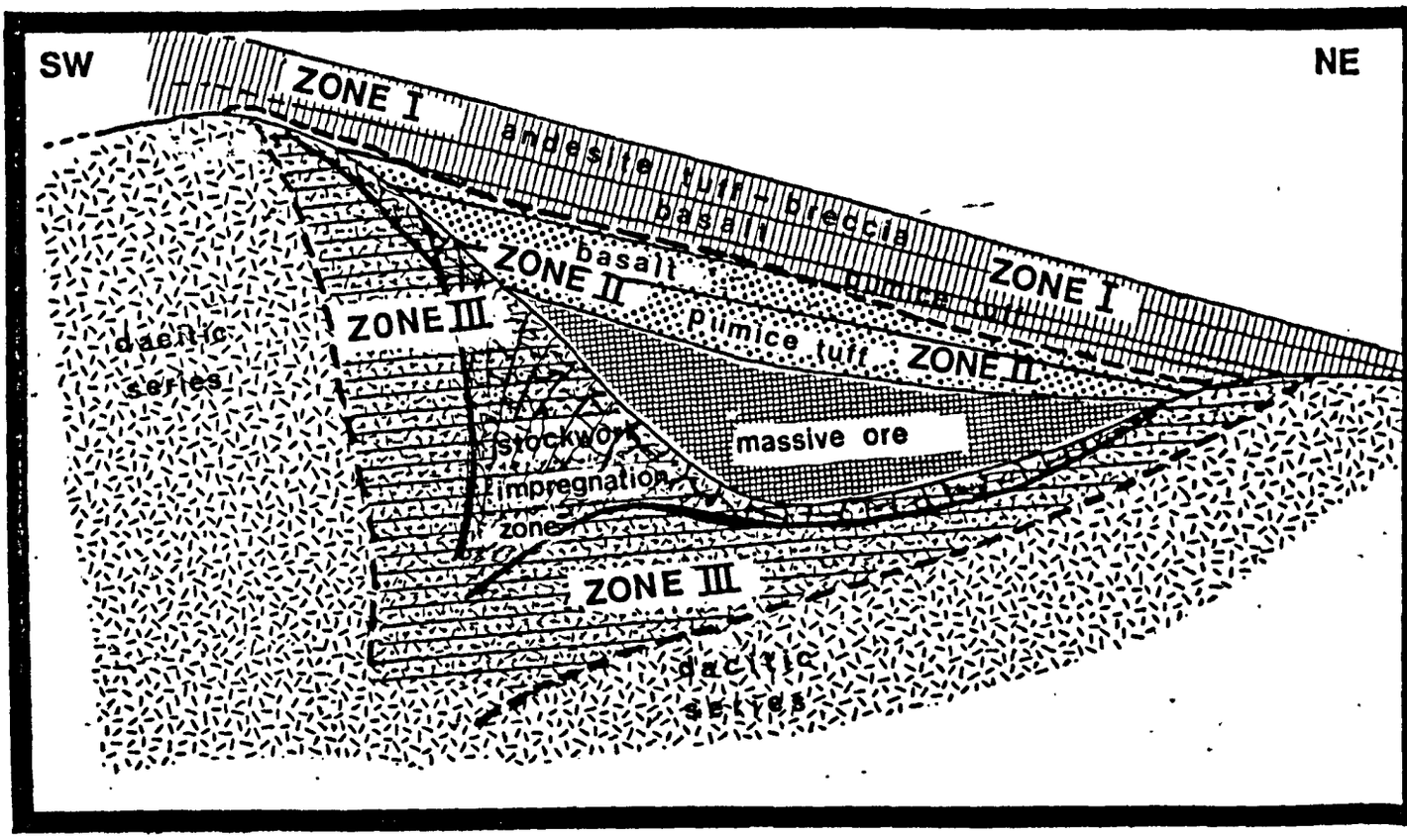


Figure 8.8 Idealized cross section showing the spatial association of the Madenköy massive sulphide deposit and the hydrothermal alteration zones. (Zone I Montmorillonite - calcite ± illite ± chlorite ± kaolinite ± dolomite ± hematite; Zone II Kaolinite - mixed-layered sericite - montmorillonite - dolomite ± siderite ± hematite; Zone III Illite-Sericite - kaolinite - dolomite ± siderite.

In either case the stability of the kaolinite under later, alkaline conditions is remarkable. The various sulphide grains in the pumice tuffs are regarded as detrital, being derived from the erosion of the sulphide ore below.

The mixed-layer sericite-montmorillonite clay probably represents a transition between sericite and montmorillonite with the change in conditions of alteration. Montmorillonite in Zone 1 was formed by the reaction of alkaline hydrothermal solutions (mixed with sea water) with the feldspars and volcanic glass. Silica from the volcanic glass were probably responsible for the silicification of the footwall dacitic rocks and the hanging wall pumice tuffs. This silica probably resulted from the reaction of the glass with hydrothermal solutions to produce hydrothermal quartz, possibly through an unstable low cristobalite phase.

In the Madenköy area the most intensive and extensive hydrothermal alteration occurs towards the southwest of the Madenköy map area (Figure 8.1, 8.2, and 8.10). An idealized cross section illustrating the spatial association of the ore and hydrothermal alteration zones is given in Figure 8.8.

All other studied mineralized zones, except Sarisu, have similar alteration mineral assemblages, but these are somewhat different from those present at the Madenköy deposit. In other mineralized zones the absence of kaolinite and montmorillonite is a common feature, and magnesium metasomatism manifests itself in the form of chloritization rather than dolomitization.

The porous, glassy nature of the dacitic rocks seems to have played a major role in the extensive nature of the alteration zones in all of the mineralized areas.

8.2.9 Hydrothermal Alteration as a Guide to Ore

8.2.9.1 Introduction

Most of the earlier work related to the use of hydrothermal alteration as a guide to ore has been done on porphyry copper deposits (Schwartz, 1955, 1956; Creasey, 1959, 1966; Gupta et al., 1965; Lowell and Guilbert, 1970; Hausen and Kerr, 1971). These workers attempted to delineate certain phases of hydrothermal alteration associated with the productive ore-forming stages through studies of mineral paragenesis and physical and chemical changes involved in the different phases of alteration.

Studies of hydrothermal alteration related to volcanogenic massive sulphide deposits, and their use in exploration, have recently become available. These investigations are reviewed in Chapters 1 and 2.

It is evident from the detailed descriptions of hydrothermal alteration described in the previous section that certain general features can be used in exploration. In particular, the assemblage of illite-sericite (± kaolinite) alteration minerals associated with the mineralizing processes in the Eastern Black Sea Ore Province appears to be significant. Another feature of the alteration zones that emerged from the studies described above is the marked alteration of feldspars. The assessment of feldspar alteration and its use in mineral exploration is described below.

8.2.9.2 Use of Feldspar Alteration As a Guide to Ore

The hydrothermal alteration of feldspars to montmorillonite-kaolinite, and illite-sericite-groups of clay

minerals has been well documented (Schwartz, 1955; Creasey, 1959; Meyer and Hemley, 1967; and others). Present day alteration of plagioclase feldspar in pyroclastic rocks by thermal spring waters to form montmorillonite, kaolinite, and sericite has been reported from Wairakei, New Zealand and Nevada, U.S.A. (White, 1955).

The author's examination of several thin sections of the dacitic rocks and pumice tuffs in the Madenköy area revealed extensive increasing feldspar alteration as the ore body is approached. This led the author to evaluate the feldspar alteration in the mineralized zones studied. The feldspar, clays, and carbonates were measured by a simple X-ray diffraction analysis under a constant set of conditions such as even grain size and packing and constant operating conditions of the X-ray diffractometer. It is assumed that this ensures that the peak intensity for a particular X-ray reflection of a mineral is directly proportional to its amount. The arbitrary values of the peak intensities can only be compared for samples of the same rock type (i.e. the same matrix). A detailed account of the analytical technique is given in section 5.10.

The feldspars generally alter to montmorillonite, kaolinite, and illite-sericite clay minerals. In hydrothermally altered dacitic and pumaceous rocks, clay minerals are also formed by the alteration of volcanic glass and pumice. The contribution from these can be assumed to be constant for the dacites and pumice tuffs. The ratio "clay (montmorillonite - kaolinite - illite-sericite)/Feldspar" should, prove, therefore, to be an effective indicator of hydrothermal alteration. In the mineralized areas this ratio

was found to be the best index for assessing the degree of hydrothermal activity associated with mineralization. Based on the frequency distribution of this ratio, intervals of 0-0.2, 0.3-0.7, 0.8-6.5, and > 6.5 were selected for purposes of pattern recognition.

A reconnaissance bedrock survey in the Çayeli area, covering the Madenköy, Sirtköy, and Sarisu deposits and mineralized zones, and detailed studies of the Madenköy, Kutlular, Kotarak Dere, and Tunca deposits were carried out to assess the effectiveness of this ratio. In the reconnaissance survey, areas of strong alteration as indicated by the clay/feldspar ratio, correspond to the Madenköy, Sirtköy, and Sarisu deposits and mineralized zones (Figure 8.9). There is little difference in the intensity of alteration in these areas, and the ratio is, therefore, indicative of hydrothermal alteration only and not of deposit type. In the Sarisu disseminated pyrite deposit the dacites are highly altered, but the basalts are only slightly altered. In the Sirtköy area the dacites, and to a lesser extent the basalts, are strongly altered near the focus of mineralization. Outside of the mineralized zone at Sirtköy the dacites and the basics show no sign of alteration. In the large but discontinuous exposure of dacitic rocks in the Madenköy area, the clay/feldspar ratio outlines an alteration halo in the dacitic rocks around the deposit. An alteration halo is also exhibited in the pumice tuffs overlying the concealed massive ore. This zone is about 200 m in width and 500 m in lateral extent. Compared to the primary F and As halos over this deposit, the clay/feldspar halo is more extensive.

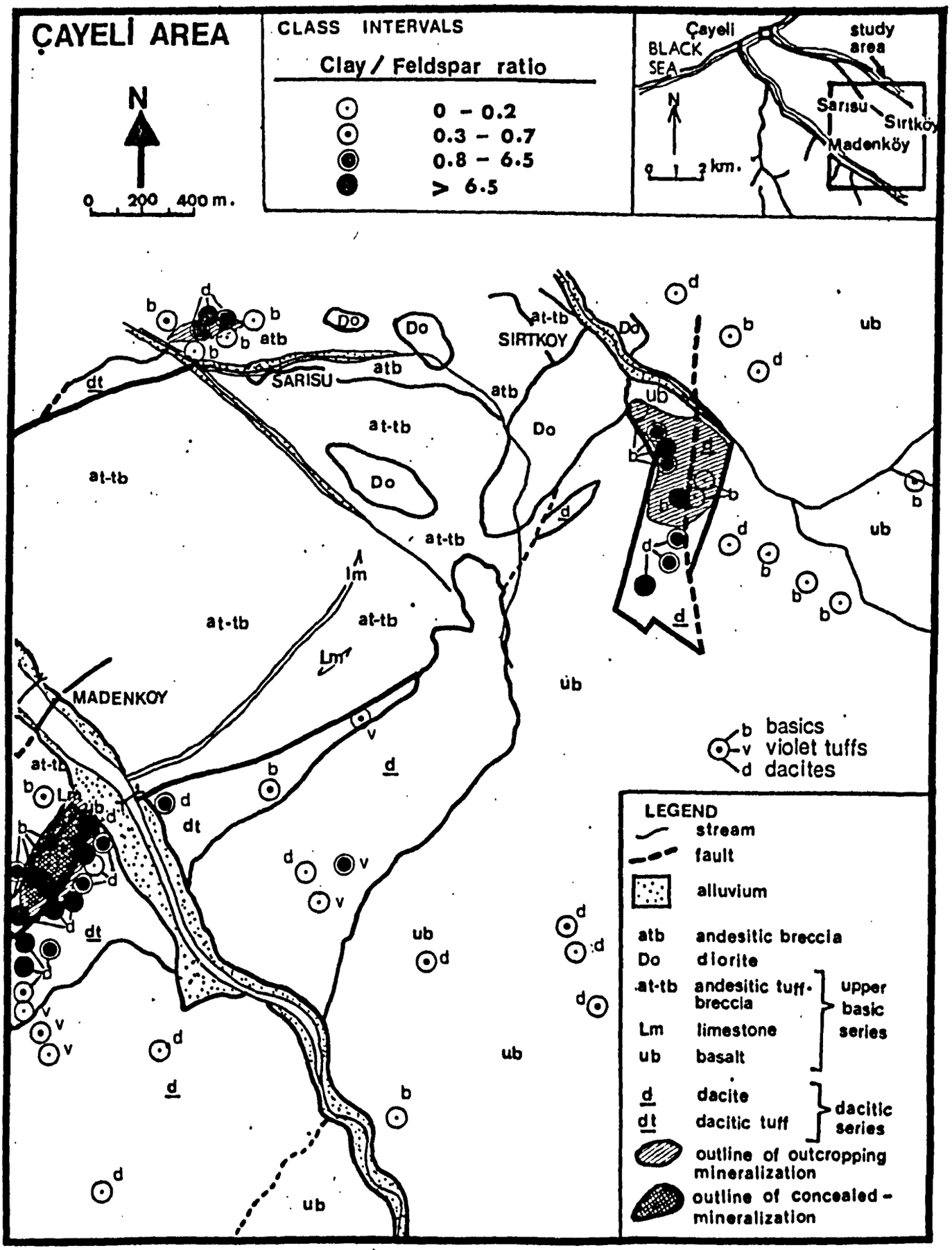


Figure 8.9 Clay/feldspar ratio of bedrocks, Cayeli area.

In the immediate vicinity of the Madenköy deposit an extensive zone of alteration extends along the entire pumice tuff-dacitic tuff contact (Figure 8.10). Above the ore zone, only the pumice tuffs display an anomalous alteration pattern; the basalts, andesite tuff-breccia, and sandstone show little alteration, and the clay/feldspar halo in the hanging-wall rocks is, therefore, not as pronounced as the primary elemental halo for F, Pb, and Ag. Intense alteration in both the dacites and pumice tuffs continues for about 300 m SW of the massive ore zone; this trend is also evident for the base metals, F and As. The alteration halo in the dacites is much more uniform than the primary halos for the indicator elements.

In the Kutlular and Kotarak Dere areas, the ratio outlines extensive alteration halos in the footwall dacites (Figure 8.11 and 8.12), especially in the former area where all the samples collected from the footwall dacites were practically devoid of fresh feldspars. The hanging-wall dacitic agglomerates also show strong alteration in this deposit. In these two areas the clay/feldspar ratio exhibits a more extensive halo than the primary dispersion of many indicator and pathfinder elements.

In the Tunca area the ratio is highly anomalous for all samples collected within the dacite window (Figure 8.13). The hematitized dacites stratigraphically overlying the ore show some alteration whereas the diabase is only slightly altered.

The present studies show that the feldspar/clay ratio and the relative distributions of the clay alteration

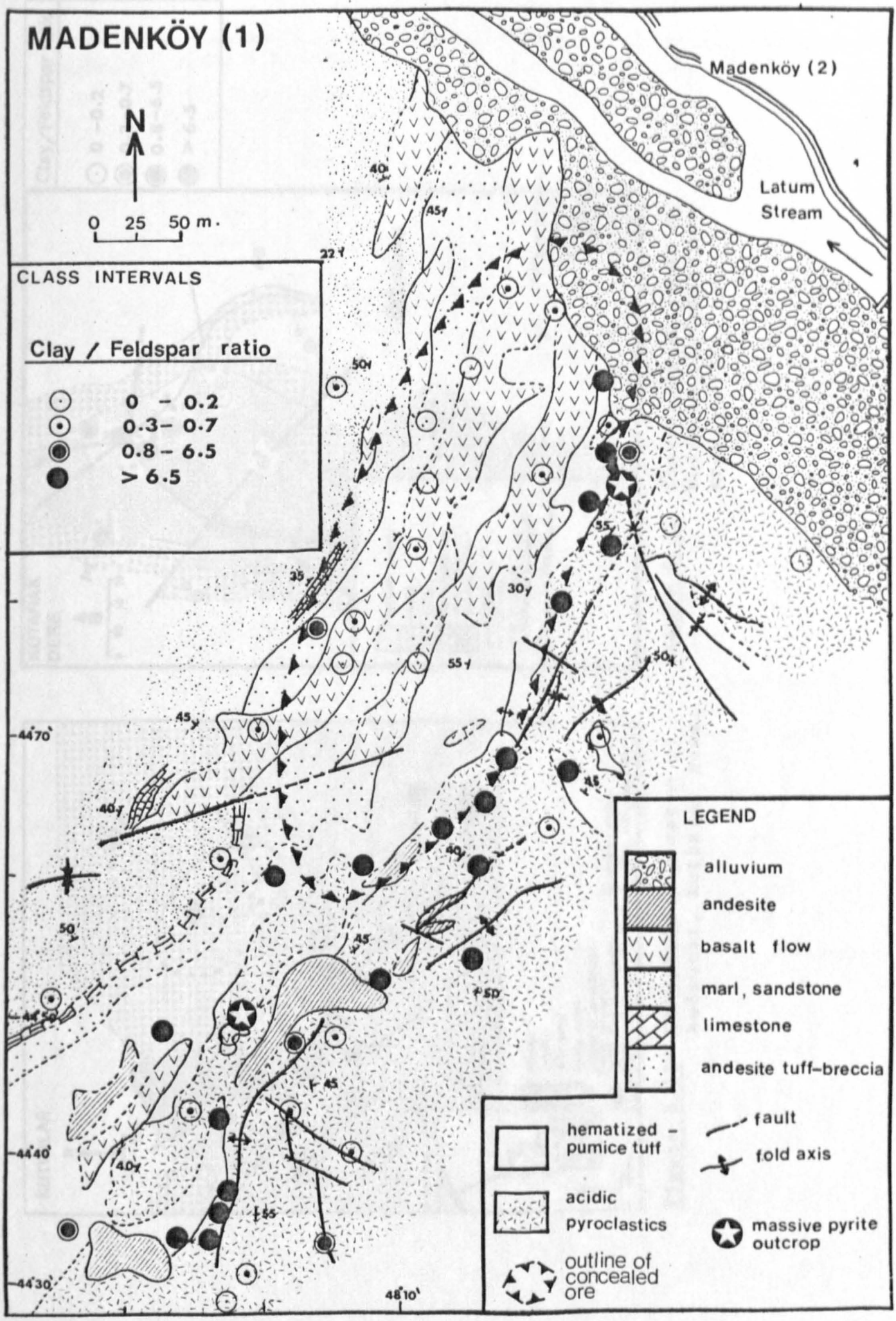


Figure 8.10 Clay/feldspar ratio of bedrocks, Madenköy area.

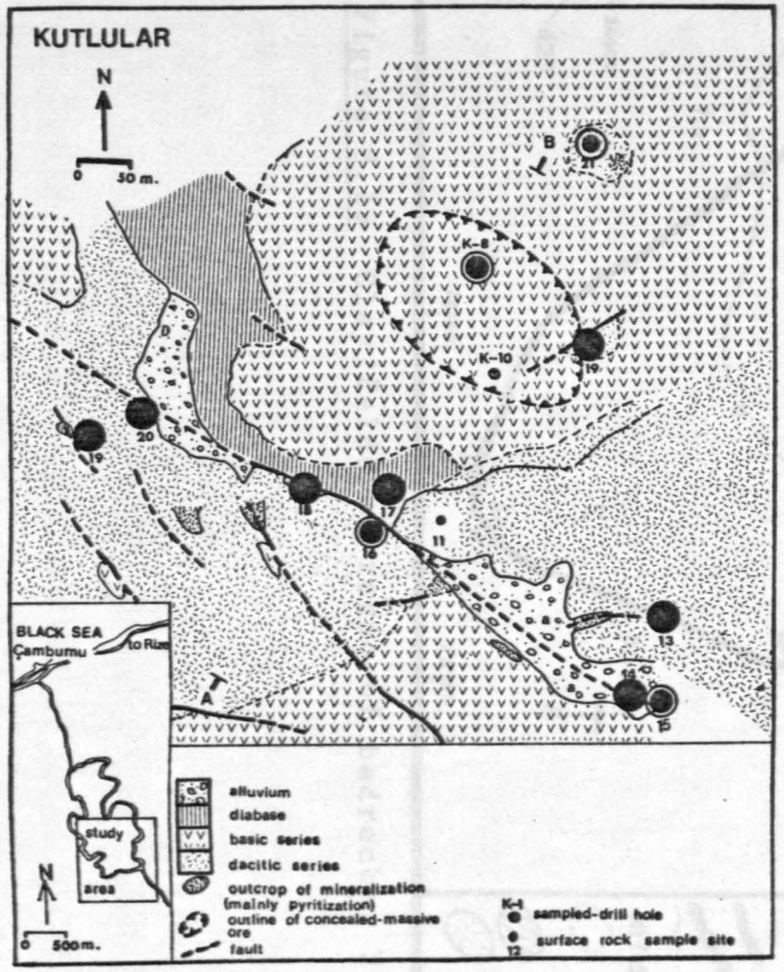


Figure 8.11 Clay/feldspar ratio of bedrocks, Kutlular area.

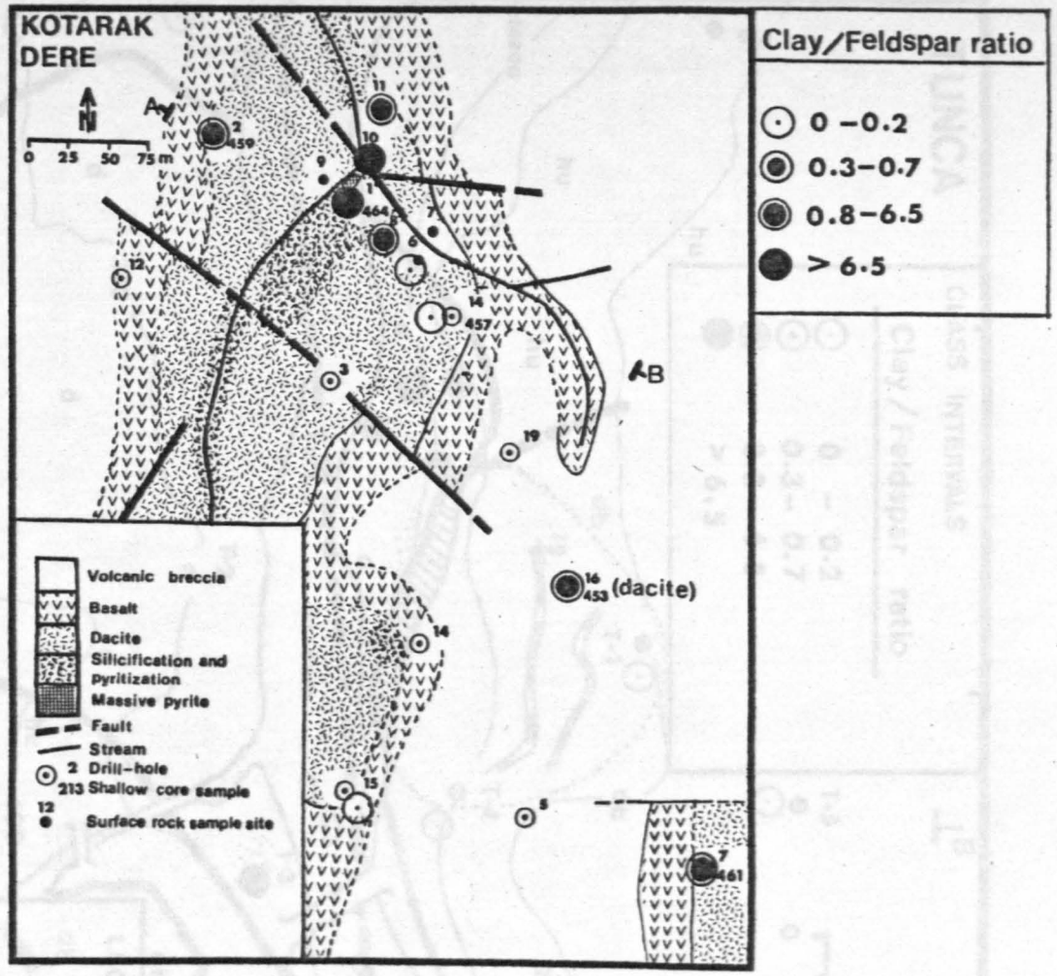


Figure 8.12 Clay/feldspar ratio of bedrocks, Kotarak Dere area.

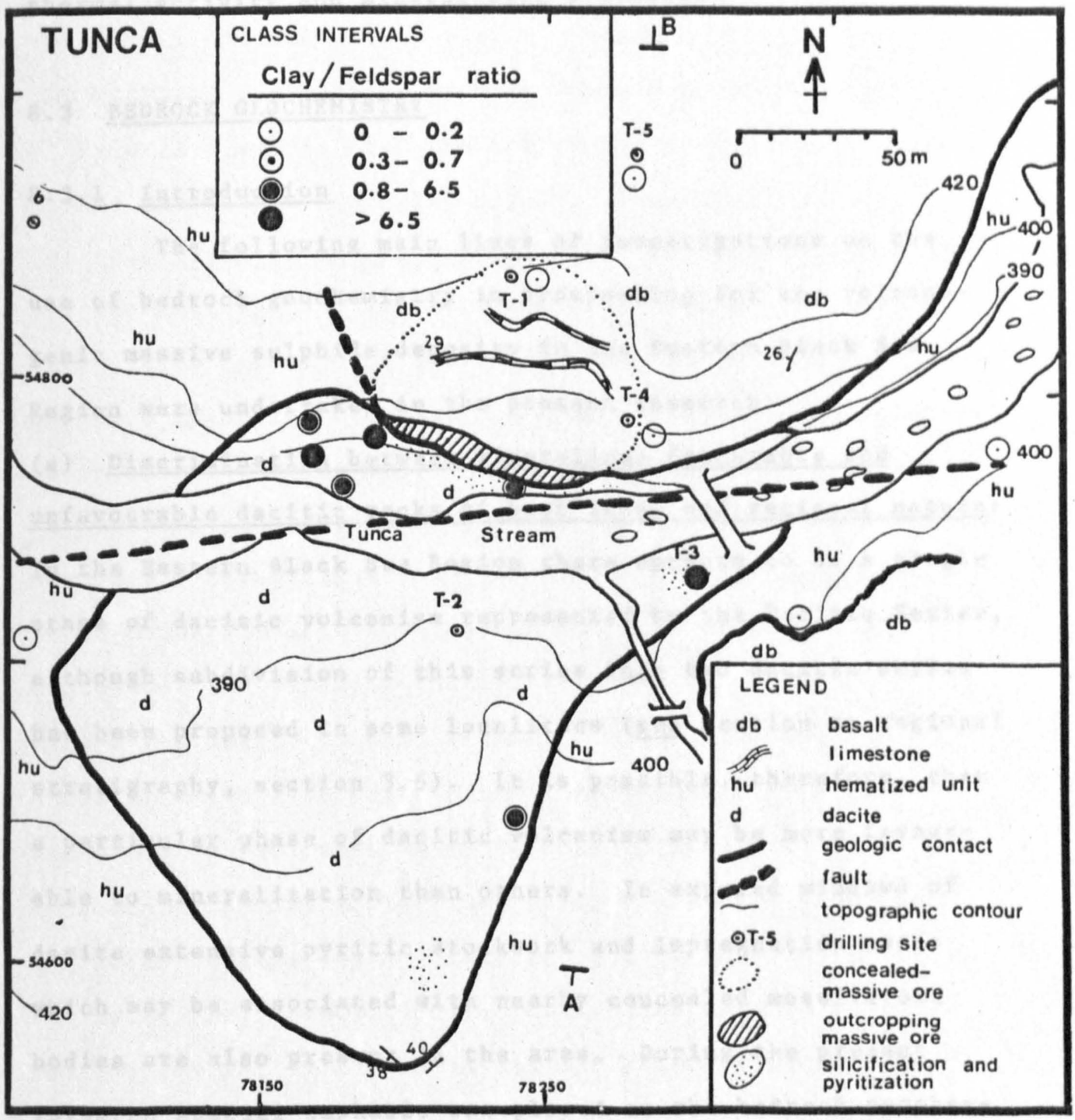


Figure 8.13 Clay/feldspar ratio of bedrocks, Tunca area.

products can be used to estimate the magnitude of hydrothermal activity and mineralizing processes.

8.3 BEDROCK GEOCHEMISTRY

8.3.1 Introduction

The following main lines of investigations on the use of bedrock geochemistry in prospecting for the volcanogenic massive sulphide deposits in the Eastern Black Sea Region were undertaken in the present research:

(a) Discrimination between mineralized favourable and unfavourable dacitic rocks of both local and regional nature: In the Eastern Black Sea Region there appears to be a single stage of dacitic volcanism represented by the Dacitic Series, although subdivision of this series into two dacitic series has been proposed in some localities (see section on regional stratigraphy, section 3.6). It is possible, therefore, that a particular phase of dacitic volcanism may be more favourable to mineralization than others. In exposed windows of dacite extensive pyritic stockwork and impregnation zones which may be associated with nearby concealed massive ore bodies are also present in the area. During the present research special emphasis was placed on the bedrock geochemistry of the host dacitic rocks with the objective of assessing the regional and local favourability of dacitic rocks for mineralization.

(b) Detection of elemental halos in both the hanging-wall and footwall formations of concealed ore deposits: Chemical data obtained during reconnaissance and detailed geological mapping can be used to outline primary halos associated with

suboutcropping or blind ore deposits. Subsurface and surface rock geochemistry around the six deposits and mineralized zones were studied with a view to determining the nature of the vertical and lateral primary dispersion characteristics of several elements that could be used as directional vectors in the search for concealed massive orebodies.

(c) Detection of Exhalite Zones: In the Eastern Black Sea Ore Province typical exhalite horizons such as jaspers, ferruginous cherts, and iron formations associated with the sulphide mineralization are not common; instead the volcanogenic sulphide zones in this region are commonly overlain by hematitized pyroclastics, sediments, or volcanics that may extend laterally beyond the dimensions of the deposits. These rocks are also enriched in Mn (e.g. Madenköy, Harşit-Köprübaşi, and Harköy deposits) and have thicknesses varying from a few metres to tens of metres. For example, the Madenköy massive sulphide deposit is overlain by a hematitized pumice tuff unit which is intercalated with pumaceous sandstones and red marly limestones; the Harşit-Köprübaşi and Harköy deposits are blanketed by a ferruginous chert (D. Egin, pers. comm., 1977); the Lahanos massive sulphide body is covered by a hematitized marly limestone unit (D.W. Hattie, pers. comm., 1977); and the Tunca, Israil, and Murgul deposits are overlain by hematite-impregnated and hematite-veined dacitic rocks. On the other hand, deposits such as Kutlular, Kotarak Dere, and Kizilkaya have beleached pyroclastic cover rocks immediately overlying the deposits. When present the hematitized rock formations usually form an ideal horizon for primary halo studies. Detailed petrochemical studies of the hematitized pumice tuffs at the Madenköy

deposit were made to elucidate their origin, determine their relationship to the ore deposit, and thus to detect any primary elemental halos that could be useful in exploration. (See section 4.2.2.3.1 for petrological description, and section 8.2 for alteration characteristics of these rocks).

For the bedrock geochemical studies a total of 483 diamond drill-core samples from the Madenköy, Kutlular, Kotarak Dere, and Tunca deposits and 203 surface and shallow drill-core samples from all six deposits and mineralized zones and surrounding areas were collected and analysed for 27 elements by various analytical techniques. Not all the samples were analysed for the full range of elements. For the methods of sample collection, sample preparation, and analysis the reader is referred to Appendix A.1.1, Appendix A.2.2, and Chapter 5 respectively.

8.3.2 Data Processing and Presentation

The results of the analyses of the surface and shallow drill-core samples were statistically processed, and arithmetic and logarithmic histograms and cumulative frequency plots were computed for each of the rock types in mineralized and unmineralized areas (see Appendix C). For the elements investigated their distribution in the various rock types were best approximated by a $\log_{10}$ normal distribution. As an estimate of the dispersion of the data about the mean, the means plus one standard deviation for all elemental distributions in the various rock types were calculated and are shown in Tables 8.4 and 8.5.

Class intervals for distribution plots of As, Cu, Zn, Pb, and F correspond to the 20th, 50th, 80th, and 95th

Table 8.4 Composition of Dacitic Rocks Associated with Volcanogenic Sulphide Mineralization in the Eastern Black Sea Region. Values are given for the Mean and Mean + One Standard Deviation (in italics) of Log_{10} Transormed Data (all values are in ppm except where otherwise noted).

	UNMIN-ERALIZED DACITES (19)	MIN-ERALIZED DACITES (83)	MASSIVE SULPHIDE DEPOSITS			STOCKWORK DEPOSITS		BARREN
			MADENKÖY (36)	KUTLULAR (10)	TUNCA (7)	KOTARAK DERE (14)	SIRTKÖY (16)	SARISU (10)
Fe %	1.2 *(4.4)*	2.5 *(6.0)*	1.8 *(3.7)*	2.0 *(3.6)*	2.9 *(8.9)*	3.0 *(6.4)*	5.2 *(6.8)*	5.3 *(7.4)*
Mn	303 *(1080)*	400 *(1125)*	362 *(860)*	208 *(365)*	279 *(720)*	537 *(1472)*	675 *(2167)*	248 *(700)*
As	3 *(9)*	6 *(26)*	7 *(22)*	21 *(97)*	40 *(156)*	3 *(9)*	7 *(28)*	2 *(4)*
Cu	13 *(42)*	36 *(215)*	40 *(295)*	32 *(131)*	120 *(845)*	38 *(260)*	43 *(272)*	26 *(79)*
Pb	14 *(27)*	21 *(63)*	25 *(83)*	29 *(126)*	70 *(367)*	17 *(32)*	13 *(23)*	16 *(27)*
Zn	72 *(142)*	95 *(475)*	184 *(627)*	11 *(27)*	505 *(4850)*	148 *(895)*	74 *(170)*	20 *(63)*
Ag	<0.1 *(-)*	0.2 *(1.0)*	0.2 *(1.2)*	0.5 *(2.8)*	1.3 *(7.5)*	0.3 *(1.1)*	0.1 *(0.3)*	0.1 *(-)*
Cd	1 *(2)*	2 *(6)*	2 *(8)*	1 *(2)*	5 *(29)*	2 *(8)*	2 *(2)*	2 *(3)*
Mo	1 *(3)*	2 *(6)*	2 *(4)*	10 *(30)*	2 *(9)*	3 *(7)*	2 *(4)*	2 *(4)*
Ba	84 *(270)*	113 *(437)*	90 *(356)*	226 *(525)*	816 *(2770)*	208 *(757)*	90 *(323)*	50 *(84)*
Sr	27 *(60)*	25 *(82)*	23 *(75)*	9 *(13)*	33 *(142)*	11 *(25)*	40 *(104)*	73 *(260)*
V	17 *(36)*	28 *(94)*	11 *(22)*	24 *(38)*	29 *(36)*	37 *(70)*	87 *(337)*	305 *(577)*
Co	3 *(7)*	3 *(9)*	2 *(5)*	2 *(3)*	2 *(4)*	4 *(10)*	12 *(35)*	7 *(35)*
Ni	12 *(35)*	13 *(36)*	13 *(29)*	22 *(48)*	24 *(47)*	24 *(37)*	7 *(17)*	9 *(29)*
Cr	20 *(48*	21 *(54)*	20 *(40)*	32 *(62)*	38 *(59)*	33 *(61)*	8 *(22)*	41 *(145)*
Ti	914 *(2430)*	1075 *(3515)*	454 *(1336)*	955 *(1810)*	1680 *(1995)*	1660 *(3148)*	2570 *(7870)*	5148 *(8055)*
F	201 *(432)*	306 *(740)*	466 *(1100)*	154 *(250)*	750 *(1406)*	360 *(711)*	173 *(587)*	284 *(385)*
Be	0.2 *(0.2)*	0.3 *(0.6)*	0.3 *(0.5)*	0.3 *(0.4)*	0.2 *(-)*	0.2 *(0.3)*	0.4 *(1.1)*	0.2 *(0.3)*
Li	10 *(26)*	5 *(23)*	11 *(40)*	3 *(10)*	7 *(26)*	1 *(2)*	2 *(7)*	2 *(4)*
Sc	2 *(9)*	4 *(14)*	3 *(9)*	8 *(11)*	6 *(12)*	7 *(16)*	8 *(24)*	19 *(30)*
Ga	21 *(26)*	17 *(27)*	16 *(25)*	8 *(18)*	18 *(22)*	19 *(29)*	19 *(23)*	20 *(30)*
K %	1.1 *(2.3)*	1.1 *(2.3)*	1.1 *(2.4)*	1.2 *(2.1)*	2.1 *(3.9)*	1.3 *(2.9)*	0.8 *(1.9)*	0.6 *(1.5)*
Ca %	0.4 *(0.9)*	0.4 *(1.3)*	0.5 *(1.4)*	0.2 *(0.5)*	0.4 *(1.2)*	0.3 *(0.4)*	1.1 *(3.6)*	1.0 *(2.4)*
Mg %	0.4 *(1.2)*	0.6 *(1.8)*	0.6 *(1.4)*	0.3 *(0.4)*	0.8 *(2.8)*	1.0 *(3.0)*	0.5 *(1.2)*	0.7 *(1.4)*
Al %	8.1 *(9.5)*	8.5 *(22.7)*	6.4 *(11.2)*	8.0 *(9.4)*	8.5 *(10.6)*	9.5 *(12.4)*	7.9 *(10.5)*	11.3 *(17.5)*
Si %	38.1 *(47.9)*	36.6 *(49.5)*	35.3 *(43.7)*	46.6 *(46.9)*	37.0 *(46.9)*	44.3 *(48.4)*	31.8 *(47.8)*	35.6 *(51.4)*

* From Cayeli area

\+ Includes dacites from all deposits except Sarisu

Note: Numbers in brackets for the various areas represent the number of outcrops from which the composite chip samples were taken.

Table 8.5

Composition of Cover Rocks Associated with Volcanogenic Sulphide Mineralization in the Çayeli Area, Eastern Black Sea Region. Values are given for the Mean and Mean + One Standard Deviation (in italics) of Log_{10} Transformed Data (all values are in ppm except where otherwise noted).

			MADENKÖY		SIRTKÖY
	BACKGROUND UPPER BASICS *(11)*	BACKGROUND PUMICE TUFFS *(9)*	UPPER BASICS *(19)*	PUMICE TUFFS *(31)*	UPPER BASICS *(9)*
Fe %	6.7 *(8.5)*	2.3 *(3.7)*	4.1 *(5.2)*	2.8 *(4.5)*	9.6 *(4.8)*
Mn	1850 *(3640)*	457 *(1007)*	1415 *(2300)*	730 *(2650)*	2400 *(5860)*
As	2 *(5)*	2 *(4)*	3 *(6)*	5 *(21)*	7 *(19)*
Cu	27 *(132)*	8 *(21)*	77 *(181)*	19 *(110)*	171 *(703)*
Pb	23 *(39)*	9 *(14)*	32 *(53)*	21 *(70)*	18 *(32)*
Zn	90 *(175)*	60 *(95)*	100 *(345)*	123 *(330)*	106 *(255)*
Ag	0.1 *(-)*	<0.1 *(-)*	0.3 *(1.3)*	0.7 *(2.5)*	<0.1 *(-)*
Cd	2 *(3)*	1 *(2)*	2 *(3)*	2 *(3)*	2 *(3)*
Mo	1 *(2)*	1 *(2)*	2 *(4)*	2 *(3)*	2 *(4)*
Ba	64 *(146)*	20 *(39)*	90 *(214)*	86 *(257)*	146 *(430)*
Sr	65 *(197)*	61 *(145)*	127 *(272)*	34 *(79)*	20 *(62)*
V	238 *(367)*	15 *(20)*	145 *(345)*	23 *(53)*	316 *(435)*
Co	21 *(42)*	33 *(49)*	19 *(35)*	4 *(12)*	17 *(66)*
Ni	12 *(28)*	10 *(35)*	36 *(105)*	13 *(73)*	14 *(37)*
Cr	15 *(38)*	17 *(51)*	108 *(415)*	17 *(41)*	26 *(59)*
Ti	5566 *(8340)*	703 *(1470)*	2870 *(4305)*	790 *(2000)*	5956 *(7762)*
F	140 *(237)*	105 *(160)*	256 *(482)*	450 *(1365)*	115 *(191)*
Be	0.2 *(-)*	0.2 *(-)*	0.2 *(0.4)*	0.4 *(1.0)*	0.2 *(-)*
Li	5 *(21)*	8 *(17)*	13 *(44)*	21 *(59)*	1 *(4)*
Sc	15 *(19)*	1 *(7)*	11 *(5)*	3 *(12)*	20 *(31)*
Ca	23 *(31)*	19 *(24)*	16 *(20)*	20 *(28)*	24 *(28)*
K %	0.4 *(1.6)*	0.7 *(2.0)*	0.9 *(1.6)*	1.2 *(2.7)*	1.2 *(4.0)*
Ca %	1.9 *(2.8)*	0.2 *(0.5)*	3.1 *(7.0)*	0.6 *(1.6)*	1.7 *(4.2)*
Mg %	2.5 *(6.8)*	0.2 *(0.5)*	2.1 *(6.6)*	0.6 *(1.9)*	0.7 *(1.9)*
Al %	8.0 *(10.4)*	7.9 *(9.1)*	7.4 *(9.4)*	7.6 *(10.1)*	8.7 *(10.4)*
Si %	25.8 *(35.2)*	43.0 *(45.0)*	21.4 *(29.3)*	33.2 *(45.4)*	30.5 *(40.3)*

Note (1) Numbers in brackets below each rock type represent the number of outcrops from which composite chip samples were taken.

(2) Upper basic rocks represent basalts and spilites.

percentiles of the $\log_{10}$ transformed data for dacitic rocks. Distribution patterns in the dacites and overlying pumice tuffs (these rocks have a similar composition to dacites) can be interpreted directly; the basalt samples collected from the Upper Basic Series are interpreted in the light of the mean concentrations for the elements compiled in Table 8.5.

The As, F, Cu, Zn, and Pb concentrations in the Çayeli and Madenköy areas were plotted on maps. The data for the Kutlular, Kotarak Dere, and Tunca areas were not plotted. However, the sample sites for these areas are given in Figures 4.8, 4.9, and 4.11, and the data for As, F, Cu, Zn, and Pb are compiled in Appendix D.

The results of the drill-core sample analyses from the Madenköy and Kutlular, Kotarak Dere, and Tunca deposits in profile form along logged drill-core samples are shown in Figures 8.14, 8.15, 8.16, 8.17, 8.18, and 8.19.

8.3.3 Reconnaissance Bedrock Survey in the Çayeli Area

Where possible, composite chip samples of available bedrock exposures were taken during reconnaissance geological mapping. The Çayeli area, which contains all three types of mineralization mentioned previously, is typified by an extensive cover of basalts and andesitic-tuff breccias of the Upper Basic Series (Figure 8.20). Andesitic breccias, probably of the Young Basic Series, occur only in the northern part of the area around the Sarisu pyritic impregnation occurrence. Intrusive bodies of diorite are confined to the area between Sirtköy and Sarisu. Exposed within the cover of Upper Basic Series are three windows of dacitic rocks at Madenköy, Sirtköy, and Sarisu.

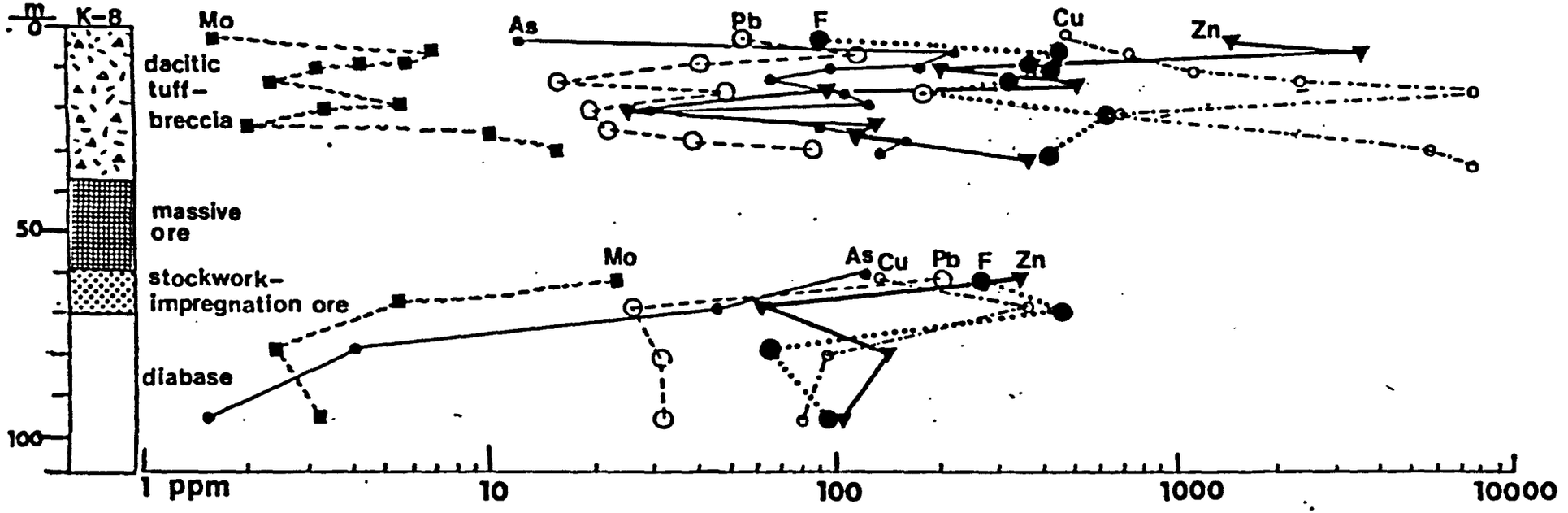


Figure 8.17 Vertical elemental profiles in drill-hole K-8, the Kutlular deposit.

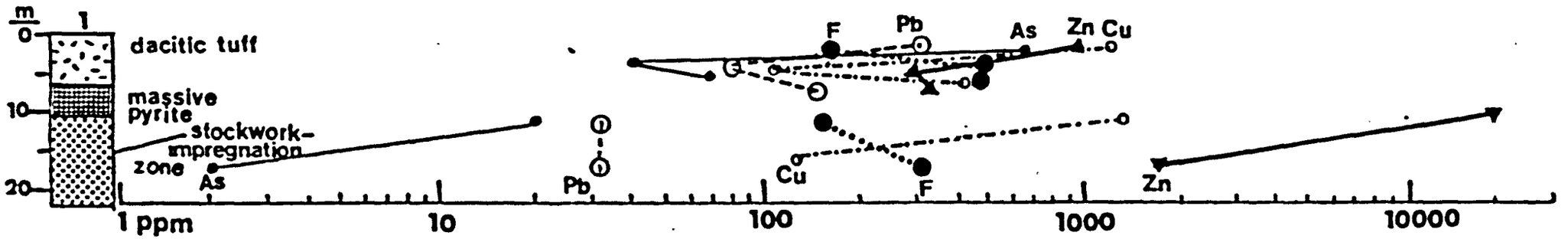


Figure 8.18 Vertical elemental profiles in drill-hole 1, the Kotarak Dere deposit.

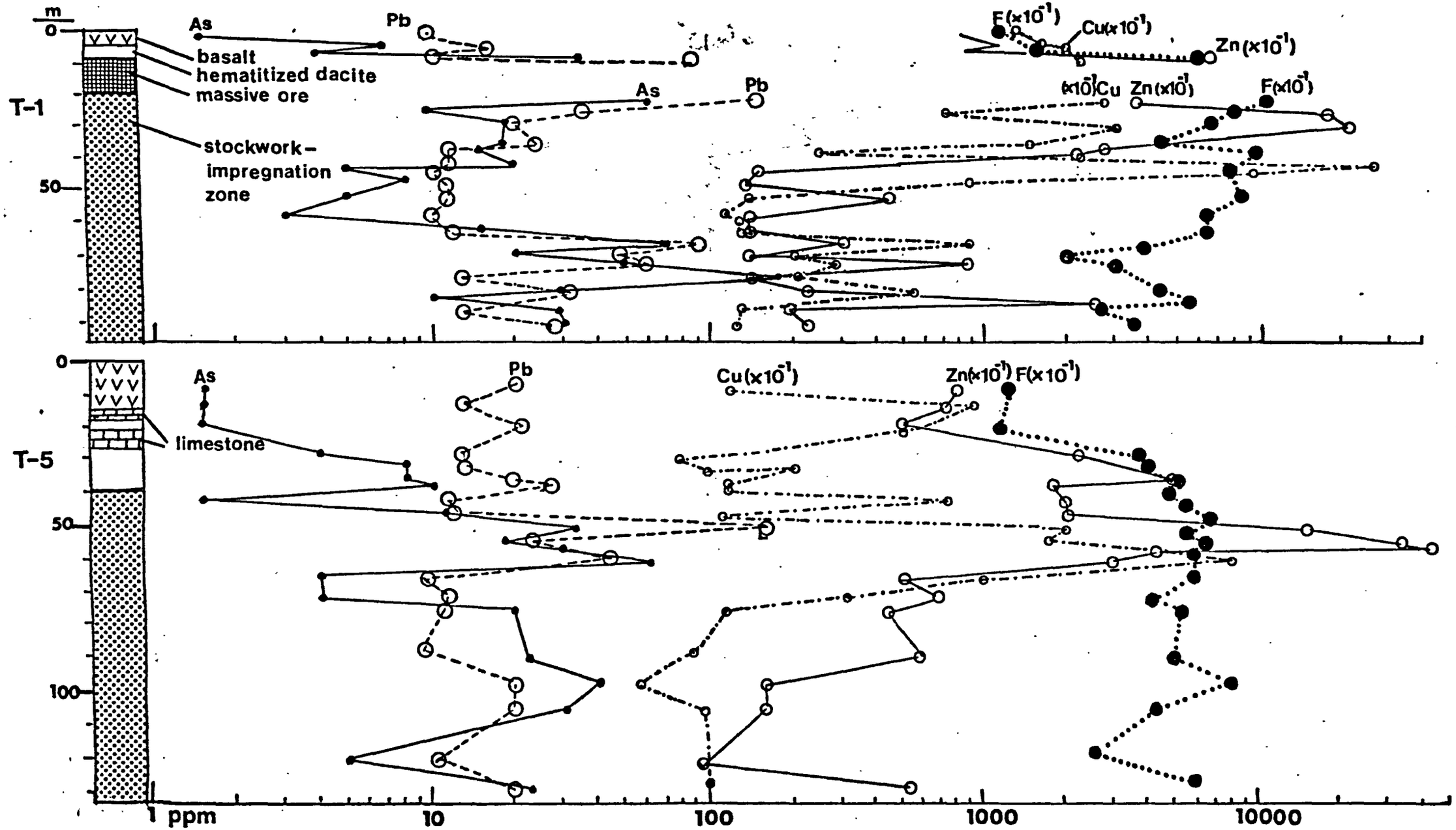


Figure 8.19 Vertical elemental profiles in drill-holes T-1 and T-5, the Tunca deposit.

Exposure in the area as a whole is unfortunately not very good, due mainly to a heavy vegetation and soil cover; the greatest amount of exposure occurs in areas where extensive block faulting in NE-SW and NW-SE directions has occurred (Madenköy, Sirtköy, and Sarisu).

For reconnaissance surveys, As (Figure 8.20), F (Figure 8.21), Pb (Figure 8.22), Zn (Figure 8.23), and Cu (Figure 8.24) were found to be of most value for detecting and differentiating between the three types of mineralization. Fluorine and As are sensitive indicators of hydrothermal activity and mineralizing processes (pyritization) respectively. Thus, in the Madenköy area both elements demonstrate good vector properties in pointing out mineralization. Over the blind Madenköy ore body, the primary halos of F and As have dimensions of the order of 200 x 400 metres, extending over both the dacites and basic cover rocks.

In the Sirtköy area F shows a slight enrichment in parts of the dacitic exposure within the stockwork zone; the basics overlying mineralization show no enrichment. Arsenic on the other hand is anomalous in both the mineralized dacites and overlying basics. Outside of the mineralized zone at Sirtköy, As and F exhibit background values in both the dacites and basics.

At Sarisu F is enriched in the hydrothermally altered dacites and displays only background values in the surrounding basics. Arsenic shows no enhancement whatsoever in the mineralized dacites and would therefore appear to be an active mineralizer only during processes of pyritization associated with stockwork and massive sulphide mineralization.

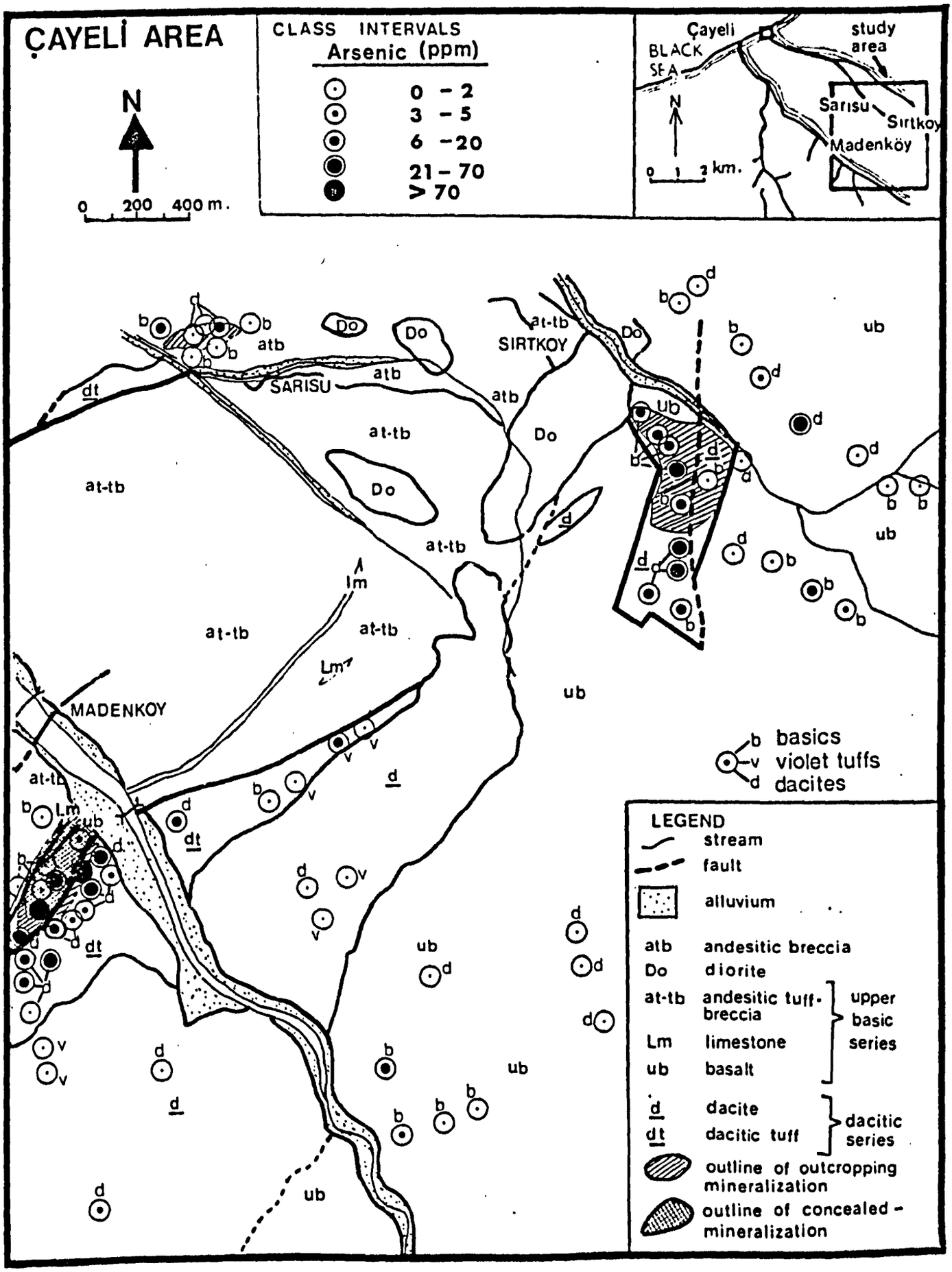


Figure 8.20 As contents of bedrocks, Cayeli area.

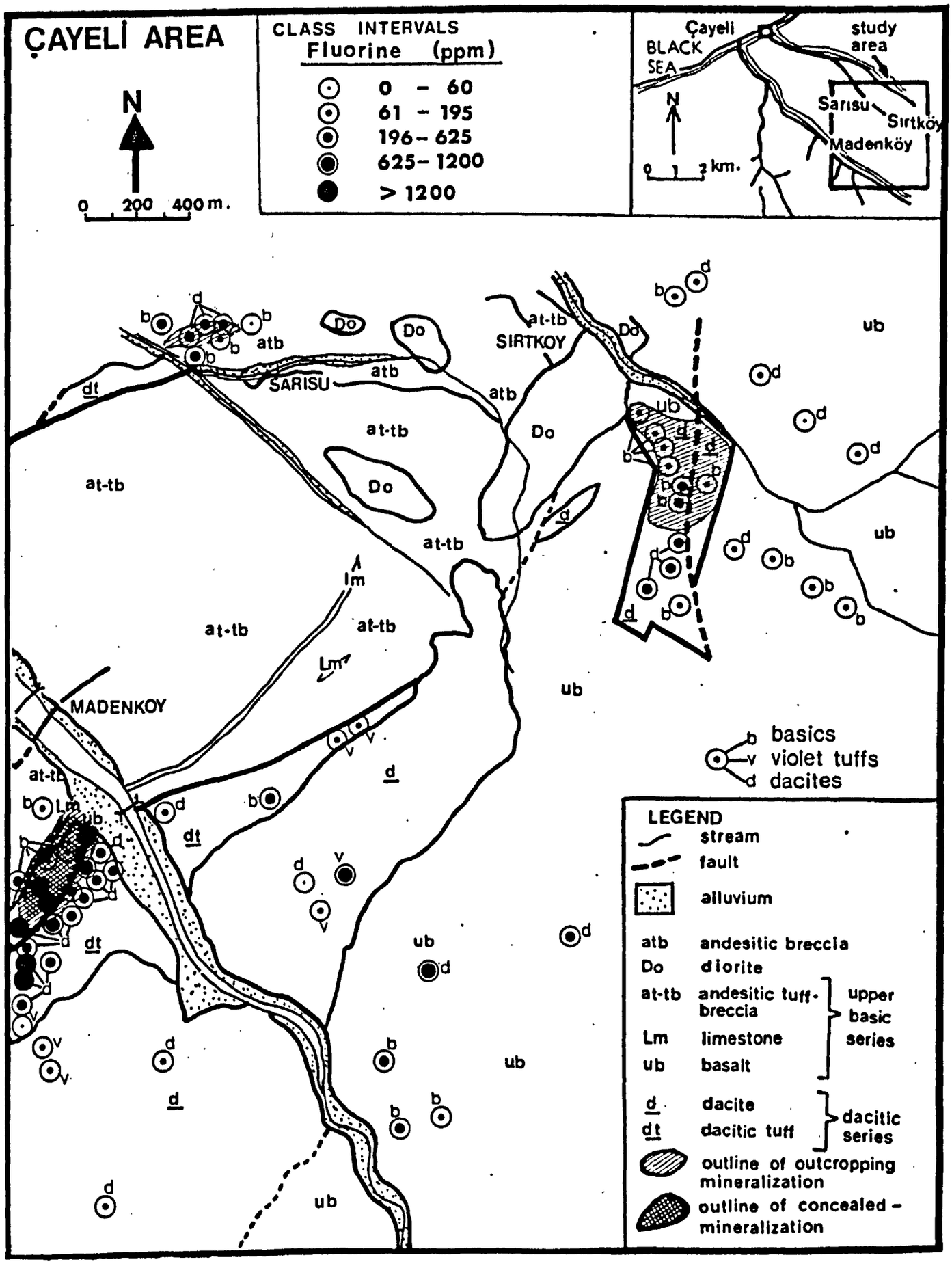


Figure 8.21 F content of bedrocks, Çayeli area.

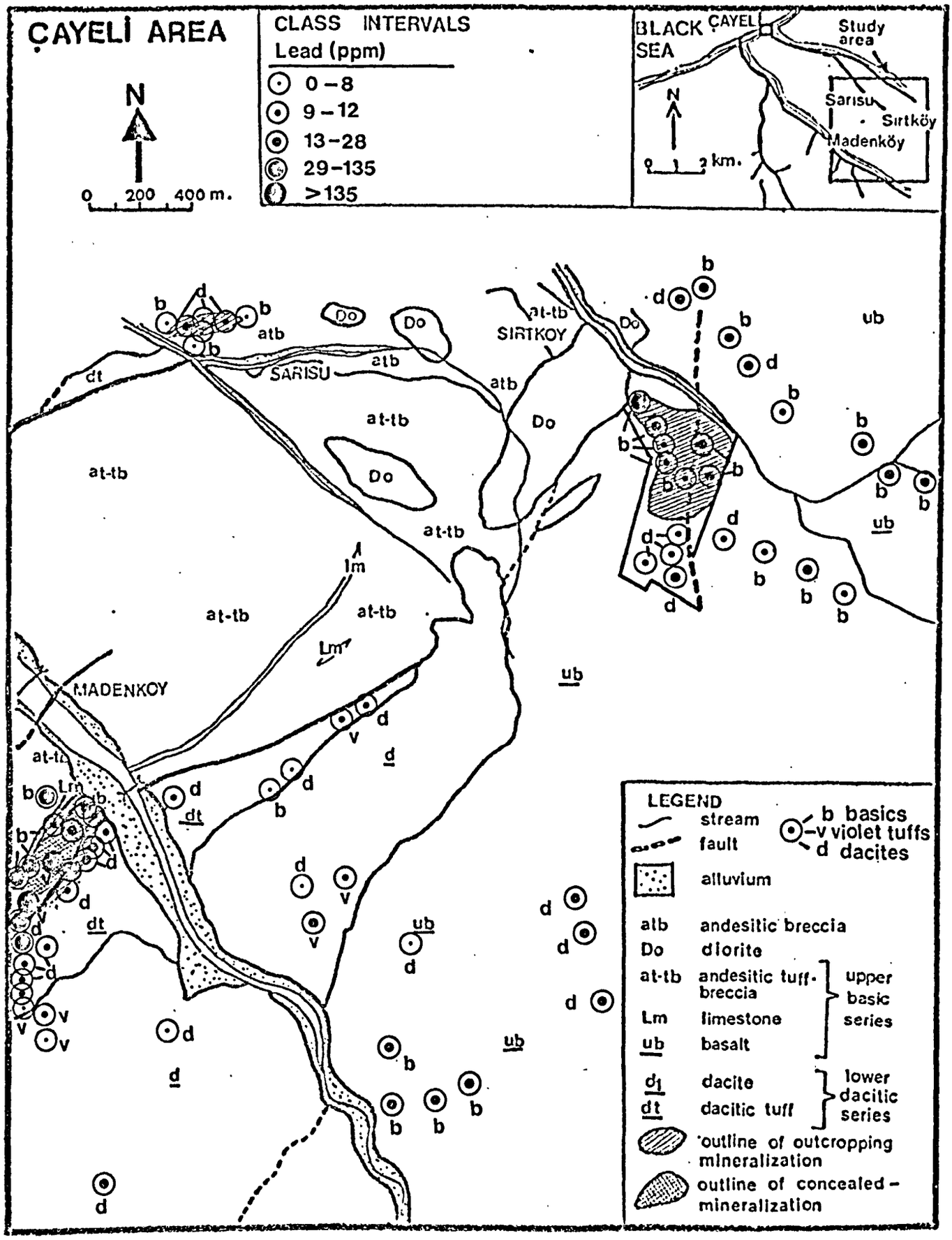


Figure 8.22 Pb content of bedrocks, Çayeli area.

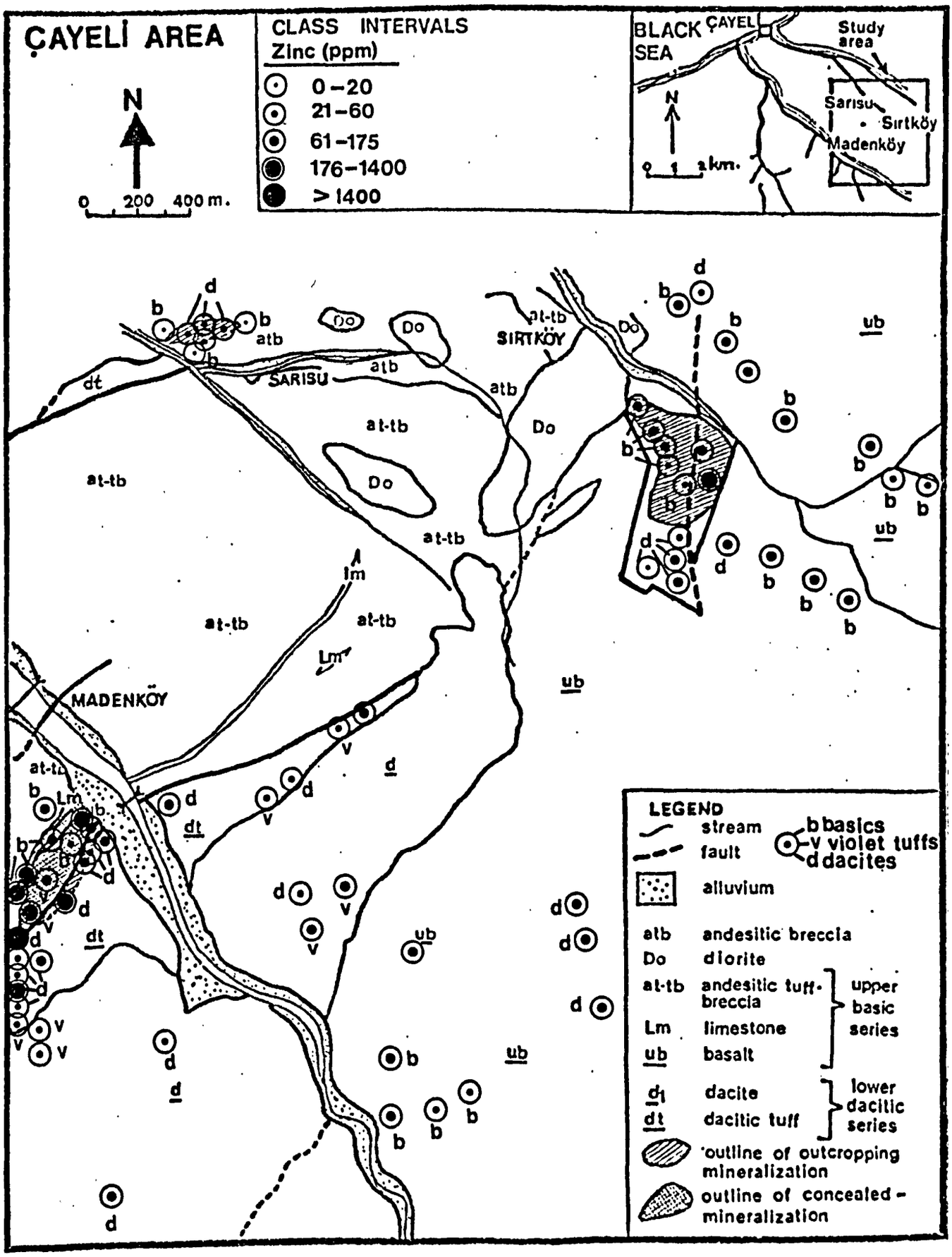


Figure 8.23 Zn content of bedrocks, Çayeli area.

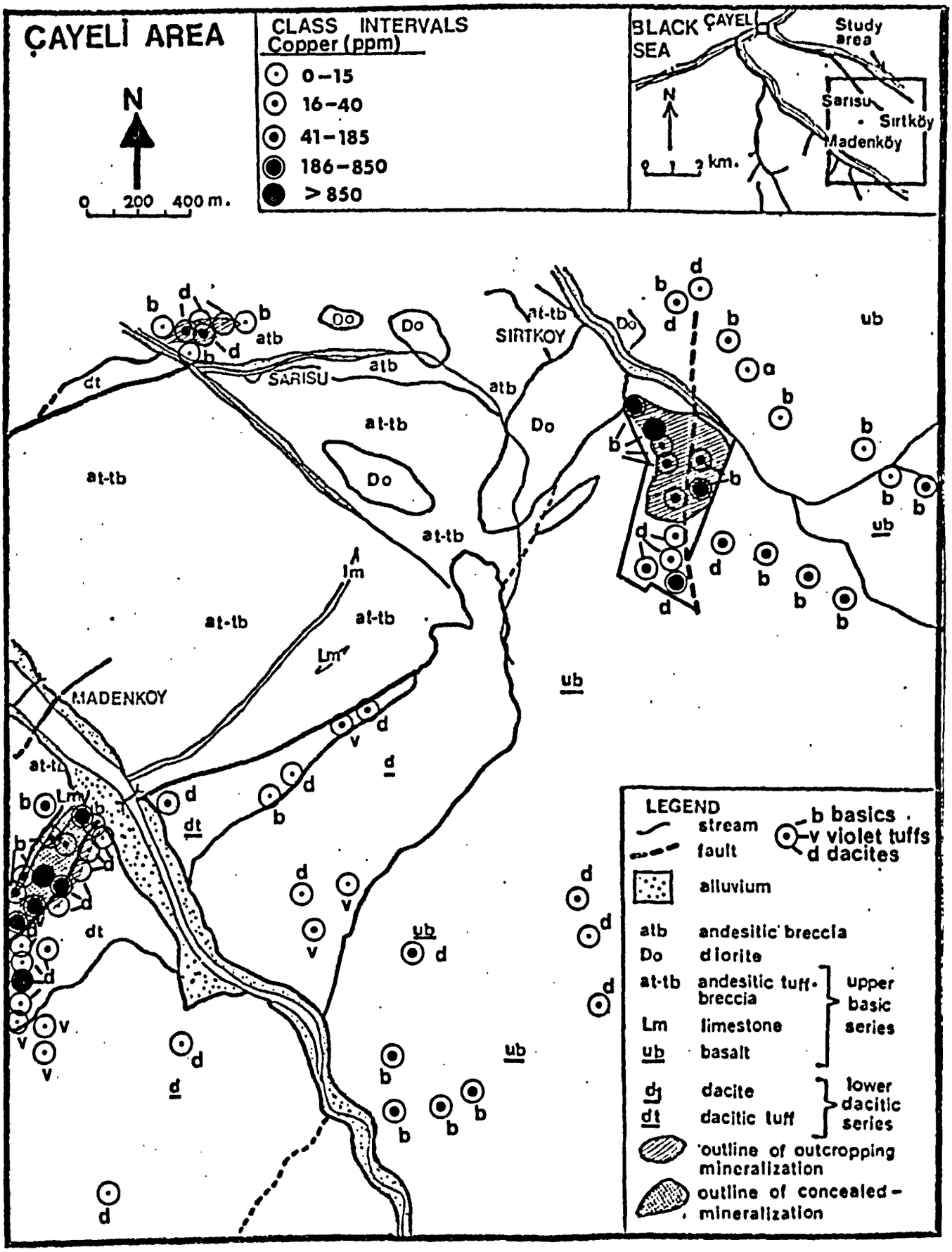


Figure 8.24 Cu contents of bedrocks, Çayeli area.

Pb and Zn are also good lithogeochemical indicators in this province; both elements clearly show stronger anomalies in the vicinity of massive sulphide mineralization (Madenköy) as compared to the stockworks (Sirtköy) and disseminated pyrite (Sarisu) occurrences (Figures 8.22 and 8.23; see also Table 8.4). Copper is not a particularly sensitive indicator of the type of mineralization present, although it is anomalous in mineralized dacites as a whole.

These results suggest that As, F, Zn, Pb, and Cu in rocks sampled during reconnaissance surveys are good indicators of mineralization. This should permit both detection of mineralization and a certain degree of diagnosis as to its type.

8.3.4 Detailed Bedrock Surveys

Detailed geochemical bedrock surveys were carried out over the Madenköy, Kutlular, Kotarak Dere, and Tunca deposits with the following results.

8.3.4.1 Primary Halos in Dacitic Host Rocks

Dacitic rocks hosting economic massive sulphide ore bodies generally contain a stockwork zone surrounded by more extensive pyritic impregnation and argillic alteration zones. In the vicinity of suspected ore, the dispersion patterns of certain indicator elements in the dacitic host rocks may be useful in indicating both the presence and position of massive ore. As was indicated by the results of the reconnaissance survey in the Çayeli area the initial exploration depends to a large extent on such detailed bedrock studies

as those for As, F, Zn, Pb, and Cu in exposed dacitic windows within the Upper Basic Series.

The exposed section of the dacitic rocks near the Madenköy deposit shows distinct signs of hydrothermal alteration and pyritic impregnation; only a very small portion of the stockwork zone is exposed. Arsenic, F, and especially Pb and Zn form anomalous halos in the dacitic tuffs along the entire length of the dacite-pumice tuff contact (Figures 8.25, 8.26, 8.27, and 8.28). Although the average F and As contents (466 and 7 ppm respectively, Table 4.4) of the Madenköy dacites are significantly higher than those for unmineralized dacites (201 and 3 ppm respectively) their distribution in the footwall rocks are marked by only a few sporadic anomalies; Cu displays a similar pattern to As (Figure 8.29). On the other hand Pb and Zn exhibit almost continuous anomalies in the footwall zone and form a lateral halo extending almost 300 m to the south of the concealed ore zone. On a plan view the primary halos for As, Pb, Zn, and F in the footwall zone appear to extend 100-200 m outward from the dacitic tuff-pumice tuff contact, but due to later tectonic tilting these halos may actually be smaller in size. Alternatively, the true lateral extent of these halos out of the map plane (SE of the massive ore zone) may have been greater than their present observed width. Unfortunately none of the drill-holes were deep enough to locate the extention of the halos below the massive ore. However, drill-holes 4 and 73 traversing the dacitic footwall rocks give an idea of the dispersion of As, Pb, Cu, and Zn in these rocks (Figure 8.14). The concentrations of these elements are variable in the

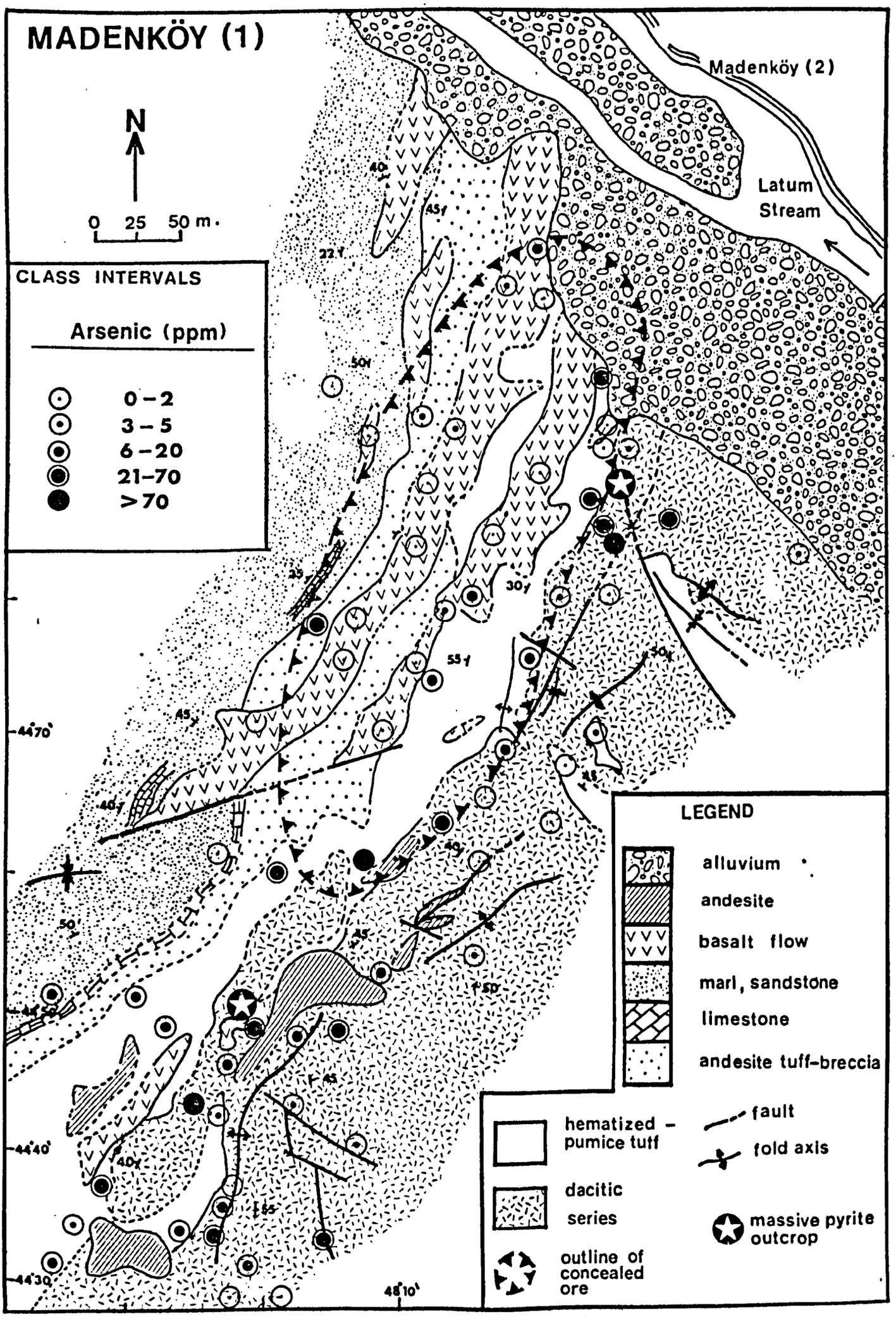


Figure 8.25 As content of bedrocks, Madenköy area.

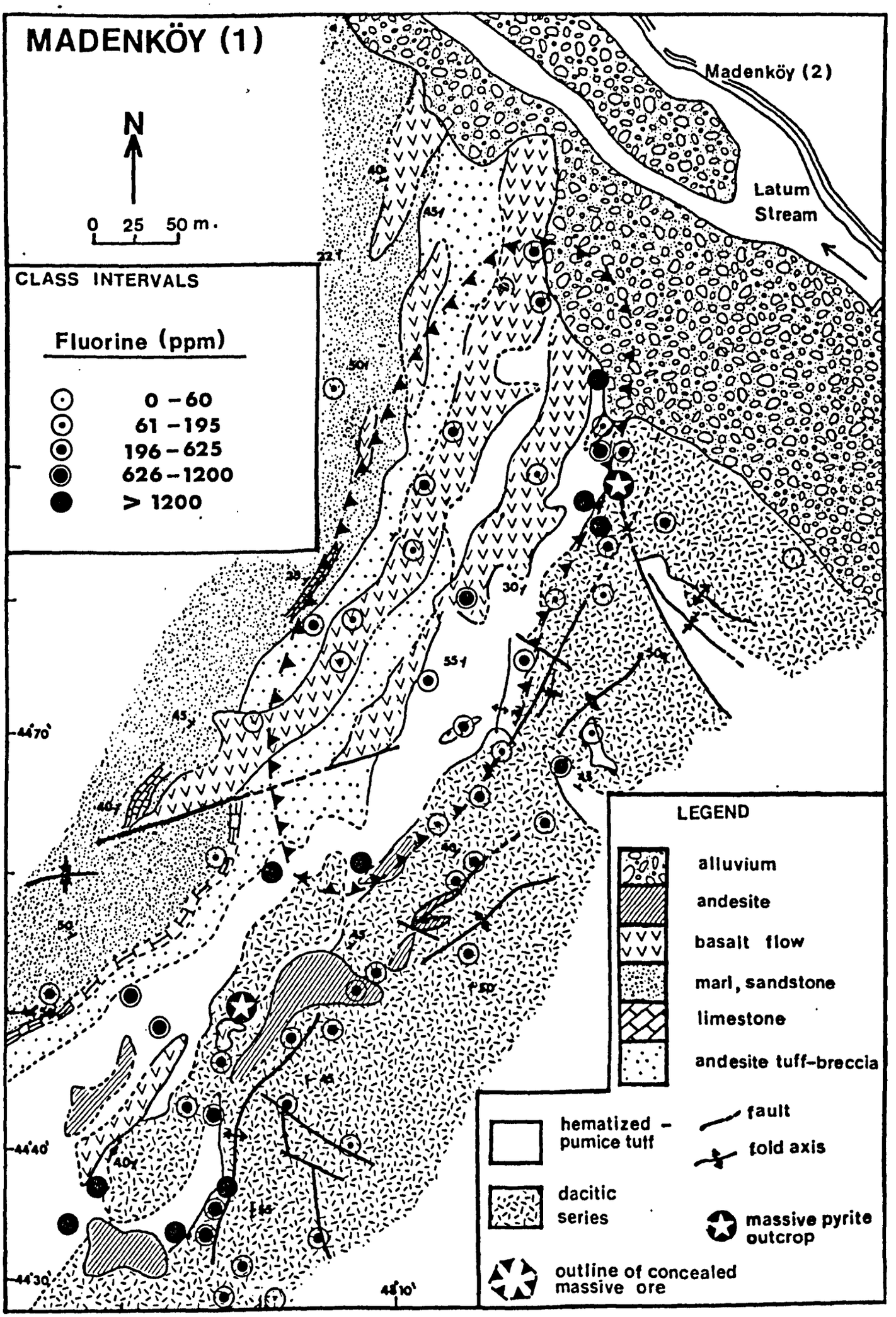


Figure 8.26 F content of bedrocks, Madenköy area.

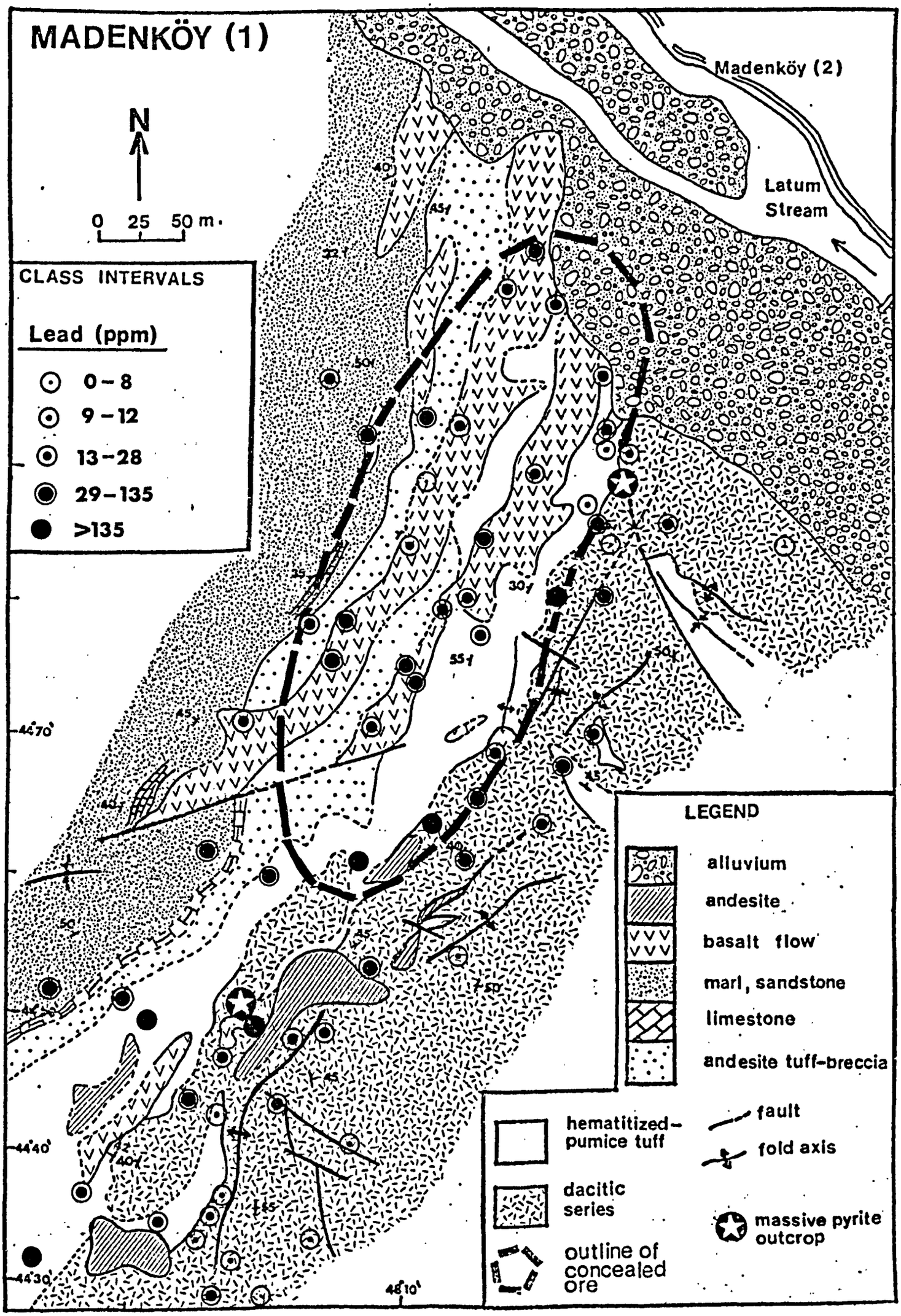


Figure 8.27 Pb content of bedrocks, Madenköy area.

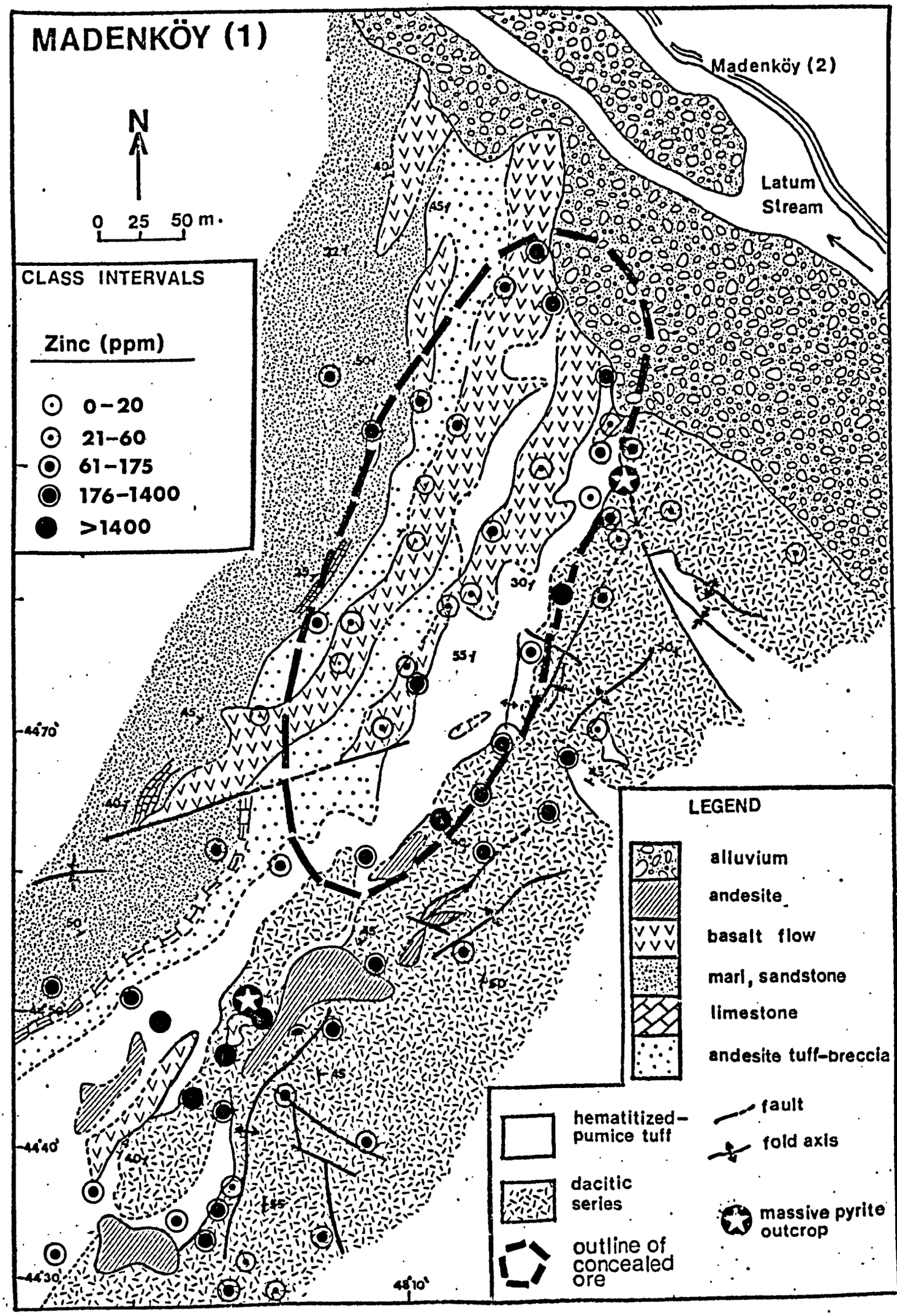


Figure 8.28 Zn content of bedrocks, Madenköy area.

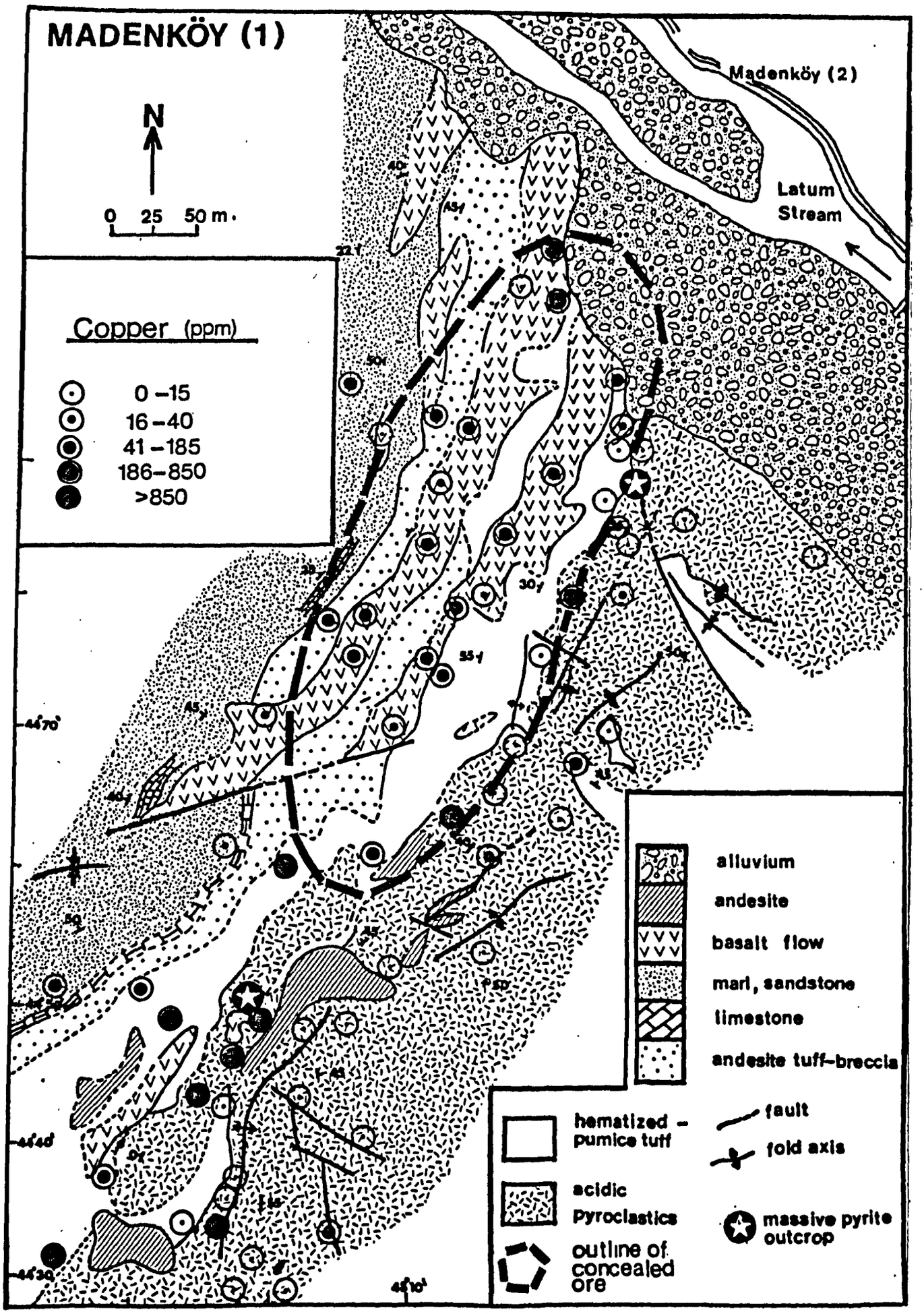


Figure 8.29 Cu content of bedrocks, Madenköy area.

footwall dacites along the core sections, wide dispersions being demonstrated by Zn, As, and Cu.

In drill-hole 110 Hg decreases sharply with depth in the impregnation zone, and within 40 m from the massive ore the element is present in background concentrations (about 60 ppb). Fluorine on the other hand increases from values of about 200 ppm just below the massive ore to more than 1500 ppm within 40 m of it (Figure 8.15). Thus, F is concentrated in a zone about 20 m outward from the massive ore body, having a halo whose observable width is about 300 metres within the dacitic footwall rocks. Such dispersion features emphasize the important role of this element during mineralizing processes.

As discussed below, in a section on the Regional Assessment of Mineralized Stockwork and Impregnation Zones (see also Table 8.4), the footwall dacites in the Kutlular, Kotarak Dere, and Tunca deposits display anomalously high concentrations of As, F (except at Kutlular), Cu, Zn, Pb, Ag, Cd, Ba, and Mo. The drill-core profiles for As, F, Cu, Zn, Pb, and Mo also demonstrate the high contents of these elements in the stockwork and impregnation zones of these deposits (Figures 8.17, 8.18 and 8.19). The mineralizing ore fluids circulating through impervious dacitic rocks have produced elemental halos that are extensive as well as intensive in places (e.g. Kutlular).

8.3.4.2 Primary Halos in Hanging-wall Rocks

Exposures of the Lower Dacitic Series in the Eastern Black Sea Region are sparse, and there is much geological evidence to suggest that massive sulphide deposits are only

preserved (e.g. Madenköy and Kutlular) if they have a sufficient capping of cover rocks, generally of the Upper Basic Series. Detailed mapping in the Madenköy and Sirtköy areas and drill-core sampling in the Madenköy, Kutlular, Kotarak Dere, and Tunca Deposits was carried out to confirm the existence of primary elemental halos in the hanging wall rocks, some of which were observed (e.g. As and F) during the initial reconnaissance survey of the Çayeli area.

In the Madenköy area, pumice tuffs (violet tuffs) and intercalated tuffaceous sandstones lie directly over the massive sulphide orebody and extend laterally about 300 m to the SW and NE. In terms of chemical composition these rocks are similar to dacites, a major exception being an excess Fe content represented by hematitization. Compared to the basalts they have much lower contents of Mn, V, Co, Ni, Cr, and Ti. On a visual basis, the pumice tuffs from background and mineralized areas cannot be differentiated. The surface pumice tuffs collected close to the mineralization, however, are significantly enriched in elements such as As, F, Pb, Zn, Ag, Ba, Mn, and to a lesser extent Fe, Cu, and Mo (Table 4.5). For most of these elements their means exceed even the mean plus one standard deviation for the background tuffs. For the Madenköy pumice tuffs, As, Pb, Zn, and F form anomalous halos along the full length of the footwall-hanging wall contact zone and extend for more than 200 m SW of the ore zone. The vertical distributions of As, F, Zn, Pb, Cu, and Mo in drill-cores through this deposit also confirm the existence of primary halos in the pumice tuffs (Figures 8.14, 8.15, and 8.16). The contents of As, Fe, Zn, Pb, and Mo in

these rocks generally increase as the orebody is approached (e.g. drill core sections 101 and 110, Figure 8.15).

The minor elements such as As, Cu, Zn, Pb, and Mo in the pumice tuffs probably occur as sulphides (for Cu, Zn, Pb) or as minor elements in sulphides (for As and Mo) which are occasionally present as disseminations. In addition considerable contents of these elements are thought to occur in clays (especially the mixed-layered sericite montmorillonite and montmorillonite), and iron and manganese oxides as suggested by the three different selective extraction procedures carried out on these rocks (Table 8.6). Especially indicative in this respect is the strong relationship between As and Fe as shown by the ammonium oxalate extraction (See section 5.8 for details of the analytical procedures for these techniques, and see section 9.5 for their extractive properties).

Table 8.6 Mean extractabilities of metals from 16 pumice tuff drill-core samples for three types of extraction procedures [extractability expressed as (reagent extractable metal/HNO_3 + $HClO_4$ extractable metal) x 100].

Type of extraction	Percentage of Fe extracted	Percentage of Mn extracted	Percentage of Cu extracted	Percentage of Zn extracted	Percentage of Pb extracted	Percentage of As extracted
E D T A (pH:4.65)	1.3	14.4	16.2	6.9	25.1	No detectable extraction
Hydroxylamine hydrochloride (pH:1.3)	6.3	62.4	37.9	34.0	34.4	No detectable extraction
Ammonium oxalate (pH:3.3)	18.2	19.8	25.7	13.1	-	45.0

Compared to their background counterparts the basalts overlying the Madenköy deposit are considerably enriched in F,

Pb, and Ag (Table 8.5), and these elements are, therefore, good indicators of underlying sulphide mineralization. As, Cu, Zn, Sr, and Ba are only slightly enriched in the Madenköy basalts, but as a group they may also aid interpretation. The drill-core profiles for F, Zn, Pb, and As also suggest enrichment of these elements in the basalts (Figures 8.14, 8.15, and 8.17).

The dispersion of Hg in drill-cores 101 and 110 above the Madenköy sulphide orebody produced dissappointing results (Figure 8.15). Despite the fact that the ore contains as much as 7 ppm Hg, the overlying rocks rarely report values greater than 40 ppb.

The Upper Basic Series (mainly spillites and basalts) stratigraphically overlying the Sirtköy pyritic stockwork deposit have increased concentrations of As and Cu only, thus reflecting the type of mineralization over which they lie. There is a distinct diagnostic difference between the composition of basic rocks overlying the Madenköy massive sulphide ore (high F, Pb, Ag) and those overlying the pyritic stockwork mineralization (high As and Cu only). These parameters can, therefore, be used to indicate the type of ore underlying anomalous zones in the Upper Basic Series.

The cover rock exposure (tuffs and basalts) around Sarisu is restricted; the results obtained for the basalts (4 samples) reveal a general absence of primary anomalies for any of the elements.

The Kutlular massive sulphide deposit is overlain by a dacitic-tuff breccia unit which is mineralized. Veinlets and disseminations of pyrite and chalcopyrite are common in these rocks. The dacitic-tuff breccia is in turn followed

by a thin cover of basalts which has largely been eroded. A few surface samples of the dacitic tuff-breccia and the vertical profiles for As, Mo, Cu, Zn, and Pb in drill-core K-8 indicate a strong enrichment of these elements (Figure 8.17) in the cover rocks. Fluorine is generally low in the hanging-wall rocks as in the footwall dacites of this deposit.

In the Kotarak Dere deposit, the dacitic tuffs covering the massive pyrite contain high concentrations of As, Cu, Zn, and Pb in drill-core 1 (Figure 8.18).

In the Tunca deposit As, F, Cu, Zn, and Pb are slightly enriched in the hanging-wall hematitized dacites. The profiles for As, F, Cu, Zn, and Pb in drill-cores T-1 and T-5 also suggest enrichment of the above mentioned elements in the hematitized dacites whereas background concentrations of these elements occur in the overlying baslats (Figure 8.19).

In general, it can be concluded that the dispersion of As, F, Pb, Zn, Ag, and Cu in hanging-wall rocks are useful indicators of underlying mineralization. The hematitized rocks, when present, constitute an ideal horizon to sample during detailed surveys. Dispersion of elements such as As and F can also be used as possible directional indicators of underlying mineralization.

8.3.5 Regional Assessment of Mineralized Stockwork and Impregnation Zones

Mineralized zones in dacites have a widespread occurrence in the Black Sea region. Many of these mineralized-altered zones bear no relationship to massive sulphides or productive stockwork deposits. Thus, in order to formulate

initial priorities for detailed exploration of exposed mineralized zones, these areas must first be assessed on a regional basis. With this in mind the possibility of developing certain geochemical criteria by which to judge the mineral potential of the numerous stockwork and impregnation occurrences in the Black Sea region was investigated. The importance of developing such criteria is further emphasized by the fact that the larger massive sulphide deposits are completely concealed beneath a protective cover of Upper Basics, and a portion of their mineralized footwall rocks may be the only signature of the deposits at the surface. Bedrock sampling was carried out in stockwork-impregnation zones for which a priori information with regard to mineral potential was known (Madenköy, Kutlular, Tunca, Kotarak Dere, Sirtköy, and Sarisu).

It is extremely unlikely that a proper assessment and hence criteria can be obtained if unbiased sampling is carried out in these mineralized zones (i.e. sampling of sulphide and sulphide-free material). In many cases the exposure and demarcation between these zones is not good, and a confident decision as regards mineral potential can only be made if care is taken to sample the same type of material at each outcrop. For this reason it was decided that only altered rocks visibly free of sulphides should be sampled, as this type of material represents the largest percentage of the available exposure in these rocks. Since it is often difficult, with limited exposure, to determine whether the stockwork or impregnation (or transitions between the two) are being sampled, it was decided on logistical grounds to classify exposures merely as mineralized dacites

noting any observations that might aid interpretation. For the Madenköy deposit, Cu was the only element to show a marked difference in concentration between stockwork and impregnation zones. Fortunately this element is not a strong indicator of deposit type.

The average compositions (and mean + one standard deviation) of the mineralized dacites associated with massive sulphide bodies, Cu-pyrite stockworks, and barren pyritic impregnation zones are given in Table 8.4. The compositions of the mineralized dacites as a whole (excepting those of Sarisu) and the unmineralized dacites from the Çayeli area are also given.

Compared to their background counterparts, rocks taken from the mineralized stockwork-impregnation zones (whole population) are significantly enriched in Fe, As, Cu, Pb, Zn, and F, and to a lesser extent in Ag, Cd, Mo, and Ba. Mn, Sr, Co, Ni, and Ti are not noticeably enhanced in these mineralized zones, indicating their lack of participation in mineralizing processes.

The results for the individual deposits indicate that no one element can be adequately used as a discriminator. For example, due probably to a much higher level of hydrothermal activity at Kutlular, some of which post-dates mineralization, the more readily leached elements such as Zn, Sr, and F show a considerable depletion. Furthermore, Mo, which is only slightly anomalous in other deposits, displays a very high mean concentration in the Kutlular dacites; to a lesser extent the same is also true for Ag and Ba. With the exception of Tunca, As has its highest concentration in the Kutlular dacites. A further problem affecting the interpretation

of single element data relates to the proximity of the sampled zone to ore. For the Tunca dacites, the relatively high concentrations observed for all of the indicator elements is related to the fact that a fault bisects the ore zone thus permitting the stockwork-impregnation zone immediately below the ore to be exposed.

Since each of the massive sulphide deposits have different characteristics as regards tenor or ore, degree of hydrothermal activity, and degree of exposure, an adequate assessment of mineralized dacitic exposures can only be made by examining, on a relative basis, a more comprehensive selection of trace elements. Thus the dacites associated with massive sulphide ores form a clearly anomalous group having abnormally high concentrations of most and in some cases (Madenköy, Tunca) all of the base metal indicators (Cu, Pb, Zn, Ag) as well as As and F. Compared to the other types of mineralization outlined in Table 4.1, Pb is the only element which is consistantly higher in the footwall rocks of massive sulphide deposits; greater weight can therefore be given to the observed levels for this element.

Although the Kotarak Dere occurrence has been classed in Table 4.1 as a stockwork deposit, there is strong evidence to suggest that it represents the exposed root of an eroded massive sulphide deposit. A small remnant of massive sulphide mineralization occurs in the middle of the exposure and disseminations of sphalerite (unlike Sirtköy) have been found in the stockwork zone. Geochemically the Kotarak Dere dacites are similar to the footwall rocks of the Madenköy deposit; only As and Pb exhibit lower levels in these rocks. Although it would appear likely that massive sulphides have

been eroded away, it is still possible that ore is present under the covered flanks of the dacite. Present drilling has been confined to assessing the mineral potential of the stockwork zone. As its chemistry fits the criteria mentioned above for mineralized dacites associated with massive sulphides, it is suggested that drilling be extended over the flanking Upper Basic Series.

The altered dacites in the Sirtköy stockwork deposit have a chemistry distinctly different from dacites related to massive sulphide mineralization. Of the ore indicators, only Fe, As, and Cu are enriched in this deposit. The other base metals, together with F, have values very similar to those for unmineralized dacites. The basic elements Mn, V, Co, and Ti are also high in these rocks, but Ni and Cr are not. The same trend for the above mentioned basic elements was also observed for the Sarisu dacites. The differences in the concentrations of these elements in the Sirtköy and Sarisu dacites, and those of dacites from other areas may be attributed to one of two factors as follows:

(1) The possible existence of more than one dacitic phase of volcanism which probably followed different differentiation trends. However, the occurrence of the Madenköy and Sirtköy windows along the same trend and the absence of any multiphase characteristics are evidence against this possibility.

(2) The possible incorporation of the basic elements as the result of contact-metamorphic processes between intrusive dacites and the basalts and spilites of the Upper Basic Series. The basic elements may therefore be used to indicate

stockwork and impregnation deposits having more of an intrusive nature rather than a submarine exhalative one.

The above results suggest that the basic elements may be useful in regional assessment of dacitic rocks in the Eastern Black Sea Region. However more regional data on the content of these elements in the dacitic rocks of this region is needed to reach any firm conclusions.

The Sarisu impregnation deposit is characterized by high levels of Fe and Cu only. Geochemically, deposits of this type can be differentiated from more productive mineralized zones by their lack of base metal (excepting Cu), As, and F contents.

Finally, the major elements such as K, Ca, Fe, and Mg in the dacites from the mineralized areas follow trends in accordance with the alteration patterns described in section 8.2 (Table 8.7). For example, enrichment of Fe, Ca, and Mg in the Madenköy dacites compared with the unmineralized dacites is in accordance with the mineralogical changes (dolomite and siderite formation) that took place during alteration.

Depending on the degree of exposure, a minimum of 10-15 samples, areally representing the mineralized zone should be taken for regional assessment. Where only single mineralized outcrops are exposed care should be taken to sample material free of sulphides. This method of a visual cut-off in sampling was found to give the most meaningful results in the Eastern Black Sea Province. Exposures which have higher than normal contents of most of the base metals (particularly Pb) as well as As and F should be given a high

Table 8.7 Variations in some major element contents of dacitic rocks from various mineralized areas compared with unmineralized dacites from the Madenköy area.

Element	Madneköy mineralized dacites	Kutlular dacites	Kotarak Dere dacites	Tunca dacites	Sirtköy dacites	Sarisu dacites
K	±	+	+	+	-	-
Ca	+	-	-	±	+	+
Fe	+	+	+	+	+	+
Mg	+	-	+	+	+	+
Al	-	±	+	+	-	+

+ Indicates addition of element

- Indicates substraction of element

± Indicates no significant change

priority for detailed surveying. For a technique such as this, analytical precision is imperative.

CHAPTER 9

PEDOGEOCHEMICAL EXPLORATION

9.1 INTRODUCTION

Residual soil surveys have been extensively and successfully used in geochemical exploration (Warren and Delavault, 1966; Hawkes and Webb, 1962, p. 203). In the U.S.S.R., "metallometric surveys", which usually involve the sampling of soils, have been widely used in mineral exploration and geological mapping (Schirokow and Kowaljowa, 1961; Isaregradskiy, 1962). Because residual soils are formed as a result of in-situ weathering their chemical features will generally reflect faithfully the chemistry of the parent bedrock. In areas of deep residual soil cover and limited bedrock exposure residual soil surveys may, therefore, be effectively used in geochemical prospecting. In the Eastern Black Sea Region this is especially true, the limited rock exposure in some localities makes residual soil sampling an ideal adjunct to bedrock surveys in geochemical exploration.

The soils in this region are generally undifferentiated, immature mountain soils that have developed under humid, moderate climatic conditions. The soils are slightly acid (pH about 4.5), and because of the relatively high relief are well aerated and drained. Their thickness rarely exceeds 1m and their constituent clay minerals are mainly illite and vermiculite types. The carbon content of the topsoils ranges up to 6.23% and 19.48% for tea-planted and forested areas respectively.

Because of undifferentiated nature of the soils, samples were taken at an arbitrary horizon (30 cm below the

surface). Two hundred and twenty-one soil samples were collected along several traverses in the Madenköy, Sirtköy, Sarisu, Kutlular, and Kotarak Dere areas (Figures 9.1, 9.2, 9.3, and 9.4). A minus 80 mesh (-200μ) size fraction was analysed for (a) Fe, Mn, Cu, Zn, Pb, and Cd by atomic absorption spectrometry after a hot nitric acid digestion, (b) As and Mo by colorimetric methods, (c) Ba and Ag by direct reading optical spectrography, and (d) Hg by a flameless atomic absorption method. Not all the samples were analysed for the full range of elements. For the details of sample collection, sample preparation, and analysis, the reader is referred to Appendix A.1.2, Appendix A.2.3, and Chapter 5 respectively.

Selective extraction experiments involving EDTA, hydroxylamine hydrochloride, and ammonium oxalate solutions on selected soil samples were carried out to enhance anomalies over concealed massive sulphide deposits and to elucidate the mode of occurrence of the various metals.

9.2 DATA PROCESSING AND PRESENTATION

Elemental concentrations for all the soil samples were entered on computer cards and processed to obtain simple statistical parameters such as range, arithmetic and logarithmic means, standard deviations, 50th percentiles, and correlation coefficients. The results are given in Table 9.1. The frequency histograms and cumulative frequency diagrams were also plotted (see Appendix C). From these plots it was evident that all of the elements were best approximated by a lognormal distribution. However, Cd and Ag show some deviation from both the normal and lognormal distributions,

Table 9.1 Statistical summary of total soil data (total number of samples is 221*).

Element (in ppm unless stated)	Number of samples	Range of values	Means		50th percentile (Log_{10} distrn)	Std. deviations		Correlation Coefficients									
			Arith.	Geom.		Arith.	Geom.	As	Cu	Zn	Pb	Ag	Cd	Mo	Hg	Ba	Mn	Fe
As	221	1.5-780	15	7.5	6.5	20	3.4	1.00										
Cu	221	4-1890	45	72	58	217	3.3	0.18										
Zn	221	15-4000	185	112	73	335	2.4	0.13	0.44									
Pb	221	8- 760	55	34	24	82	2.4	0.71	0.34	0.31								
Ag	150	0.1-17.0	0.6	0.2	0.1	1.7	3.2	-0.05	-0.04	-0.01	-0.04							
Cd	210	0.5-17	1.5	1.2	0.9	1.5	1.9	0.08	0.42	0.91	0.31	-0.01						
Mo	147	0.5-18.1	3.3	2.3	2.1	2.9	2.5	0.64	0.22	0.15	0.46	0.03	0.21					
Hg(ppb)	148	11-624	86	70	65	65	1.9	0.2	0.13	0.40	0.23	0.67	0.37	0.21				
Ba	150	42-1619	145	113	101	173	1.8	0.2	0.08	0.51	0.28	0.64	0.51	0.20	0.77			
Mn	124	30-6500	1075	592	824	1023	3.8	-0.13	0.34	0.17	-0.13	0.01	0.15	-0.37	0.22	-0.08		
Fe%	124	0.7-15.0	4.9	3.8	3.9	3.5	2.3	0.20	0.15	-0.06	0.24	-0.15	-0.14	-0.17	0.20	-0.26	0.22	1.00

*Not all samples were analysed for all elements

partly due to low analytical sensitivity and high detection limits.

The elemental concentrations in soils along the various traverses were plotted in profile form on a $\log_{10}$ scale and are presented in Figures 9.5 to 9.16.

9.3 THE pH OF SOILS

The pH of soils was determined in the laboratory by soaking ten grams of -2 mesh soil in 20 ml of a 0.01 M calcium chloride ($CaCl_2$) solution for 30 minutes and measuring the pH using an electrode and mV meter (see section 5.9.1 for the method).

The pH measurements of 100 soils from all study areas ranged from 3.5 to 6.7 with an average of 4.5. pH values between 5 and 6.7 were rare and only observed in a few soil samples collected over the cover rocks of the Madenköy massive sulphide body (Figure 9.10). These relatively high pH values are believed to be related to the presence of pumice tuffs and red limestones constituting the hanging-wall rocks in the area.

9.4 DISPERSION OF METALS IN SOILS

9.4.1 Introduction

Three soil traverses (A-A', B-B', and C-C') were run across the strike of the Madenköy massive sulphide deposit (Figures 9.1 and 9.2). For comparison with the Madenköy (1) area, soils were collected over a traverse (2M-2M') in the Madenköy (2) area where similar rock types occur and where there is no known mineralization (Figure 9.5). Another soil

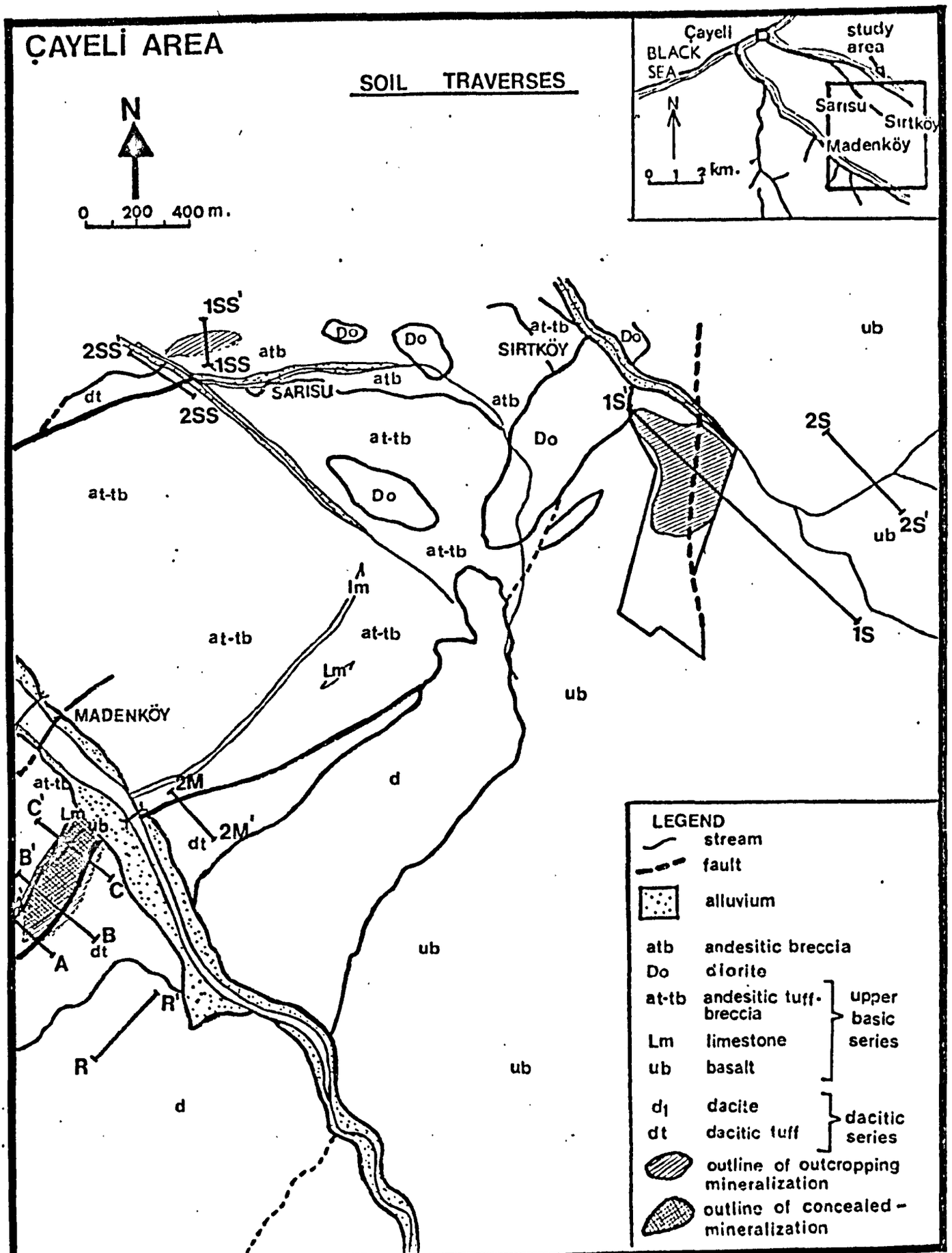


Figure 9.1 Location of soil traverses, Çayeli area.

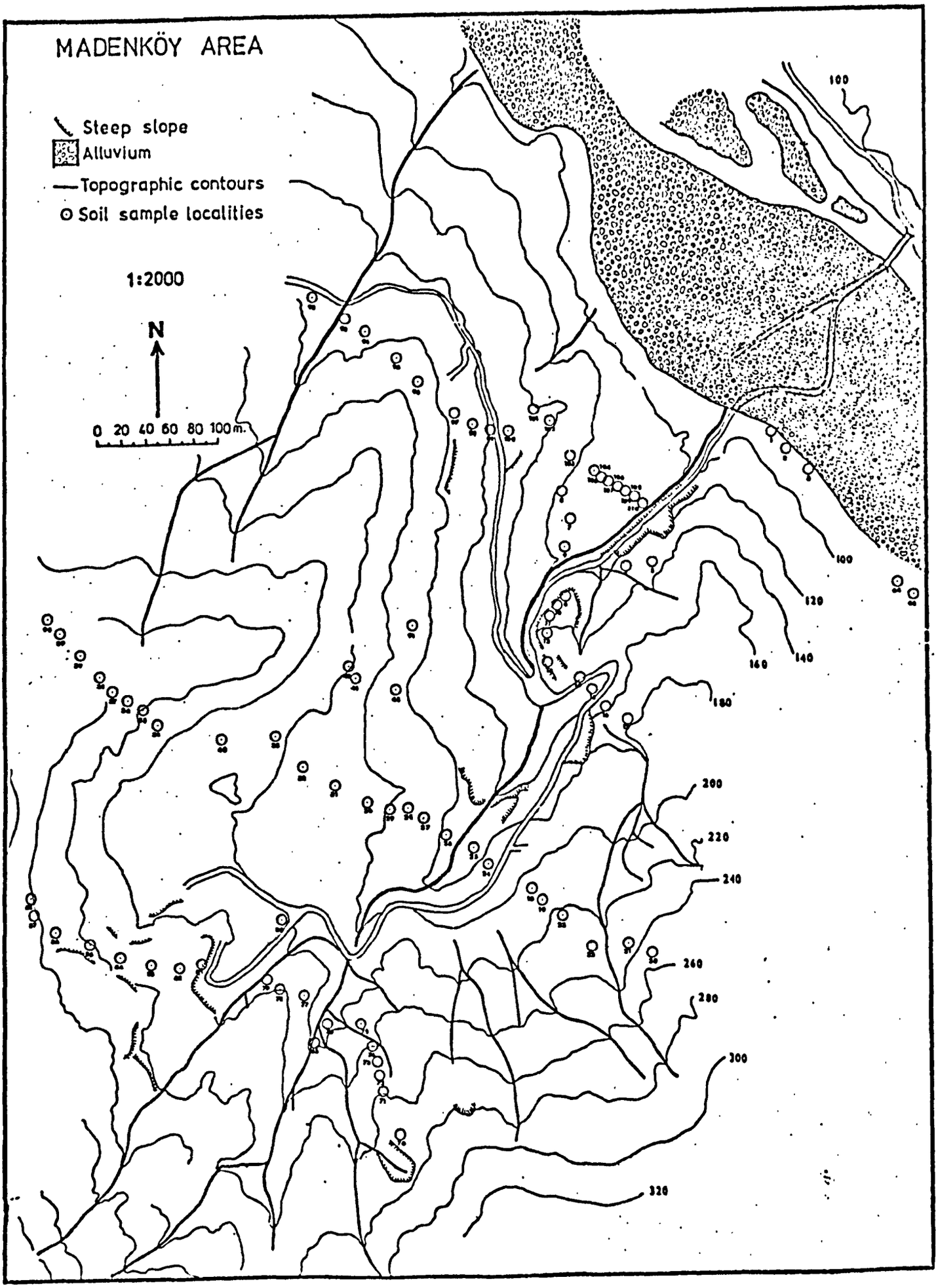


Figure 9.2 Soil sample locality map, Madenköy (1) area.

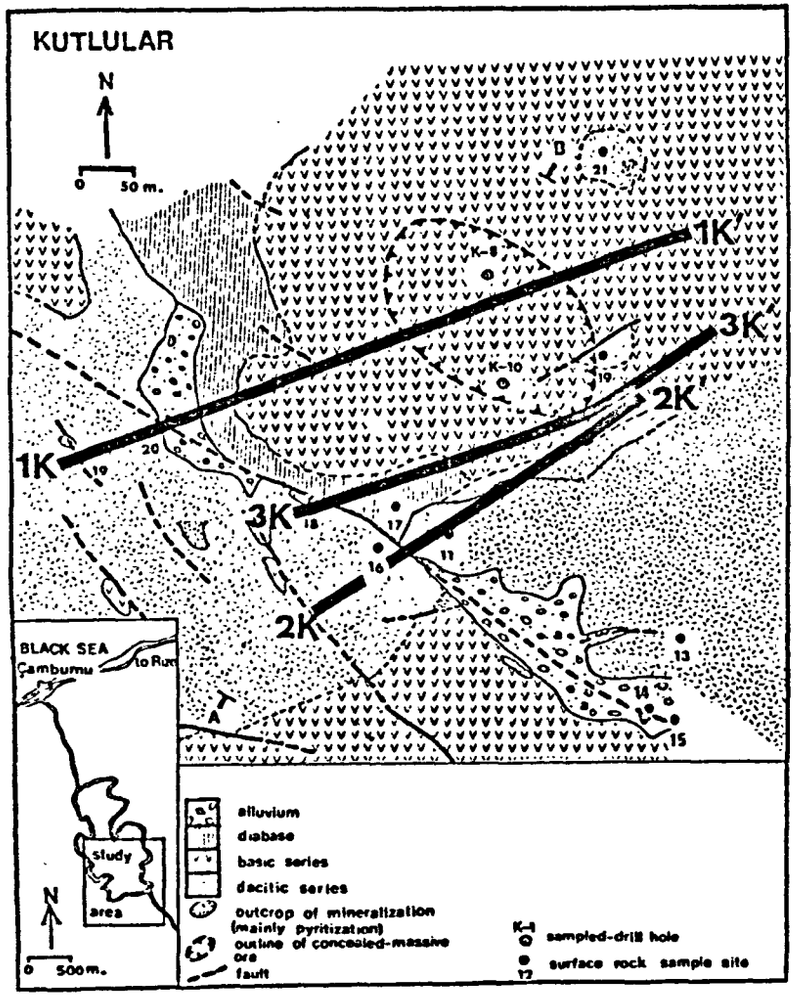


Figure 9.3 Location of soil traverses, Kutlular area.

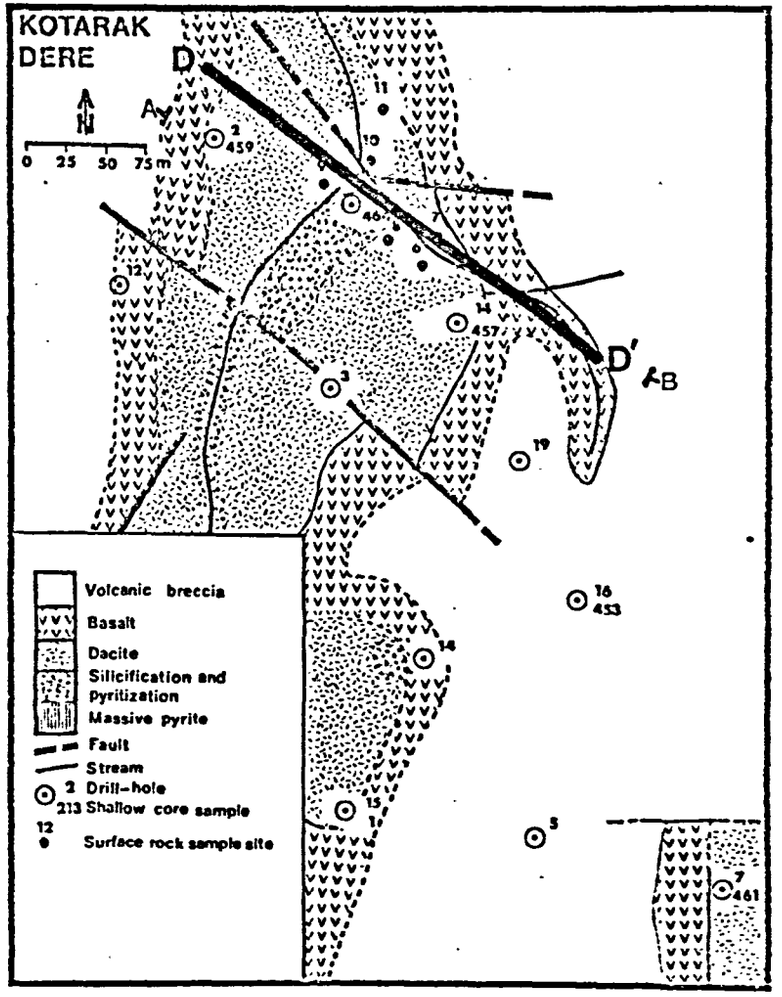


Figure 9.4 Location of soil traverse, Kotarak Dere area.

traverse (R-R') was run over dacites to the south of the Madenköy deposit to obtain background concentrations for metals in soils developed over dacitic rocks (Figure 9.6). Two soil traverses in the Sirtköy area, one (1S-1S') across the mineralized zone (Figure 9.15) and another (2S-2S') over unmineralized basic rocks (Figure 9.7) were run (see Figure 9.1 for locations). Soil traverses were also run over the Sarisu (1SS-1SS and 2SS'-2SS'), Kutlular (1K-1K', 2K-2K', and 3K-3K'), and Kotarak Dere (D-D') mineralized zones.

The soil traverses in the Madenköy (1) and (2), Sarisu and Kutlular areas are located on cultivated (mainly tea-planted) fields whereas those at Sirtköy and traverse R-R' south of Madenköy are on uncultivated ground.

9.4.2 Dispersion of Metals

The three soil traverses over the Madenköy massive sulphide deposit show strong well developed anomalies for Pb, Zn, Cu, Ba, and As over the partly exposed stockwork zone of this deposit (Figures 9.8, 9.9, 9.10, and 9.11). The maximum anomaly/background ratios for these elements over the stockwork zone are approximately 30, 14, 10, 11, and 10 respectively. The high Pb anomaly/background ratio indicates the general association of lead with massive sulphide deposits as well as its immobile nature in a secondary environment characterized by acid leaching. Compared with the stockwork zone, the soils over the hanging-wall rocks display only slightly anomalous concentrations of the above elements. Arsenic occurs in weakly anomalous contents, and Pb, Zn, Ba, and Cu exhibit maximum anomaly/background ratios of 4, 2.5, 2, and 1.5 respectively.

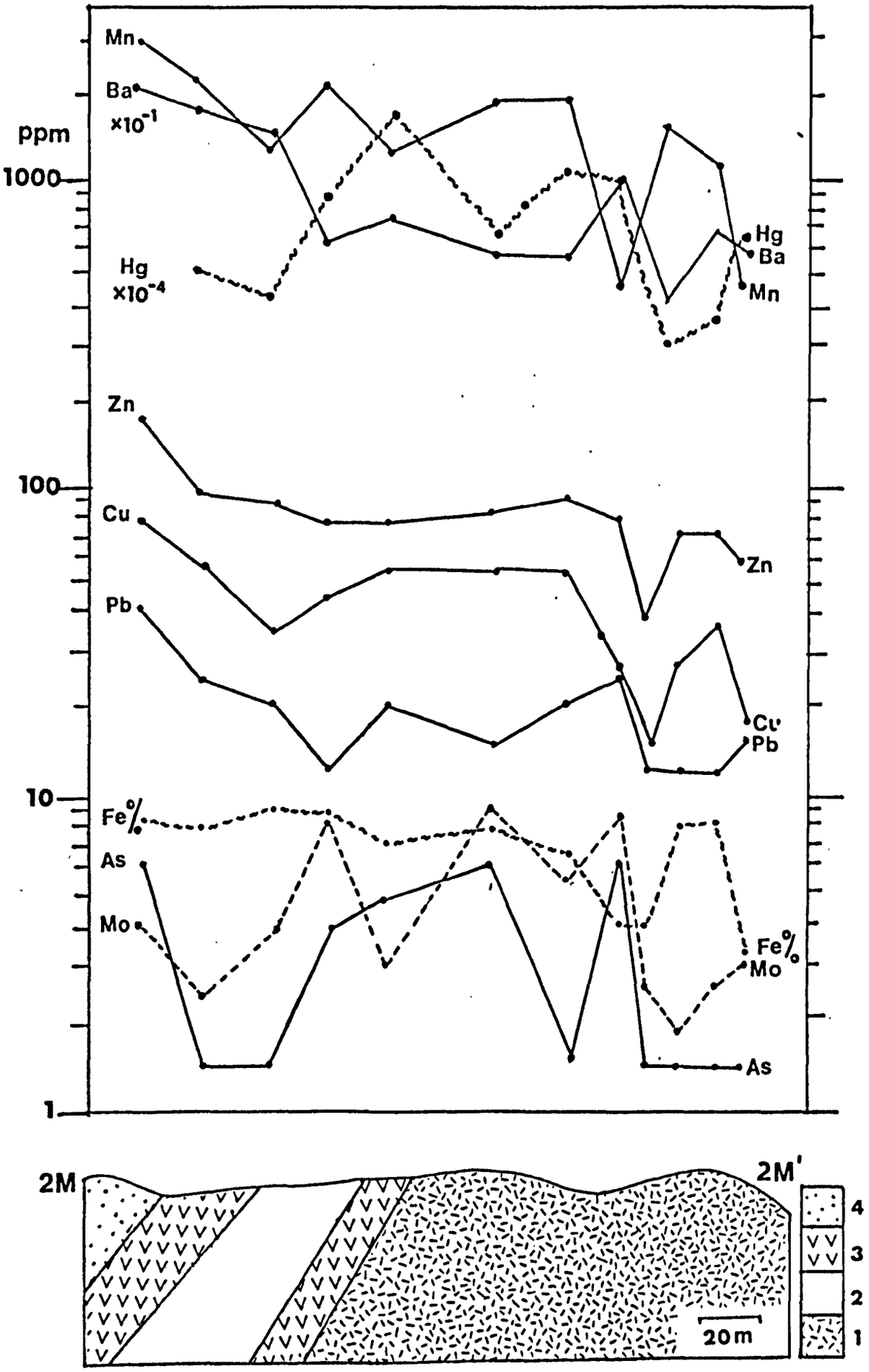


Figure 9.5 Elemental profiles along soil traverse 2M-2M', Madenköy (2) area. All concentrations in ppm unless otherwise noted. (Legend: 1- Dacitic Series, 2- pumice and dacitic tuff, 3- Basalt, 4- andesite-tuff breccia).

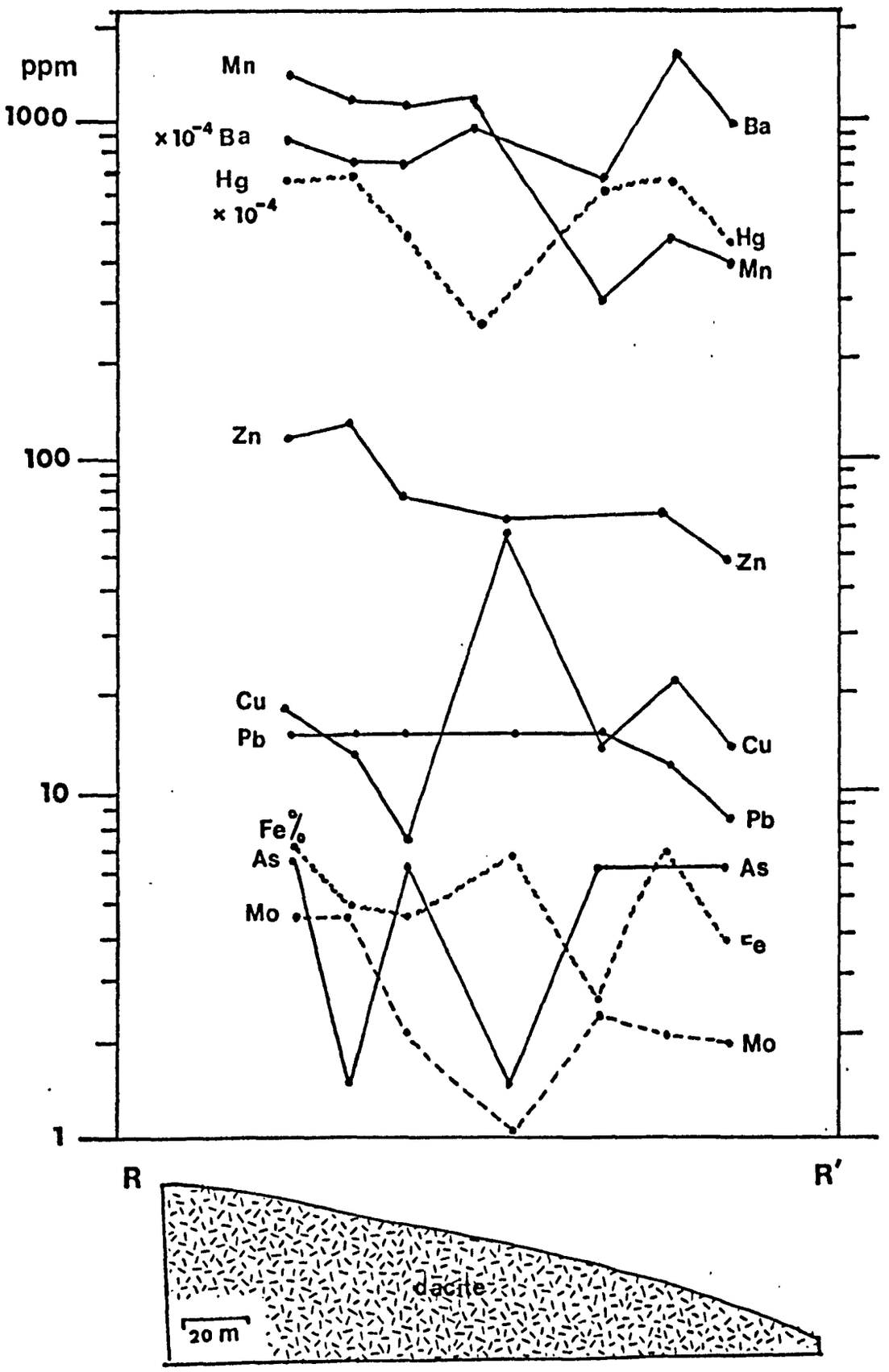


Figure 9.6 Elemental profiles along soil traverse R-R', south of the Madenköy area. All elemental concentrations in ppm unless otherwise noted.

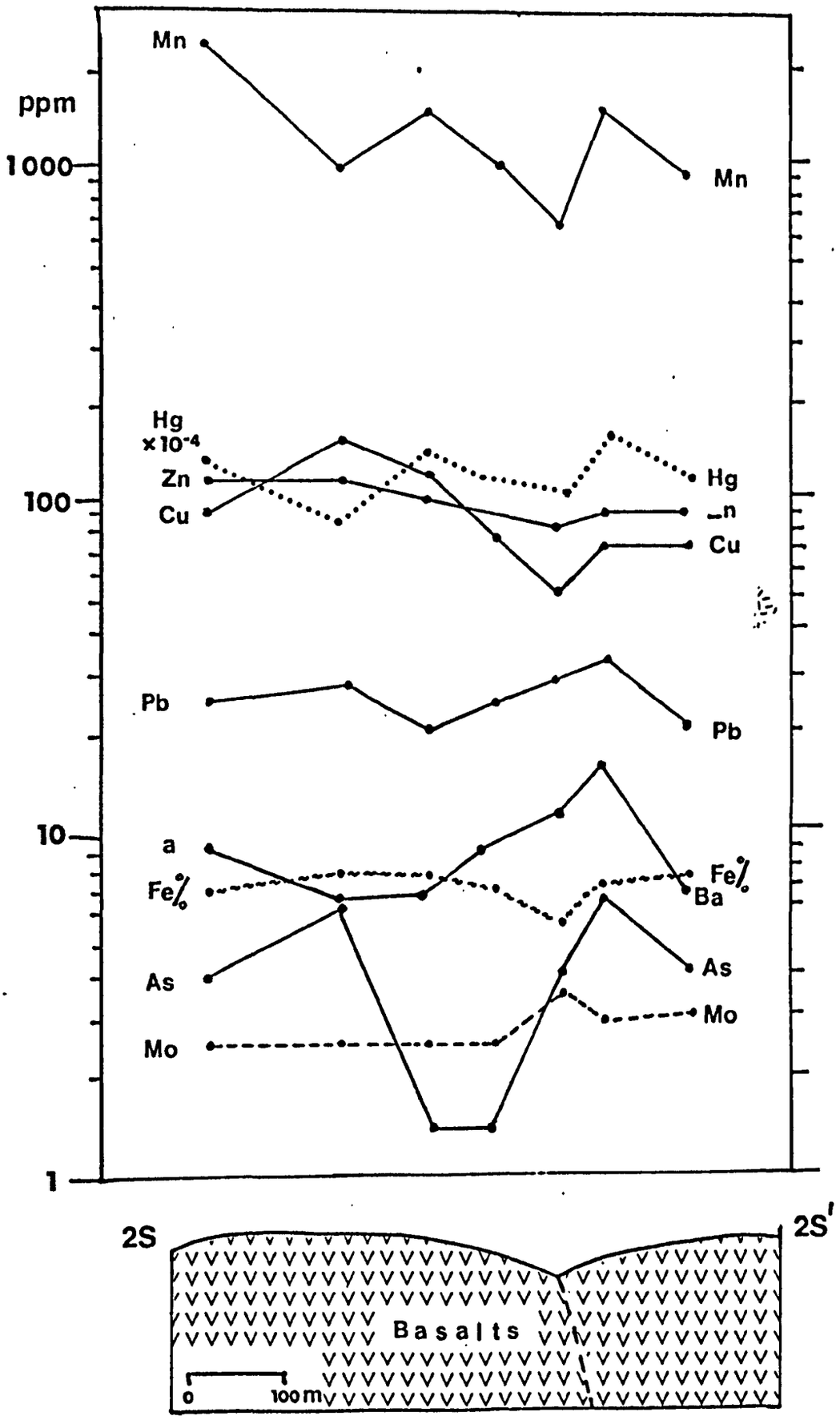


Figure 9.7 Elemental profiles along soil traverse 2S-2S', Sirtköy area. All concentrations in ppm unless otherwise stated.

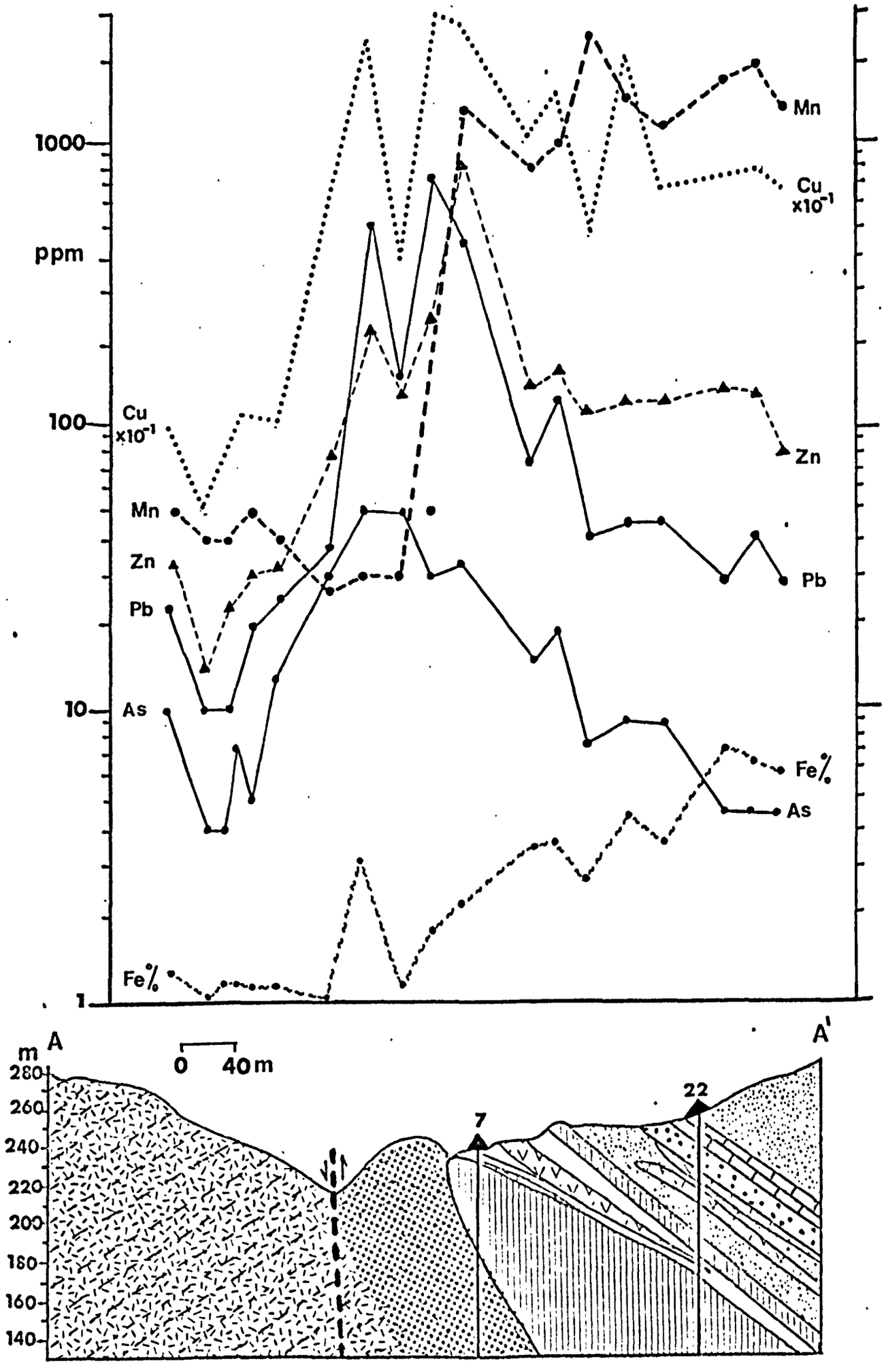


Figure 9.8 Elemental profiles along soil traverse A-A' over the Madenköy massive sulphide deposit. All concentrations in ppm unless otherwise stated. For geological legend see Figure 9.11.

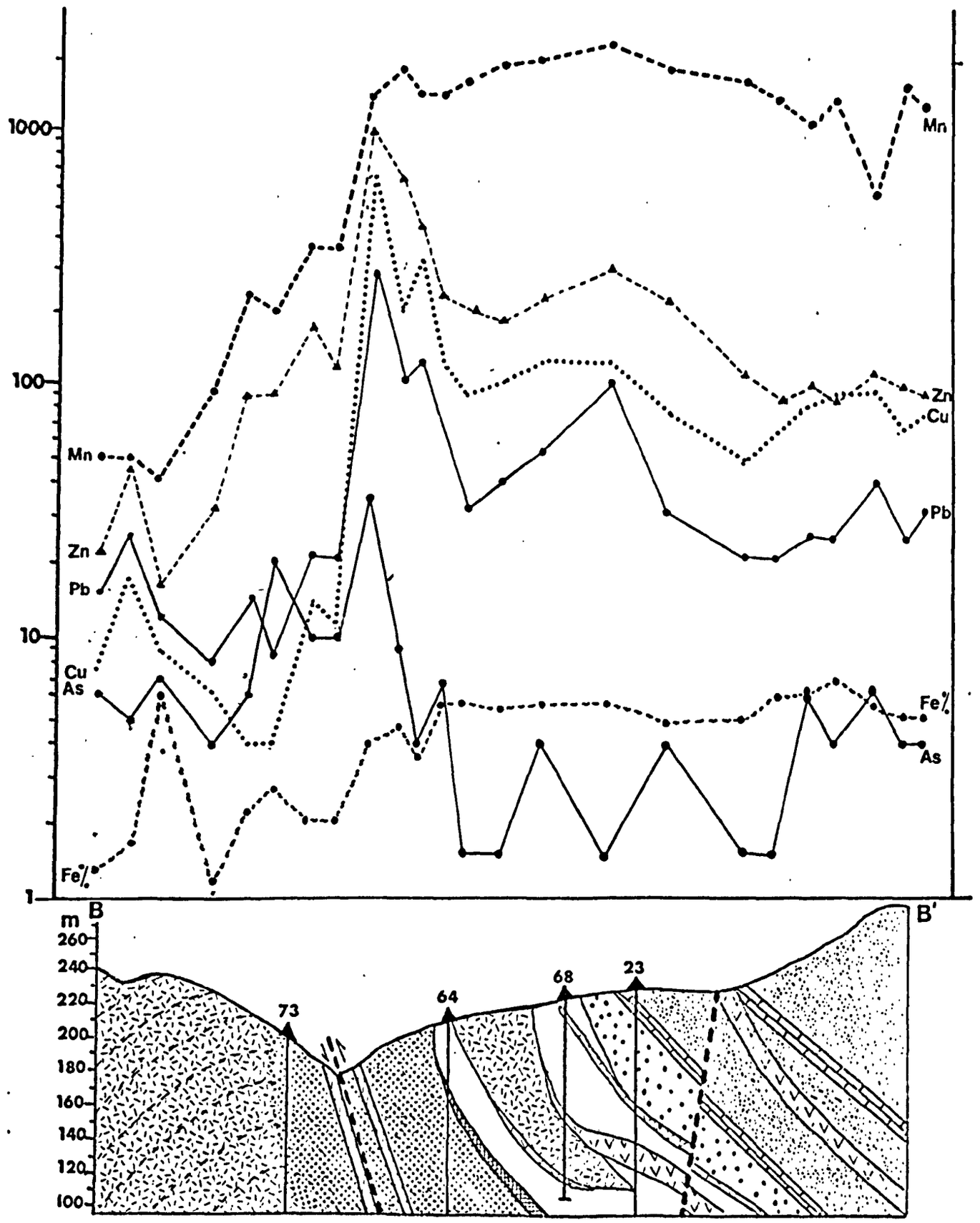


Figure 9.9 Elemental profiles along soil traverse B-B' over the Madenköy massive sulphide deposit. All concentrations in ppm unless otherwise stated. For geological legend see Figure 9.11.

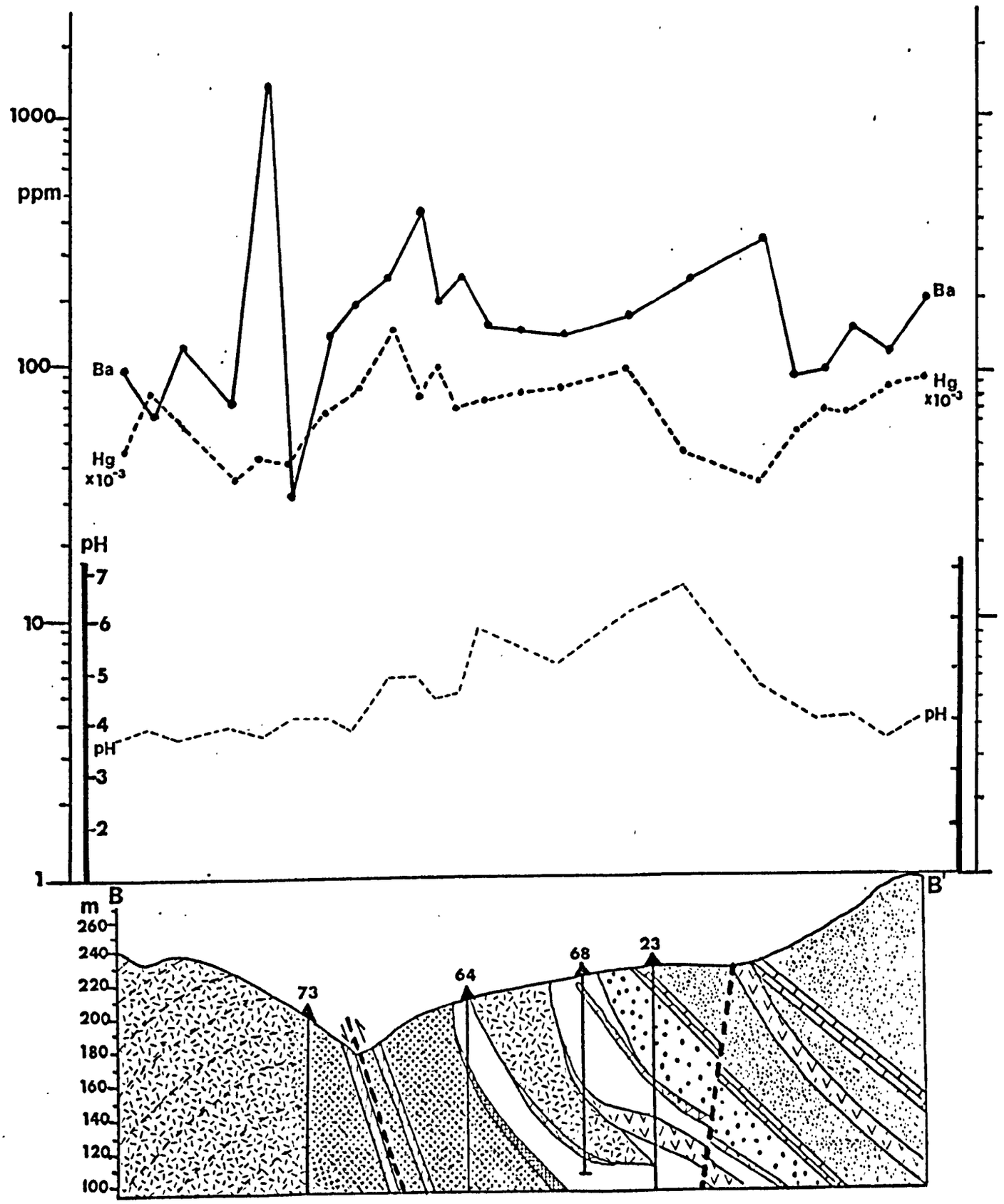


Figure 9.10 Hg and Ba contents, and the pH of soils along traverse B-B' over the Madenköy massive sulphide deposit. Elemental concentrations in ppm. For geological legend see Figure 9.11.

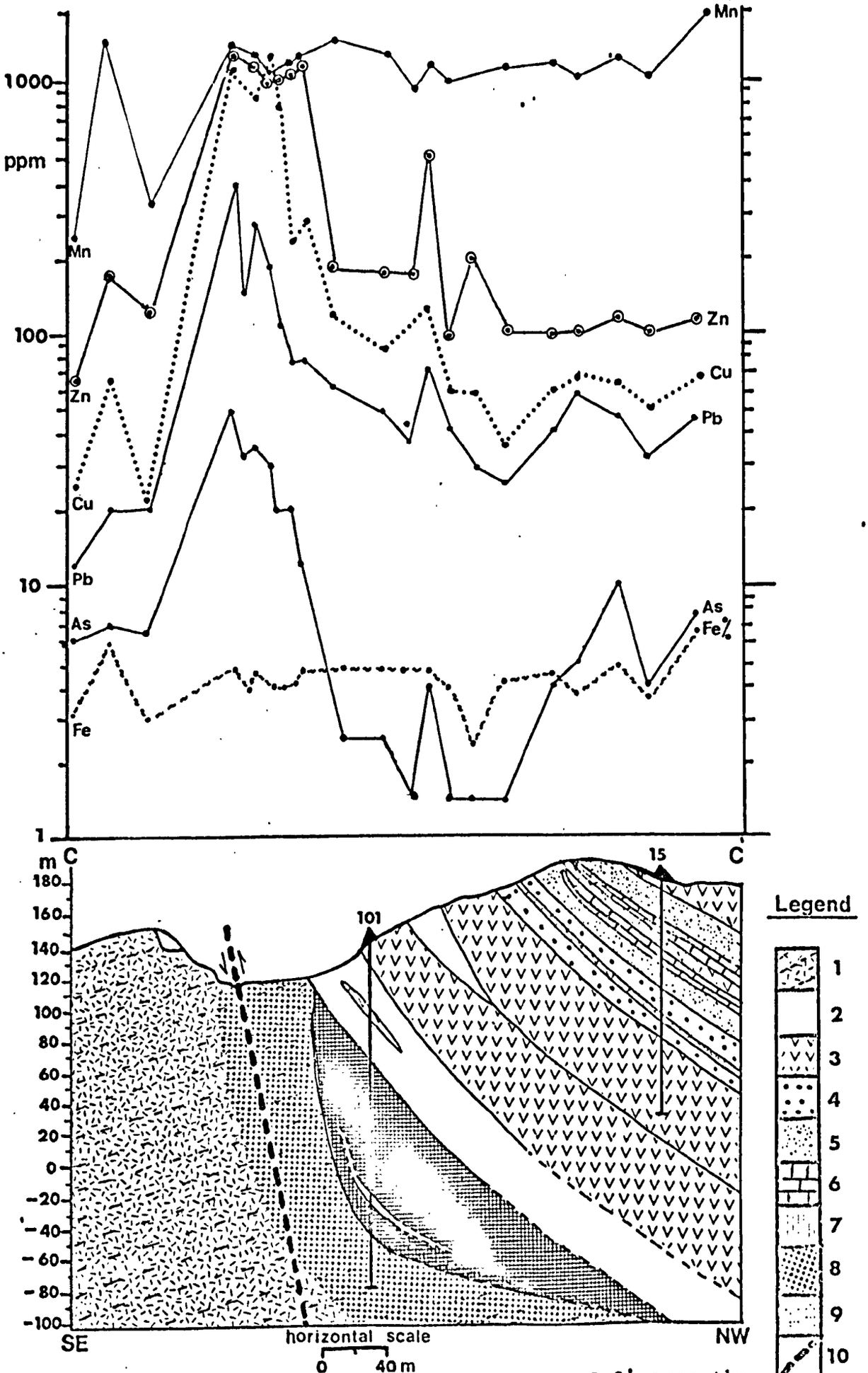


Figure 9.11 Elemental profiles along soil traverse C-C' over the Madenköy massive sulphide deposit. All concentrations in ppm unless otherwise stated. (1- Dacitic Series, 2- pumice tuffs, 3- basalts, 4- andesitic tuff-breccia, 5- sandstone, 6- limestone, 7- andesite, 8- stockwork-impregnation zone, 9- massive ore, 10- fault, 11- drilling site).

In contrast to the Madenköy deposit, soils over the Kutlular deposit exhibit strong Pb, Cu, Zn, and As anomalies over the cover rocks, the maximum/background ratios being about 40, 25, 6, and 20 respectively. These results reflect the mineralized nature of the hanging-wall rocks as well as the thin and eroded features of the basalt cover (Figures 9.12 and 9.13). High concentrations of Pb, Cu, Zn, and As were observed in cover rocks penetrated by drill-core K-8 (Figure 8.17). The maximum anomaly/background ratios of these elements over the stockwork zone at Kutlular are about 10, 6, 2, and 8 respectively. The anomaly/background ratio for Ba was found to be about 2 for soils developed over both the cover rocks and stockwork zone.

Over the Kotarak Dere stockwork deposit, the elemental concentrations in the soils are low compared with those obtained over the Madenköy and Kutlular deposits (Figure 9.14). The highest contents of As, Zn, Cu, and Ba occur slightly to the southeast of the known stockwork-impregnation zone in the Kotarak Dere stream, suggesting a probable extention of the mineralized zones in this direction. Over the Kotarak Dere deposit the highest anomaly/background ratio was again shown by Pb (about 3) followed by Cu, As, Zn, and Ba with ratios of 2.5, 2, 1.5 and 1.5 respectively.

In the Sirtköy area, Cu, As, and Ba occur in anomalous concentrations over the mineralized zone (Figure 9.15). These elements exhibit maximum anomaly/background ratios of 14, 5, and 3 respectively. Arsenic and Ba register high values over the mineralized dacites around the Gümüşdere stream whereas Cu and Zn occur in high concentrations over the mineralized basic rocks. Over the mineralized dacites Zn

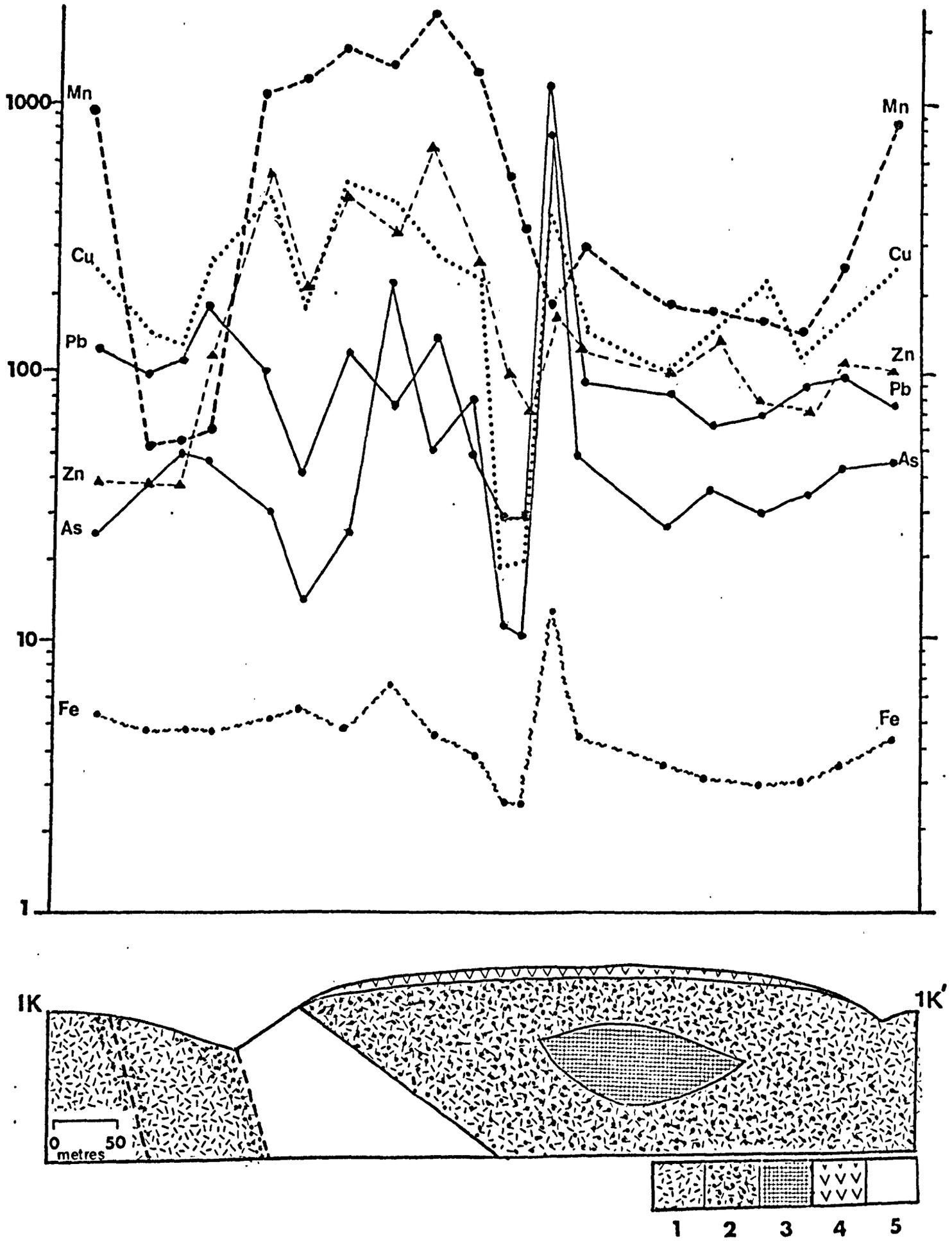


Figure 9.12 Elemental profiles along soil traverse, 1K-1K' over the Kutlular massive sulphide deposit. All concentrations in ppm unless otherwise stated. (1- Dacitic Series, 2- pyritized and silicified zone, 3- massive ore, 4- basalt, 5- diabase).

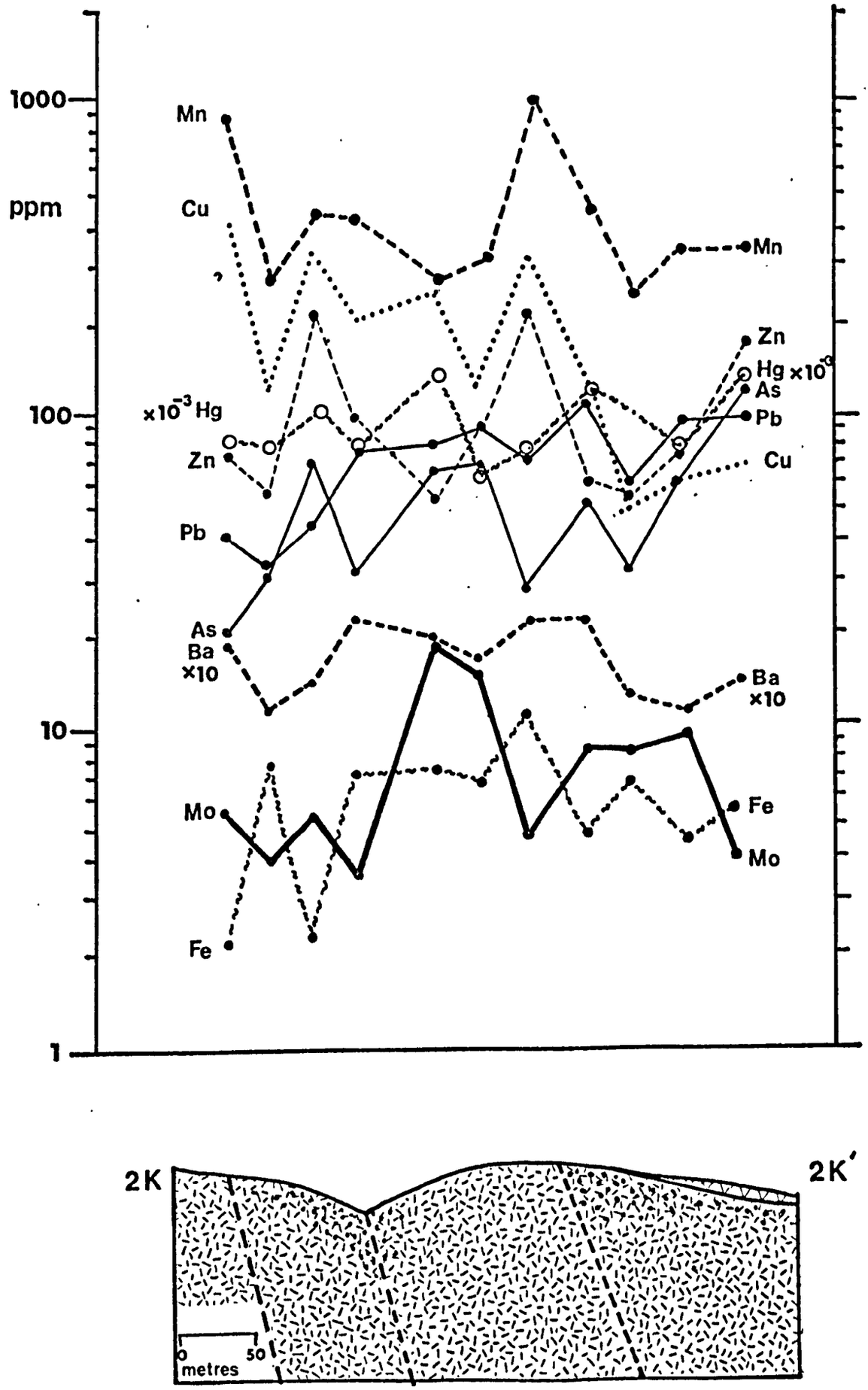


Figure 9.13 Elemental profiles along soil traverse 2K-2K' over the Kutlular massive sulphide deposit. All concentrations in ppm unless otherwise stated. For geological legend see Figure 9.12.

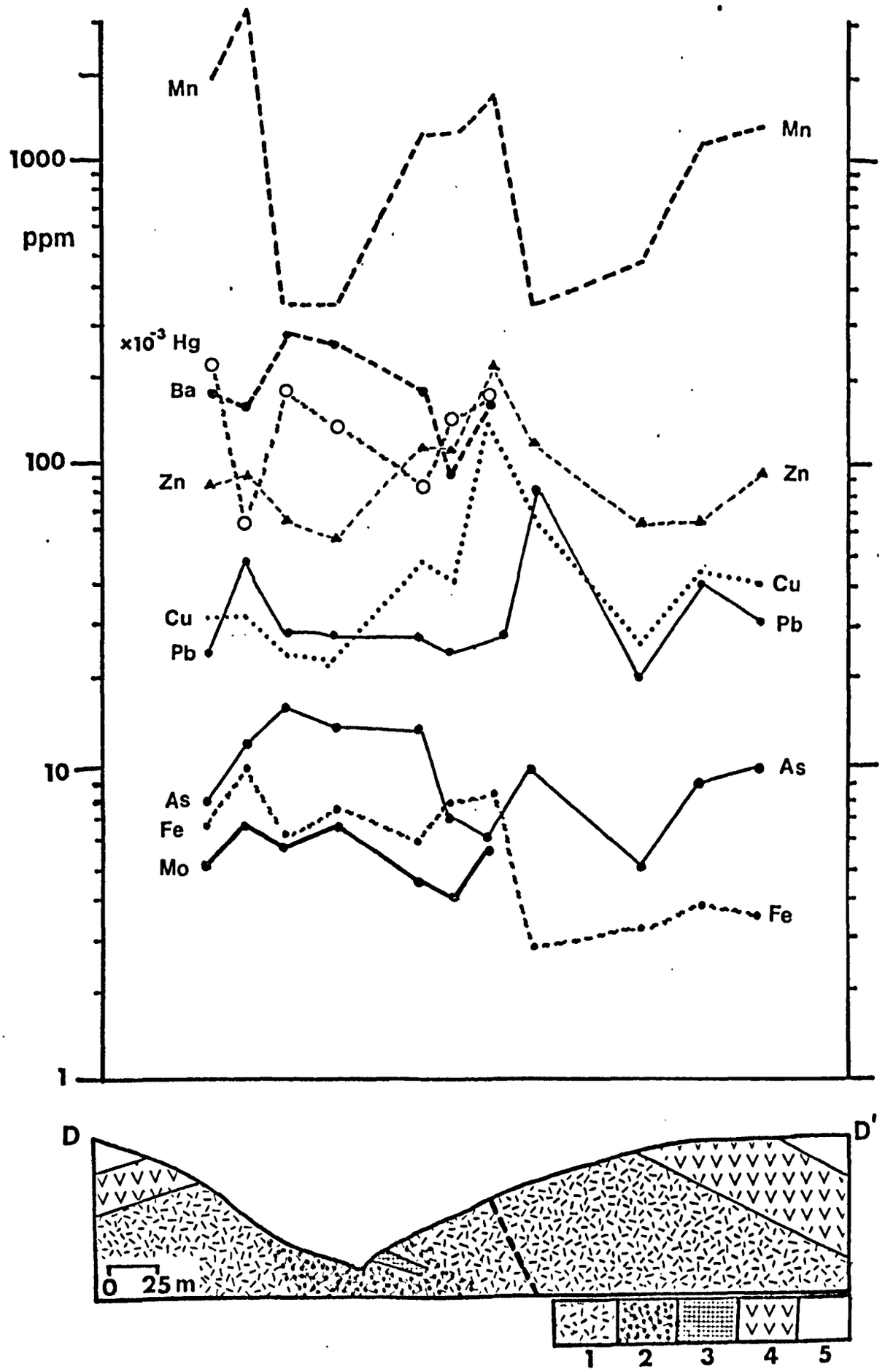


Figure 9.14 Elemental profiles along soil traverse D-D' over the Kotarak Dere deposit. All concentrations in ppm unless otherwise stated. (1- dacite, 2- silicification and pyritization, 3- massive pyrite, 4- basalt, 5- volcanic breccia).

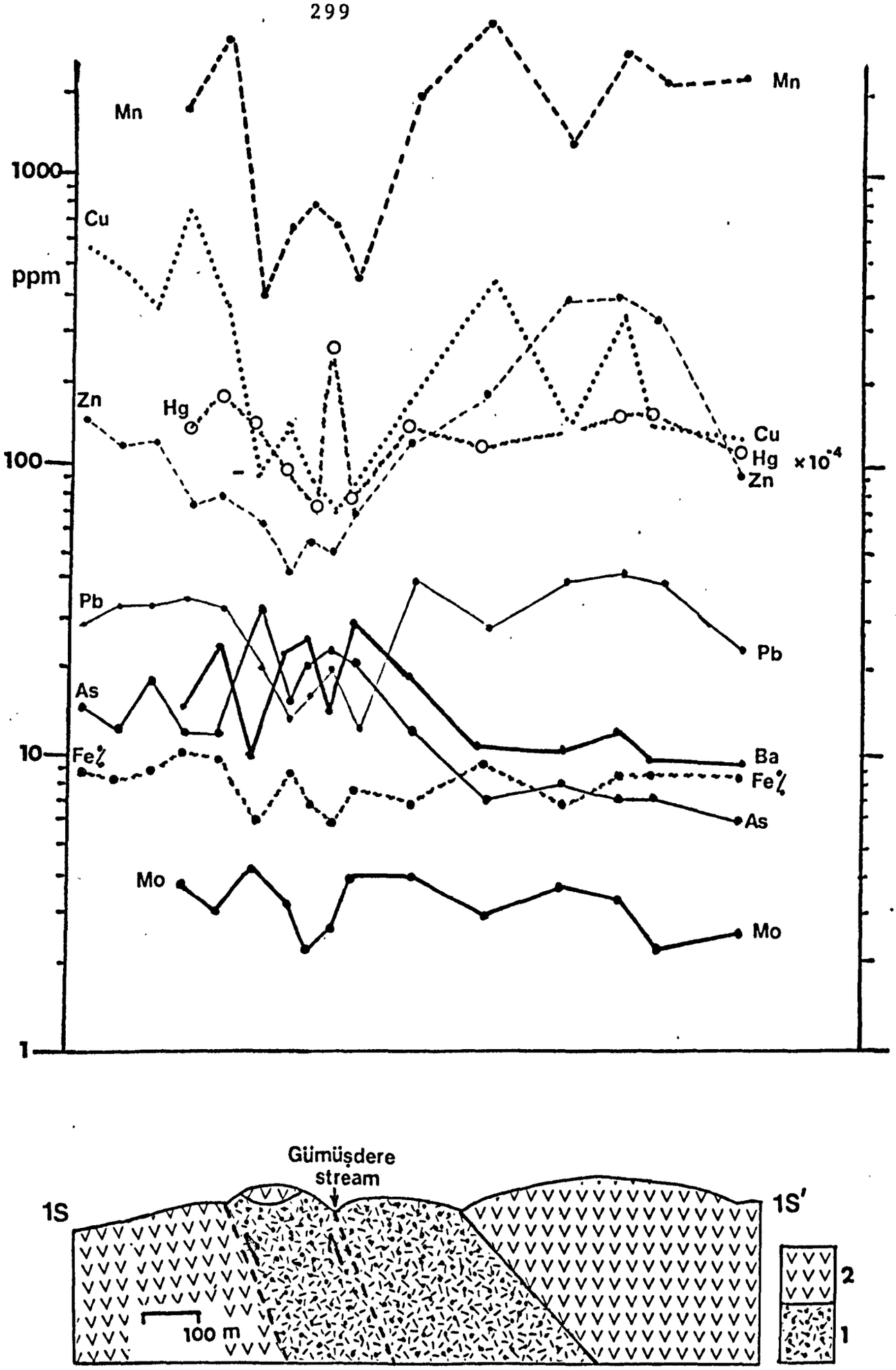


Figure 9.15 Elemental profiles along soil traverse 1S-1S', Sirtköy area. All concentrations in ppm unless otherwise stated. (1- pyritized and silicified dacite, 2- basalt).

and Pb are present in slightly higher concentrations than their background levels over this rock type. These dispersion features for As, Ba, Cu, Zn, and Pb in the Sirtköy soils reflect the results of the bedrock survey.

In the Sarisu area, As and to some extent Cu demonstrate a slight enrichment over the impregnation zone (Figure 9.16). Other elements such as Zn, Pb, and Ba occur in concentrations close to their background values, thus indicating the barren nature of this mineralization.

Cadmium and Ag occur in high concentrations over the stockwork zones of the economic sulphide mineralizations (e.g. Madenköy and Kutlular). These two elements are also enriched in soils over the cover rocks of the Kutlular massive ore. However, their dispersion in soils is restricted, and their anomaly background ratios are somewhat low due to the high detection limits and low analytical sensitivities of the elements.

Molybdenum is present in anomalous concentrations over mineralized zones in general, but its dispersion is erratic, and the element exhibits no regular dispersion pattern which could be useful in a directional vector sense to outline concealed massive sulphide mineralization.

Mercury displays no significant anomalies over the various mineralized zones (Figures 9.5, 9.6, 9.7, 9.10, 9.13, 9.14, 9.15, and 9.16). Its concentrations in soils over the stockwork impregnation zones does not appear to be related to the type of mineralization, the mean contents for the soils over the stockwork-impregnation zones of the Madenköy and Kutlular deposits and the Sirtköy mineralization being 73, 85, and 135 ppb respectively. Vapour evolution phase analysis

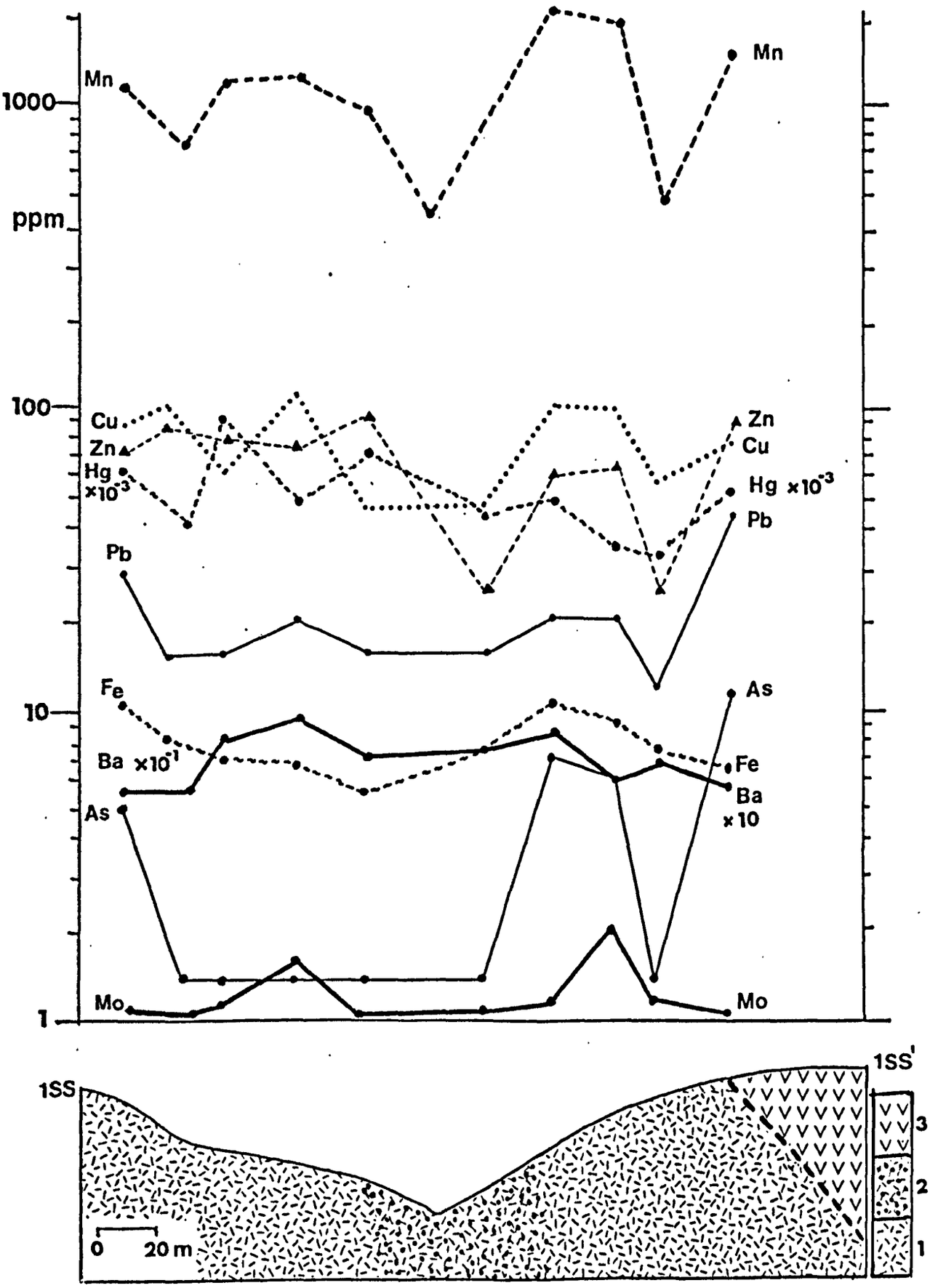


Figure 9.16 Elemental profiles along soil traverse 1SS-1SS', Sarisu area. All concentrations in ppm unless otherwise stated. (1- dacite, 2- pyrite impregnation in dacite, 3- basalt).

of mercury was carried out for selected soil samples from mineralized and background localities. Tentative interpretation of the evolution profiles obtained suggests that mercury occurs mainly in sulphide form (Table 9.2). However, in a few samples the presence of adsorbed mercury, mercuric chloride ($HgCl_2$), mercuric sulphate ($HgSO_4$), and mercuric oxide (HgO) are also suggested. No significant difference was found in the mode of occurrence of mercury in soil samples from background and mineralized localities.

These interpretations for mercury are only tentative, for example adsorbed mercury can also be evolved at 200°C and 430°C, thus interfering with the sulphate evolution peaks (R. Halenko, pers. comm., 1975). From this it follows that more research is required before a sound interpretation of results based on mercury phase analysis can be made.

The distribution of Fe and Mn in the soils generally reflects the chemistry of the underlying bedrock. For example, compared to the dacitic footwall rocks, Mn and to some extent Fe are present in higher concentrations in the soils over the cover rocks of the Upper Basic Series which include pumice tuff, basalts, and andesite breccias, all of which are primarily rich in Mn and Fe (Figures 9.8, 9.9, and 9.11).

9.5 SELECTIVE EXTRACTION TECHNIQUES

9.5.1 Introduction

Selective extraction techniques have been employed in geochemical surveys (soil and stream sediment) for increasing

Table 9.2 Mercury phase analysis of selected soil samples

Sample Number	Type of zone from which sample collected	Mercury compound present					
		Adsorbed mercury (100-180°C)	Hg_2Cl_2 (180°C)	$HgCl_2$ (200-210°C)	HgS (270-310°C)	$HgSO_4$ (440°C)	HgO (150,270,520°C)
Madenköy							
MS-7	stockwork	±			+		±
MS-21	stockwork				+	±	
MS-26	stockwork				+		
MS-30	hanging-wall				+		
MS-33	hanging-wall				+		
MS-37	hanging-wall			±	±		
MS-39	hanging-wall	±					
Kutlular							
K-2	hanging-wall				+		
K-26	hanging-wall			±			
Kotarak Dere							
K-12	stockwork				+	±	
Sirtköy							
SS-3	background			+	+	±	±
SS-5	background			+	+	+	
SS-13	stockwork				+	±	

+ indicates presence of mercury compound

± indicates presence of minor amounts of mercury compound

anomaly contrast as well as studying the mode of occurrence, mobility, and general behaviour of elements under different natural environmental conditions (Hawkes and Webb, 1962, p. 151; Ellis et al., 1967; Horsnail et al., 1969; Rose, 1975).

Trace elements in the secondary environment may occur as major elements in a minor secondary mineral, as minor elements in a primary detrital mineral, and as adsorbed ions on clay minerals, iron and manganese oxides and hydroxides, and organic matter. By using relatively weak sample digestion techniques involving a specific reagent one can selectively dissolve one or more elements of the components of a geochemical sample. For example, EDTA has been used to extract the exchangeable and readily soluble elemental phase in soils (Lakanen and Erviö, 1971); hydroxylamine hydrochloride has been employed to dissolve Mn-oxides (Chester and Hughes, 1967; Chao, 1972); and ammonium oxalate has been used to selectively dissolve Fe and Mn oxides and hydroxides (Le Riche and Weir, 1963; Horsnail et al., 1969). Other reagents employed in selective leaching of geochemical samples include 1 M neutral ammonium acetate solution and 0.2% hydroquinone in 1 M neutral ammonium acetate buffer for extracting exchangeable Mn (Sherman et al., 1942; Horsnail et al., 1969); calcium nitrate for extracting Mn from soils (Page, 1964); dithionite in acid solution for dissolving Mn and Fe (Anderson and Jenne, 1970); and hydrogen peroxide for dissolving organic matter together with Mn-oxides and sulphides (Rose and Suhr, 1971).

In geochemical exploration involving the sampling of the secondary environment, "total" attacks using reagents such as hydrofluoric acid and/or perchloric acid or

perchloric-nitric acids usually reflect the bedrock geochemistry and cause high background noise in which hydromorphic anomalies may be lost. When bedrock information is not required the weaker, cold-extractable methods have often been found to give better anomaly contrasts, more emphasis being thus placed on the detection of hydromorphic anomalies by diminishing the background variations due to bedrock geochemistry (Coope and Webb, 1963; Ellis et al., 1967; Bradshaw et al., 1974).

In the present study selected residual soils from Madenköy (23 samples on traverse B-B'), Sirtköy (13 samples on traverse 1S-1S', and 7 background samples on traverse 2S-2S'), and Kutlular (7 samples on traverse 3K-3K') were subjected to three extraction procedures involving 0.05 M ammonium EDTA (pH:4.65), 1 M hydroxylamine hydrochloride in acetic acid (pH:1.3), and 0.157 M ammonium oxalate in oxalic acid (pH:3.3). The extractive capability of these three reagents can be summarized as follows:

EDTA, being a strong chelating agent, extracts and complexes the exchangeable and easily soluble fractions such as calcium carbonate and the trace elements bound by organic matter.

Hydroxylamine hydrochloride, a reducing agent, dissolves the Mn-oxide fraction (up to 90% of the total) and only minor amounts of Fe oxides. This reagent also extracts the exchangeable and readily soluble fractions.

Ammonium oxalate, being a stronger reducing agent than hydroxlamine hydrochloride, dissolves under the catalytic action of ultra-violet light Fe oxides (up to 60% of the total)

in addition to Mn oxides and hydroxides, and the exchangeable and readily soluble fractions.

The author investigated the solubility of the common sulphide minerals in these reagents. The results are presented in Table 9.3.

The main aims of the present selective extraction studies were to enhance anomalies in general and especially to increase the anomaly contrast over concealed massive ore bodies similar to Madenköy; in addition a knowledge of the forms in which the trace elements occur in the soils was sought. The elements studied were Cu, Zn, Pb, Fe, and Mn. Arsenic analysis and Hg vapour-phase analysis were also carried out in the leached residues. For the selective extraction methods the reader is referred to section 5.8.

9.5.2 Results

The means and ranges of the percentage of extractability* for Cu, Zn, Pb, Fe, and Mn by the three extraction techniques are given in Tables 9.4, 9.5, and 9.6.

The EDTA extraction dissolves only a minor amount of the total Fe (mean of about 0.2%) and a small percentage of the Mn, Cu, and Zn (means of about 7, 8 and 3%) from all the soils. However, considerable amounts of Pb (average of 18% of the total) are extracted by this reagent. The order of extractability of the metals by the EDTA extraction technique is Pb > Mn = Cu > Zn > Fe.

---

* Extractability is expressed as (amount of extractable metal in ppm/amount of 'total' metal in ppm as determined by nitric acid-perchloric acid attack) x 100 for all metals except Pb, the total of which was determined by a nitric acid attack.

Table 9.3 Solubility (g/l) of sulphides in three types of extraction media (experiments were carried out under the same conditions as the extraction of samples, see section 5.8 for conditions)

TYPE OF EXTRACTION	PYRITE	CHALCOPYRITE	GALENA	SPHALERITE
E D T A extraction (pH:4.7)	0.0857	0.0238	8.0811	0.2681
Hydroxylaminae hydrochloride extraction (pH:1.3)	1.2257	0.4533	46.1776	2.2008
Ammonium oxalate extraction (pH:3.3)	1.6029	1.4959	0.9236	0.9393

Table 9.4 Extractability* of elements from soil samples by 0.05 M ammonium EDTA (pH:4.65).

Locality (no. of samples, soil traverse)	Extractability of elements (wt %)									
	Cu		Zn		Pb		Fe		Mn	
	Mean	Range	Mean	Range	Mean	Range	Mean	Range	Mean	Range
Madenköy (23 samples on traverse B-B')	16.6	2.0-35.9	6.0	0.4-16.2	33.2	12.5-62.5	0.4	0.1-1.9	15.2	1.3-44.0
Kutlular (7 samples on traverse 2K-2K')	7.6	1.9-15.3	2.5	0.9- 4.6	20.0	13.6-31.3	0.3	0.1-0.7	5.1	2.0-11.8
Sirtköy (13 samples on traverse 1S-1S')	4.2	0.5- 7.5	2.0	0.5- 4.8	21.1	3.3-28.6	0.2	0.1-0.4	5.8	2.0-15.3
Sirtköy (7 background samples on traverse 2S-2S')	2.1	0.5- 3.4	1.0	0.4- 2.5	8.5	3.3-17.1	0.1	0.1-0.2	1.7	0.8- 3.0

*Extractability expressed as (EDTA extractable metal/nitric acid + perchloric acid extractable metal) x 100 for all metals except Pb for which "nitric acid + perchloric and extractable metal" is replaced in the formula by "nitric acid extractable metal".

Table 9.5 Extractability* of elements from soils by 1M hydroxylamine hydrochloride solution in acetic acid (pH:1.3).

Locality (No. of samples, soil traverse	Extractability of elements (wt %)									
	Cu		Zn		Pb		Fe		Mn	
	Mean	Range	Mean	Range	Mean	Range	Mean	Range	Mean	Range
Madenköy (23 samples on traverse B-B^1)	20.7	3.0-66.7	13.2	1.5-44.0	37.3	10.0-72.7	4.9	0.8-13.3	66.7	18.8-83.3
Kutlular (7 samples on traverse 2k-2k^1)	12.1	1.3-37.7	12.6	9.4-17.2	39.0	20.8-54.7	4.6	0.5-9.3	40.7	28.3-56.2
Sirtköy (13 samples on traverse 1s-1s^1)	5.9	1.8-9.4	8.9	2.0-23.0	36.0	24.0-57.1	4.8	2.3-7.7	51.2	13.6-83.8
Sirtköy (7 background samples on traverse 2s-2s^1)	4.4	2.1-7.5	3.7	0.8-9.2	31.6	25.0-40.0	3.9	3.1-5.8	54.7	44.0-75.2

*Extractability expressed as (hydroxylamine hydrochloride extractable metal/nitric acid + perchloric acid extractable metal)x 100 for all metals except for Pb for which "nitric acid + perchloric acid extractable metal is replaced in the formula by nitric acid extractable Pb".

Table 9.6 Extractability* of elements from soil samples by 0.157 M ammonium oxalate solution (pH:3.3)

Locality (no. of samples, soil traverse)	Extractability of metals (wt %)									
	Cu		Zn		Pb		Fe		Mn	
	Mean	Range	Mean	Range	Mean	Range	Mean	Range	Mean	Range
Madenköy (23 samples on traverse B-B')	39.3	28.6-58.6	34.6	10.8-51.8	25.0	0.50.0	39.8	22.9-62.5	69.2	42.2-87.6
Kutlular (7 samples on traverse 2K-2K')	22.4	4.5-42.9	15.8	5.9-31.5	21.7	8.8-4.0	28.5	13.1-34.4	59.1	43.3-82.4
Sirtköy (13 samples on traverse 1S-1S')	20.4	9.4-36.3	10.0	2.2-31.9	10.8	0.28.0	27.3	13.7-39.8	59.0	5.7-96.2
Sirtköy (7 background samples on traverse 2S-2S')	22.9	6.0-44.3	15.1	2.1-34.2	10.3	0.32.0	37.9	32.5-50.0	67.5	54.1-84.8

*Extractability expressed as (ammonium oxalate extractable metal/nitric acid + perchloric acid extractable metal) x 100 for all metals except Pb for which "nitric acid + perchloric acid extractable metal is replaced in the formula by nitric acid extractable metal.

Hydroxylamine hydrochloride solution extracts more than half the total manganese, about 5% of the total Fe and approximately 35%, 11%, and 10% respectively of the total Pb, Cu, and Zn from all the soils. The order of extractability of metals by hydroxylamine hydrochloride is Mn > Pb > Cu ≥ Zn > Fe.

The ammonium oxalate extraction results in the solution of approximately 35%, 65%, 28%, 20%, and 17% of the total Fe, Mn, Cu, Zn, and Pb respectively with the order of extractability being Mn > Cu > Fe > Zn > Pb.

Arsenic analyses of the leached residues were also carried out. In the case of the EDTA and hydroxylamine hydrochloride extracted residues no detectable differences were found between the As contents of leached and unleached samples. However, for the ammonium oxalate leached residues it was found that a mean of 24% and a range of 3-55.6% of the total As was extracted in 15 soil samples from the Madenköy and Kutlular areas.

Mercury phase analysis was done on the leached soil samples. A comparison of the results obtained with those for the original unleached samples demonstrates that the absorbed mercury (evolved between 100 and 210°) is leached by the EDTA and the hydroxylamine hydrochloride solutions. However, these reagents had no effect on the mercuric sulphide phase. The ammonium oxalate solution removes all the peaks representing adsorbed Hg and sulphide Hg and yields a sharp peak at about 180°C, probably representing mercurous chloride (Hg_2Cl_2). The extractants had no effect on mercury evolved at about 440°C and 520°C (i.e. HgO and $HgSO_4$).

All three extraction procedures removed larger amounts of each of the metal from the Madenköy soils than from the soils of other areas (Tables 9.4, 9.5 and 9.6). In the case of the EDTA and hydroxylamine hydrochloride extraction methods the lowest amounts of metals were extracted from the background soils of the Sirtköy area, thus demonstrating the efficiency of these techniques in enhancing the anomaly contrast (Tables 9.4 and 9.5). The results obtained with the ammonium oxalate extraction technique (Table 9.6) suggests that this technique is not effective in increasing the anomaly contrast. For example, this method extracts more Zn, Fe, and Mn from the background Sirtköy soils than from the Sirtköy soils collected on traverse 1S-1S' over the mineralized zone. Further comparison of the extractabilities of metals in soils from mineralized areas with those from the background Sirtköy Soils by the three extraction procedures demonstrates that the EDTA, and to a lesser extent the hydroxylamine hydrochloride, are the best extraction procedures for increasing the anomaly/background ratio (Tables 9.4, 9.5 and 9.6). For example, the ratios of extractabilities by the EDTA procedure for Cu, Pb, and Zn from the Madenköy soils to those from the background soils are about 8, 4, and 6; the corresponding ratios for the hydroxylamine chloride procedure are approximately 5, 1.2, and 3.5, and for the ammonium oxalate procedure 1.5, 2.5, and 2.3.

Considering the Madenköy soils on traverse B-B', the EDTA and hydroxylamine hydrochloride extractable metals, in particular Zn and Pb, display the highest enhancement of anomalies over the concealed massive ore-body compared to the stockwork-impregnation zone (Figure 9.17 and 9.18). With

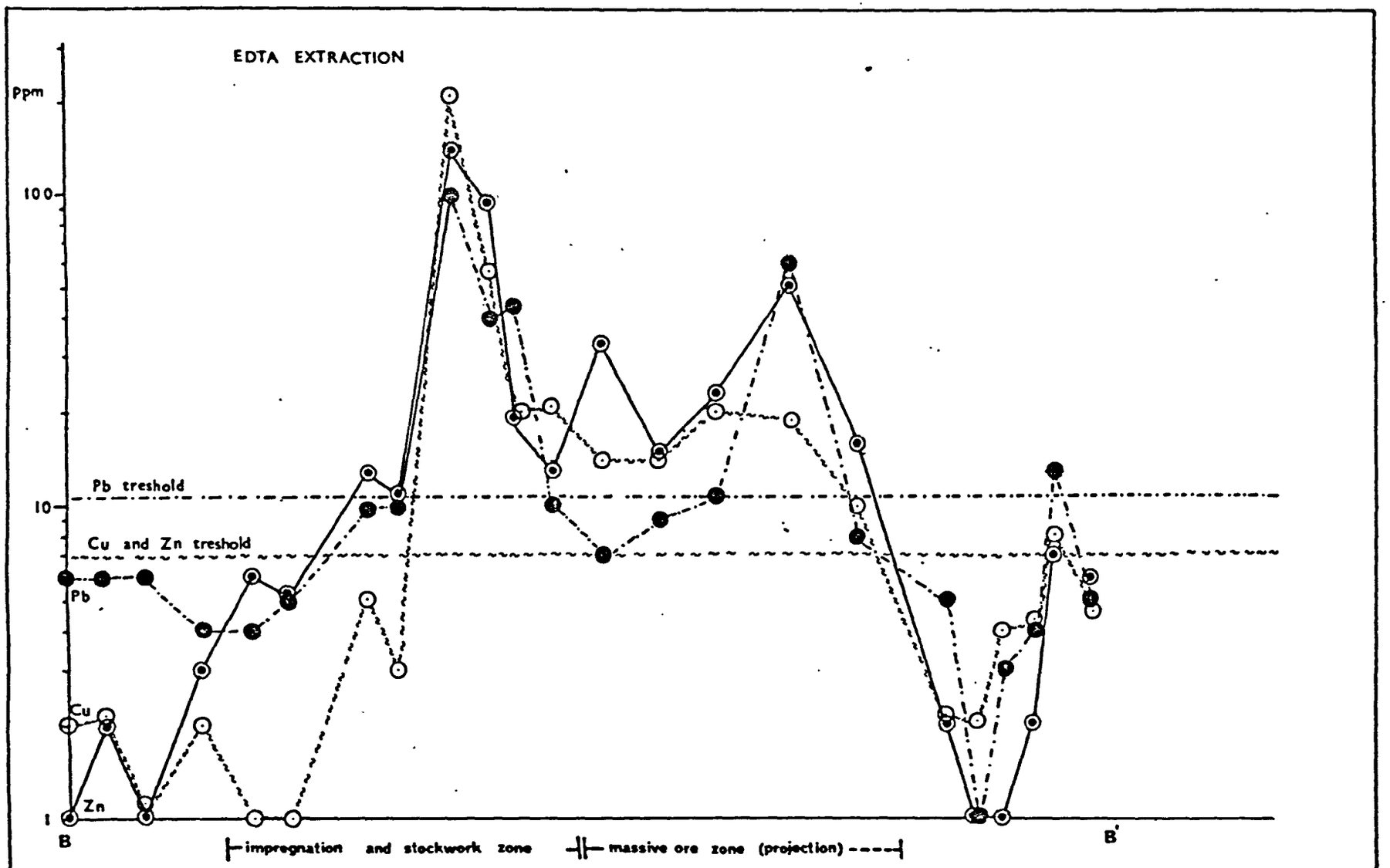


Figure 9.17 EDTA extractable Cu, Zn, and Pb in soils along traverse B-B', over the Madenköy massive sulphide deposit. (For cross-section along traverse B-B' see Figure 9.10).

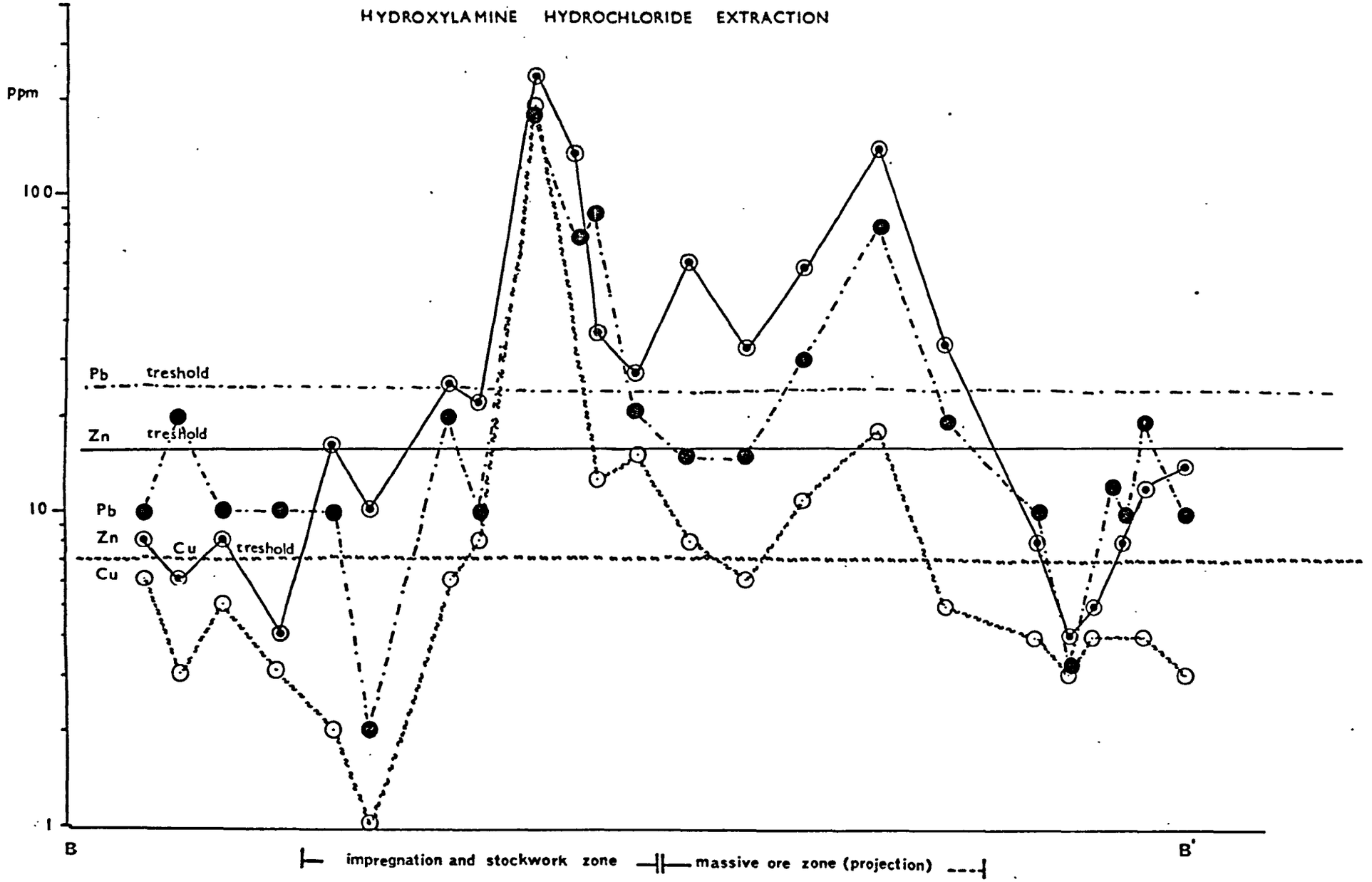


Figure 9.18 Hydroxylamine hydrochloride extractable Cu, Zn, and Pb in soils along traverse B-B' over the Madenköy massive sulphide deposit. (For cross-section along traverse B-B' see Figure 9.10).

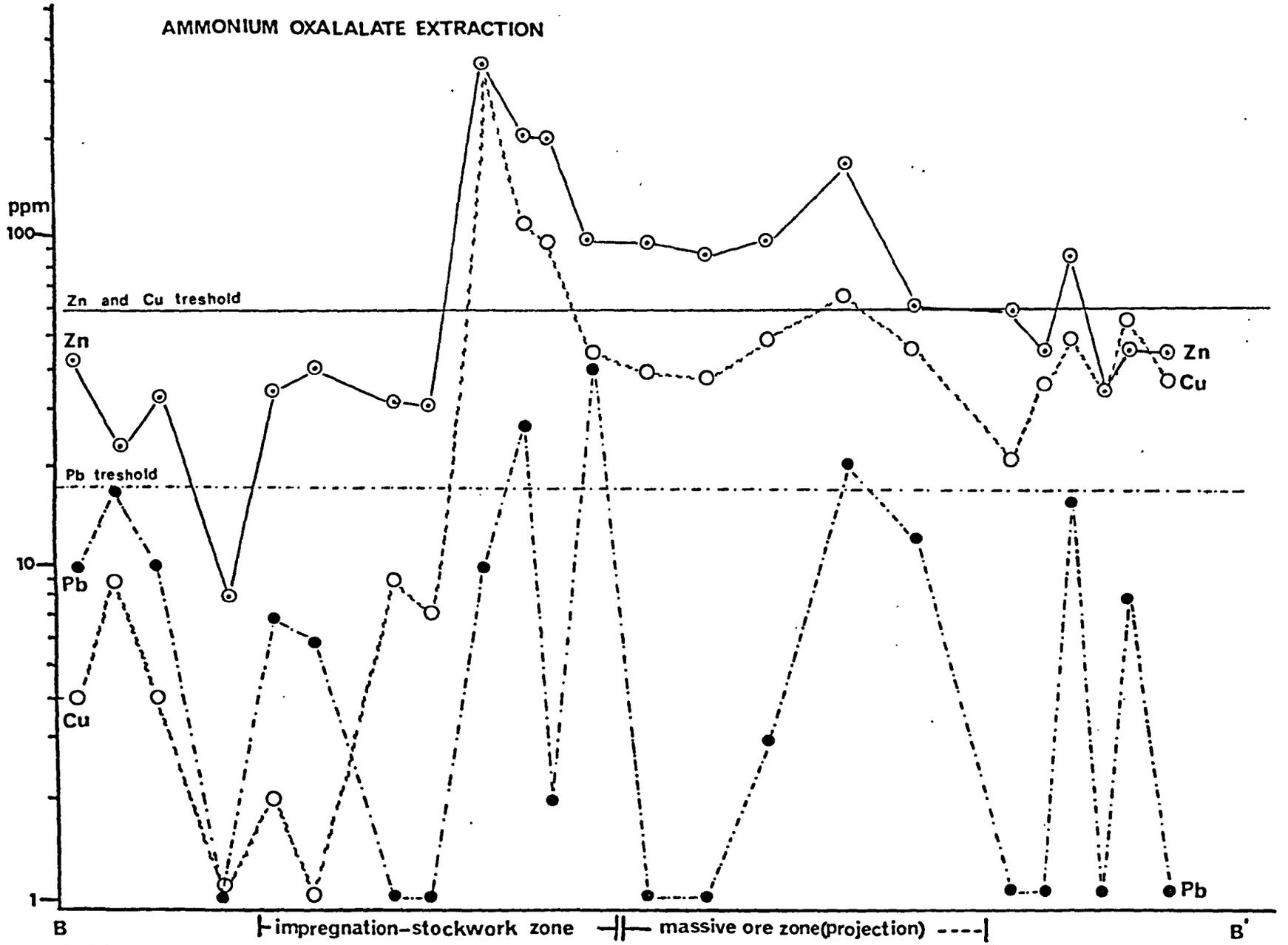


Figure 9.19 Ammonium oxalate extractable Cu, Zn, and Pb in soils along traverse B-B' over the Madenköy massive sulphide deposit. (For cross-section along traverse B-B' see Figure 9.10).

these two methods more Zn and Pb, and less Cu, were extracted from soils over the cover rocks of the massive ore body than from those over the stockwork and impregnation zones. The ammonium oxalate extractable metals, on the other hand, display no anomaly enhancement over the massive ore body when compared with the nitric acid extractable metals (Figure 9.19).

9.6 DISCUSSION AND CONCLUSIONS

Copper, and to a lesser extent As, in soils were found to delineate all three types of mineralization in the Eastern Black Sea Ore Province. The strongest anomalies for these elements are located over the economic massive sulphide deposits at Madenköy and Kutlular; moderately strong anomalies are displayed over the Kotarak Dere and Sirtköy mineralized zones, and only weak anomalies exist over the Sarisu barren pyrite occurrence.

Lead was found to be an excellent indicator of massive sulphide-type mineralization, with anomaly/background ratios of up to 40 over the stockwork zone as well as high ratios over the cover rocks of the massive sulphides; these high anomaly contrasts are due to the immobile nature of this element. Zinc also displays high anomaly/background ratios (up to 14) over the stockwork zone and cover rocks of the massive sulphides. Lead and Zn, on the other hand, display relatively weaker anomalies over the Kotarak Dere deposit and occur at or near background concentrations over the Sirtköy and Sarisu mineralized zones.

Barium demonstrates useful dispersion patterns related to massive sulphide-type and stockwork sulphide-type mineralization. Over the Sarisu barren pyrite occurrence the

element is present at background concentrations. In general barium exhibits much lower anomaly contrasts than Pb and Zn.

Mercury is not a useful indicator of mineralization in this area. No significant differences in the form of occurrence of this element in background and mineralized area soils were detected.

Molybdenum exhibits an erratic dispersion pattern. Although high contents of the element are clearly associated with sulphide mineralization it cannot be used to differentiate between the various types.

Despite the fact that acid leaching of the soils in the area would be expected to eliminate most of the hydromorphic anomalies, weak extractions such as EDTA and hydroxylamine hydrochloride were found to increase the anomaly contrasts considerably and to enhance Zn and Pb anomalies over the cover rocks of the Madenköy massive sulphide ore body relative to the stockwork and impregnation zones. Ammonium oxalate, which is a stronger extractant than either EDTA or hydroxylamine hydrochloride, was not effective in enhancing anomalies and increasing anomaly/background ratios. Considering the long and expensive procedure, involving two analytical steps (which also doubles the analytical error), the ammonium oxalate extraction technique is not recommended for further pedogeochemical exploration studies in this region.

The research described in this chapter indicates that the pedogeochemical dispersion characteristics of the elements discussed above are similar to their primary lithogeochemical trends. Thus, in the Eastern Black Sea Region the soils can provide an alternative or adjunct sampling media to rocks where the latter have a limited exposure in a particular area.

CHAPTER 10

GUIDELINES FOR EXPLORATION AND RECOMMENDATIONS FOR FURTHER RESEARCH

10.1 GUIDELINES FOR EXPLORATION

The problems of geochemical exploration for volcanogenic massive sulphide deposits in the Eastern Black Sea Ore Province include not only the detection of mineralized zones but also differentiating between the various types, including impregnation, stockwork, and massive sulphide types. The methods of geochemical exploration should, therefore, take into account methods of discriminating between these various types of mineralization with the ultimate objective of discovering economic massive sulphide bodies following delineation of mineralized zones with cost-effective, geochemical reconnaissance techniques.

Based on the present studies the following conclusions and guidelines for exploration can be stated:

1. Regional detection of mineralized zones: Regional geochemical exploration using stream sediment sampling is an effective technique for outlining mineralized zones in general because a well developed dendritic drainage pattern is present, and the streams generally follow tectonic lines (lines of block faulting) where the dacitic rocks (host rocks to sulphide mineralization) are usually exposed. However, due to the high stream gradients and frequent floods there is often significant erosion or elimination of hydromorphic dispersion trains. Close interval sampling (sampling densities less than 1 sample per square km) of second and even third order streams is required for effective reconnaissance

surveys. Arsenic is the best elemental pathfinder for outlining the sulphide mineralization in general, and Pb, Zn, Ag and high contents of As and Cu are good indicators of massive sulphide-type mineralization. The barren stockwork and impregnation deposits are generally characterized by anomalous contents of one or more of As, Cu, and Mo. The in-situ measurements of stream and spring water pH can be used to detect oxidizing sulphide zones.

2. Regional and Detailed Assessment of Mineralized Zones (Bedrock surveys): The Dacitic Series are associated with widespread mineralized zones in the Eastern Black Sea Region. Diagnostic parameters have been formulated to assess on a regional basis the mineral potential of exposed stockwork and impregnation zones in dacitic host rocks. Barren pyritic impregnation occurrences (e.g. Sarisu) have anomalous Fe and Cu contents, whereas pyritic stockwork zones, not associated with massive sulphide ore (e.g. Sirtköy), are enriched in Fe, As, and Cu. Stockwork - impregnation zones associated with massive sulphides are significantly enriched in most but not necessarily all of the following elements: Fe, As, F, Cu, Pb, Zn, Ag, Cd, and Mo.

Depending on the degree of exposure a minimum of 10 to 15 samples free of sulphides representing the areal extent of the mineralized zones should be taken for regional assessment. Mineralized zones, which have higher than normal contents of base metals (especially Pb), As, and F should be given high priority for detailed surveying.

Bedrock surveys, utilizing samples of host dacitic rocks and cover rocks involving different units of the Upper

Basic Series, have proven effective in outlining various types of primary halos associated with sulphide mineralization. For reconnaissance surveys As, F, Pb, and Zn are of most value for detecting and differentiating between the three types of mineralization. Fluorine and As are sensitive indicators of hydrothermal activity and mineralizing processes (pyritization) respectively; these elements consequently possess good directional (vector) properties for pointing out mineralization on a reconnaissance level. On a detailed basis it has been shown that F, As, Pb, Zn, and Cu have characteristic primary halos with high anomaly contrasts in the dacitic rocks around mineralization. The concentrations of these indicator elements increase significantly in the direction of massive sulphide mineralization and can, therefore, be used as directional vectors during drilling programs. When present, the hematitized rock units overlying the Dacitic Series were found to be the best sampling medium within the sequence of cover rocks. These hematitized rocks are marked by halos of As, F, Cu, Pb, Zn, Cd, Ag, Ba, and Mn over the mineralizations. The basic cover rocks (basalts) over mineralized zones, on the other hand, display elemental halos which are generally characterized by sporadic highs. The basalts over the Madenköy massive ore body contain high concentrations of F, Pb, and Ag. During reconnaissance bedrock surveys basic rocks exhibiting higher than normal contents of indicator elements such as F, Pb, Ag, As, Zn, and Cu should be studied in more detail to permit comparison of local population statistics similar to those generated in Chapter 8 (Table 8.5) with background data in

order to assess the possibility that they are cover rocks over blind ore.

Semi-quantitative evaluation of the "clay/feldspar" ratio is useful in detecting the presence and intensity of the hydrothermal activity related to sulphide mineralization. The "clay/feldspar" ratio as well as the zonation of alteration minerals (clays and carbonates) can also be used as directional vectors during drilling programs.

Limited data on the trace element chemistry of pyrite from the various deposits suggest that pyrite from barren stockwork and impregnation zones is characterized by high Co and Ni and low As contents. More data are required however to support the reliability of the As/(Ni + Co) ratio in assessing the mineral potential of mineralized zones in dacitic host rocks.

3. Use of soil sampling as an alternative or adjunct to bedrock surveys in areas of limited bedrock exposure: In many areas in the Eastern Black Sea Region the efficacy of bedrock surveys is severely affected by limited exposure; for this reason studies were also directed towards determining whether primary haloes in the basic cover rocks have signatures in the overlying soils. It has been shown that soil surveys can be successfully employed in this region as an alternative or adjunct to bedrock surveys.

The As and hot nitric acid extractable Cu, Zn, and Pb contents of the soils are good indicators of sulphide mineralization; Pb and Zn and high contents of As and Cu are indicative of massive sulphide mineralization. In detailed follow-up studies selective extraction techniques involving hydroxylamine hydrochloride and EDTA can be used to increase

the anomaly contrast. Furthermore, these two reagents are effective in enhancing Zn and Pb anomalies developed in soils on the cover rocks of concealed massive sulphide bodies.

To summarize: Guidelines for exploration in the Eastern Black Sea Region of Turkey are dependent upon a sound knowledge of the chemistry and alteration characteristics of both the dacitic rocks and cover rocks of the Upper Basic Series, the genetic and structural features of the various types of deposits, and adequate orientation data on the concentration levels and dispersion patterns exhibited by the various indicator elements in the primary and secondary environments.

10.2 RECOMMENDATIONS FOR FURTHER RESEARCH

The following recommendations are made for further research in this region:

(1) A regional stratigraphic correlation should be worked out in the Eastern Black Sea region on the basis of available geological mapping at 1/50,000, 1/25,000 and 1/10,000 scales. Consequent upon these stratigraphic and geological mapping studies, outcrops of the Dacitic Series and stratigraphic boundaries between this Series and the Upper Basic Series should constitute initial target areas for geochemical exploration.

(2) More data on the distribution of elements such as V, Ti, Sc, Co, and Ni in mineralized dacitic rocks associated with the various types of sulphide mineralization and unmineralized dacitic rocks should be useful in differentiating between different phases of dacites (which may possibly be present in the region) associated with the various

types of sulphide mineralization. An optical spectrographic method (such as the one used in the present study) covering a wide range of elements will provide the necessary data.

(3) More data on the minor element chemistry (especially the Co, Ni, and As contents) of pyrite from the different types of volcanogenic sulphide zones may prove to be useful in exploration. Electron microprobe analyses should be useful in eliminating the problems associated with separating pyrite free of included or exsolution material.

(4) The present studies indicate a marked relationship of fluorine with volcanogenic sulphide mineralization. In view of the fact that F in the Eastern Black Sea Region migrates great distances in the footwall and hanging-wall rocks from the focus of mineralization and also shows a larger anomaly contrast than other elements investigated, it would be worthwhile to study the behaviour of this element in the other types of volcanogenic sulphide deposits in different geological settings.

REFERENCES

ACAR, E., 1974. The economic importance of some trace elements within the province of Giresun, Eastern Black Sea Region. M.T.A. Bull., 82: 136-146 (in Turkish).

AHRENS, L.H., and TAYLOR, S.R., 1961. Spectrochemical Analysis. Addison-Wesley Publishing Company, Inc., 2nd edition 545 pp.

AKINCI, O.T., 1974. The Geology and Mineralogy of Copper Lead, Zinc Sulphide Veins from Bulancock, Turkey. Unpublished Ph.D. thesis, University of Durham.

ALDOUS, K.M., DAGNALL, R.M., SHARP, B.L., and WEST, T.S., 1971. A microwave-induced argon plasma system suitable for trace analysis. Anal. Chim. Acta, 54: 233-244.

ALLEN, R.J., CAMERON, E.M., and DURHAM, C.C., 1973. Reconnaissance geochemistry using lake sediments of a 36,000 square mile area of the northwest Canadian Shield (Operation Bear-Slave, 1972). Geol. Surv. Canada. Paper 72-50, 70 p.

ALTUN, Y., 1972. Geology of Madenköy (1) area. Unpublished M.T.A. Report, No. 553 (in Turkish).

ANDERSON, B.J. and JENNE, E.A., 1970. Free iron and manganese oxide content of reference clays. Soil Science, 109: 163-169.

APPLIED GEOCHEMISTRY RESEARCH GROUP TECHNICAL COMMUNICATION REPORT, 1971. Determination of Mo and As, provisional method.

APPLIED GEOCHEMISTRY RESEARCH GROUP TECHNICAL COMMUNICATION REPORT NO. 59, 1973. Direct reading optical spectrographic Emission System (System C).

ASLANER, G., 1971. Mineralogical study of the Kutonit mineralization (Eastern Black Sea Region) and its genetic implications. M.T.A. Bull., 77:38-56 (in Turkish).

ASLANER, G., and CAGATAY, A., 1973. Mineralogical study of the Piraziz mineralization and its genetic implications. M.T.A. Bull., 81:26-30 (in Turkish) (Also in German: M.T.A. Bull., foreign addition, 81:26-30).

ATABEK, S., 1940. Copper, zinc, and manganese deposits of Cayeli and Aytanos. Unpublished M.T.A. Report, No. 1061 (in Turkish).

ATAMAN, G., BUKET, E., and CAPAN, U.Z., 1975. Could North Anatolian Fault zone be a paleo Benioff zone? M.T.A. Bull., 84:97-102.

AUGER, P.E., 1941. Zoning and district variations of the minor elements in pyrite of Canadian gold deposits. Econ. Geol., 36:401-423.

AYDINÖZ, F., 1971. Geological map of Sarisu area, Cayeli district, Rize Province (1:2,000 scale). M.T.A. Map No. 23603.

BAILEY, E.H., BARNES, J.W., and KUPFER, D.H., 1966. Geology and ore deposits of the Küre District, Kastomonu Province, Turkey. In: Cento Summer Training Program in Geological Mapping Techniques. Office of U.S. Economic Coordination for Cento Affairs, Ankara, pp. 17-33.

BARAGAR, W.R.A., 1968. Major-element geochemistry of the Noranda volcanic belt Quebec-Ontario, Canadian Jour. Earth. Sci., 5:773-790.

BETHKE, P.M., and BARTON, P.B., Jr., 1971. Minor elements between coexisting sulphide minerals. Econ. Geol., 66:140-163.

BOYLE, D.R., 1976. The geochemistry of fluorine and its application in mineral exploration. Unpublished Ph.D. thesis, University of London.

BOYLE, D.R., and TROUP, A.G., 1975. Copper-molybdenum porphyry mineralization in central British Columbia: in Jones, M.J. (ed.), Prospecting in areas of glaciated terrain 1975, Instn. Min. Metall., p. 6-15.

BOYLE, R.W., 1974. The use of major elemental ratios in detailed geochemical prospecting utilizing primary halos. J. Geochem. Explor., 3:345-369.

BRADSHAW, P.M.D., THOMSON, I., SMEE, B.W., and LARSSON, J.O., 1974. The application of different analytical extractions and soil profile sampling in exploration geochemistry. J. Geochem. Explor., 3:209-225.

BRINKMANN, R., 1974. Geologic relations between Black Sea and Anatolia: in Degens, E.T., and Ross, D.A. (eds.), The Black Sea - Geology, Chemistry, and Biology. The American Association of Petroleum Geologists Mem., No. 20, pp. 63-76. Collegiate Press, 633 p.

BRUNFELT, A.O., and STEINNES, E., 1967. Determination of selenium in standard rocks by neutron activation analysis. Geochim. Cosmochim. Acta, 31:283-285.

BURNHAM, C.W., 1962. Facies and types of hydrothermal alteration. Econ. Geol., 57:768-784.

BUSER, S., and CVETIC, S., 1973. Geology of the Murgul deposit and surrounding area. M.T.A. Bull., 81:22-45 (in Turkish); also in German: M.T.A. Bull., foreign edition, 81:1-25).

ÇAĞATAY, A., 1968. Erzmikroskopische untersuchung des Weiss-Vorkommens bei Ergani Maden, Turkei, und genetische deutung der Kupfererzlager stätten von Ergani Maden. Neues Jahrb. Mineralogie Abh., 109:131-155.

ÇAĞATAY, A. (in press). Some thoughts on the genesis of the copper deposits and occurrences in southeastern Turkey through geological and mineralogical studies. M.T.A. Bull. (in Turkish).

ÇAĞATAY, M.N., and BOYLE, D.R. (in press). Geochemical prospecting for volcanogenic sulphide deposits in the Eastern Black Sea Region, Turkey. J. Geochem. Explor., 8th International Geochemical Exploration Symposium, Sydney, Australia, 1976, Vol. 8.

ÇALGIN, R., 1976. Preliminary report on the geology and mineralization of the Siirt-Madenköy copper deposit. Unpublished M.T.A. Report, No. M. 254 (in Turkish).

CAMERON, E.M., 1975. Geochemical methods of exploration for massive sulphide mineralization in the Canadian Shield: in Elliott, I.L., and Fletcher, W.K. (eds.), Geochemical exploration 1974 (Elsevier, Amsterdam), pp. 21-50.

CAN, M., 1975. Geology map of Tunca area (1:2,000 scale), Unpublished M.T.A. Map.

CHENG, K.L., 1956. Determination of traces of selenium 3,3' diaminobenzidine as Se (IV) organic reagent. Analytical Chemistry, 28:1738-1742.

CHAO, T.T., 1972. Selective dissolution of manganese oxides from soils and sediments with acidified hydroxylamine hydrochloride. Soil Sci. Am. Proc., 36:764-768.

CHESTER, R. and HUGHES, M.J., 1967. A chemical technique for separation of ferro-manganese minerals, carbonate minerals and adsorbed trace-elements. Chemical Geology, 2:249-262.

ÇOĞULU, H.E., 1970. Comparative petrological and geochronological study of the Gümüshane and Rize plutons. Post-doctoral thesis presented at Technical University of Istanbul, Turkey.

CONSTANTINOU, G., and GOVETT, G.J.S., 1972. Genesis of sulphide deposits, Ochre and Umber of Cyprus. Trans. Instn. Min. Metall., 81:B34-B36.

CONSTANTINOU, G., and GOVETT, G.J.S., 1973. Geology, geochemistry, and genesis of Cyprus sulphide deposits. Econ. Geol., 68:843-858.

COOPE, J.A., and WEBB, J.S., 1963. Copper in stream sediments near disseminated copper mineralization, Cebu, Phillipine Republic. Trans. Instn. Min. Metall., 72:397-406.

CREASEY, S.C., 1959. Some phase relations in hydrothermally altered rocks. Econ. Geol., 54:351-373.

CREASEY, S.C., 1966. Hydrothermal alteration: in Titley, S.R. and Hicks, C.L. (eds.), Geology of the porphyry copper deposits. Tuscan, Univ. of Arizona Press.

DALTON, E.F. and MALANOSKI, H.J., 1971. Note on the determination of arsenic by atomic absorption by arsine generation into an argon-hydrogen entrained air flame. Atomic Absorption Newsletter, 10:92-93.

DAVENPORT, P.H., and NICHOL, I., 1973. Bedrock geochemistry as a guide to areas of base-metal potential in volcano-sedimentary belts of the Canadian Shield: in Jones, M.J. (ed.), Geochemical exploration 1972, Instn. Min. Metall., p. 45-58.

DE GEOFFROY, J., 1960. Geology and mineral deposits of Cayeli, Pazar and Ardesen districts. Unpublished M.T.A. Report, No. 3073 (in Turkish).

DESCARREAUX, J., 1973. Petrochemical study of the Abitibi volcanic belt and its bearing on the occurrences of massive sulphide ores. Can. Inst. Min. Metall. Bull., 66 (730):61-69.

DEWEY, J.F. and BIRD, J.M., 1970. Mountain belts and the new global tectonics. J. Geophysical Research, 75(14): 2625-2647.

DEWEY, J.F., PITMAN, W., RYAN, W., and BONNIN, J., 1973. Plate tectonics and evolution of the Alpine system. Geol. Soc. Am., Bull., 84:3137-3180.

DIETZ, R.S., 1963. Alpine serpentinites on oceanic ridge fragments. Geol. Soc. Am. Bull., 74:947-952.

DIXON, C.J., and PEREIRA, J., 1974. Plate tectonics and mineralization in the Tethyan Region. Mineralium Deposita, 9(3):185-198.

ELLIS, A.J., TOOMS, J.S., WEBB, J.S., and BICKNELL, J.V., 1967. Application of solution experiments in geochemical prospecting. Trans. Instn. Min. Metall., 63:B25-B39.

FALLGATTER, K., SVOBODA, V., and WINEFORDNER, J.D., 1971. Physical and analytical aspects of a microwave excited plasma. Applied Spectroscopy, 25:347-352.

FERGUSON, J., LAMBERT, I.B., and JONES, H.E., 1974. Iron sulphide formation in an exhalative-sedimentary environment, Talassea, New Britain, P.N.G. Mineralium Deposita, 9:33-47.

FERNANDEZ, F.J., 1973. Atomic absorption determination of gaseous hydrides utilizing sodium borohydride reduction. Atomic Absorption Newsletter, 12:93-97.

FERNANDEZ, F.J., and MANNING, D.C., 1971. The determination of As at sub-microgram levels by atomic absorption spectrophotometry. Atomic Absorption Newsletter, 10:86-88.

FLEISCHER, M., 1955. Minor elements in some sulphide minerals. Econ. Geol., 50th anniversary volume (part 2):970-1024.

FRANKLIN, J.M., KASARDA, J., and POULSEN, K.H., 1975. Petrology and chemistry of the alteration zone of the Mattabi massive sulphide deposit. Econ. Geol., 70:63-79.

GATTINGER, T.E., ERENTÖZ, C., and KETİN, I., 1962. Explanatory text of the geological map of Turkey - Trabzon sheet, 1:500,000 scale. M.T.A. publication, Ankara.

GILMOUR, P., 1971. Stratabound massive sulphide deposits - a review. Econ. Geol., 66:1239-1244.

GOODFELLOW, W.D., 1975. Major and minor element halos in the volcanic rocks at Brunswick No. 12 deposit, N.B., Canada: in Elliott, I.L. and Fletcher, W.K. (eds.), Geochemical exploration 1974 (Elsevier, Amsterdam), pp. 279-293.

GOODWIN, A.M. and RIDLER, R.H., 1970. The abitibi orogenic belt: in Basins and geosynclines of the Canadian Shield. Geol. Surv. Canada Paper 70-40:1-30.

GÖKSU, E., PAMİR, N.H., and ERENTÖZ, C., 1974. Explanatory text of the geological map of Turkey - Samsun sheet, 1:500,000 scale. M.T.A. publication, Ankara.

GOVETT, G.J.S., 1972. Interpretation of a rock geochemical exploration survey in Cyprus - statistical and Graphical Techniques. J. Geochem. Explor., 1:77-102.

GRANT, J.N.M., 1974. Some aspects of Tectonics, magmatism and mineralization in the Tethyan Region. Unpublished M.Sc. dissertation, Imperial College, University of London.

GREENFIELD, S., McGEACHIN, H. McD., and SMITH, P.B., 1975a. Plasma emission sources in analytical spectroscopy - I. Talanta, 22(1):1-16.

GREENFIELD, S., McGEACHIN, H. McD., and SMITH, P.B., 1975b. Plasma emission sources in analytical spectroscopy - II. Talanta, 22(7):553-562.

GREENFIELD, S., JONES, I.LL., McGEACHIN, H. McD., and SMITH, P.B., 1975c. Automated multi-sample simultaneous multi-element analysis with H.F. plasma torch and direct reading spectrometry. Anal. Chim. Acta, 74:225-245.

GRIFFITS, W.R., ALBERS, J.P., and ONER, O., 1972. Massive sulphide deposits of the Ergani-Maden area, South-eastern Turkey. Econ. Geol., 67:701-716.

GRUNER, J.W., 1944. The hydrothermal alteration of feldspars in acid solutions between 300°C and 400°C. Econ. Geol., 39:578-589.

GUILD, P.W., 1972. Metallogeny and new global tectonics: in 24th Int. Geol. Congress, Ottawa, Canada, section 4, pp. 17-24.

GÜMRÜKCÜ, A., 1973. Geological map of Kutlular area (1:2,000 scale), Trabzon, Turkey. M.T.A. Map No. 26747.

GÜMRÜKÇÜ, A. and TAKAOGLU, S., 1974. Geological map of Kotarak Dere area (1?2000 scale), Trabzon, Turkey. M.T.A. Map No. 28630.

GÜMÜŞ, A., 1970. Turkiye metallojenisi, 1:2,500,000 ölcekli Turkiye metallojenik haritasinin izahi (Metallogenic map of Turkey and explanatory text, in Turkish). M.T.A. publication No. 144, Ankara.

GUPTA, S.P., GUPTA, D., SEN, P.R., and MURPHY, M.V.N., 1965. Nature and significance of wall rock alteration in some hydrothermal ore deposits in India. Econ. Geol., 60:1702-1708.

HALENKO, R. (in prep.). Mercury phase analysis and the mode of occurrence of mercury in primary haloes associated with ore deposits. Ph.D. thesis, University of London.

HAMAMCIOĞLU, A. and SAWA, T., 1971. Black Sea Region copper-lead-zinc deposits under light of the new developments. Presented at a symposium of the Society of Turkish Mining Engineers (in Turkish).

HAUSEN, D.M. and KERR, P.F., 1971. X-ray diffraction methods of evaluating potassium silicate alteration in porphyry mineralization: in Boyle, R.W. (ed.), Geochemical exploration symposium, Can. Instn. Min. Metall., Special Volume 11, pp. 334-340.

HAWKES, H.E. and WEBB, J.S., 1962. Geochemistry in mineral exploration. Harper and Row (publishers), 415 p.

HAWLEY, J.E., 1952. Spectrographic studies of pyrite in some Eastern Canadian gold mines. Econ. Geol., 47:260-304.

HAWLEY, J.E. and NICHOL, I., 1959. Selenium in some Canadian sulphides. Econ. Geol., 54:608-628.

HAWLEY, J.E. and NICHOL, I., 1961. Trace elements in pyrite, pyrrhotite and chalcopyrite of different ores. Econ. Geol., 56:467-487.

HEMLEY, J.J., MONTOYA, J.W., NIGRINI, A., and VINCENT, H.A., 1971. Some alteration reactions in the system CaO-Al_2O_3-SiO_2-H_2O: in IMA-IAGOD Meetings '70. Joint Symposium Volume. Soc. Min. Geol. Japan, Special Issue 2, pp. 58-63.

HEWETT, D.F., 1928. Dolomitization and ore deposition. Econ. Geol., 23:821-863.

HOFFMAN, S.J., and WASKETT-MYERS, M.J., 1974. Determination of molybdenum in soils and sediments with a modified zinc-dithiol procedure. J. Geochem. Explor., 3:61-66.

HOLAK, W., 1969. Gas-sampling technique for arsenic determination by atomic absorption spectrophotometry. Analytical chemistry, 41:1712-1713.

HONNOREZ, J., HONNOREZ-GUERSTEIN, B., VALETTE, J., and WAUSCHKUHN, A., 1973. Present day formation of an exhalative sulphide deposit at Vulcano (Tyrrhenian Sea), Part II: Active crystallization of fumarolic sulphides in the volcanic sediments of the Baia di Levante: in Amstutz, G.C. and Bernard, A.J. (eds.), Ores in sediments (VIII. International Sedimentological Congress, Heidelberg, 1971), Intn. Union Geol. Sci., Series A, No. 3 (Springer-Verlag), pp. 139-166.

HORIKOSHI, E., 1969. Volcanic activity related to the formation of the Kuroko-type deposits in the Kosaka district, Japan. Mineralium Deposita, 4:321-345.

HORSNAIL, R.F., NICHOL, I., and WEBB, J.S., 1969. Influence of variations in secondary environment of the metal content of drainage sediments. Quart. Colorado School of Mines, 64(1):307-322.

HUTCHINSON, R.W., 1965. Genesis of Canadian massive sulphides reconsidered by comparison to Cyprus Deposits. Can. Instn. Min. Metall. Trans. Symposium Volume, 68:286-300.

HUTCHINSON, R.W., 1973. Volcanogenic sulphide deposits and their metallogenic significance. Econ. Geol., 68:1223-1246.

IIJIMA, A., 1974. Clay and zeolitic alteration zones surrounding Kuroko deposits in the Hokuroku district, Northern Akita, as submarine hydrothermal-diagenetic alteration products, in Ishihara, S. (ed.), geology of Kuroko deposits, the Society of Mining Geologists of Japan, Special Issue, No. 6, pp. 267-290.

ISACS, B., OLIVER, J., and SYKES, L.R., 1968. Seismology and the new global tectonics. J. Geophysical Research, 73:5855-5899.

ISHIKAWA, H., KURODA, R., and SUDO, T., 1962. Minor elements in some altered zones of "Kuroko" (Black Ore) deposits in Japan. Econ. Geol., 57:785-789.

JAKES, P. and WHITE, A.J., 1972. Major and trace element abundances in volcanic rocks of orogenic areas. Geol. Soc. Am. Bull., 83:29-40.

JAMES, C.H., and WEBB, J.S., 1964. Sensitive mercury vapour meter for use in geochemical prospecting. Trans. Instn. Min. Metall., 73:633-641.

KAJIWARA, Y., 1971. Sulfur isotope study of the Kuroko-ores of the Shakanai No. 1 deposits, Akita Prefrecture, Japan. Geochemical Journal: 4(4):157-181.

KANEHIRA, K. and TATSUMI, T., 1970. Bedded cupriferous iron sulphide deposits in Japan, a review: In Tatsumi, T. (ed.), Volcanism and ore genesis, Tokyo, Tokyo University Press, pp. 51-76.

KAWADA, K. and ENGIN, A., 1972. Geology and geological structure of Çayeli, Rize, Turkey. Unpublished M.T.A. Report No. 1135.

KAWADA, K. and SARMAN, E., 1973. Geological map of Cayeli district. M.T.A. Map No. 27354.

KENTS, P., 1963. Hydrothermal developments in the Andes. Econ. Geol., 58:1110-1118.

KERR, P.F., 1955. Hydrothermal alteration and weathering. Geol. Soc. America, Special Paper 62, pp. 525-544.

KETİN, I., 1959. The orogenic evolution of Turkey. M.T.A. Bull., 53:82-88.

KETİN, I., 1966. Tectonic units of Anatolia (Asia Minor). M.T.A. Bull., 66:23-34.

KIESL, W., GRASS, F., BÖKL, R., and PONTA, U., 1970. Cosmochemical abundances of trace elements in Meteorites. I. Determination of Se, Te, Tl, Sr, Ba, and Ta in chondrites. J. Radioanalytical Chemistry, 6:447.

KIRKBRIGHT, G.F. and WARD, A.F., 1974. Atomic emission spectrometry and induction-coupled high-frequency plasma torch. Talanta, 21:1145-1165.

KIRKBRIGHT, G.F., WARD, A.F., and WEST, T.S., 1972. The determination of sulphur and phospho us by atomic emission spectrometry with an induction-coupled high-frequency plasma source. Anal. Chim. Acta, 62:241-251.

KIRKBRIGHT, G.F., WARD, A.F., and WEST, T.S., 1973. Atomic emission spectrometry with an induction coupled high frequency plasma source. Determination of iodine, mercury, arsenic and selenium. Anal. Chim. Acta, 64:353-362.

KRÄEFF, A., 1963a. A contribution to the geology of the region between Sirya and Ardanuc. M.T.A. Bull., 60:37-44.

KRÄEFF, A., 1963b. Geology and mineral deposits of the Hopa-Murgul region (western part of the province of Artvin, NE Turkey). M.T.A. Bull., 60:45-60.

KRONBERG, P., 1970. Photogeological results on the tectonics of the Eastern Black Sea Mountains (northeastern Turkey). M.T.A. Bull., 74:57-65 (in Turkish) (Also in German: M.T.A. Bull., foreign edition, 74:24-33).

LAKANEN, E. and ERVIÖ, R., 1971. A comparison of eight extractants for the determination of plant available micronutrients in soils. Soumen Maatalaustieelisen Seuran Julkaisuja 123, Acta Agralia Fennica.

LAKIN, H.W., 1959. Field test for selenium: in Geochemical Exploration Symposium, Mexico, 1959, pp. 453-459.

LAMBERT, I.B. and SATO, T., 1974. The Kuroko and associated ore deposits of Japan: a review of their features and metallogenesis. Econ. Geol., 69:1215-1236.

LEEPER, G.W., 1947. The forms and reactions of manganese in the soil. Soil Sci., 63:79-94.

LEITCH, C.H.B., 1975. Lateral distribution of trace metals in two Turkish volcanogenic sulphide deposits. M.Sc. thesis, Imperial College, University of London.

LE RICHE, H.H. and WEIR, A.H., 1963. A method of studying trace elements in soil fractions. J. Soil Sci., 14:225-235.

LICHTE, F.E. and SKOGERBOE, R.K., 1973. Analysis of solution samples by microwave induced plasma excitation. Analytical Chemistry 45:399-401.

LOFTUS-HILLS, G. and SOLOMON, M., 1967. Cobalt, nickel, and selenium in sulphides as indicators of ore genesis. Mineralium Deposita, 2(3):228-242.

LOVERING, T.S., 1949. Rock alteration as a guide to ore - East Tintic District, Utah. Econ. Geol. Monograph No. 1, 61 p.

LOWELL, J.D. and GUILD, J.M., 1970. Lateral and vertical alteration-mineralization zoning in porphyry ore deposits. Econ. Geol., 65:373-408.

LUKE, C.L., 1959. Determination of traces of selenium or tellerium in lead or copper. Analytical Chemistry, 31:572-574.

MABUCHI, H. and NAKAHARA, H., 1963. Colorimetric determination of traces of selenium with dithizone. Bull. Chem. Soc. Japan, 36:151-155.

MADO, H., 1972. Geology and mineralization of the copper ore deposits in the Murgul mine, northeastern Turkey. Unpublished M.T.A, Report No. 1103.

MADSEN, R.E., JR., 1971. Determination of arsenic subsequent to arsine reaction with 0.01M silver nitrate. Atomic Absorption Newsletter, 10:57-58.

MATSUKUMA, T. and HORIKOSHI, E., 1970. Kuroko deposits in Japan, a review: in Tatsumi, T. (ed.), Volcanism and ore genesis, Tokyo, University of Tokyo Press, pp. 153-179.

MEYER, C. and HEMLEY, J.J., 1967. Wall rock alteration: in Barnes, H.L. (ed.), Geochemistry of hydrothermal ore deposits, Holt, Rinehart and Winston, Inc., pp. 166-235.

MEYER, W.T., 1973. Development and application of thermally evolved vapor analysis in exploration geochemistry. Ph.D. thesis, University of London.

MEYER, W.T. and LAM SHANG LEEN, K.C.Y., 1973. Microwave-induced argon plasma emission system for geochemical trace analysis: in Jones, M.J. (ed.), Geochemical exploration 1972, Instn. Min. Metall., pp. 325-335.

MILLOT, G., 1970. Geology of clays; weathering, sedimentology, geochemistry. New York, Springer-Verlag, 429 p.

MITCHELL, A.H.G. and BELL, J.D., 1973. Island-arc evolution and related mineral deposits. Journal of Geology, 81:381-405.

MIYASHIRO, A., 1973. The Troodos ophiolite complex was probably formed in an island arc. Earth and Planetary Science Letters, 19:218-224.

MIYASHIRO, A., 1974. Volcanic rock series in island arcs and active continental margins. Am. Jour Sci., 274:321-355.

MURATOV, 1966. History of the Tectonic development of the Alpine folded region of southeastern Europe and Asia Minor - New data on the tectonic structure and history of development of the Alpine zone of Europe. Intn. Geol. Rev: 6(1):99-118.

MURAYAMA, S., MATSUNO, H., and YAMAMOTO, M., 1968. Excitation of solutions in a 2450 MHz discharge. Spectrochimica Acta, 23B:513-520.

NEBİOĞLU, T.Y., 1975. Geological map of Madenköy (1) area (1:1,000 scale), M.T.A. Map No. 31134.

NEPROCHNOV, Yu.P., 1959. Deep structure of earth's crust underneath Black Sea, southwest of Crimea, from seismic data. Akad. Nauk SSSR Doklady, 126(5):1119-1122.

NILSSON, C.A., 1968. Wall rock alteration at the Boliden deposit, Sweden. Econ. Geol., 63:472-494.

OAKES, H., 1959. Soils of Turkey. The Society of the Agricultural Engineers of Turkey publication, No. 18.

OGURA, Y., 1972. Geology and "Kuroko" ore deposit of the Hanaoka-Matsumime mine, northern Japan: in 24th Int. Geol. Congress, Ottawa, Canada, section 4, pp. 318-325.

O'NEILL, T.F., 1948. Hydrothermal alteration of feldspars at 250 to 400°C. Econ. Geol., 43:167-180.

OVCHINIKOV, L.H. and BARANOV, E.N., 1972. Endogenic geochemical halos of pyritic ore deposits. Int. Geol. Rev., 14 (5):419-429.

PAGE, E.R., 1964. Extractable manganese of soil. J. Soil Sci., 15:93-102.

PANTAZIS, T.H.M. and GOVETT, G.J.S., 1973. Interpretation of a detailed rock geochemical survey around Mathrati mine, Cyprus. J. Geochem. Explor., 2:25-36.

PEARCE, J.A., 1975. Basalt geochemistry used to investigate past tectonic environments on Cyprus. Tectonophysics, 25:41-67.

PEARCE, J.A. and GALE, G.H., 1976. Identification of ore-deposition environments from trace-element geochemistry. Paper presented at the Joint meeting of the Institution of Mining and Metallurgy and the Volcanic Studies Group of the Geological Society of London on "Volcanic Processes in Ore Genesis", 21-22 January.

PEARSE, R.W.B. and GRAYDON, A.G., 1950. Identification of molecular spectra. London, Chapman and Hall Ltd., 276 p.

PENROSE, R.A.F., JR., 1894. The superficial alteration of ore deposits. Journal of Geology, 2:314-318.

PEREIRA, J. and DIXON, C.J., 1971. Mineralization and plate tectonics. Mineralium Deposita, 6:404-405.

POLLOCK, E.N. and WEST, S.J., 1972. The determination of antimony at submicrogram levels by atomic absorption spectrophotometry. Atomic Absorption Newsletter, 11:105-106.

POLLOCK, E.N. and WEST, S.J., 1973. The generation and determination of covalent hydrides by atomic absorption. Atomic Absorption Newsletter, 12:6-8.

POPOVIC, R., 1975. Some of the structural and genetic characteristics and the zonal distribution of nonferrous metals deposits in eastern Pontides. M.T.A. Bull., 85:1-16.

REZANOV, I.A. and CHAMO, S.S., 1969. Reasons for absence of a "granitic" layer in basins of the South Caspian and Black Sea type. Canadian J. Earth Sci., 6 (4):671-678.

RIDLER, R.H. and SHILTS, W.W., 1974. Exploration for Archean polymetallic sulphide deposits in permafrost terrains: an integrated geological/geochemical technique; District of Keewatin, Kaminak Lake Area. Geol. Surv. Canada Paper 73-34, 33 p.

ROBINSON, W.D., DUDLEY, H.C., WILLIAMS, K.T. and BYERS, H.G., 1934. Determination of selenium and arsenic by distillation in pyrites, shales, soils, and agricultural products. Ind. Eng. Chemistry, Anal. Ed., 6:274-276.

ROSCOE, S.M., 1965. Geochemical and isotopic studies, Noranda and Matagami areas. Trans. Can. Instn. Min. Metall., Symposium Volume, 68:279-289.

ROSE, A.W., 1975. The mode of occurrence of trace elements in soils and stream sediments applied to geochemical exploration: in Elliott, I.L. and Fletcher, W.K. (eds.), Geochemical Exploration 1974 (Elsevier, Amsterdam), pp. 691-705.

ROSE, A.W. and SUHR, N.H., 1971. Major element content as a means of allowing for background variation in stream sediment geochemical exploration: in Boyle, R.W. (ed.), Geochemical exploration symposium, Can. Instn. Min. Metall., Special Volume, 11:587-593.

SAKRISON, H.C., 1967. Rock geochemistry - its current usefulness on the Canadian Shield. Canadian Instn. Min. Metall. Bull., 64:28-31.

SANGSTER, D.F., 1972. Precambrian volcanogenic massive sulphide deposits in Canada: a review. Geol. Surv. Canada Paper 72-22, 44 p.

SATO, T., 1972. Behaviours of ore-forming solutions in sea water. Mining Geol., 22:31-42.

SATO, T., 1973. A chloride complex model for Kuroko mineralization. Geochemical Journal, 7:245-270.

SAWA, T., SAWAMURA, K., and TEŞREKLİ, M., 1972. Geological survey report of the Murgul mine and surrounding copper mineralizations. Unpublished M.T.A. Report No. 2343.

SAWAMURA, K. and YILMAZ, S., 1971. Geology and ore mineralization at the Sürmene district, Trabzon, Turkey. Unpublished M.T.A. Report No. 1034.

SCHIROKOW, A.S. and KOWALJOWA, A.A., 1961. Application of metallometric investigations to geological reconnaissance. Zeitchrift für Angewandte Geologie, 7 (1):19-23 (in German with English summary).

SCHNEPFE, M.M. and FLANAGAN, F.J., 1973. The selenium content of U.S.G.S. standard rocks. Chemical Geology, 12:77-80.

SCHULTZE-WESTRUM, H-H., 1961. Das geologische profil des Aksu dere bei Giresun - Ein beitray zur geologie und lagerstättenkunde der Ostpontischen erz - und mineral provinz, NE - Anatolien. M.T.A. Bull., 57:65-74.

SCHWARTZ, G.M., 1955. Hydrothermal alteration as a guide to ore. Econ. Geol., 50th Anniversary Volume (part 1), pp. 300-323.

SCHWARTZ, G.M., 1956. Argillic alteration and ore deposits. Econ. Geol., 51:407-414.

SCOTT, R.H. and KOKOT, M.L., 1975. Application of inductively coupled plasmas to the analysis of geochemical samples. Anal. Chim. Acta; 75:257-272.

SHAW, H.F., 1971. Clay mineralogy of Recent sediments in the Wash, eastern England. Unpublished Ph.D. thesis, University of London.

SHEPPARD, S.M.F., 1976. Identification of the origin of ore-forming solutions by use of stable isotopes. Paper presented at the Joint meeting of the Institution of Mining and Metallurgy and the Volcanic Studies Group of the Geological Society of London on "Volcanic Processes in Ore Genesis", 21-22 January, 1976.

SHERMAN, G.P., McHARGUE, J.S., and HODGKISS, W.S., 1942. Determination of active manganese in soil. Soil Sci., 54:253-257.

SHIIKAWA, M., WAKASA, K., and TONO, N., 1975. Geochemical exploration for Kuroko deposits in north east Honshu, Japan: in Elliott, I.L. and Fletcher, W.K. (eds.), Geochemical exploration 1974 (Elsevier, Amsterdam), pp. 65-76.

SHIROZU, H., 1974. Clay minerals in altered wall rocks of the Kuroko type deposits, in Ishihara, S. (ed.), geology of Kuroko deposits, the Society of Mining geologists of Japan, Special Issue, No. 6, pp. 303-310.

SILLITOE, R.H., 1972. Formation of certain massive sulphide deposits at sites of sea-floor spreading. Trans. Instn. Min. Metall., 81:B141-B148.

SINCLAIR, W.D., 1971. A volcanic origin for the No. 5 Zone of the Horne Mine. Econ. Geol., 66:1225-1231.

SINDEEVA, N.D., 1964. Mineralogy and types of deposits of Selenium and tellerium. New York, Interscience (publishers), 363 p.

SMIRNOV, V.I., BORODAYEV, YU.S., and STAROSTIN, V.I., 1969. Pyritic ores and deposits of Japan. Intern. Geol. Rev., 11 (8):845-856.

SMITH, A.G., 1971. Alpine deformation and the oceanic areas of the Tethys, Meditterranean, and Atlantic geology. Geol. Soc. Am. Bull., 82:2039-2070.

SPOONER, E.T.C. and HEATON, T.H.E., 1976. Isotopic evidence for the origin of mineralization associated with the ophiolitic rocks of the Troodos Massif, Cyprus. Paper presented at the joint meeting of the Institution of Mining and Metallurgy and the Volcanic Studies Group of the Geological Society of London on "Volcanic Processes in Ore Genesis", 21-22 January, 1976.

STANTON, R.E., 1966. Rapid methods of trace analysis for geochemical applications. Edward Arnold (publishers) Ltd. London, 96 p.

STANTON, R.E. and McDONALD, J., 1965. The determination of selenium in soils and sediments with 3,3' - diaminobenzidine. Analyst, 90:497-499.

STRINGHAM, B., 1952. Fields of formation of some common hydrothermal alteration minerals. Econ. Geol., 47:661-664.

SUPERCEANU, C.I., 1971. The Meditterranean - Iranian Alpine copper-molybdenum belt: in Takeuchi, Y. (ed.), Proceedings of the IMA-IAGOD meetings '70 IAGOD volume, the Society of Mining Geologists of Japan, Special Issue No. 3, pp. 393-398.

TANRIVERDI, F., 1973. Surveys in recreation planning of the Eastern Black Sea Region, Turkey. Atatürk University, Erzurum, Ankara basim ve cilt evi (publishers) (in Turkish).

TATSUMI, T. and CLARK, L.A., 1972. Chemical composition of acid volcanic rocks related to formation of the Kuroko deposits. Journal Geol. Soc. Japan, 78:191-201.

THOMPSON, K.C. and THOMERSON, D.R., 1974. Atomic-absorption studies on the determination of antimony, arsenic, bismuth, germanium, lead, selenium, tellerium and tin by utilizing the generation of covalent hydrides. Analyst, 99:595-601.

TODOROVIC, Z., and NEBİOĞLU, T.Y., 1972. Copper mineralization in Tunca area, Ardesen, Turkey. Unpublished M.T.A. Report No. 1069.

TOKEL, S., 1973. The stratigraphical and volcanic history of the Gümüshane area, northeast Anatolia. Unpublished Ph.D. thesis, University of London.

TSAREGRADSKY, V.A., 1962. Metallometric surveying in Kazakhstan. Intn. Geol. Rev., 4 (12):1337-1349.

TUĞAL, H.T., 1969. Pyritic sulphide deposits of the Lahanos mine area, Eastern Black Sea Region, Turkey. Unpublished Ph.D. thesis, University of Durham.

TUĞAL, H.T. and PHILLIPS, R., 1971. Pyritic sulphide deposits, Eastern Black Sea area, Turkey: in Takeuchi, Y. (ed.), Proceedings of the IMA-IAGOD meetings '70, IAGOD volume, the Society of Mining Geologists of Japan, Special Issue No. 3, p. 309 (abstract only).

TURHAN, K., 1968. Geological map of Sirtköy-Gümüshane area, Cayeli, Rize: 1 cm to 20 m scale. M.T.A. Map No. 20398.

UZKUT, I., 1971. Turkish manganese mining industry and its future. M.T.A. Bull., 77:99-112 (in Turkish; also in German: M.T.A. Bull., foreign edition, 77:39-53).

VELCHEV, V. and TOKMAKCHIEVA, M., 1971. Preliminary results on the primary deep geochemical aureoles of elements in the Radka pyritic copper mine (Bulgaria), in Boyle, R.W. (ed.), Geochemical exploration symposium, Can. Instn. Min. Metall., Special Volume, 11, p. 397 (abstract only).

VUJANOVIC, V., 1974. The basic mineralogic, paragenetic and genetic characteristics of the sulphide deposits exposed in the eastern Black Sea coastal region (Turkey). M.T.A. Bull., 82:21-26.

WALTHAM, A.C., 1968. Classification and Genesis of some massive sulphide deposits in Norway. Trans. Instn. Min. Metall., 77:B153-B161.

WARREN, H.V. and DELEVAULT, R.E., 1956. Soils in geochemical prospecting. Mining Eng., 8:992-996.

WATLING, R.J., DAVIS, G.R., and MEYER, W.T., 1973. Trace identification of mercury compounds as a guide to sulphide mineralization at Keel, Eire: in Jones, M.J. (ed.), Geochemical exploration 1972, Instn. Min. Metall., pp. 59-69.

WHITE, D.E., 1955. Thermal springs and epithermal ore deposits. Econ. Geol., 50th Anniversary volume (part 1), 99-154.

WHITE, D.E., 1968. Environment of generation of some base-metal ore deposits. Econ. Geol., 63:301-335.

WHITEHEAD, R.E.S. and GOVETT, G.J.S., 1974. Exploration rock geochemistry-detection of trace element halos at Heath Steele Mines (N.B., Canada), by discriminant analysis. J. Geochem. Explor., 3:371-386.

YEGÜLALP, M., ACAR, B.H., and BOYABATLI, A., 1971. Regional geochemical survey between Rize and Findikli. Unpublished M.T.A. Report No. 1121 (in Turkish).

YILMAZ, Y., 1973. The petrology and structure of the Gümüshane granite and the surrounding rocks, north-east Anatolia. Unpublished Ph.D. thesis, University of London.

ZANKL, H., 1961. Magmatismus and bauplan des Ostpontischen gebirges im querprofil des Harsit-Tales, NE Anatolien. Geol. Rundschau, 51 (1):218-239.

APPENDIX A

SAMPLE COLLECTION AND SAMPLE PREPARATION

A.1 SAMPLE COLLECTION

A.1.1 Rock and Ore Sampling

Each rock sample was collected from an outcrop of 1 m in diameter and consisted of representative composite chips within that area. Special care was taken to collect fresh samples free of weathering. Each sample, weighing between 0.5 and 1.5 kg, was placed in a cloth sample bag together with a label and was described in the field notebook. Drill core samples were collected at about 5 m intervals. However, the sample density was usually increased to 1-2 m near the ore bodies. Core samples were composed of representative chips within a particular interval and weighed about 0.3 - 1.0 kg. The depth from which the sample was taken and a sample description were compiled in tables.

Ore samples from the surface and drill cores were collected following the same procedure as that used for rock sampling.

A.1.2 Soil Sampling

The soils in the study areas are undifferentiated. Thus, only an arbitrary soil horizon could be sampled. In this case about 30 cm below the surface was sampled. Each sample covered an area of 1 m in diameter in which three points were sampled to obtain a representative composite sample weighing about 0.5 - 1.0 kg. Samples were placed in labelled, water-resistant Kraft sample bags.

A.1.3 Stream Sediment Sampling

Stream sediment samples were collected in the middle of the active stream beds. They were placed in labelled, water-resistant Kraft paper bags. Average sample weight was about 0.5 kg.

A.2 SAMPLE PREPARATION

A.2.1 Introduction

The methods of preparation of rock, soil, and stream sediment samples are described. The methods described also include clay separation from rocks and pyrite separation from ores.

A.2.2 Preparation of Rock Samples

Representative chips of rock samples weighing between 60 and 120 g were reduced to 20-mesh (B.S.S.) (aperture size 750μ) using a tungsten carbide mortar and pestle. The sample was then ground in an agate "tema" mill for five minutes. The grain size at the end of this process was 200-mesh (B.S.S.) (aperture size 75μ), and the sample was well homogenized.

A.2.3 Preparation of Soil Samples

Soil samples were air dried in the field camp and broken up in a porcelain mortar until they passed a 2-mesh sieve (B.S.S.) (aperture 750μ). Some of this 2-mesh size fraction was kept for the pH determinations of soils in the laboratory. The rest was sieved through an 80-mesh sieve (B.S.S.) (aperture 200μ). This 80-mesh sieve fraction was used for all the analyses.

A.2.4 Preparation of Stream Sediment Samples

Stream sediment samples were air dried in the field camp. The dried samples were disintegrated by gentle pestle action in a porcelain mortar and sieved through a 40-mesh sieve (B.S.S.) (aperture 375μ). The 40-mesh fraction was further sieved through a 80-mesh sieve. Some samples from Madenköy were separated into -20 - 60-mesh (B.S.S.) (-750-250μ), -60-80 mesh (B.S.S.) (-250-200μ), -80-100-mesh (B.S.S.) (-200-150μ) and -100 mesh (B.S.S.) (-150μ) size fractions.

A.2.5 Clay Separation Method for Rock Samples

The rock sample was crushed using a tungsten carbide mortar and pestle to pass a 20-mesh (B.S.S.) (750μ aperture) sieve and then frequently sieved through a 200-mesh (B.S.S.) sieve (aperture 75μ). In this way the contribution from the soft minerals such as feldspars is minimised. Ten grams of -200-mesh size fraction were then placed in a 400 ml beaker full of deiomized water and mixed thoroughly. The suspension was transferred into plastic centrifuge bottles and centrifuged at 500 cps for 12 minutes. The supernatant water contains the clay fraction. Some of this clay for X-ray diffraction analysis was filtered through a mounted disc by vacuum filtering; the rest was transferred to another plastic centrifuge bottle and centrifuged at 3000 cps for one hour to obtain the clay fraction. This clay fraction was then air dried and used for further X-ray diffraction analysis.

A.2.6 Pyrite Separation Techniques for Mineralized Samples

About 250g of sulphide-rich sample was crushed using a tungsten-carbide mortar and pestle. From the crushed

material -100-140-mesh (-150-180μ) and -140-200 mesh (-108μ -75μ) fractions were sieved and placed in separate sample bags. The latter fraction was taken in case the liberation of pyrite grains was not complete in the coarser fraction. The two fractions were put in two separate beakers and washed with deionized water several times until a clear solution was obtained above; the fractions were then finally washed with acetone and air dried on filter papers.

A combination of micropanner (Chas. W. Cook and Sons Ltd., Birmingham) and an Isodynamic Franz magnetic separator was used to separate pyrite from the rest of the minerals. For most samples the Iosdynamic Franz separator was sufficient for the separation. When the samples were quartz-rich pyrite could not be adequately separated from the quartz; in such cases, the micropanner was employed. Generally the -100-140 mesh (-150-108μ) fraction was used. At the end of each step of the separation procedure the purity of pyrite sample was checked with a binocular microscope.

The operating conditions for both of the above mentioned instruments varied considerably from sample to sample. The best conditions for separating pyrite were found by trial and error for each sample. Thus, no attempt will be made to give a list of operating conditions.

APPENDIX B

ANALYTICAL METHODS

B.1 SAMPLE DIGESTION PROCEDURES FOR ATOMIC ABSORPTION SPECTROMETRY

B.1.1 Nitric Acid Digestion

Reagents (All chemicals are Analar grade)

(a) Nitric acid

(b) Deionised water

Apparatus

(a) Test tubes (18 x 180 mm)

(b) Hot plate

(c) Adjustable Oxford dispensor

(d) Whirly mixer

Procedure

(a) Weigh 0.25 g sample and place in a test tube.

(b) Add 1 ml of nitric acid.

(c) Heat at 115^{o}C for one hour on a hotplate in a fume cupboard. The oxidizing procedure is generally complete within one hour.

(d) Leave tube to cool.

(e) Make up to 10 ml with 9 ml of deionised water.

(f) Mix the whole contents and leave overnight to obtain a clear supernatent liquid for analysis.

The dilution factor is 40 and the final solution is of 1M strength.

B.1.2 Nitric Acid/Perchloric Acid Digestion

Reagents (All chemicals are Analar grade)

(a) Nitric acid

(b) Perchloric acid

(c) Acid mixture: mixture of nitric and perchloric acids in 4:1 volumetric proportion

(d) Hydrochloric acid

(e) 6 M hydrochloric acid: mix 240 ml of hydrochloric acid with 200 ml of deionised water.

Apparatus

(a) Test tubes

(b) Hot plate

(c) Adjustable Oxford dispensor

(d) Whirly mixer

Procedure

(a) Weigh 0.25 g sample and place in a test tube.

(b) Add 5 ml of acid mixture.

(c) Evaporate slowly and carefully to dryness on a hot plate in a fume cupboard.

(d) When just dry and cream coloured, leave tubes to cool.

(e) Leach with 2 ml of 6 M hydrochloric acid.

(f) Make up to 12.5 ml with deionised water.

(g) Mix and leave overnight to settle.

The dilution factor is 50.

B.1.3 Bromine/Nitric Acid digestion for Sulphide Analysis

Reagents (All chemicals are Analar grade)

(a) Bromine - carbon tetrachloride mixture: mix bromine and carbon tetrachloride in a 2:3 volumetric proportion

(b) Nitric acid

(c) 6 M nitric acid

Apparatus

(a) 100 ml beaker

(b) Watch glass

(c) Hot plate

(d) Adjustable Oxford dispensor

Procedure

(a) Weigh 0.25 g sample and place in a 100 ml beaker.

(b) Add 3 ml of bromine and carbon tetrachloride mixture.

(c) Cover and set aside for ½ hour with occasional swirling.

(d) Add 5 ml of nitric acid and set aside for another ½ hour with occasional swirling.

(e) Heat gently on a hot plate for one hour.

(f) Displace cover and increase heat and gently evaporate the mixture just to dryness.

(g) Leach the residue in 2 ml of 6 M nitric acid.

(h) Dilute to 12.5 ml.

The dilution factor is 50.

B.2 DIRECT READING OPTICAL SPECTROGRAPHIC ANALYSIS - SAMPLE PREPARATION AND OPERATING CONDITIONS

Reagents (All chemicals are Analar grade)

(a) Buffer: 1 part w/w sodium fluoride and 2 parts w/w carbon powder

Apparatus

(a) Direct reading optical spectrophotometer with a computer program, together called System C, details of which are given in Applied Geochemistry Research Group Technical Communication Report No. 59 (1973).

Procedure

(a) Mix 100 mg sample with 150 mg buffer.

(b) Lode carbon electrode by pressing it into mixture (a). The amount of sample contained in the electrode is approximately 15 mg.

(c) Place electrode in burner system and arc electrode in air with a D.C. arc using cathode excitation of 8.0 amperes. The time of excitation is 60 seconds for Cd, Pb, Zn, Li, Mo, and As and 90 seconds for the rest of the elements.

B.3 COLORIMETRIC ANALYSIS

B.3.1 Arsenic Analysis

Reagents (All chemicals are Analar grade)

(a) Potassium bisulphate (powder)

(b) 6 M hydrochloric acid: Mix 240 ml of concentrated hydrochloric acid with 200 ml of deionised water.

(c) 1.5% stannous chloride: dissolve 35 g stannous chloride in 250 ml of concentrated hydrochloric acid and dilute 10 times with deionised water

(d) Dilute potassium iodide solution: dissolve 10 g potassium iodide in 400 ml deionised water

(e) Zinc pellets (activated with copper)

(f) Mercuric chloride paper (ex. Johnsons)

Apparatus

(a) Borosilicate test tube

(b) Primus and bunsen burner

(c) Gutzeit tube

Procedure

(a) Weigh 0.25 g sample and place in a borosilicate test tube.

(b) Mix with 1 g potassium bisulphate and first fuse on a primus and then on a bunsen burner until a quiescent melt is obtained.

(c) When cool leach with 10 ml of 6 M hydrochloric acid

(d) Mix tube contents and set aside overnight to settle

(e) Take 5 ml of the clear liquid for Mo analysis. To the remaining liquid and residue add 2 ml of dilute potassium iodide solution.

(f) Add 4 ml of 1.5% stannous chloride solution and mix

(g) Add about 2 g zinc pellets and without delay connect a Gutzeit tube loaded with mercuric chloride paper.

(h) Remove the mercuric chloride paper after one hour and compare the spot with the standards. Standards are prepared by using solutions containing 0, 0.5, 0.75, 1, 2, 3, 4, 5, 6, 7, 8, 9, 10 and 12 µg/ml arsenic in 6 M hydrochloric acid.

B.3.2 Molybdenum Analysis

From step (e) of the previous procedure related to As analysis, the following reagents, apparatus and procedure are used for Mo analysis.

Reagents (All chemicals are Analar grade)

(a) Reducing solution: dissolve 75 g of citric acid and 150 g of ascorbic acid in 2 l of water

(b) Concentrated potassium iodide solution: dissolve 500 g potassium iodide in 500 ml of deionised water

(c) Dithiol Solution: dissolve 20 g of sodium hydroxide and 3.0 g of zinc dithiol in 20 ml of ethanol and 40 ml of deionised water and then add a further 500 ml of deionised water

(d) Thioglycollic acid (50%)

(e) Toluene

Apparatus

(a) Test tube (150 mm long; 15 mm in diameter) and silicon rubber stopper

(b) Adjustable Oxford dispensor

(c) Mechanical tube shaker (Griffin flask shaker)

(d) Gilford 300 N spectrophotometer

Procedure

(a) Add 4 ml of reducing solution to 5 ml of sample solution and leave for 5-10 minutes.

(b) Add 2 ml of concentrated potassium iodide solution.

(c) Add 50 µl thioglycollic acid.

(d) Add 1 ml of zinc dithiol solution and allow to stand for ten minutes.

(e) Add 3 ml toluene.

(f) Stopper the test tube, shake mechanically for 5 minutes, and set aside for 10 minutes.

(g) Measure the absorption of the toluene layer by using Gilford 300 N spectrophotometer at 680 mm.

(h) Obtain a calibration curve by running standards which have been treated by the same procedure. It is important that the standard solutions should have the same acidity.

(i) Convert absorbances into concentrations by means of the calibration curve. Dilution factor is eight for the Mo analysis.

B.4 FLUORINE ANALYSIS (after Boyle, 1976)

Reagents (All chemicals are Analar grade)

(a) Concentrated NaOH solution. In a thick walled 2 litre

polythene bottle containing 1 litre deionised water dissolve 1 kg of NaOH in small portions, waiting for each portion to dissolve before adding the next. Shake the solution until all the NaOH has dissolved.

(b) Citrate-acetate buffer: To a 20 l container add 2.5 kg sodium citrate and 500 gm sodium chloride. Make up to 20 l mark with deionised water adding 550 ml of glacial acetic acid before mark is reached. Shake until all chemicals have dissolved. Check effectiveness of buffer by adding 3.0 ml of the concentrated NaOH solution to 100 ml of the buffer. The pH should be in the range of 7.0-7.5. If the pH is too alkaline then slowly add more acetic acid continually checking until the correct pH range is achieved. Similarly if the pH is too acidic add 5 M NaOH.

(c) Calibration standards. These should be made up in the citrate-acetate buffer solution to which has been added enough concentrated NaOH (approximately 30 ml/l of buffer) to give a pH of 7.0-7.5. For a stock solution of 1,000 µg/ml F^- dissolve 2.108 gm NaF (which has been dryed at 110°C for 24 hours) in one litre of the above solution. For a working solution of 100 µg/ml F^- dilute 100 ml of stock solution to one litre using the adjusted buffer solution. Make up calibration standards of 10, 1, and 0.1 µg/ml F^- by diluting 100 ml, 10 ml, and 1 ml of working solution respectively to one litre with the adjusted buffer solution. Standards will have the same solution matrix as the sample solution.

(d) Isopropyl alcohol

Apparatus: (for 100 determinations)

(a) Muffle furnace

(b) One hundred 20 ml nickel crucibles and lids

(c) Six crucible racks made from 1/16" sheet steel with three rows of six holes and the corners turned down for legs. Racks can be labelled using metal stamps.

(d) Metal tongs and asbestos sheets to put hot racks on

(e) Drying oven capable of 200°C

(f) One hundred 100 ml polypropylene beakers

(g) Magnetic stirrer and magnets

(h) Pipette calibrated to deliver 3.0 ml and fitted with a suction bulb

(i) pH paper covering neutral range

(j) Fluoride specific ion electrode, reference electrode, and Ionanalyser (Orion) or mullivolt meter (Fig. 2.1).

Procedure: (for 100 determinations)

Weigh 0.25 gm of sample into a nickel crucible. Do this for 100 samples (including replicates and blanks). Add to each crucible 3.0 ml of concentrated NaOH solution. Add 1 to 2 ml isopropyl alcohol to facilitate the mixing of the sample and flux.

Place the rack of samples in a drying oven at 200°C for 1 to 1½ hours or until all of the water has been evaporated from the flux. Remove each rack in turn from the drying oven and place nickel lids on the crucibles. Place each rack in turn in a muffle furnace at 420°C for 20 minutes, after which remove the rack and let the samples cool. Racks of samples should be left in the heating oven until it is time for them to be fused. This prevents the flux from taking on water which may result in a violent reaction in the muffle furnace.

After the samples have cooled put the crucibles and lids in polypropylene beakers containing 100 ml of citrate-acetate buffer. Let the fused samples soak in the buffer solution for 10 to 15 minutes with the crucibles on their sides. Stir the samples using a plastic stirring rod until the fusion is completely disintegrated. Remove the crucibles and lids and add a magnetic stirrer to each beaker. Test the final pH with pH paper to ensure a pH of 7.0 to 7.5. If the pH is outside this range add dropwise 1 M NaOH or 1 M HCl, whichever is required, until the correct pH is attained. Allow sample solutions to cool to room temperature before analysis.

Calibrate fluoride electrode system using 10, 1, and 0.1 µg/ml F^- standards and adjust for temperature variation if necessary.

Sample concentrations can be measured using the following formula

$$\text{Concentration } (\mu g/gm) = \frac{\mu g/ml \times 100 \text{ ml}}{0.25 \text{ gm}}$$

The theoretical detection limit is 8 µg/gm (based on the solubility product of the LaF_3 membrane).

Although the use of a muffle furnace greatly increases production, fusions can be done over a bunsen burner, and the method can easily be adapted for use in a mobile laboratory.

B.5 MERCURY ANALYSIS - FLAMELESS ATOMIC ABSORPTION METHOD

B.5.1 Total Mercury Analysis

Reagents (All chemicals are Analar grade)

(a) Concentrated nitric acid

(b) 10% stannous chloride solution. Dissolve 10 g of stannous chloride in 1 litre of 1 M hydrochloric acid

(c) Nitrogen

(d) Calibration standards. Prepare standards of 0, 20, 100, 200, 300, 400, and 500 ppb Hg in the same solution matrix as the sample solution. For a stock solution of 1000 µg/ml Hg dissolve 1.4789 of $HgSO_4$ in 1 l of 1 M nitric acid.

Apparatus

The analytical system for total mercury analysis is described in Chapter 5.7. The apparatus used during the sample preparation is:

(a) Test tube

(b) Hot plate

Procedure

(a) Weigh 100 mg sample and place in a test tube.

(b) Add 2 ml of nitric acid.

(c) Heat at 80°C to 90°C for three hours.

(d) When cool transfer the contents into wash bottle and make up to 50 ml with washings of deionised water.

(e) Add 2 ml of stannous chloride.

(f) Close the wash bottle with the Sinta glass bubbler and open the first stopper and the two-way stopper so that the nitrogen passes through the wash bottle only. Employ a nitrogen flow rate of 4 litre/min. (i.e. 2 litre/min. each flow meter).

(g) Obtain mercury concentration from the calibration graph.

B.5.2 Mercury Thermal Evolution Profile Analysis

Details of the instrumentation is given in chapter 5.7. A detailed description of the procedure follows:

Procedure

(a) Weigh 100 mg sample

(b) Place the sample in the micro-crucible of the furnace

(c) Let the nitrogen flow at a rate of 4 litre/min.

(d) Heat the sample at a rate of 30°C/min.

(e) Record mercury evolved and the temperature on each channel of the recorder.

(f) Compare the profiles with the standard profiles.

B.6 SELECTIVE EXTRACTION METHODS

B.6.1 EDTA Extraction

Reagents (All chemicals are Analar grade)

(a) 0.05 M ammonium EDTA solution (pH:4.65). Dissolve 18.12 g of ammonium EDTA in 1 litre of deionised water.

(b) Standard solutions. Prepare standard solutions for Fe, Mn, Cu, Zn, and Pb in 0.05 M ammonium EDTA solutions.

Apparatus

(a) Test tube (150 mm long and 14 mm in diameter)

(b) Silicon-rubber cork to fit the tube

(c) Mechanical shaker (Griffin flask shaker)

(d) Filter paper (Watman 40, ashless, 110 mm in diameter)

(e) pH paper covering acid range

(f) Drying oven

Procedure

(a) Weigh 0.5 g sample and place in a test tube.

(b) Add 10 ml of the EDTA solution.

(c) Stopper the tube and shake on a mechanical shaker for one hour.

(d) Filter the mixture through the filter paper into another test tube. Keep the residue after washing it twice with distilled water and drying it.

(e) Check pH. If below 4.0 adjust pH to 4.5-5.0.

The filtered solution can be directly sprayed into the flame of the atomic absorption spectrophotometer for Fe, Mn, Cu, Zn, and Pb analyses.

B.6.2 Acidified Hydroxylamine Hydrochloride Extraction

Reagents (All chemicals are Analar grade)

(a) Acidified 1 M hydroxylamine hydrochloride solution (pH:1.3). Dissolve 50 g of hydroxylamine hydrochloride in 900 ml of 35% acetic acid.

(b) 35% (v/v) acetic acid. Dilute 450 ml glacial acid to 1:1 with deionised water

(c) Concentrated nitric acid

(d) 6 M hydrochloric acid. Mix 240 ml of concentrated hydrochloric acid and 200 ml of deionised water.

Apparatus

(a) 50 ml centrifuge tube

(b) 10 ml pipette

(c) 50 ml beaker

(d) Centrifuge machine

(e) Hot plate

(f) Adjustable Oxford dispensor

(g) Drying oven

Procedure

(a) Weigh 0.5 g sample and place in a centrifuge tube.

(b) Add 25 ml of the acidified hydroxylamine hydrochloride.

(c) Mix occasionally during a four hour-period and leave overnight.

(d) Centrifuge at 5,000 rev/min for five minutes.

(e) Take 10 ml aliquot of the supernatent solution and transfer into a beaker.

(f) Place the beaker on a hot plate and add concentrated nitric acid slowly until all the reaction has ceased. Evaporate just to dryness.

(g) Leach the residue with 2 ml of 6 M hydrochloric acid.

(h) Make up to 10 ml with deionised water in a test tube. This solution is ready for atomic absorption analyses. The residue left after stage (e) was washed twice with deionised water. It was kept for further analysis after drying at 50°C.

B.6.3 Ammonium Oxalate Extraction

Reagents (All chemicals are Analar grade)

(a) 0.157 M ammonium oxalate in oxalic acid (pH:3.3). Mix 0.275 M solutions of ammonium oxalate and oxalic acid in 100:75 volumetric proportions

(b) 0.275 M ammonium oxalate solution. Dissolve 39.08 g ammonium oxalate in 1 l of deionised water

(c) 0.275 m oxalic acid. Dissolve 34.67 g oxalic acid in 1 l of deionised water.

Apparatus

(a) 50 ml centrifuge tube

(b) Magnetic stirrer

(c) Hanovia UV lamp (Model 16)

(d) Centrifuge machine

(e) Drying oven

Procedure

(a) Weigh 1.0 g sample and place in a centrifuge tube.

(b) Add 50 ml of the ammonium oxalate in oxalic acid (pH:3.3).

(c) Leach samples for five days.

(d) Stir samples using magnetic stirrer under ultra-violet light.

(e) Centrifuge to separate the attached sample and wash it three times with deionised water.

(f) Dry the residue at 50°C.

(g) Reweigh it.

(h) Analyse the leached residue by atomic absorption spectrometry after a nitric/perchloric acid digestion (see Appendix B.1.2).

(i) Apply weight-loss correction if necessary.

(j) Subtract from the total elemental concentrations to find the amount extracted by the ammonium oxalate solution.

B.7 COLORIMETRIC METHOD OF SELENIUM ANALYSIS

Reagents (All chemicals are Analar grade)

(a) Acid mixture. Mix concentrated nitric and perchloric acids in 1:1 volumetric proportion

(b) 6 M hydrochloric acid. Mix 240 ml of concentrated hydrochloric acid and 200 ml of deionised water

(c) Sodium arsenite solution. Dissolve 250 mg of As_2O_3 and 2g NaOH in 200 ml of deionised water

(d) Hypophosphorous acid. 50% w/w

(e) EDTA solution. Dissolve 25g EDTA disodium salt in 500 ml water

(f) 10 M ammonia solution

(g) Formic acid

(h) Buffer solution. Dissolve 60 g of ammonium formate in 500 ml of deionised water. Add 200 ml of formic acid, followed by 6 M hydrochloric acid until the pH is 1.6 and finally dilute to 1 l with deionised water

(i) 3,3'-diaminobenzidine solution. Dissolve 0.5 g of 3,3'-diaminobenzidine in 100 ml of deionised water. This solution should be freshly prepared. Note: 3,3'-diaminobenzidine is a very carcinogenic chemical

(j) Toluene

(k) Selenium standards. Dissolve 100 mg Se in 20 ml of nitric acid and dilute to 1 l with deionised water. From this 100 ppm Se solution prepare 0.5, 1,2,3,5,10, 15,20 and 30 ppm Se standards.

Apparatus

(a) 50 ml beakers

(b) Auto pipette

(c) Hot plate

(d) Filter paper. Whatman No. 540 (90 mm in diameter)

(e) Test tube (18 x 180 mm) calibrated at 10 and 14.5 ml

(f) Mechanical Tube shaker (Griffin flask shaker)

(g) Unicam SP spectrophotometer

Procedure

(1) Weigh 1 g sample into a beaker.

(2) Add 10 ml of acid mixture.

(3) Add a further 10 ml acid mixture after all the effervescence has subsided.

(4) Evaporate the solution to fumes of perchloric acid until volume is between 1 and 2 ml.

(5) Filter the hot solution through a filter paper into a second beaker to remove the residue with 6 M hydrochloric acid.

(6) Wash the first beaker and residue with 6 M hydrochloric acid.

(7) Add 2 ml of sodium arsenite solution.

(8) Add 5 ml of hypophosphorus acid.

(9) Cover beaker and boil solution until precipitate has flocculated.

(10) Filter solution through filter paper and discard filtrate

(11) Wash beaker and residue with 6 M hydrochloric acid and discard filtrate.

(12) Place filter paper in beaker and add 20 ml acid mixture

(13) Cover beaker and heat so that precipitate and filter paper completely dissolves.

(14) When oxidation is complete evaporate solution to fumes of perchloric acid until solution is between 1 and 2 ml.

(15) When cold, place solution into a test tube with water washings from beaker.

(16) Add 1 ml EDTA solution.

(17) Add ammonian solution until colour of indicator is orange.

(18) Dilute solution to 10 ml with water.

(19) Add 2 ml buffer solution.

(20) Add 0.5 ml of 3,3'-diminobenzidine solution and leave for ½ hour.

(21) Add 2 ml of ammonia solution to increase pH within range 4.3 - 10.3, after selenium complex has formed This pH is optimum for toluene extraction.

(22) Add 4 ml toluene.

(23) Cork tube and shake for 15 minutes by mechanical shaker.

(24) Prepare standard selenium solutions of 0.5, 1,2,3,5, 10,20, and 30 ppm concentrations in test tubes and treat them as described in stages 16 to 23 of the procedure.

(25) Measure absorption through toluene phase of standards and samples at 420 Å by spectrophotometer.

(26) Read Se concentration from calibration graph.

APPENDIX C

DATA PROCESSING

Data on the elemental contents of stream sediment, soil, and rock samples were processed by two computer programs. The first is called "MRSTAT" which computes the simple statistical parameters such as, means, ranges, standard deviations, and correlation coefficients. The second is called "RAWFREQ" which plots the arithmetic and logarithmic relative frequency and cumulative frequency diagrams for the elemental distributions.

Where a sample was not analysed for a particular element the element was coded as -1. The programs were modified to take into account missing data.

Examples of the outputs of these two programs are given in Figures C.1, C.2, and C.3.

D=DR DATA A=AADATA

NO. OF VARIABLES = 14 NO. OF SAMPLES = 203

MISSING DATA (CODED -1) HAS BEEN OMITTED

VARIABLE	MEAN	SD	MIN	MAX	RANGE	C.V.	S.E.	N
V	108.001	129.452	5.000	595.000	590.000	119.862	9.154	200
CO	11.183	15.066	.100	117.000	116.900	134.729	1.065	200
NI	21.435	26.829	1.000	128.000	127.000	97.094	1.473	200
CR	46.995	71.658	1.000	524.000	523.000	152.481	5.067	200
GA	19.385	7.973	1.000	81.000	80.000	41.127	.564	200
TI	2583.845	2371.283	31.000	9999.000	9968.000	91.773	167.675	200
BE	.304	.493	.200	2.400	2.200	128.417	.035	200
MG	1.473	1.512	.100	7.700	7.600	102.677	.107	200
CA	1.522	1.983	.000	11.710	11.710	130.225	.140	200
SR	75.265	127.321	4.000	1336.000	1332.000	169.163	9.007	200
BA	263.628	649.122	5.000	6776.000	6771.000	246.227	46.015	199
K	1.329	.949	.100	4.400	4.300	71.407	.067	200
LI	14.606	19.468	0.000	144.000	144.000	133.295	1.377	200
SC	8.693	6.369	.100	33.700	33.600	73.268	.450	200

CORRELATION MATRIX
SAMPLE SIZE = 203

	V	CO	NI	CR	GA	TI	BE	MG	CA	SR	BA	K	LI	SC
V	1.000													
CO	.505	1.000												
NI	.082	.222	1.000											
CR	.245	.312	.772	1.00										
GA	.17	.41	-.173	-.11	1.0									
TI	.710	.415	-.110	.033	.201	1.000								
BE	-.158	-.024	-.156	-.151	-.049	-.263	1.000							
MG	.339	.357	.299	.46	.076	.284	-.177	1.000						
CA	.768	.476	.331	.482	-.167	.237	-.122	.519	1.000					
SR	.184	.147	.096	.226	-.139	.227	-.084	.200	.403	1.000				
BA	-.111	-.000	-.012	-.037	.003	-.061	-.060	-.114	-.134	-.012	1.000			
K	-.124	-.096	-.117	-.176	.281	.002	-.127	-.225	-.768	-.248	.225	1.000		
LI	-.242	-.194	-.132	-.147	.062	-.245	.196	.245	.116	.167	-.163	-.244	1.000	
SC	.725	.457	.111	.224	.151	.760	-.242	.416	.406	.241	-.051	-.079	-.248	1.000

NUMBER OF SAMPLES USED IN CALCULATION
ALLOWING FOR MISSING DATA VALUES

	V	CO	NI	CR	GA	TI	BE	MG	CA	SR	BA	K	LI	SC
V	203.													
CO	203.	203.												
NI	203.	203.	203.											
CR	200.	200.	200.	203.										
GA	200.	200.	200.	200.	203.									
TI	203.	203.	203.	203.	203.	203.								
BE	203.	203.	203.	203.	203.	203.	203.							
MG	200.	200.	200.	200.	200.	200.	200.	203.						
CA	200.	200.	200.	200.	200.	200.	200.	200.	203.					
SR	203.	203.	203.	203.	203.	203.	203.	203.	203.	203.				
BA	199.	199.	199.	199.	199.	199.	199.	199.	199.	199.	199.			
K	200.	200.	200.	200.	200.	200.	200.	200.	200.	200.	196.	203.		
LI	200.	200.	200.	200.	200.	200.	200.	200.	200.	200.	196.	200.	203.	
SC	200.	200.	200.	200.	200.	200.	200.	200.	200.	200.	199.	200.	200.	203.

Figure C.1 Statistical parameters (mean, standard deviation and correlation coefficients) for 14 elements in all surface rock samples as computed by program "MRSTAT" (arithmetic data).

Figure C.2 Histogram for log(10) transformed Cu concentrations of 221 soil samples as plotted by program "RAWFREQ".

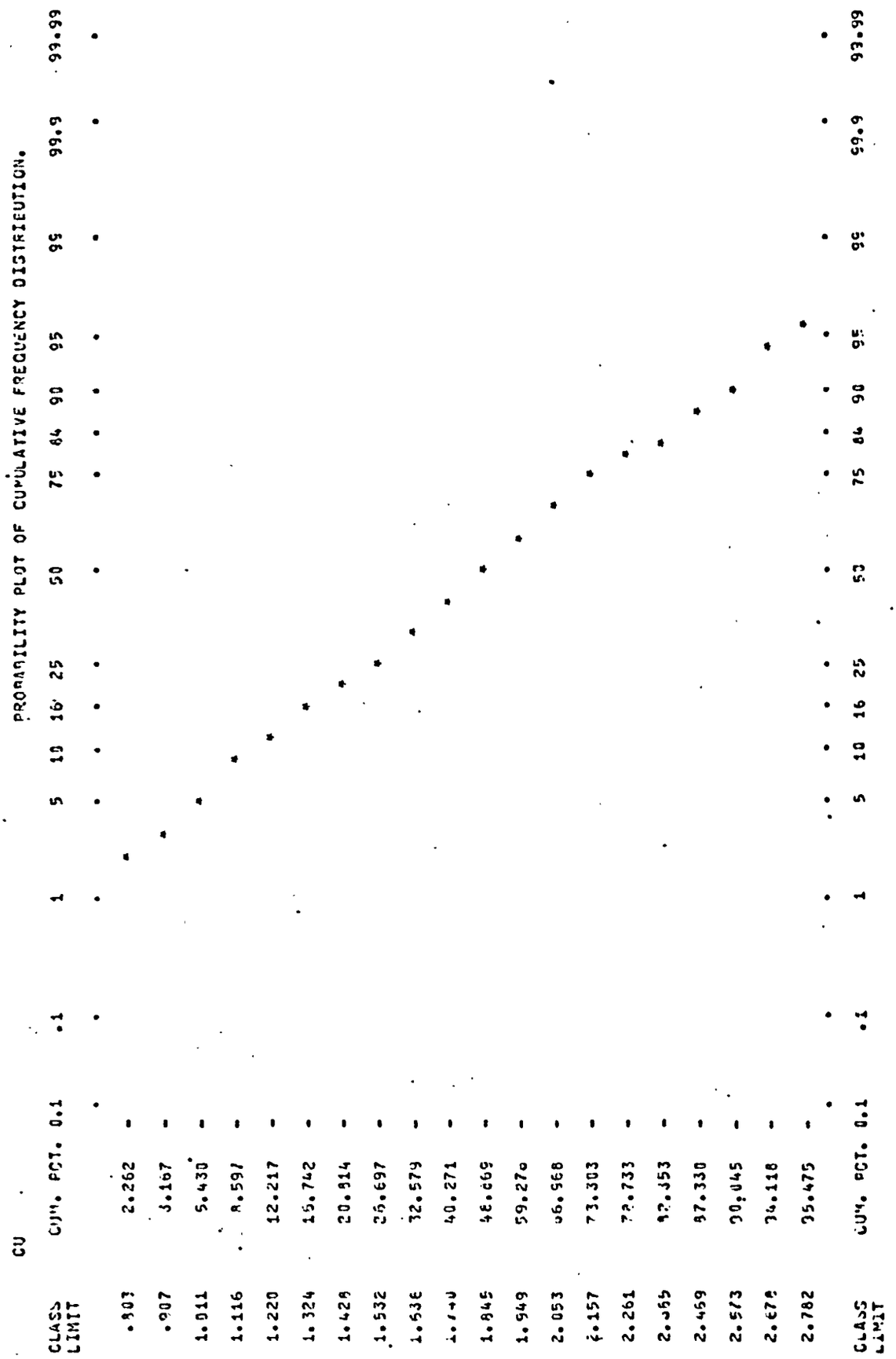


Figure C.3 Probability plot of cumulative frequency distributions for log (10) transformed Cu concentrations in 221 soil samples as plotted by program "RAWFREQ".

APPENDIX D

BEDROCK DATA FOR KUTLULAR, KOTARAK DERE, AND TUNCA AREAS

Table D.1 Bedrock data, Kutlular area. For locations of samples See Figure 4.8. All concentrations are in ppm.

Sample No.	Rock type*	As	F	Cu	Pb	Zn
11	1	20	92	8	10	4
12	1	16	116	25	10	4
13	1	72	208	75	180	33
14	1	7	148	12	35	14
15	1	200	260	112	10	12
16	1	10	124	30	10	4
17	2	1.5	400	410	45	460
18	1	150	224	300	356	11
19	1	1.5	216	9	10	5
20	1	36	240	160	172	16
21	1	6	60	7	10	56
390	2	225	480	2300	120	3500

* Rock type 1 indicates dacitic rocks
2 indicates basic rocks

Table D.2 Bedrock data, Kotarak Dere. For location of samples see Figure 4.9. All concentrations are in ppm.

Sample No.	Rock type *	As	F	Cu	Pb	Zn
1	1	1.5	312	11	20	113
2	1	4	600	3	10	86
6	1	1.5	640	85	60	190
7	1	1.5	144	5	10	30
8	1	-	152	77	10	44
9	1	24	630	23	28	27
10	1	1.5	600	430	10	6900
11	1	1.5	620	18	10	108
12	1	1.5	880	5	10	125
453	1	9	264	80	44	58
457	1	4	128	59	10	59
459	1	1.5	368	4	10	69
461	1	13	600	460	24	160
464	1	10	160	1300	30	9900

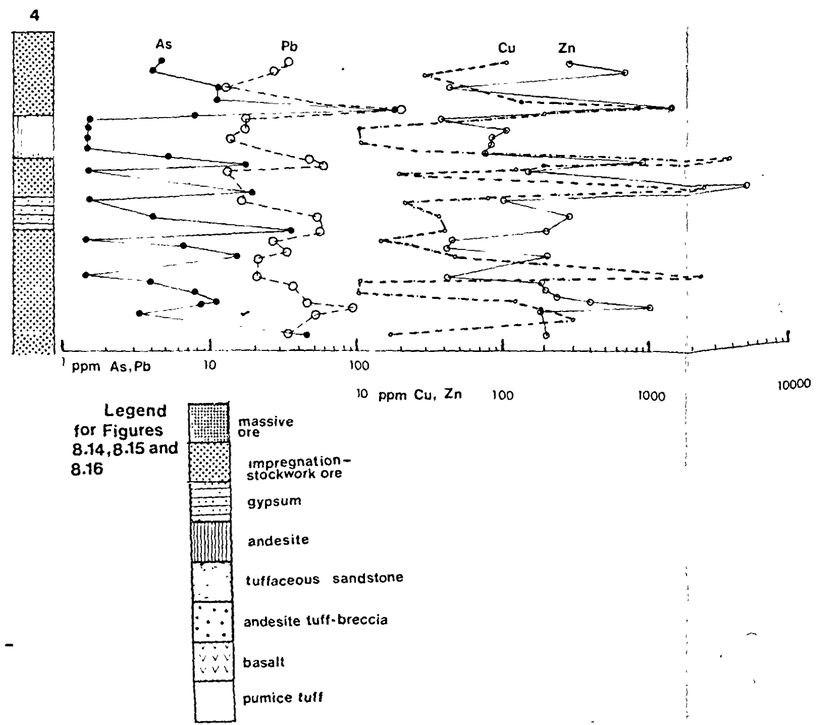
* Rock type 1 indicates dacite

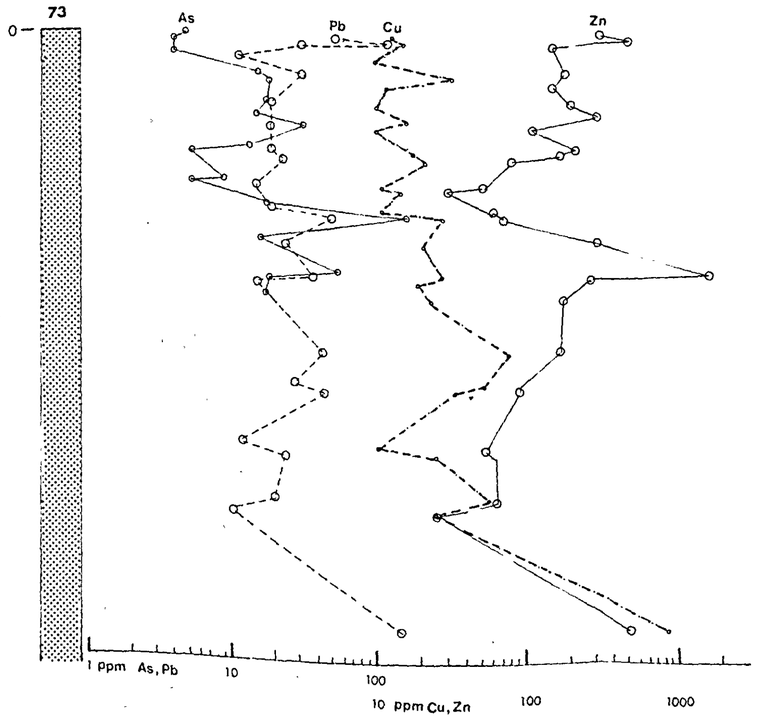
Table D.3 Bedrock data, Tunca area. For locations sample sites see Figure 4.11. All concentrations are in ppm.

Sample Number	Rock Type*	As	F	Cu	Pb	Zn
1	2	1.5	220	91	20	90
2	2	1.5	368	122	20	60
3+	1	400	352	761	1738	5197
4	1	58	800	230	50	300
5	1	250	1080	2100	1400	5500
6	1	4	560	29	20	810
7	1	32	1080	30	10	29
8	1	18	1920	8	40	6500
9	1	30	300	140	40	61
10	3	1.5	500	8	10	510
11	3	6	300	19	10	180
12+	1	650	230	690	300	1100
14	1	150	440	710	1200	1500
15	3	175	920	37	10	290
401	2	7	140	150	14	109
424	2	1.5	124	12	20	69

* Rock type 1 indicates dacitic rocks
2 indicates basic rocks
3 indicates hematitized dacite

\+ Denotes exclusion of data for this sample during statistical treatment.





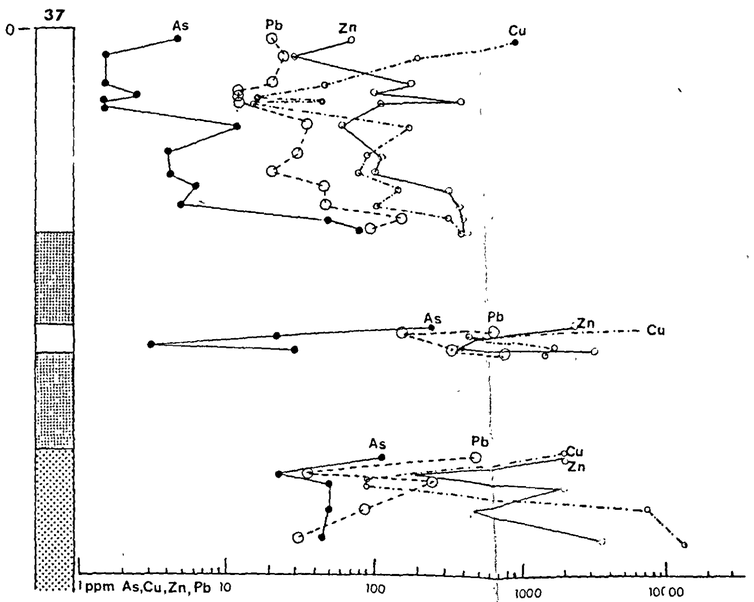
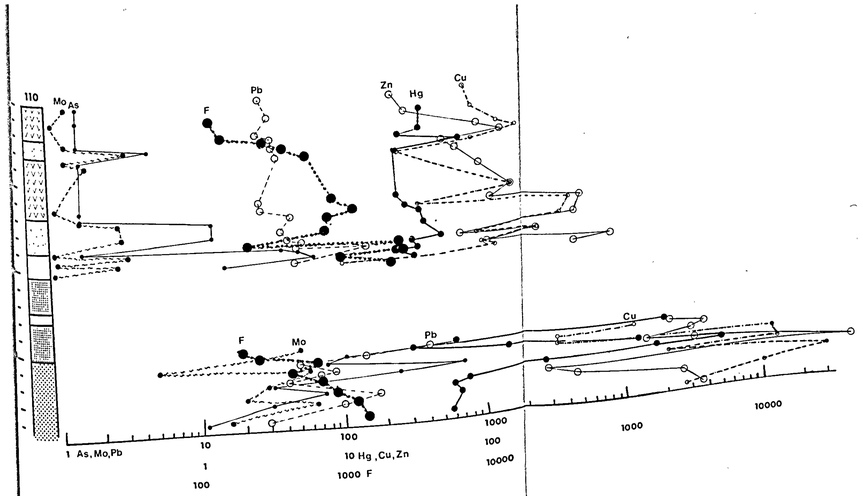
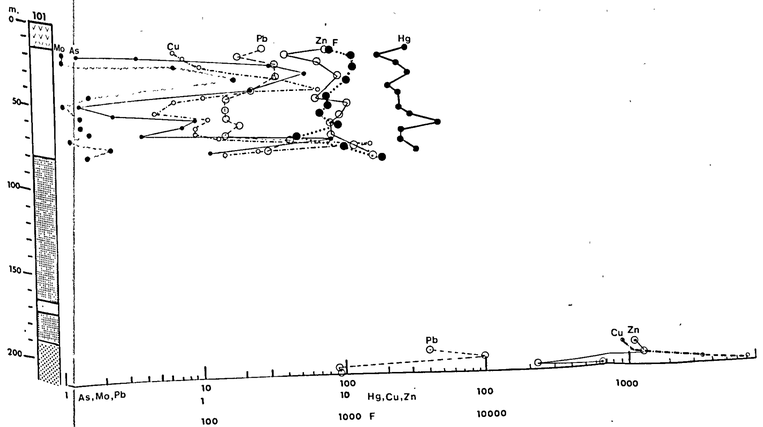


Figure 8.14 Vertical elemental profiles in drill-holes 4, 73, and 37, the Madenköy deposit.

Page 250





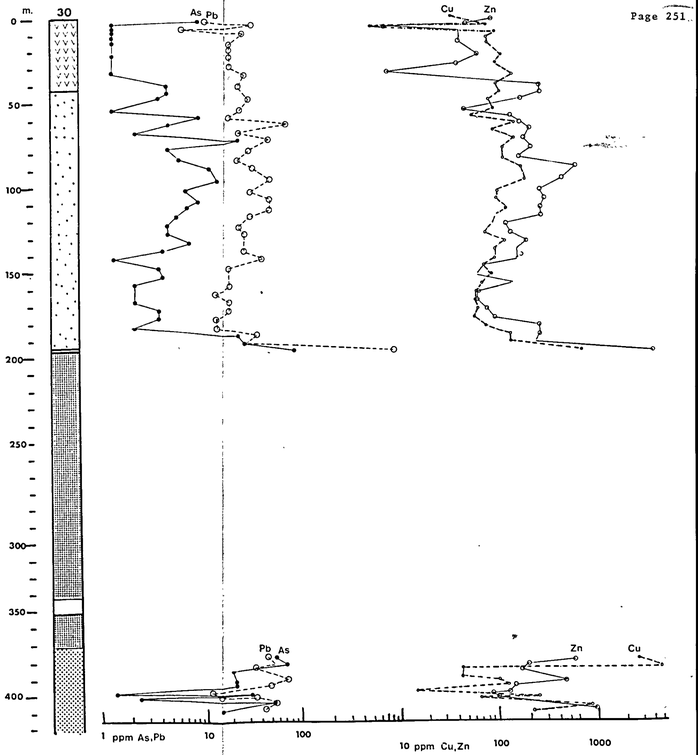


Figure 8.15 Vertical elemental profiles in drill-holes 110, 101 and 30, the Madenköy deposit.

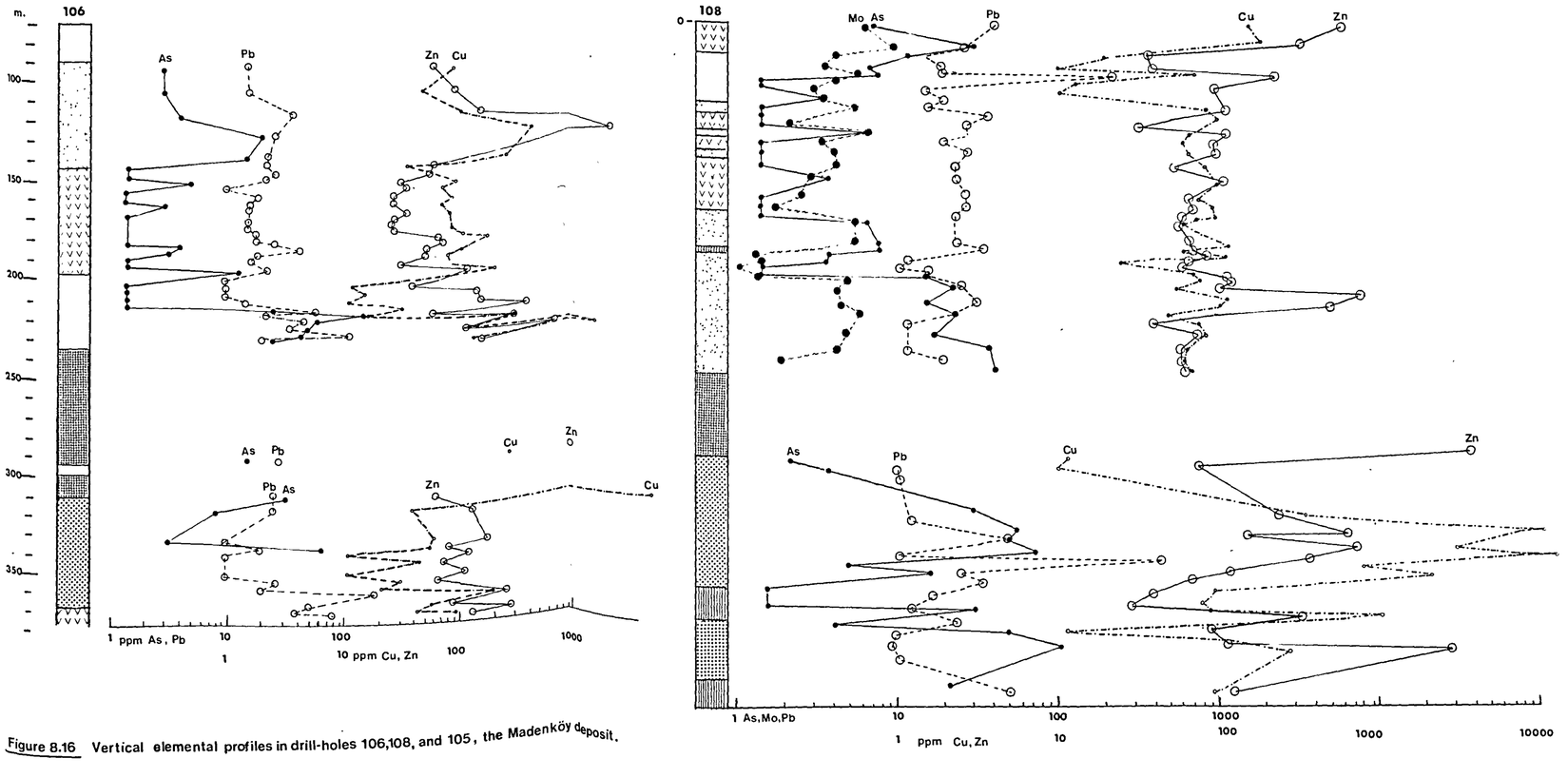


Figure 8.16 Vertical elemental profiles in drill-holes 106,108, and 105, the Madenköy deposit.